JOURNAL OF GEOPHYSICAL RESEARCH

The continuation of

TERRESTRIAL MAGNETISM AND ATMOSPHERIC ELECTRICITY

(1896-1948)

An International Quarterly

VOLUME 56 September, 1951 NUMBER 3

CONTENTS

(Contents concluded on outside back cover)

PUBLISHED BY

THE WILLIAM BYRD PRESS, INC.

P. O. Box 2-W—Sherwood Ave. and Durham St., Richmond 5, Virginia

FOR THE JOHNS HOPKINS PRESS, BALTIMORE 18, MARYLAND

EDITORIAL OFFICE:

5241 Broad Branch Road, Northwest, Washington 15, D.C., U.S.A.

THREE DOLLARS AND FIFTY CENTS A YEAR SINGLE NUMBERS, ONE DOLLAR

JOURNAL OF GEOPHYSICAL RESEARCH

The continuation of

Terrestrial Magnetism and Atmospheric Electricity

(1896-1948)

An International Quarterly

Founded 1896 by L. A. BAUER *Continued 1928–1948 by* J. A. FLEMING

Fields of Interest

Terrestrial Magnetism
Atmospheric Electricity
The Ionosphere
Solar and Terrestrial Relationships
Aurora, Night Sky, and Zodiacal Light
The Ozone Layer
Meteorology of Highest Atmospheric Levels
The Constitution and Physical States of t Upper Atmosphere
Special Investigations of the Earth's Cru and Interior, including experimental seism waves, physics of the deep ocean and oce bottom, physics in geology
And similar topics

This Journal serves the interests of investigators concerned with terrestrial magnetism and ele tricity, the upper atmosphere, the earth's crust and interior by presenting papers of new analy and interpretation or new experimental or observational approach, and contributions to int national collaboration. It is not in a position to print, primarily for archive purposes, extensi tables of data from observatories or surveys, the significance of which has not been analyzed.

Forward *manuscripts* to the editorial office of the Journal at 5241 Broad Branch Road, Northwe Washington 15, D. C., U.S.A., or to one of the Associate Editors. It is preferred that manuscri be submitted in English, but communications in French, German, Italian, or Spanish are a acceptable. A brief abstract, preferably in English, must accompany each manuscript. A *publi tion charge* of $4 per page will be billed by the Editor to the institution which sponsors the work any author; private individuals are not assessed page charges. Manuscripts from outside t United States are invited, and should not be withheld or delayed because of currency restrictio or other special difficulties relating to page charges. Costs of publication are roughly twice t total income from page charges and subscriptions, and are met by subsidies from the Carne Institution of Washington and international and private sources.

Back issues and *reprints* are handled by the Editorial Office, 5241 Broad Branch Road, N. Washington 15, D.C., U.S.A.

Subscriptions are handled by The Johns Hopkins Press, Baltimore 18, Maryland, U.S.A.

THE JOHNS HOPKINS PRESS

Baltimore 18, Maryland

Entered as second-class matter at the Post Office at Richmond, Virginia, under the act of March 3, 1879.

Journal of

GEOPHYSICAL RESEARCH

The continuation of

Terrestrial Magnetism and Atmospheric Electricity

OLUME 56 SEPTEMBER, 1951 No. 3

ON THE AUTOMATIC CHEMICAL DETERMINATION OF ATMOSPHERIC OZONE*

BY I. GERALD BOWEN AND VICTOR H. REGENER

Department of Physics, The University of New Mexico, Albuquerque, N. M.

(Received April 18, 1951)

ABSTRACT

A chemical method for the automatic and quantitative recording of atmospheric ozone near the ground, from aircraft, or by means of sounding balloons, is described. A network of surface ozone recording stations is now being established in New Mexico and one airborne unit has been flown in an airplane. Preliminary recordings are communicated.

I—INTRODUCTION

Ozone as a constituent of the atmosphere occupies a peculiar place due to its rtical distribution. The partial pressure of ozone near the ground is, on the aver-e, only one-tenth of that which is found near the ozone maximum at an altitude of out 20 km. The ratio of the number of ozone molecules to the number of air lecules has an average value of 2×10^{-8} near the ground and reaches a maximum lue of about 6×10^{-6} somewhere between 20 and 30 km in the stratosphere. The oduction of ozone in the stratosphere due to the photochemical dissociation of the ygen molecule by ultra-violet solar radiation has been quantitatively established theoretical investigations [see 1 of "References" at end of paper].

*A preliminary report of this work was given by one of the authors (V. H. R.) at the Los geles meeting of the American Physical Society on December 30, 1950.

The photochemical mode of production of the ozone molecule is no longer pre below an altitude of about 18 km. In the absence of other mechanisms which m form ozone at lower altitudes [2], one is led to the current assumption that the oz measured in the troposphere and at the earth's surface is the result of mechan transport from the ozonized stratosphere [3]. The term *mechanical transport* i include the lateral advection due to large-scale movement of air masses as wel the more localized convection such as that which leads, in the extreme case under otherwise favorable conditions, to thunderstorms. Ordinary diffusion due gradient of concentration is, below 30-km altitude, a slow process compared mechanical transport and its effect can be neglected [4].

This transport should in the course of time have established a uniform rati ozone to air at altitudes lower than 18 km. However, the strong fluctuations of ozone content of the troposphere, coupled with the fact that the ozone/air ratio to 18 km is not constant with height, leads to the assumption that the ozone m cule is destroyed in the troposphere and at the ground. This results in a net flu ozone from the stratosphere to the troposphere and the surface of the earth.

There are four processes which lead to the destruction of the ozone molecul altitudes lower than 18 km:

(1) Oxidation of foreign particles suspended in the atmosphere or catal destruction of the ozone molecule on these particles.
(2) Oxidation of objects on the surface of the earth or catalytic destruc of the ozone molecule on these objects.
(3) Solar radiation in the orange (Chappuis absorption bands) and at long-wave end of the Hartley absorption band near 3000 Å.
(4) Thermal dissociation of the ozone molecule.

The first two mechanisms are probably predominant and are held primarily sponsible for the existence of an ozone flux to the earth and, in conjunction with fluctuating processes of mechanical transport in the atmosphere, for the contin absence of a stationary state of this ozone flux [5]. Liquid water in clouds and on surface, as well as water vapor, are to be included as ozone-destroying agent under (1) and (2).

Regarding processes (3) and (4), and also in the case of the "catalytic" proce referred to under (1) and (2), it must be kept in mind that the oxygen atom w appears during the destruction of the ozone molecule would tend to again for ozone molecule in a three-body collision with an oxygen molecule as one of collision partners [6]. However, in the presence of foreign particles and of wat water vapor, one must consider the possibility that the oxygen atom is interce by a foreign particle or by water prior to an ozone-forming three-body collisio

One would thus consider the atmosphere above 18 km a source region whe equilibrium value of the ozone concentration tends to be reestablished af mechanical disturbance and the atmosphere below 18 km, especially the layers the ground, a sink region where the ozone molecule disappears due to its che activity. The fraction of ozone which disappears per unit time at each level dep on the prevailing abundance of oxidizable substances and catalyzers, and also lesser extent, on the presence of solar radiation and on the temperature.

The foregoing considerations received their impulse from the many observations ich showed that the ozone concentration near the ground is subject to very strong ne variations and that these variations are correlated to meteorological condi-ns [7, 8].

Continuous recordings of the ozone concentration near the ground, coupled with easurements of the vertical ozone distribution from airplane and balloon flights, omise to become a valuable source of information on the air transport mechanism tween stratosphere and troposphere. Even though the situation is complicated by e variability of the conditions which lead to the destruction of ozone during its nsport, there is hope that an extensive series of such ozone measurements will entually allow significant interpretations in the sense indicated. Plans were thus ade at the University of New Mexico in 1947 to set up a network of recording ations for surface ozone in conjunction with simultaneous ozone measurements in e troposphere and stratosphere [9].

II—CHOICE OF THE METHOD

The ozone concentration near the earth's surface is extremely difficult to measure cause of its small magnitude. On the other hand, the time fluctuations of this ncentration are very large. The average value is 2 ozone molecules per 10^8 air olecules, but values anywhere from near zero to 6 ozone molecules per 10^8 air olecules can be recorded within a short time interval. An instrumental accuracy of few per cent can be considered sufficiently good for the purpose.

There is a choice between spectrographic and chemical methods. The spectro-aphic method has the advantage of being immediately specific to ozone. It makes e of the very strong absorption of the ozone molecule in the center of the artley band near 2500 Å. However, a path length of several kilometers is needed r sufficiently accurate determinations of surface ozone by conventional means. ther complications which forbid the use of the spectrographic method for the con-nuous recording of ozone are selective extinction due to variable conditions of haze nd precipitation, need for quartz optics, and restriction to night-time measure-ents. The chemical method, on the other hand, while not *a priori* specific to ozone, n be adapted to the automatic and continuous determination of surface and upper-r ozone.

The quantitative production of free iodine by ozone in a neutral aqueous solution potassium iodide according to the formula

$$O_3 + 2KI + H_2O \longrightarrow 2KOH + O_2 + I_2$$

a very efficient reaction and, when used with certain precautions, the most suit-ble for automatic recording.

The potassium iodide method, after having been adapted to the non-automatic easurement of surface ozone in as little as 15 liters of air [10], has been used with eat success by Auer [7] and Ehmert [8] for an analysis of time variations of ozone connection with meteorological conditions [11]. Later, Ehmert [12] introduced ectrolytic titration, which further simplified the procedure over the earlier use of starch indicator. Gluckauf, Heal, Martin, and Paneth [13] also used electrolytic ration in equipment which was, for the first time, automatic to the extent that it

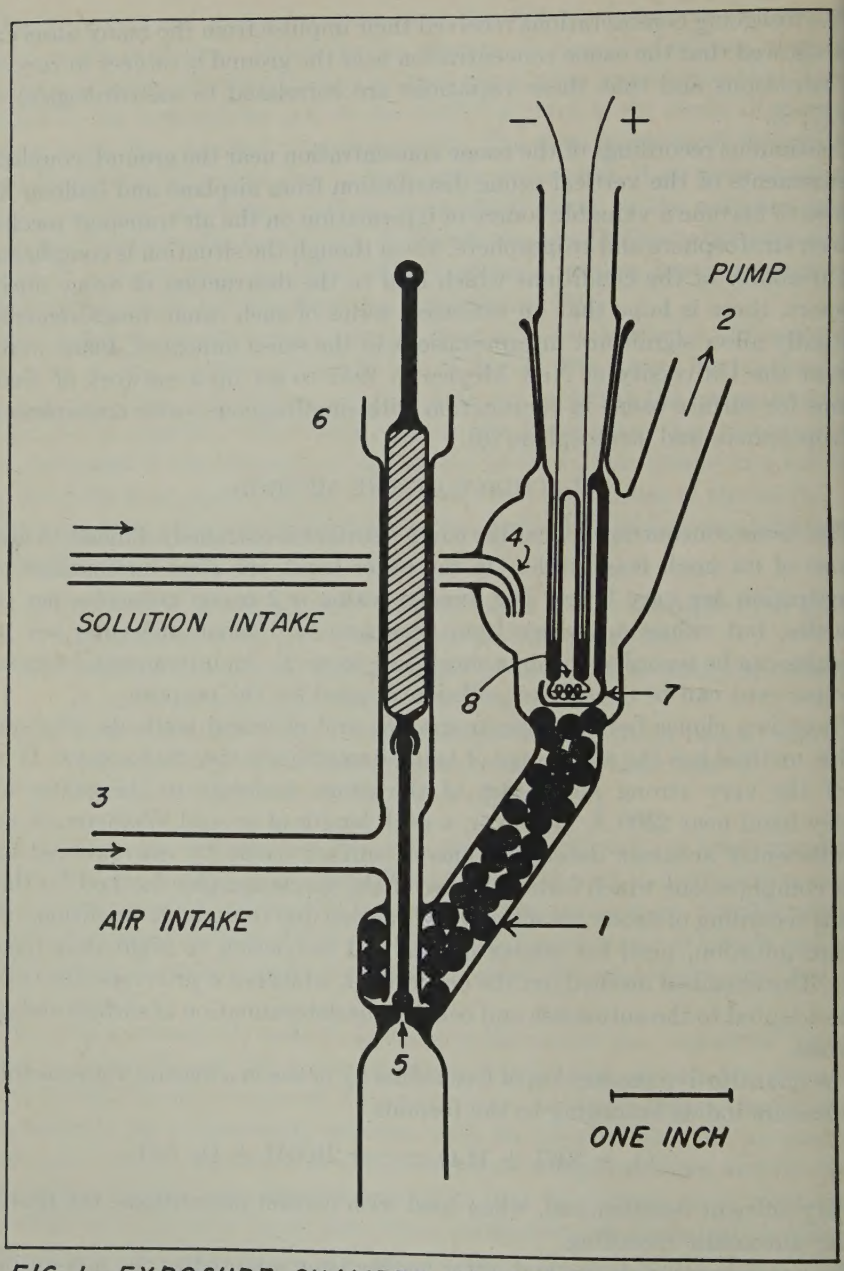

FIG. 1—EXPOSURE CHAMBER, ELECTROLYTIC CUP, AND DRAIN VALVE

wed the continuous measurement of surface ozone concentrations over a period 4 hours.

The equipment described below records ozone on the ground without attendance one week with an accuracy of a few per cent and is characterized by relatively ple and inexpensive construction. The instrument is also adapted to recording ing airplane flights and to sounding balloon work with radio transmission to the und.

III—DESCRIPTION OF THE EQUIPMENT

A known amount of sodium thiosulfate is added beforehand to several liters of a assium iodide "storage" solution. A small amount of this solution, the "charge," rought into close contact with the air stream of which the ozone concentration is be determined.

While the air stream passes through the charge, iodine is continuously freed by ozone, but it reacts immediately with the sodium thiosulfate. As soon as the ium thiosulfate is used up, free iodine appears and is then promptly detected by depolarizing effect on a platinum cathode. The small electrolytic current which v flows is used to automatically "cycle" the instrument; the charge is discarded l a new charge is injected from the storage solution into the reaction chamber. e actual ozone measurement consists of recording the volume of air which had to s through the reaction chamber in order to cause the instrument to cycle.

The essential parts of the exposure apparatus where the air makes contact with potassium iodide solution are shown in Figure 1. The air is drawn through the ction chamber *1* at a rate of about 1.5 liters per minute by a small pump con- ted at *2*; the outside air intake is at *3*. The chamber *1* is filled with glass balls for d contact between the air and the solution. The solution is injected in the ount of 8 cm^3 at *4* after the previous charge has been drained through the valve *5* raising the piston in the medical glass syringe *6* for a short time. The valve stem astened to the lower end of the piston by means of a ball-and-socket connection. e valve seat is ground against the valve with fine emery. The piston of the syringe ufficiently tight to prevent admission of room air in competition with the outside Some mercury can be placed at *6* for an additional seal if this appears desirable. After the solution is injected at *4* by the mechanism described below, it is kept tated by the air rising through it. The charge of 8 cm^3 is large enough to reach up bout 1 cm above the edge of the small cup *7* which surrounds the two electrodes Thus, the electrodes are continuously rinsed with solution due to the agitation sed by the air flow without being touched by air bubbles and without being in ger of drying when the solution is drained from the chamber. There is enough ess of solution above the cup to allow for evaporation in case the same charge uld remain in the chamber for many hours due to a low ozone concentration.

The charge remains in the reaction chamber until the presence of free iodine is icated by a current of about 2×10^{-9} ampere between the electrodes *8*. This rent is amplified and triggers a relay to actuate the motor-driven cycling mechan- . The current flow is a consequence of the depolarizing action of the neutral ne as it is transported to the cathode by the agitation of the liquid [14]. Both trodes consist of clean platinum wire 0.5 mm in diameter. The cathode is in the

form of a helix and the anode passes through its axis. A constant potential differen of 22 millivolts is maintained between the electrodes by means of a battery.*

The charge is taken from the storage solution of two per cent potassium iod in carefully distilled water with the addition of Merck reagent sodium thiosulfa to make a 5×10^{-6} normal solution. The addition of $Na_2S_2O_3$ ahead of the exposu of the charge to the air, apart from allowing a convenient automatic determinati of the end-point for the ozone-iodine reaction, also serves to prevent volatile f iodine from entering the air stream and thus from escaping detection [10]. Enou storage solution is made, approximately 5 liters, to last for one week under abo average ozone conditions. Using the sodium thiosulfate concentration quoted abo the instrument cycles every 30 minutes when the ozone concentration is avera In spite of the small concentration of sodium thiosulfate, the solution keeps for c week without noticeable change in sodium thiosulfate. The keeping quality is, course, very sensitive to the purity of the distilled water. Commercial distilled wa is re-distilled in a glass still with the addition of some potassium permangana Dissolved gases are boiled off before the beginning of the distilling operation. shown below, the volume freed in the storage flask by the consumption of solut during the week is not replaced by air but by argon.

Figure 2 shows the exposure chamber along with mechanical parts of the equ ment. As soon as the current in the electrolytic cup signals the appearance of f iodine, a small motor begins to turn cam *1* through one single revolution in the ti of approximately one minute. Shortly after the cam begins to turn, the lever arm drops into the recess of the cam and, by means of the string-and-pulley arrangeme raises the discharge valve which allows the charge to drain through the trap *3*. T trap is necessary because the air pump would not allow the solution to drai atmospheric pressure were present below the valve. The drain valve closes a the cam has rotated through 90°.

As the lower part of the downward stroke of the piston in the 20 cm^3 med glass syringe *4* is reached, solution from the storage flask *5* enters the syri through tube *6* and rises into the capillary *7* to a constant level determined by lower end of the argon intake tube in the storage flask.† Argon from the parti filled rubber balloon *8* replaces the volume ceded by the storage solution.

Shortly after the beginning of the upward stroke, the piston injects the cha into the reaction chamber through jet *9*. The solution does not immediately c into contact with the electrodes. As the injection nears its end, the small amoun solution which was left in the cup from the previous exposure period is replace

A small vacuum pump is attached to *10*. At installations removed from c mercial power, the pump consists of a small gasoline engine designed for m airplanes and converted into a pump.

The actual automatic measurement of the ozone concentration is accompli by recording, either photographically or with a printing recorder, the numbe

*In later models, two pieces of platinum wire with sharp tips separated by 0.5 mm are us electrodes; the potential difference has been reduced to 11 millivolts.

†In the case of the airborne unit, the argon intake tube cannot be used because of the s variations of the air pressure. In this case, the storage flask is much smaller and errors d variations of the level in capillary *7* are insignificant.

mp strokes necessary to cause the instrument to cycle. From the known amount sodium thiosulfate in each charge and from the known volume of air aspirated by ch pump stroke, the amount of ozone per unit volume of air is thus computed, thout error due to occasional changes in pumping speed.

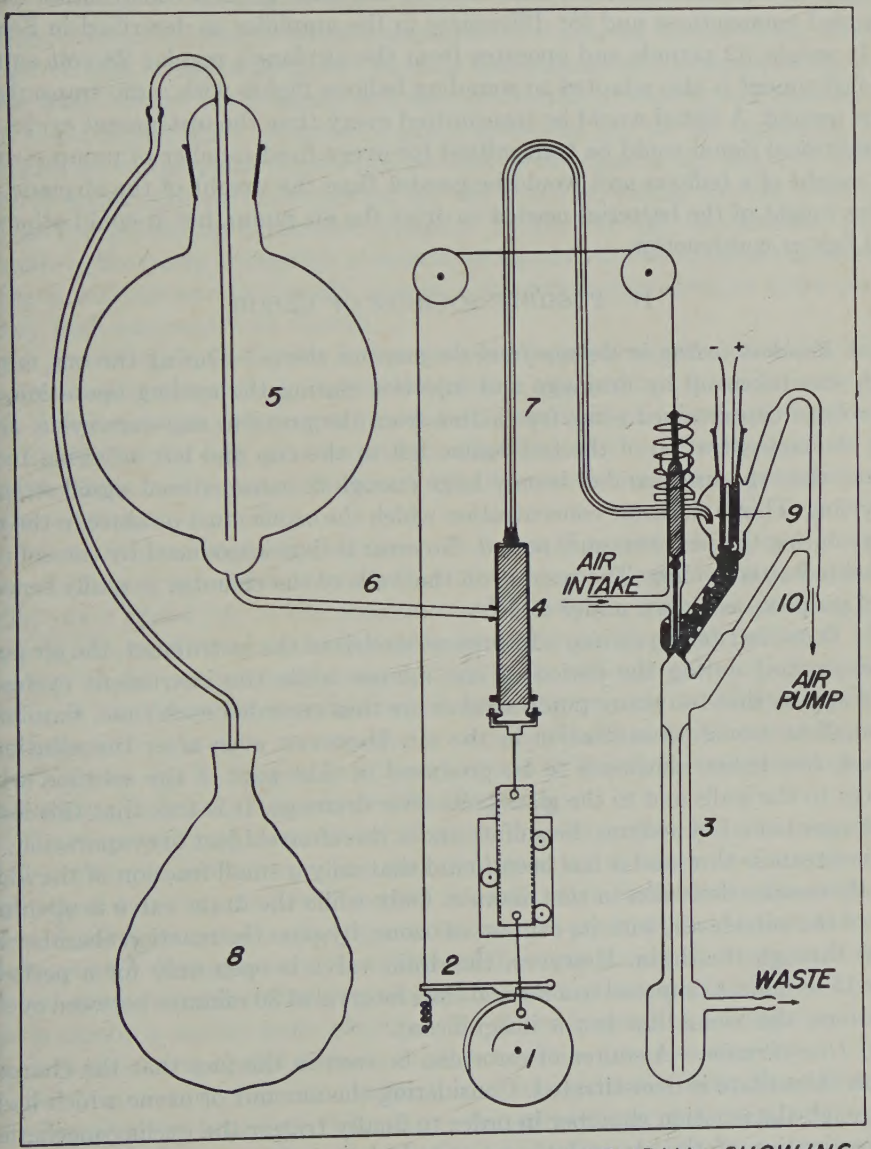

FIG. 2—COMPLETE MECHANICAL ASSEMBLY, SHOWING PROVISIONS FOR INJECTION AND DRAINAGE

The equipment shown in Figure 2 is normally mounted inside a temperature-nsulated box measuring 2 × 2 × 4 feet in the case of stationary installations. The box is electrostatically shielded and also contains the amplifier with its bat-

teries. The stationary instruments are designed to operate entirely from lead stor batteries where commercial power is not available. At present, five 6-volt batte of 125 amp-hr capacity and some dry batteries for the amplifier operate the ent equipment for one week without attendance.

One airborne unit has been built. It is of the same general construction exc for added compactness and for differences in the amplifier as described in Sect VI. It weighs 32 pounds and operates from the airplane's regular 28-volt supp The instrument is also adapted to sounding balloon flights with radio transmiss to the ground. A signal would be transmitted every time the instrument cycles a an additional signal could be transmitted for every fixed number of pump strok The weight of a balloon unit would be greater than the weight of the airplane u by the weight of the batteries needed to drive the air pump, but it could otherw be of lighter construction.

IV—POSSIBLE SOURCES OF ERROR

(*a*) *Residual iodine in the cup from the previous charge*—During the one min which was taken up by drainage and injection during the cycling operation, electrolytic cup retained some free iodine from the previous exposure cycle. H ever, the concentration of the free iodine left in the cup and left adhering to walls of the exposure chamber is only large enough to cause critical signal stren for cycling. This is the same concentration which the ozone must produce in the n charge during the next exposure period. No error is thus introduced by the solut left behind after cycling. The residue on the walls of the chamber actually serv useful purpose, as shown under (*b*).

(*b*) *Ozone lost during cycling*—In present models of the instrument, the air pu is not stopped during the period of one minute while the instrument cycles. would appear that too many pump strokes are thus recorded each time, simulat too small an ozone concentration in the air. However, even after the solutio drained, free iodine continues to be produced in that part of the solution wh adhered to the walls and to the glass balls after drainage. It is true that this io is no longer bound by sodium thiosulfate and is therefore subject to evaporation, the air stream is slow and it has been found that only a small fraction of the io actually escapes detection in this manner. Only while the drain valve is open n some of the outside air, with its content of ozone, by-pass the reaction chamber escape through the drain. However, the drain valve is open only for a perio about 15 seconds. Compared to a normal time interval of 30 minutes between cyc operations, the ozone thus lost is insignificant.

(*c*) *Over-titration*—A source of error can be seen in the fact that the charg sodium thiosulfate is over-titrated. Considering the amount of ozone which ha go through the reaction chamber in order to finally trigger the cycling mechan an examination of the electrolytic current during the exposure cycle shows roughly 90 per cent is used to bind the sodium thiosulfate in the charge and 10 per cent to produce the free iodine necessary for cycling.* The number of p

*These percentages depend on the amount of sodium thiosulfate in the charge. The fi apply to the sodium thiosulfate concentration given above.

okes needed for cycling thus appears too large by 10 per cent. This percentage mains the same for all ozone concentrations. The only rare occasion when this ror cannot be easily corrected for occurs when the ozone concentration is under- ing a very rapid change during one exposure period.

(*d*) *Changes in temperature and pressure*—The equipment counts, in effect, the mber of ozone molecules which is contained in a metered volume of air; however, e air volume is measured at the variable temperature and pressure of the pump. the temperature of the pump and the atmospheric pressure were constant, the ta could immediately be given in ozone molecules per 10^8 air molecules. If the mperature of the pump were equal to that of the outside air, the data could be ven in terms of ozone molecules per cm^3 air at the prevailing outside temperature id at the prevailing barometric pressure. In general, the temperature and the essure in the pump are neither constant nor equal to the temperature and pressure the outside air and this would require a correction amounting to a few per cent very high accuracy were desired.

(*e*) *Sensitivity to gases other than ozone*—Hydrogen peroxide and oxides of nitro- en are possible atmospheric constituents which may produce free iodine in a potas- um iodide solution. Hydrogen peroxide, however, if at all present in the lower mosphere, reacts only at a very slow rate with a two per cent potassium iodide olution [10]. As is shown in Section V (*b*), the reaction produced by ozone is very st and efficient.

Atmospheric nitrogen dioxide has been reported as present [15] in a concentra- on which is of the same order as that of ozone. At times, acetate or phosphate uffers were added [16] to the potassium iodide solution with the intention of sup- ressing the reaction of nitrogen oxides. However, as shown in Section V (*c*), the esponse of the present instrument to NO_2 has an efficiency of only five per cent. ection V (*d*) describes a method which makes it possible to distinguish between tmospheric NO_2 and O_3 on occasions when this should be found necessary.

(*f*) *Errors due to evaporation*—Water as well as free iodine may evaporate from ne solution during its exposure to the air stream.

The evaporation of water would affect the measurement only if the *concentration* the produced iodine were the quantity from which ozone is determined. The ddition of a known amount of sodium thiosulfate which binds the free iodine until ne end-point is reached, eliminates this source of error. It is true that the volume the charge decreases somewhat due to the evaporation of water and that the itical signal strength is therefore reached with somewhat less free iodine. However, his is clearly a second-order effect; at the slow air speed of 1.5 liters per minute, ne amount of evaporated water is small even when the air is very dry.

The evaporation of the free iodine during its production does not enter because is immediately bound to the sodium thiosulfate, except for the small amount hich is needed beyond the end-point of the titration in order to cause the instru- ent to cycle. The tests reported in Section V (*e*) show that the addition of sodium iosulfate does not interfere with the original reaction between ozone and potas- um iodide.

(*g*) *Significance of errors*—In view of the usually very large fluctuations of tmospheric ozone, errors up to five per cent do not need to be corrected for. The

changes of temperature and pressure in the air pump may result in a fluctuat error approaching five per cent. In the case of routine recordings, it is justifie omit corrections except for the error due to over-titration as outlined under (*c*).

V—TESTS PERTAINING TO THE CHEMICAL REACTION

(*a*) *Artificially ozonized air*—For the purposes of the tests described belo was found convenient to produce small artificial ozone concentrations in the labo tory rather than to use the highly variable atmospheric ozone.

Ozone was first removed from a stream of outside air (1.5 liters per minute) letting it pass through one meter of glass tubing (2 cm diameter) upon whic heating spiral was wound. The air stream was heated to 220°C while passing throu the tube. This removed all ozone from the air as shown by measurements with ozone recorder. Very small amounts of ozone were then added to this de-ozoni air by adding a slow (0.18 liter per minute) stream of slightly ozonized oxygen. T oxygen was ozonized by exposing it, in a quartz tube, to ultra-violet light fro Hanovia SC-2537 quartz lamp. By means of a constant voltage transformer, intensity of the quartz lamp was kept constant. This air stream with an " mospheric" ozone concentration was used for all purposes of testing. The respo of the ozone recorder to this air stream was reproducible to within three per ce

(*b*) *Test for residual ozone*—A second reaction column was connected in se with the ozone recorder to test the air which had passed through the instrument residual ozone and which might not have reacted in the chamber. The result negative, indicating that the geometry of the reaction chamber is fully efficient an air flow of 1.5 liters per minute.

(*c*) *Test for sensitivity to nitrogen dioxide*—Known amounts of NO_2 , the o oxide of nitrogen assumed to be present in the lower atmosphere [13], were added a de-ozonized air stream in order to determine if the ozone recorder reacts quanti tively to NO_2 .

The small concentration of NO_2 which was needed for this experiment was p duced by heating a known amount of $Pb(NO_3)_2$ under vacuum in a 5-liter fl Air was then admitted and a small sample of the 5-liter mixture was extracted means of a glass syringe. The content of this syringe was then added to the de-oz ized air stream by advancing the piston slowly with a motor drive at a known r

It was found that the amount of NO_2 which had to be added in order to obt a given response from the ozone recorder was roughly twenty times as large as amount which should have been needed if the recorder had been fully effici This indicates that the ozone recorder has an efficiency of only about five per c for the detection of NO_2 .

(*d*) *Discrimination against* NO_2 *in the atmosphere by means of heating*—It shown under (*a*) that ozone is destroyed quantitatively and promptly when hea to 220°C. If NO_2 is not destroyed by the same heating process, a test can be formed during atmospheric ozone recordings as a matter of routine. If heating air stream to 220°C makes the response of the ozone recorder go to zero, the sponse is due to ozone alone.

In order to make sure that NO_2 is not affected at a temperature of 220° de-ozonized air stream with an added amount of NO_2 was heated to this temp

re. For the purpose of this test, NO_2 was added to the air in sufficient quantity to tain a satisfactory response from the ozone recorder before the heater was turned . The response of the ozone recorder persisted quantitatively after the heater was rned on, indicating that NO_2 was not destroyed during the heating process and at such a heating test can be used to distinguish between atmospheric ozone and O_2.

(*e*) *The addition of sodium thiosulfate to the potassium iodide solution*—It was ecessary to show that the addition of sodium thiosulfate to the potassium iodide lution does not modify the production of free iodine according to the formula ven in Section II. This is reportedly the case [10], but a new check was made by nalyzing the artificially ozonized air stream with the manual potassium iodide ethod [10]. This older method can be used without the addition of sodium thiolfate under certain conditions. Air from the same stream was aspirated through ne ozone recorder with the result that the response of the recorder agreed quantitively.

(*f*) *Absolute calibration for ozone*—No direct comparison of this chemical method gainst the spectrographic method has been made as yet. However, the average of he measured ozone concentrations agrees with other chemical measurements and ith other spectrographic determinations. A comparison with simultaneous spectroraphic measurements is being prepared.

VI—AMPLIFIER AND RECORDER

(*a*) *The amplifier for stationary installations*—Figure 3 shows the amplifier which s used in stationary installations for ozone recording. This is a battery-operated, alvanometer-controlled d.c. amplifier with inverse feed-back. The current from the lectrolytic cup passes through the mirror galvanometer *G*, but it is almost entirely ompensated by a current from the amplifier tube as a result of the illumination of he differential photoelectric cell. Part of the current through the amplifier tube oes through the one-ohm resistor. Since the one-ohm resistor is shunted by a 100 -resistor in series with the galvanometer, the current through the one-ohm esistor and through the cycling relay in series with it is larger than the feed-back urrent through the galvanometer by a factor of 10^5. The relay is made to respond t 2×10^{-4} ampere. Using this amplifier, the critical current through the electrotic cup is thus 2×10^{-9} ampere.

(*b*) *The amplifier for portable installations*—Figure 4 shows the amplifier develped for airplane and balloon installations where vibrations and accelerations prelude the use of the simple galvanometer amplifier. The d.c. signal from the lectrolytic cup is converted into an a.c. signal by means of a Brown converter.* he a.c. signal is amplified by means of three pentode stages and, after rectification ith a 1N34 germanium diode, by a d.c. power stage. The vibrating reed of the rown converter is driven from the contacts of a commercial 6-volt vibrator modied to operate at 58 c.p.s.

This amplifier is adjusted to trigger the cycling relay at an input current of 10^{-9} mpere from the electrolytic cup and operates with a high degree of stability.

*The Brown converter is manufactured by the Brown Instrument Company, Philadelphia 44, ennsylvania.

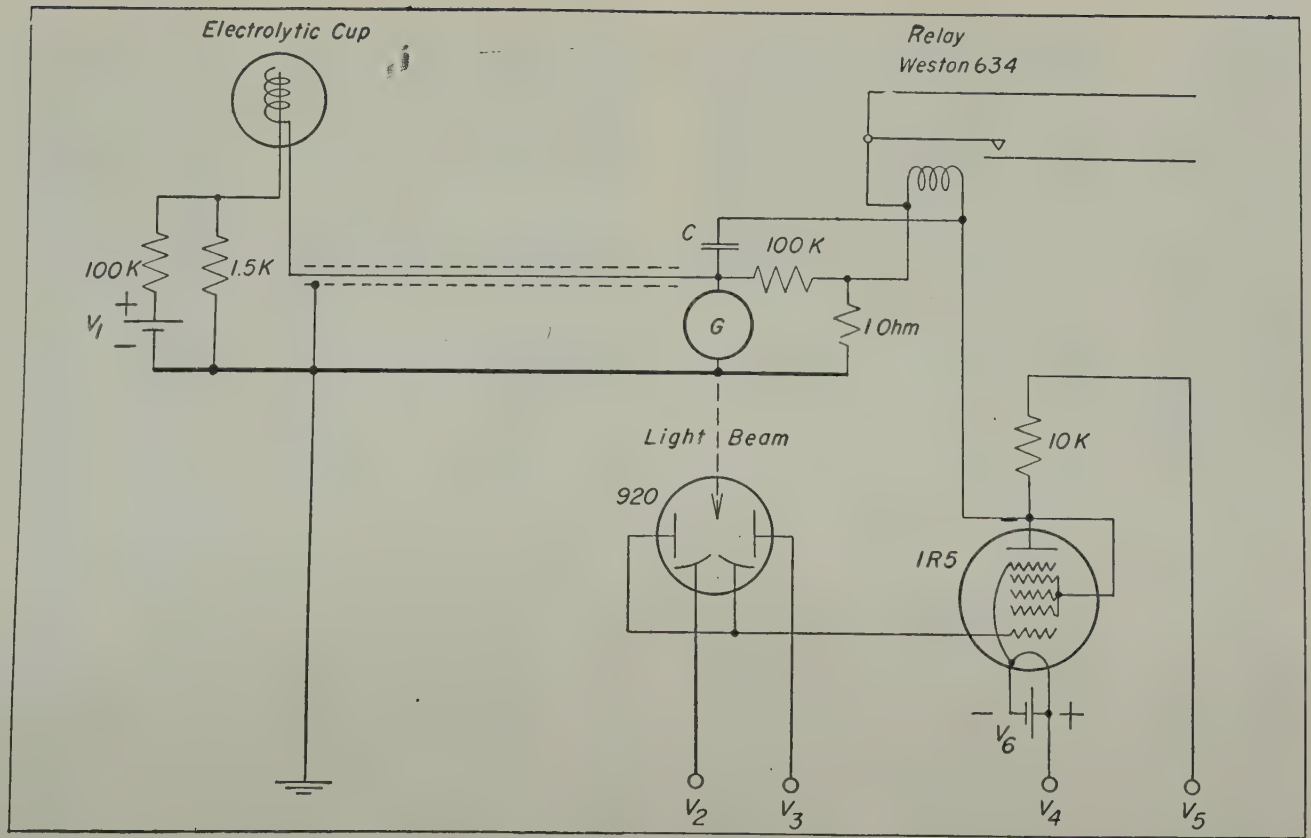

FIG. 3—AMPLIFIER FOR STATIONARY INSTALLATIONS (C, 0.005 MICROFARAD ANTI-HUNT CAPACITOR; G, GALVANOMETER—RUBICON TYPE 3406 HA, MODIFIED; V_1, 1.5 VOLTS; V_2, -90 TO -112.5 VOLTS FOR ZERO ADJUSTMENT; V_3, -45 VOLTS; V_4, -67.5 VOLTS; V_5;

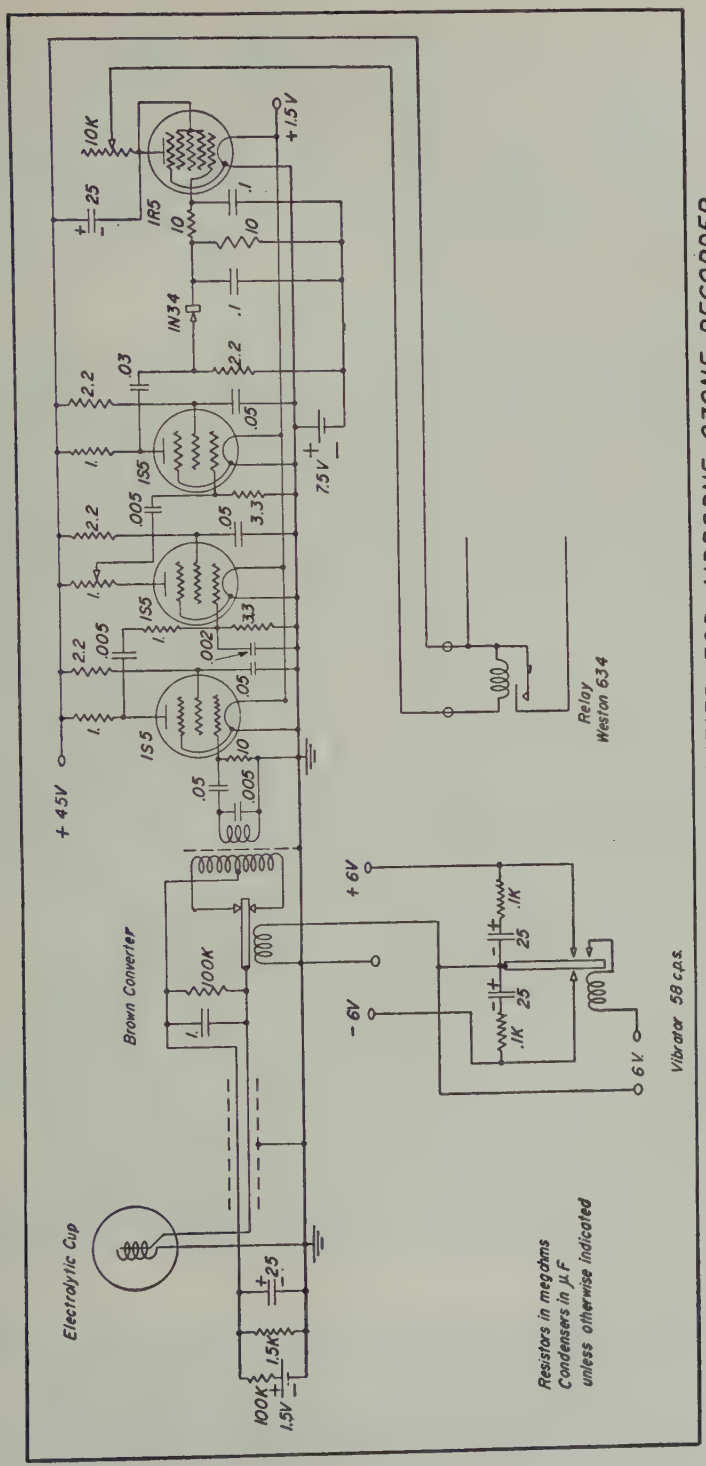

FIG. 4—BROWN CONVERTER AMPLIFIER FOR AIRBORNE OZONE RECORDER

(c) *Associated circuits*—The cycling relay drives a power relay which starts t syringe motor on its one-minute run for drainage of the old charge and injection o new one. This motor shuts itself off after one revolution, provided that the origin signal from the electrolytic cup has disappeared after one minute. This conditio is not always fulfilled because the cathode must be given time to again becom polarized after the free iodine has been removed from the cup. A time-delay circu is therefore provided to prevent the syringe motor from starting on a new run for period of two minutes after the beginning of the cycling operation.

Another auxiliary circuit provides for the recording of the number of strokes

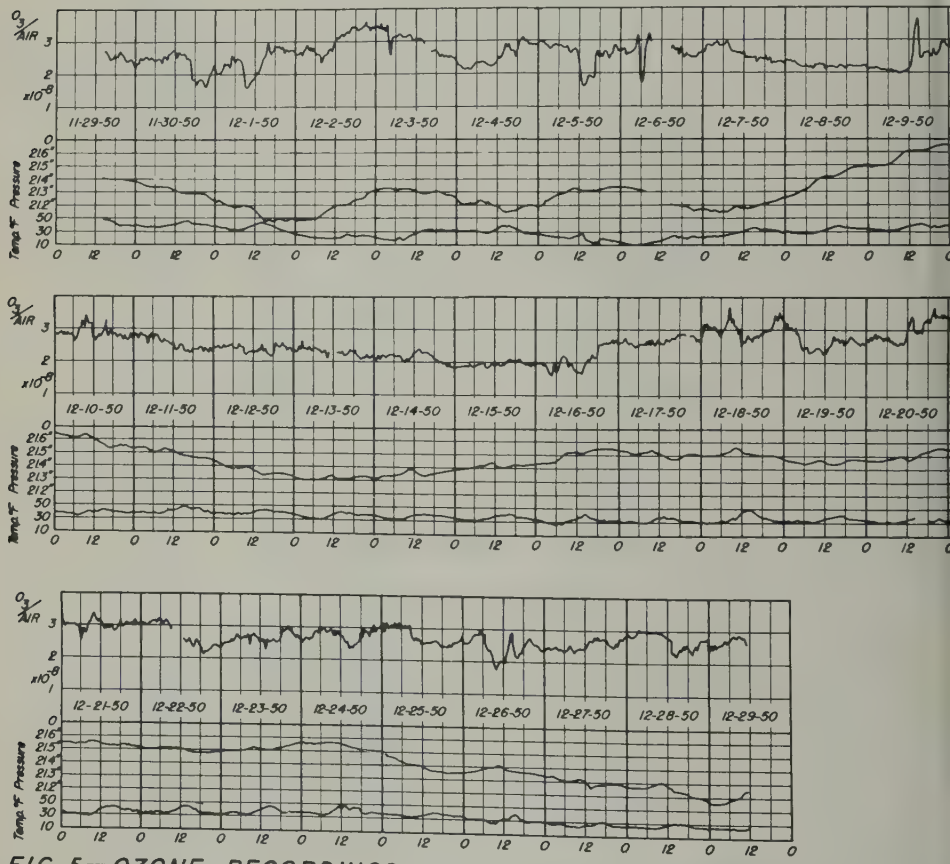

FIG. 5—OZONE RECORDINGS WITH STATION PRESSURE AND TEMPERATURE AT SOUTH CAPILLO PEAK, N.M. (ELEVATION 9200 FEET

the air pump which has occurred between cycling operations and for the simu taneous recording of the atmospheric pressure, outside air temperature, and tim

VII—PRELIMINARY AUTOMATIC OZONE RECORDINGS

Preliminary automatic ozone recordings were made at the Physics Departme of the University of New Mexico at Albuquerque, at South Capillo Peak (elevatio

00 feet), 29 miles south-southeast of Albuquerque, and at Acomita C.A.A. Air-rt, 62 miles west of Albuquerque.

Figure 5 shows ozone recordings from Capillo Peak covering the 30-day period m November 29 to December 29, 1950. The ozone record is given in terms of the io of molecules, ozone to air. It has an average resolution of 30 minutes and an curacy of ±5 per cent for each individual recorded value.* The chart also shows e atmospheric pressure as recorded at the same location, and the outside air mperature.

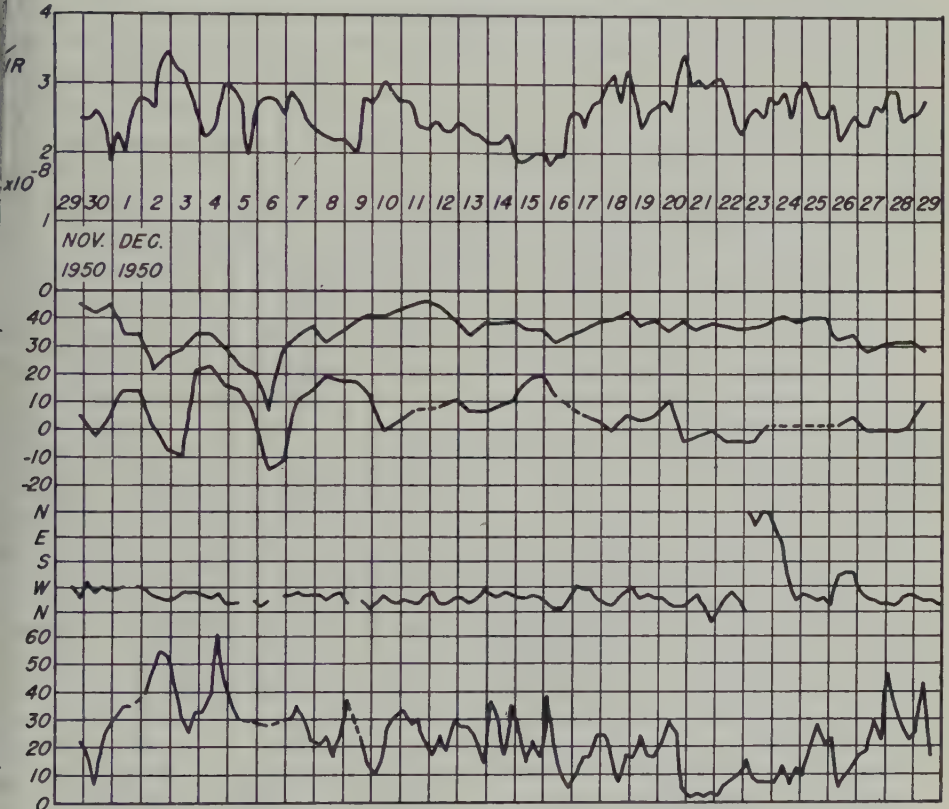

FIG. 6—OZONE RECORDINGS AT SOUTH CAPILLO PEAK, N.M. (THE TEMPERATURE AND DEW-POINT VALUES ARE WEATHER BUREAU RADIOSONDE DATA FOR 9200 FEET OVER ALBUQUERQUE; THE WIND DATA REFER TO THE 9000-FOOT LEVEL, ALSO FROM WEATHER BUREAU RECORDS AT ALBUQUERQUE)

Figure 6 shows six-hourly averages as computed from the ozone data shown in gure 5. The averages are centered at 3 and 9 o'clock every forenoon and afternoon. his chart also shows temperature and dew-point recordings taken at 9,200 feet ith radiosondes by the United States Weather Bureau at Albuquerque (elevation

*A constant correction of −10 per cent was applied to account for over-titration.

5,300 feet); these radiosonde observations are made daily at 8 a.m. and at 8 p.
Also shown in Figure 6 are the winds at the 9,000-foot level above Albuquerque; t
wind data are obtained daily at 2 a.m., 8 a.m., 2 p.m., and 8 p.m.

The material shown in Figures 5 and 6 has been studied in a tentative fashi
with regard to frontal passages at the Capillo Peak station. For this purpose, t
daily 700-mb charts published by the United States Weather Bureau were co
sulted.

Two well-defined cold fronts passed the station during the 30 days. They a
proached from the northwest and carried maritime-polar air. The pressure troug
passed the station at 3 p.m. on December 1, and at 3 p.m. on December 4. T
ozone readings began to rise at 9 a.m. on December 1, and at 3 a.m. on December

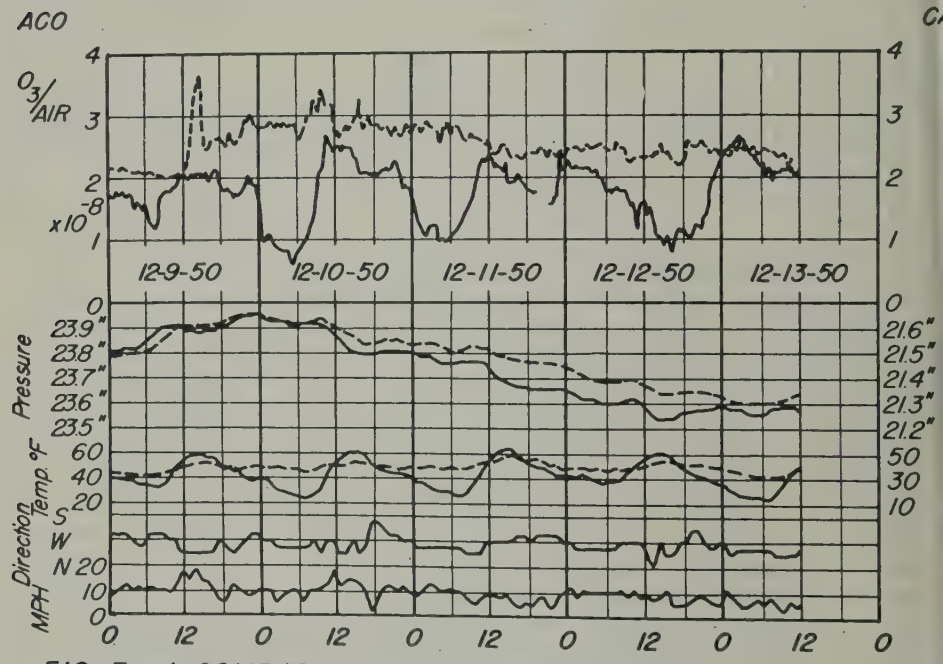

FIG. 7—A COMPARISON OF OZONE RECORDINGS FROM TWO WIDELY-SEPARATED STATIONS, CAPILLO PEAK, N.M. (CAP---) AND ACOMITA C.A.A. AIRPORT, N.M. (ACO ——)

The sudden ozone decrease on December 5 was probably caused by local precipi
tion; precipitation was not recorded but the relative humidity was 100 per cent
the afternoon of December 5.

The 700-mb charts show a warm front backing into New Mexico from the e
on December 6 and later moving out eastward again. The temperature drop a
rise accompanying this process can be seen on the records; the ozone concentrati
shows a relatively slow decrease from December 7 to December 9.

The general rise in the ozone concentration on December 9 was not accompan
by a frontal passage but by the beginning of a sharp drop in dew point. Subst

lly the same process occurred on December 16. From December 10 to December the air gradually became more moist while the ozone concentration decreased. From December 16 through December 25, the air was generally warm and dry. nigh pressure region southwest of the station dominated the circulation pattern. definite trend is shown by the ozone concentration and by the meteorological ta for the rest of the period.

In accordance with the well-established increase of the total thickness of the one layer upon influx of a polar air mass, the present data seem to indicate that rich in ozone can be brought to the earth's surface by advection from northern itudes or by subsidence of air under the influence of a high pressure area. The any short-term fluctuations of the ozone concentration shown in Figures 5 and 6 ve not yet been analyzed.

Figure 7 shows simultaneous ozone recordings from Capillo Peak and from comita Airport, covering the period from December 9 to December 13, 1950. The apillo Peak station is located on a rather exposed ridge at an elevation of 9,200 feet d some 4,000 feet above comparatively flat lands. The Acomita station, while a few ndred feet above the bottom of a valley, is at an elevation of 6,500 feet, sur-unded to the south, west, and north by mountain peaks ranging from 8,000 to ,000 feet in elevation. This station, near the Continental Divide, is located proximately 70 miles to the west of Capillo Peak. Figure 7 also shows the respec-ve station pressures and temperatures, as well as the wind for the Acomita station.

It is immediately apparent that the ozone concentration at Acomita, together th the local temperature, is subject to strong daily fluctuations, while such ctuations are quite absent at Capillo Peak. On the other hand, the ozone con-ntration at Acomita comes close to the concentration at Capillo at least once ring every day of the period. It can be inferred from the temperature record at comita that there is normally a pronounced temperature inversion at this valley cation during the early part of the day.* During the life of such an inversion, the one flux to the ground due to normal tropospheric agitation is intercepted and the one disappears near the ground due to its chemical activity. This confirms earlier dings [17] and furnishes additional evidence in favor of the view that the at-ospheric ozone near the earth's surface originates in the stratosphere.

These investigations are being continued and a detailed study of the results of ture work shall be published at a later date.

VIII—ACKNOWLEDGMENTS

The authors wish to acknowledge the aid which they have received from the embers of the Physics Department of the University of New Mexico, especially om Hyman Adler, John G. Breiland, Dorothy Capes, Raymond Jenness, and hn W. McLean.

This work has been supported by Air Force Cambridge Research Laboratories, M.C., under Contracts W28-099-ac-379 and AF 19(122)-381.

*Ozone and temperature records similar to those from Acomita are usually obtained at the iversity of New Mexico in Albuquerque, also a valley location.

References

[1] For a summary, see F. W. P. Götz, Ergebn. Kosm. Physik, **3**, 306 (1938), and S. K. Mi The Upper Atmosphere, Royal Asiatic Society of Bengal, Calcutta (1948). For a re theoretical treatment, see H. U. Dütsch, Dissertation, Zurich University, Switzerl (1946).

[2] According to G. M. B. Dobson, Bakerian Lecture, Proc. R. Soc., A, **185**, 144 (1946), *total thickness* of the atmospheric ozone layer shows a marked increase during a thun storm. It remains to be seen whether this is due to ozone production by electrical charges or due to increased mechanical transport of stratospheric ozone. Present m surements with the equipment described in this paper show no increase of the *l* ozone concentration due to atmospheric electrical discharges.

[3] S. Chapman, Zs. Geophysik **12**, 377 (1936); V. H. Regener, Zs. Physik, **109**, 642 (193

[4] P. S. Epstein, Gerland's Beitr. Geophysik, **35**, 153 (1932).

[5] E. Regener, Forschungs- und Erfahrungsberichte des Reichswetterdienstes (194 reprinted in "Ozon," Berichte des Deutschen Wetterdienstes in der U. S. Zone, No. p. 47 (1949), Bad Kissingen, Germany. This publication shall be referred to as *Gern Ozone Report* in further citations below.

[6] S. Chapman, Zs. Geophysik, **12**, 377 (1936).

[7] R. Auer, Gerland's Beitr. Geophysik, **54**, 137 (1939).

[8] A. and H. Ehmert, Forschungs- und Erfahrungsberichte des Reichswetterdienstes (194 reprinted in *German Ozone Report*—see ref. [5], p. 58; A. Ehmert, Lecture in Thara (1944); reprinted in *German Ozone Report*, p. 26; A. Ehmert, Forschungs- und Erf rungsberichte des Reichswetterdienstes (1941); reprinted in *German Ozone Rep* p. 63.

[9] V. H. Regener, Nature, **167**, 276 (1951). This is a preliminary report on recent ball measurements of the vertical ozone distribution over New Mexico.

[10] V. H. Regener, Met. Zs., **55**, 459 (1938).

[11] There are potassium iodide methods other than that quoted in ref. [10] which, e though more elaborate, operate with sufficient speed to measure (not automatica the time variations of surface ozone: H. Cauer, Zs. anal. Chemie, **103**, 166, 321, (1935); Y. Dorta-Schaeppi, and W. D. Treadwell, Helv. Chim. Acta, **32**, 356 (194 also see ref. [13]. The automatic method by Dirnagl, Bull. Amer. Met. Soc., **30**, (1949), uses KI-starch paper in equipment of commercial manufacture which has been described in detail; the apparatus records the total oxidizing power of the air bioclimatic purposes. The method by Dauvillier, J. Physique, **5**, 454 (1934), u sodium arsenite and needs such a large air volume that only daily averages of ozo not short-period changes, can be measured.

[12] A. Ehmert, Zs. Naturf., **4b**, 321 (1949).

[13] E. Gluckauf, H. G. Heal, G. R. Martin, and F. A. Paneth, J. Chem. Soc., p. 1 (1944

[14] Foulk and Bawden, J. Amer. Chem. Soc., **48**, 2045 (1926). Another interpretation ca found in ref. [12].

[15] F. A. Paneth and J. S. Edgar, Nature, **142**, 112 (1938).

[16] Gluckauf, *et al.*, ref. [13]; H. Cauer, ref. [11].

[17] R. Auer, l.c.; A. and H. Ehmert, *German Ozone Report*, p. 58.

ON THE DIURNAL VARIATION OF [OI] 5577 IN THE NIGHTGLOW

BY F. E. ROACH AND HELEN B. PETTIT

United States Naval Ordnance Test Station,
Pasadena and China Lake, California

(Received May 7, 1951)

ABSTRACT

Observations in the Mojave Desert of the diurnal variations of the zenith intensity of the forbidden oxygen line at 5577 Å for ten nights over a two-year interval are recorded. In general, a maximum of intensity occurs at local midnight, ±2.5 hours. A detailed study of one night is reported wherein the diurnal variation of regions of the sky other than the zenith are shown to follow time patterns similar in general but with significant variations in detail. The intensity changes of various parts of the sky are interpreted as geographical variations of local zenith intensity. Isophotal plots of these geographical variations throughout the night indicate the presence of definite patterns in the upper atmosphere. During the post-twilight period, an enhancement of intensity is observed in the western sky. In the predawn observations, no enhancement is noted in the eastern sky. Between the post-twilight and predawn, the intensity goes through a maximum which is partially localized to the north of our station. Evidence is presented which indicates that the over-all intensity change can be described as a fixed excitation pattern on the dark side of the earth through which a given observer seems to move with the rotation of the earth. The character of the pattern seems to change with the season. The variation of intensity with zenith distance for the whole night indicates an effective height of emission of 250 km.

I—INTRODUCTION

Many investigators [see 1 to 15 of "References" at end of paper] have reported hat the intensity of the green nightglow* line at 5577 Å has a maximum near the bserver's local midnight. The radiation results from a forbidden ($^1S_0 - {}^1D_2$) ransition of the oxygen atom in the earth's upper atmosphere. We have observed

*The general term "airglow" is used for radiations originating in the upper atmosphere. We se the term "nightglow" to connote airglow at night to distinguish it from similar radiations hich may be present (though not observable) in the daytime.

this radiation systematically over a period of more than two years. In Figures and 2 we show plots of the variation of the zenith intensity of 5577 with time f a number of nights at Cactus Peak, California (latitude 36° 04′ 41″ north, longitud 117° 48′ 54″ west, altitude 5,415 feet). The following statements can be made the basis of an inspection of the plots:

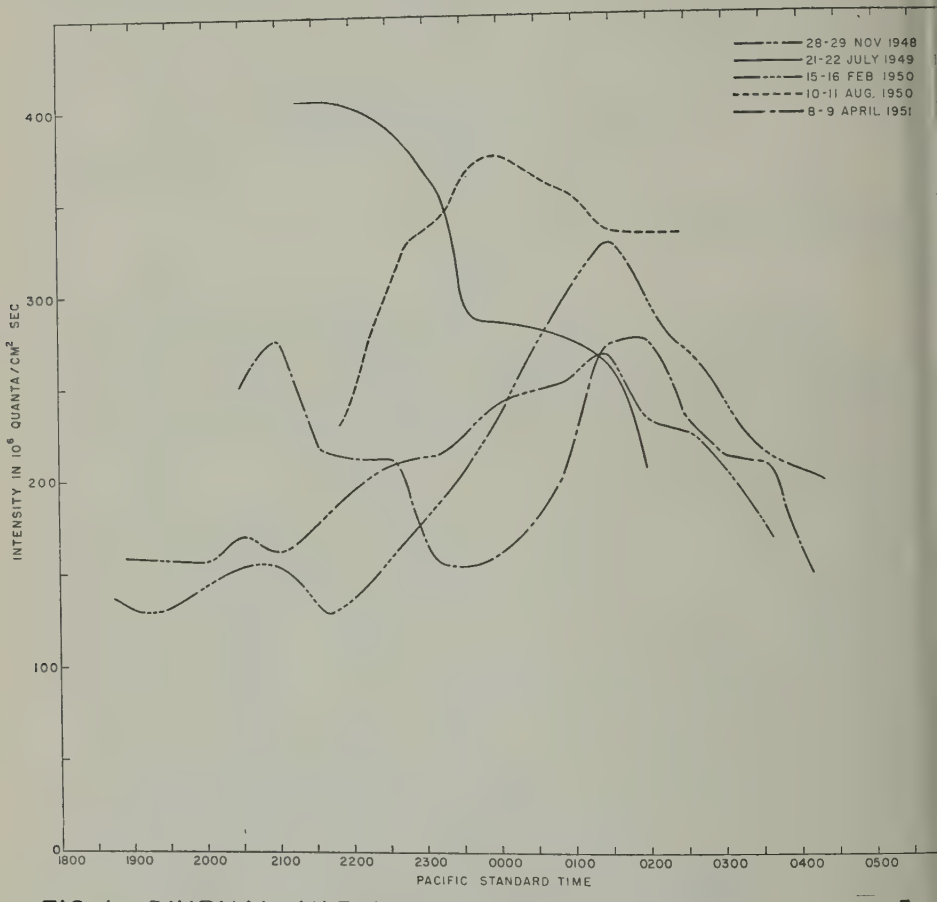

FIG. 1—DIURNAL VARIATION OF ZENITH INTENSITY OF [O
5577 AT CACTUS PEAK

(1) Without exception a maximum is observed.

(2) There is a considerable range in the time of maximum from P $21^h\ 30^m$ to PST $02^h\ 30^m$.

(3) The absolute value of the maximum ranges from 2.5×10^8 4.5×10^8 quanta/cm^2 column·sec.

(4) There is a suggestion of a seasonal variation in the time of maximu In the summer the maximum occurs before midnight and in the wi after midnight.

(5) In most cases there is an initial decline in intensity.

(6) Occasionally more than one maximum is observed.

The purpose of the present paper is to give a detailed analysis of one night nuary 6/7, 1951) during which we observed the entire sky systematically from ronomical twilight to astronomical dawn. It is thus possible to compare the rnal variation in the zenith at Cactus Peak with other parts of the sky. The l product of the investigation is a series of isophote maps of the sky throughout

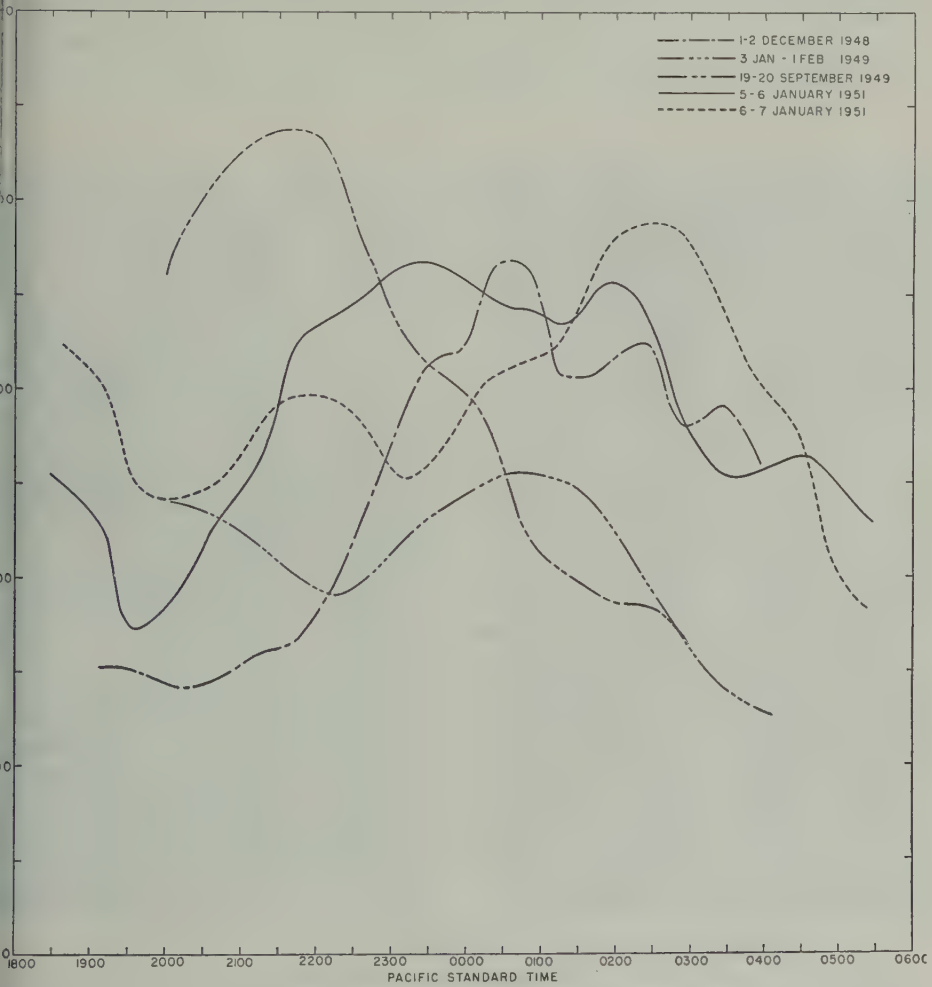

IG. 2—DIURNAL VARIATION OF ZENITH INTENSITY OF [OI] 5577 AT CACTUS PEAK

night in which the intensities are reduced to the local zenith intensity on a graphical basis. A sizable portion of the earth's surface is included in the maps, ce a low altitude observation from a given point on the earth's surface cuts the th's upper atmosphere in a region many hundreds of kilometers away from the erver. The diurnal variation in the zenith at Cactus Peak can thus be correlated h similar variations at other locations over the earth's surface in the vicinity outhwestern United States.

II—INSTRUMENTATION

Prior to January 1951, we used a two-color photometer [16]. Two interferen filters were employed, one of which included the radiation 5577 Å near its peak transmission and the other of which centered at 5200 Å and excluded 5577. T 5200 filter was used as a control. Suitable stellar calibrations were obtained, maki it possible to subtract the effect of the general radiation from stars and zodiac light from the 5577 readings [17]. In January of 1951, we put into operation Cactus Peak a new photometer capable of recording continuously in four colo as the sky was being systematically surveyed. The general construction of t

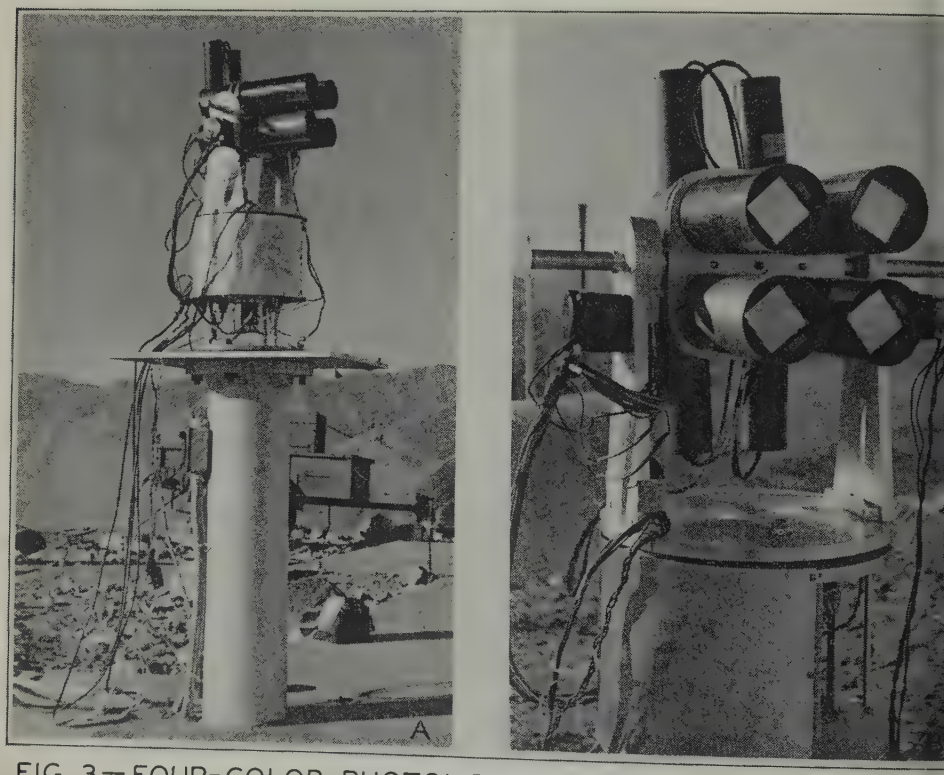

FIG. 3—FOUR-COLOR PHOTOMETER AT CACTUS PEAK: IN THE BACKGROUND OF FIGURE 3A ARE SEEN THE SIERRA NEVADA MOUNTAINS; IN FIGURE 3B THE FOUR INTERFERENCE FILTERS CAN BE SEEN IN FRONT OF THE TELESCOPE OBJECTIVES; PERMANENT HOUSING AND CONDUIT FOR THE CONTROL CABLES HAVE BEEN CONSTRUCTED SINCE THESE PHOTOGRAPHS WERE MADE

instrument is apparent from an inspection of Figure 3. A brief description of th instrument follows. A detailed description will appear elsewhere.

Optical design—There are four separate telescopes. The objective lens of eac is of 2.75-inch aperture and 9.3-inch focal length. A field lens (0.9-inch apertur

ɔuses the objective on the cathode of a 1P21 photomultiplier. The sky included a circular field 5.°0 in diameter.

The amplifiers—The potentials on the nine dynodes of the photomultiplier tube crease in steps of about 110 volts per dynode. A selector switch permits the

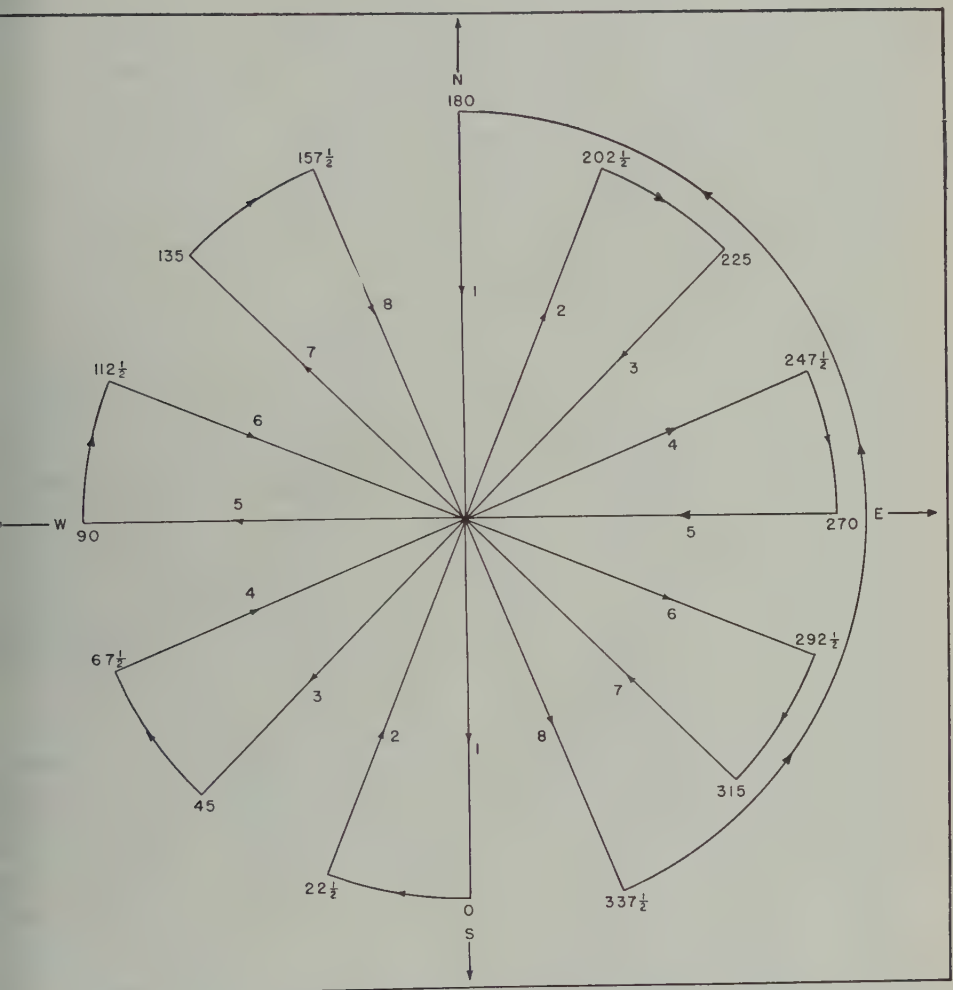

FIG. 4—CLOCK DIAGRAM SHOWING PATTERN OF SKY COVERAGE IN A COMPLETE SURVEY; EACH SWEEP FROM HORIZON TO HORIZON REQUIRES FOUR MINUTES; THE ENTIRE SURVEY REQUIRES 32 MINUTES

hoice of one of eleven load resistors for variation of the sensitivity level. The IR rop in the load resistor is applied to the grid of the first tube of a four-stage direct-urrent negative feed-back amplifier. Each photometer has a separate amplifier.

The power supply—The following voltages are furnished by a common power upply:

1,000 volts d.c. for the nine stages of the photomultiplier
+250 volts d.c.
− 90 volts d.c. } for the amplifiers
6 volts a.c. for the heaters of all vacuum tubes

The control panel—The instrument is controlled in the observing shelter, abo 100 feet from the photometer. A selector switch permits the operator to set up program of (*a*) monitoring one region of the sky, (*b*) sweeping the sky in a fix vertical circle, or (*c*) covering the entire sky in a series of eight sweeps called survey. The orientation of the photometers is indicated on the control panel synchros linked to the altitude and azimuth axes of the photometer mount.

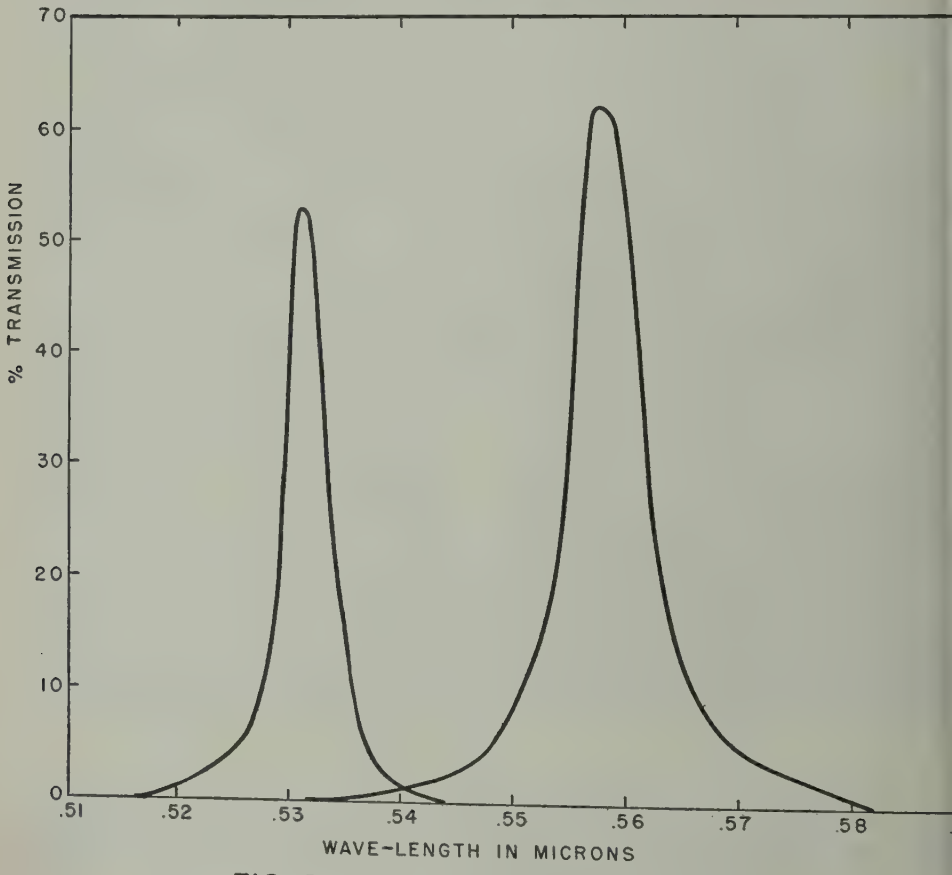

FIG. 5—FILTER TRANSMISSIONS

The recorders—Four model A.W. 0 to 1 ma Esterline-Angus recorders a driven in tandem by a single synchronous motor mounted externally to one.

III—THE OBSERVATIONS

For the night under detailed analysis in this paper (January 6/7, 1951), t observations continued in four colors throughout the night from astronomic

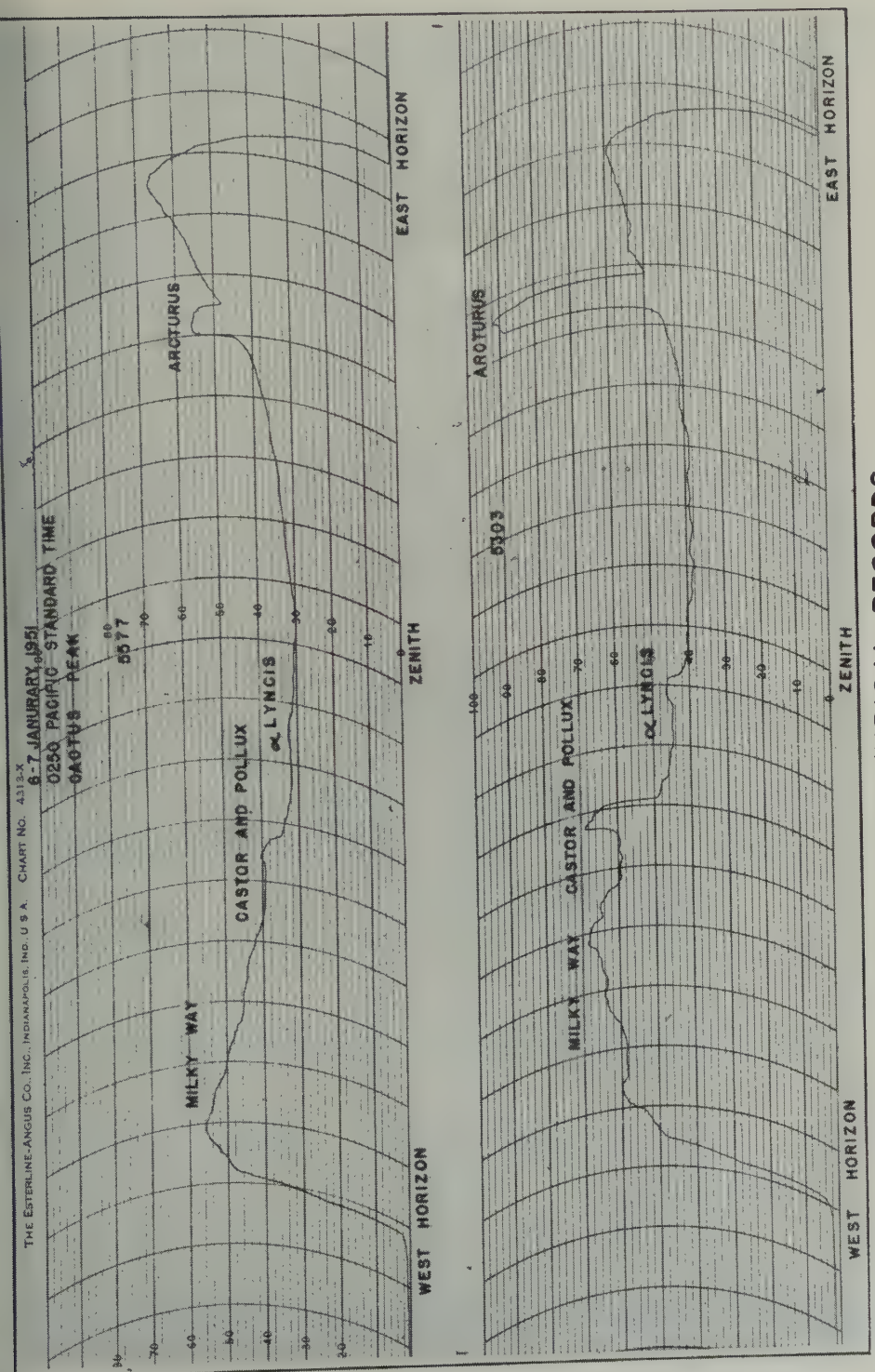

FIG. 6—TYPICAL RECORDS

twilight to astronomical dawn. In all, there were 20 surveys of the sky following the pattern illustrated in Figure 4. The atmospheric transparency was excellent to the visible horizon. The two filters* involved in this study have the characteristics shown in Table 1 and Figure 5.

TABLE 1—*Filter characteristics*

Filter No.	Peak wavelength	Peak transmission	Total integrated transmission (equivalent Ångstroms)
7-3582-5	5303	0.53	28.4
7-3470-3	5577	0.62	56.8

In the present report we include a discussion of results obtained with the 5577 filter, using the 5300 filter as a control for evaluating the intensity of the background radiation. Reports of a similar nature covering an analysis of data obtained simultaneously with the other two filters centering on NaI 5893 and [OI] 6300 will appear later. Typical tracings are shown in Figure 6.

IV—THE REDUCTION OF THE OBSERVATIONS

The most difficult part of the analysis is the evaluation of the background radiation which, in large part, is of non-atmospheric origin (integrated star light and zodiacal light). From the last column of Table 1, it is seen that our filters correspond to a band of complete transmission about 30 to 50 Ångstroms wide. Thus our photometer corresponds to a spectrograph with a wide slit opening.**

That there is a very significant amount of background light through the filters used is evident from the sensible deflections obtained with the 5303 filter which includes no upper atmosphere radiations comparable in intensity with 5577. In Figure 7 is shown a plot of the sweeps illustrated in Figure 5, with the ordinate in 10 mag. (visual) GO stars per square degree. The integrated star light and zodiacal light have been estimated from the work of Elvey and Roach [18] on the assumption that both of these components have a spectral distribution of energy corresponding to a GO star. It is noted that there is a residual in the 5303 observations after taking out these known components. We have made a systematic study of this residual throughout the night and find that its intensity and distribution over the sky are consistent with the assumption that it is due to the (6, 0) and (9, 2) bands of atmospheric OH [19]. The (7, 1) OH band transmitted by the 557

*The filters are the multilayer type manufactured by Baird Associates. In the earlier work with the two-color photometer, conventional interference filters were used.

**For example, the CI spectrograph manufactured by Huet, of Paris, has at λ 5577 a linear dispersion of 500 Å/mm. The spectrum line represents a reduction of the slit by a factor of 7. Thus our filters correspond to a slit width of 0.75 mm as compared with 0.020 mm customarily used in nightglow studies. One cannot judge properly the background intensity through one of our filters by an estimation of the background on a spectrogram, since the latter gives a "pure" spectrum by a factor of about 40.

er is of the same order of intensity as the two bands transmitted by the 5303 er, and we have adopted the practice of taking the intensity through the 5303 er as equal to that of the background light transmitted by the 5577 filter.

In order to make the correction indicated in the previous paragraph, it is cessary to put the deflections into the same units. Since this constitutes the basis the absolute values of intensity reported in this paper (and others from our boratory), the method of calibration will be given in some detail. The funda- ntal procedure would be to calibrate our instruments with a laboratory light

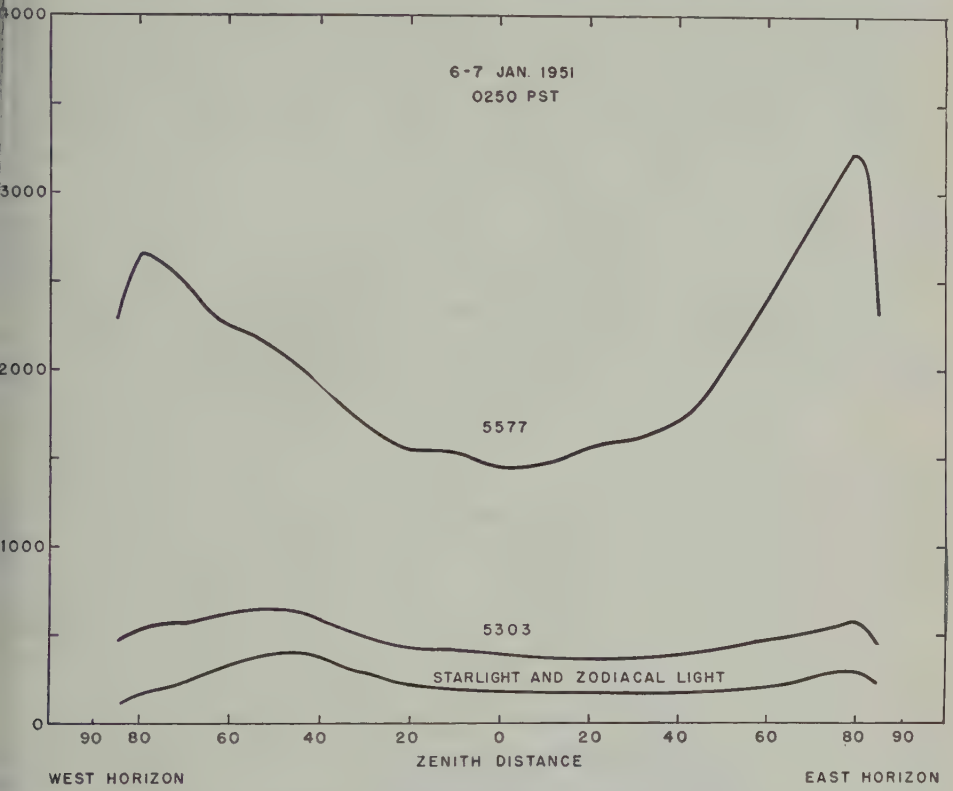

FIG. 7—THE DATA OF FIGURE 6 CONVERTED TO 10 MAG. (VISUAL) GO STARS PER SQUARE DEGREE

urce such as a black body. We have found it convenient to utilize the deflections ie to bright stars according to the following general procedure:

(1) In the course of a night's observations, many easily identifiable stellar flections can be isolated. The first step is to determine the intensity of the ar's radiation in the wave-length region in question relative to a GO star using e results of Kienle, Wempe, and Strassl [20]. From a summary of all suitable ellar observations, we thus find the mean value of the stellar magnitude (GO) rresponding to unit deflection. The field lens near the focal plane of the objective sures that the same portion of the cathode of the photomultiplier is illuminated

for a point source such as a star and for an extended surface such as the sky bac
ground. The area of the sky included by our photometer is known (19.6 squa

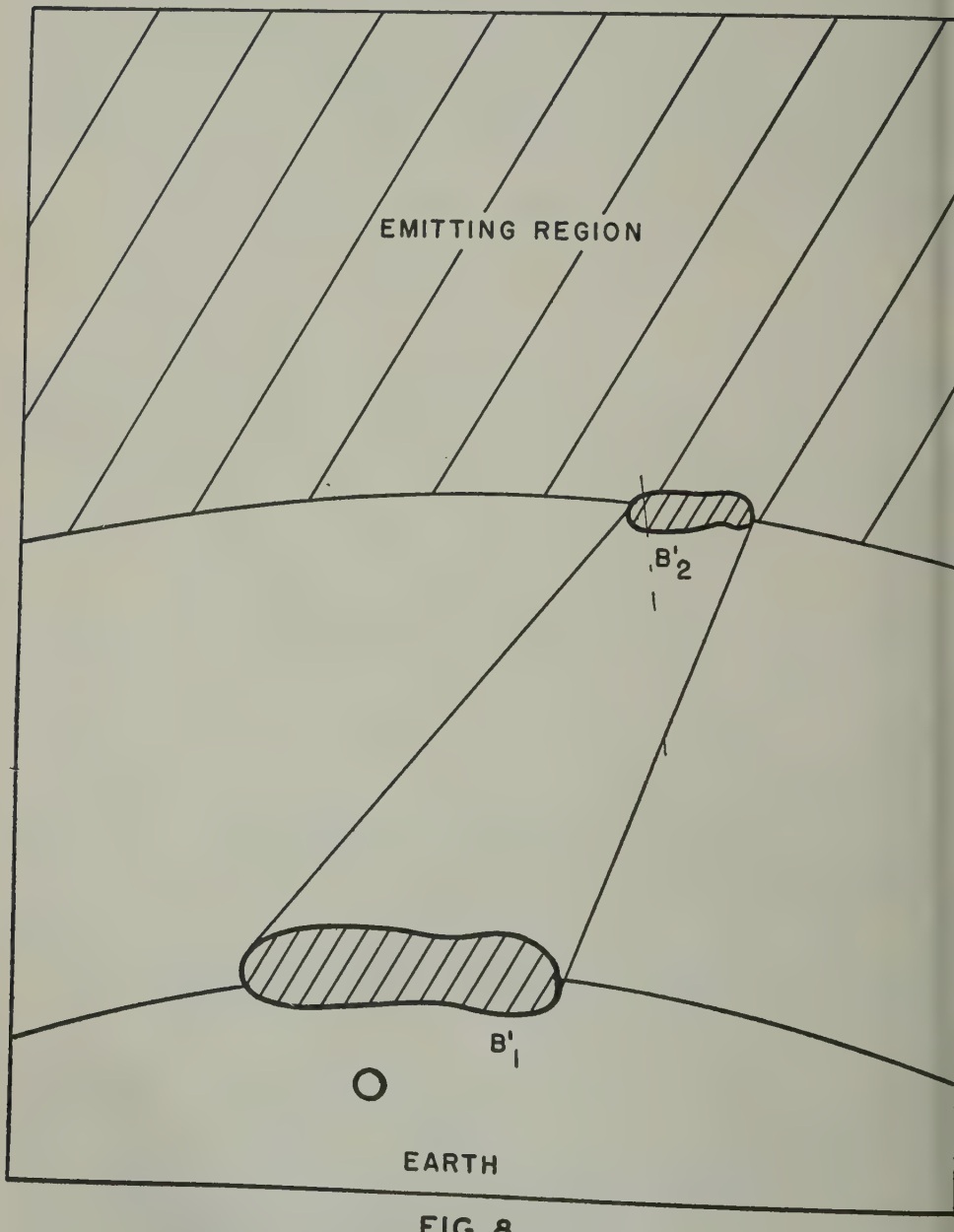

FIG. 8

degrees), so that it is possible to determine the stellar magnitude per square degree
of sky corresponding to unit deflection, or the number of 10th magnitude stars per
square degree of sky per unit deflection. This latter unit is convenient, since

antities involved in the calculations can be expressed to three significant figures thout the need of using a decimal point.

(2) For the purpose of eliminating the background light, the astronomical scale entioned above is satisfactory. However, in order to make the results useful to e upper atmosphere analyst, it is necessary to evaluate the rate of photon pro- iction in the atmosphere. Ideally, the distribution of photon production with ight is required, but *a priori* neither the effective height of the emission nor e type of variation of the emission with height is known, so that it becomes cessary to give values for the integrated rate of photon production from the server to infinity. Suppose that the emitting layer (Figure 8) may be idealized having a sharply-defined lower boundary with a surface brightness B_2' $gs/cm^2 \cdot sec \cdot steradian$ due to the summation of the emitting atoms above the wer boundary. The radiation flux emitted in a column of one square centimeter oss-section from the lower boundary to infinity will be

$$B_2 = 4\pi B_2' = 41{,}253\, B_2'' \quad \ldots\ldots (1)$$

here B_2'' is the brightness at the lower boundary in $ergs/cm^2 \cdot sec \cdot$ square degree. o convert B_2 to photons/cm^2 column·sec is straightforward for any monochro- atic radiation.

The observer at O receives radiation of brightness B_1' $ergs/cm^2 \cdot sec \cdot$ steradian r B_1'' $ergs/cm^2 \cdot sec \cdot$ square degree. Now, according to a fundamental theorem of hotometry

$$B_1' = B_2' \qquad \text{or} \qquad B_1'' = B_2'' \quad \ldots\ldots (2)$$

ence, if our photometer is calibrated in terms of flux per unit area and per unit lid angle, B_1', it is possible to evaluate B_2, the flux per square centimeter column the upper atmosphere by

$$B_2 = 4\pi B_1' = 41{,}253\, B_1'' \quad \ldots\ldots (3)$$

(3) From the calibration described in paragraph 1 above, the sensitivity of the strument is known in terms of visual stellar magnitude (GO) per square degree nd per unit deflection. Let this quantity be C. To put this into absolute units, e utilize the apparent visual magnitude of the sun (-26.72) and the determina- on of the distribution of energy in the solar spectrum made by Minnaert [21]. he quantity tabulated by Minnaert is F_λ, where πF_λ is the flux from the sun's sk in $ergs/cm^2 \cdot sec \cdot cm$ of wave-length referred to the wave-length λ. At the rface of the earth the intensity, I_λ, is given by

$$I_\lambda = \pi F_\lambda \left(\frac{R}{\rho}\right)^2 \cdot 10^{-8} \frac{\text{ergs}}{\text{cm}^2 \cdot \text{sec}} \quad \ldots\ldots (4)$$

r one Ångstrom of continuum, where R is the sun's radius and ρ is the astronomical nit.

In order to illustrate the complete procedure of calibration, we show in Table 2 e important steps for the filters used in the present investigation.

TABLE 2—*Calibration data*

Wave-length	5303	5577
Filter	Baird 7-3582-5 and Corning 3385	Baird 7-3470-3 and yellow auxiliary
Sensitivity	9	8
Apparent stellar magn (GO) of unit deflection, C	3.533	2.735
Area of photometer field (square degrees)	19.6	19.6
No. of 10 mag. vis. GO stars per sq. degree for unit deflection	19.7	48.9
$C-m_{\odot}$ (stellar magnitude)	30.253	29.455
Relative intensity (sun/star of mag. C)	1.26×10^{12}	6.05×10^{11}
I_λ for sun (ergs/cm^2·sec·Å)	198.4	194.2
I_λ for unit deflection (ergs/cm^2·sec·Å)	157.5×10^{-12}	32.1×10^{-11}
Integrated transmission of filter (equiv. Ångstroms)	28.4	56.8
I'_λ for unit deflection (ergs/cm^2 sec, total)	4473×10^{-12}	1823×10^{-11}
Transmission of filter at emission wave-length		0.62
I''_λ for unit deflection (ergs/cm^2·sec·monochromatic)		2940×10^{-11}
$h\nu$ (ergs)		3.65×10^{-12}
I'''_λ for unit deflection (quanta/cm^2 column·sec)		1.70×10^{7}

V—OBSERVATIONAL RESULTS

Measurements were made every ten degrees from the zenith to 70° and a zenith distances 75°, 80°, and 85°. There were 20 complete sky surveys for th night. For each survey, 16 different azimuths were covered (eight complete sweep from horizon to horizon), so that a total of 3,360 measurements is included in thi study for each of the two colors. For each measurement, the following procedur was adopted:

(1) Readings were converted to number of 10.0 mag. (visual) GO stars pe square degree.

(2) The intensity in the above unit for 5300 was subtracted from that for 557 for each reading.

(3) The residual was converted to transitions/cm^2 column·sec, assuming tha the entire residual is due to 5577.

(4) The converted residual for each zenith distance was plotted against azimut by surveys. At this stage of the analysis, it was possible to eliminate the effect pen lag in the recorder by a smoothing of the azimuth plots for zenith distance where the sky intensity was changing very rapidly with time. The photomete covers the sky at a rate of approximately one degree per second. The period of th Esterline-Angus recorder is about 0.5 second. Especially at zenith distance 85 where the intensity is changing rapidly with Z, is the pen lag noticeable by alte nately high and low readings for successive aximuths for which the intensity increasing with time in one case and decreasing in the next, as our survey pr gresses according to the plan of Figure 4. Actually this is a differential effect betwee 5577 and 5303.

(5) The values plotted under (4) represent slant intensities, that is, zeni

ensities for an observer some distance away increased by the greater effective
th length when viewed on a slant from Cactus Peak. The slant intensities are
xt converted into zenith intensities referred to the local geographical position
dividing the slant intensity for a particular zenith distance, Z, by the average
io, I_z/I_o , for the entire night.

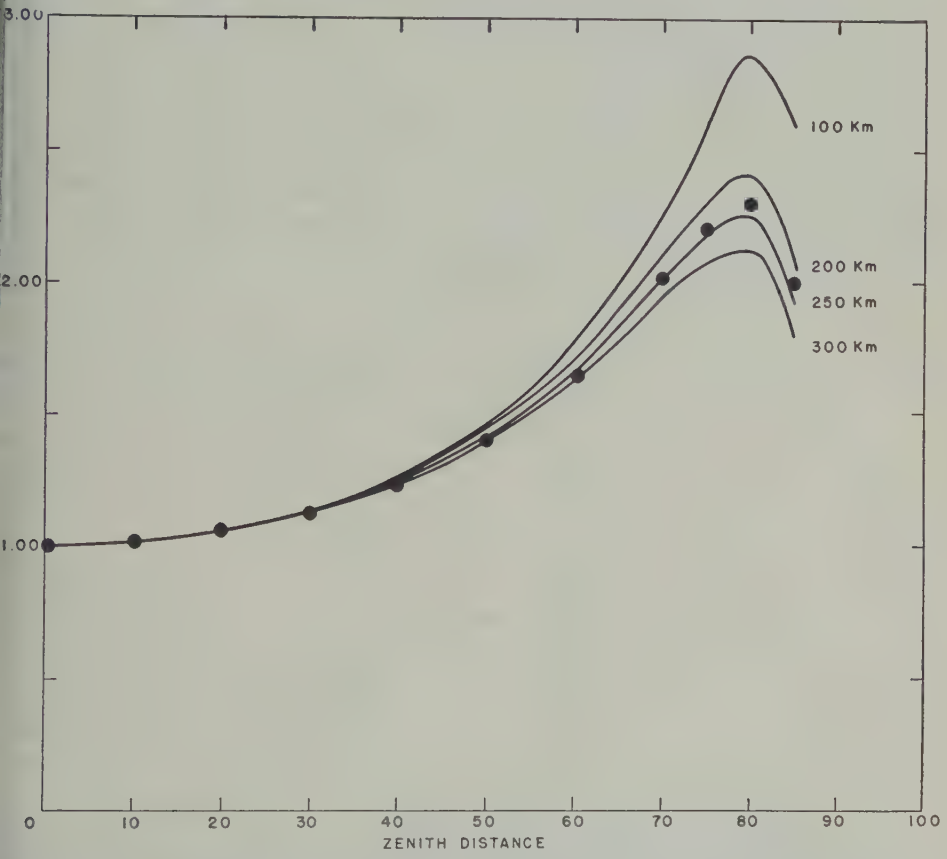

FIG. 9—MEAN VARIATION OF INTENSITY OF 5577 WITH ZENITH DISTANCE FOR THE NIGHT JANUARY 6/7, 1951 (SOLID DOTS); SOLID CURVES ARE FOR HEIGHTS 100, 200, 250, AND 300 KM BASED ON CALCULATIONS USING THE VAN RHIJN FORMULA AND AN EXTINCTION COEFFICIENT OF 0.125; FOR METHOD OF DEDUCING THEORETICAL CURVES, SEE REFERENCE [22]

(6) Since a survey requires about a half-hour, it cannot be considered that a
gle plot *versus* azimuth is a "snap shot." We therefore made detailed time plots
zenith intensities for each individual zenith distance and azimuth.

(7) Finally we prepared isophote maps of the entire sky for every hour during
night.

Steps (1), (2), (3), and (4) were done in a routine fashion. Step (5) calls for explanation. For each survey the average ratio of the intensity at each zeni distance to that at the zenith was calculated. A grand average was obtained f the whole night, as shown in Table 3 and plotted in Figure 9. No commitme need be made at this stage of the analysis as to the height of the emission in t upper atmosphere causing the increase of intensity toward the horizon. In step (we divided the individual slant intensity for a particular reading by the entry Table 3 for the zenith distance of the observation. Our procedure assumes th $I_Z \cdot (\overline{I_O/I_Z})_{Cactus}$ equals the local zenith intensity, which is true if $(\overline{I_O/I_Z})$ for Cact is the same as $(\overline{I_O/I_Z})$ in general and is a fundamental property of the upper a mosphere, not a local function. The further assumption is implied that departur from the mean are due to variations in local zenith intensity only. Other facto which might affect individual readings will cause an unavoidable uncertainty in o deduced zenith intensities. In our judgment, the procedure followed is the be available in the present state of knowledge.

TABLE 3—*Mean values of I_Z/I_O for night of January 6/7, 1951*

Z	I_Z/I_O
85	1.97
80	2.31
75	2.20
70	2.03
60	1.66
50	1.40
40	1.23
30	1.12
20	1.05
10	1.01
0	1.00

The average I_Z/I_O for the entire night probably smooths out local irregularit in time and space and our procedure will tend to minimize any systematic er that may be present, for example, in the direct subtraction of 5300 from 5577.

In Figure 10 we show time plots of intensity referred to local zenith fo zenith distance of 80° at the north and south points, together with a similar p for the Cactus zenith intensity. Similar plots have been made systematically all of the 16 azimuths at zenith distances 85°, 80°, 75°, 70°, and 0°. A numbe empirical observations are in order at this point.

(1) The general diurnal pattern noted in connection with the zenith plots Cactus Peak, shown in Figures 1 and 2, is present in all the plots covering obser tions over the entire sky. Without exception, there is a maximum of intensity w however, a wide spread in the time and intensity of the maximum. In general, maxima are higher and occur earlier in the northern part of the sky than in southern.

(2) An initial decrease in intensity occurs in all plots for this night. The m

ium between the two parts of the curve occurs early in the night for the northern rt of the sky and much later for the southern.

An examination of plots such as those in Figure 10 convinced us that the full scription of the phenomenon of the diurnal variation would best be accomplished y making isophotal maps of the entire sky interpreted in terms of a geographical stribution of local zenith intensities. The scale of the maps depends on the height the emitting layer as shown in Table 4, but the shape of the pattern is almost

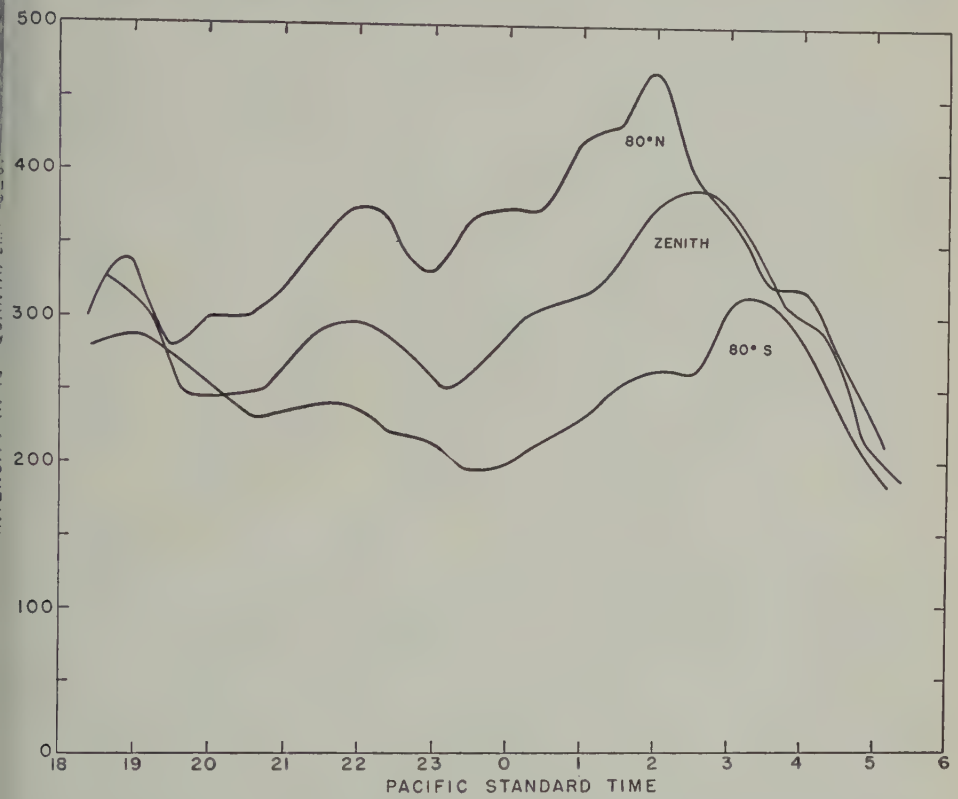

FIG. 10—TYPICAL PLOTS OF DIURNAL VARIATION OF 5577 FOR JANUARY 6/7, 1951; INTENSITIES ARE REDUCED TO LOCAL ZENITH; NOTE THE SYSTEMATIC PROGRESSION WITH TIME OF THE POSITION OF MAXIMUM INTENSITY

dependent of the height. That the shape of the geographical plots is almost indeendent of the height to the emitting layer is due to the fact that the relative stances of the intersections of the line of sight with the upper atmosphere layer main nearly constant for heights ranging from 100 to 300 km (see Table 4).

From the variation of intensity with zenith distance, heights for 5577 from ound 100 km to several hundred kilometers have been reported in the literature. or example, Roach and Barbier [22] found a value of 110 km based on observa-

tions with our two-color photometer. The results of this paper indicate a hei of 250 km, using the mean curve for the night (Figure 9) and an extinction efficient of 0.125.*

The agreement of the observed points and the theoretical curve for a hei of approximately 250 km, as shown in Figure 9, calls for an evaluation of poss systematic errors. Each plotted point is the mean of over 300 individual obse

TABLE 4—*Variation of intensity with zenith distance*

Zenith distance	Distance along earth's surface to intersection with upper atmosphere laye							
	h = 100 km		h = 200 km		h = 250 km		h = 300 km	
	Km	Relative	Km	Relative	Km	Relative	Km	Relat
85	694	1.49	1,112	1.38	1,291	1.34	1,443	1.
80	466	1.00	808	1.00	964	1.00	1,097	1.
75	338	0.72	616	0.76	744	0.77	858	0.
70	258	0.55	481	0.60	590	0.61	688	0.
60	167	0.36	322	0.40	396	0.41	467	0.
50	117	0.25	228	0.28	281	0.29	331	0.
40	83	0.18	161	0.20	201	0.21	238	0.
30	58	0.12	111	0.14	138	0.14	166	0.
20	36	0.08	71	0.09	87	0.09	103	0.
10	19	0.04	36	0.04	44	0.05	50	0.
0	0	0.00	0	0.00	0	0.00	0	0.

tions, hence it is not surprising that the scatter of the points is small. But it can be considered that a unique solution of 250 km is established, since a wide ra of equally satisfactory solutions can be obtained by a relatively small variatio the background radiation subtracted from the 5577 observations. Referring a to Figure 7, it is seen that there is an upper atmospheric residual in the 5300 servations which we have previously indicated we believe is due to radiation f the (6, 0) and (9, 2) bands of OH. We have made the assumption in our anal that the same amount of upper atmosphere background radiation must be allo for in the case of the observations with the 5577 filter. In order to indicate values for the height which would result if this assumption is wrong, we h made a calculation of the deduced heights on the basis of other assumptions.

Assumption I—There is no background component in the 5577 observat (except star light and zodiacal light). The deduced height is 300 km.

Assumption II—The background component to apply to the 5577 observat due to atmospheric radiations is twice that observed with the 5303 filter. deduced height is 150 km.

Assumption III—The background component is exactly the same for 5577 and 5303 (the basis of the results of this paper). The deduced height is 250

*The extinction coefficient τ is defined by the equation $I/I_0 = e^{-\tau m}$, where I_0 and I a intensities of radiation before and after traversing m air masses. The coefficient 0.125 is cl the value found empirically at Mt. Wilson for 5577 Å.

There is one bit of evidence suggesting that the use of Assumption III is justi-
l. In addition to the measures here reported on 5577, we have made similar
asurements for the same night for the other two photometers for the upper

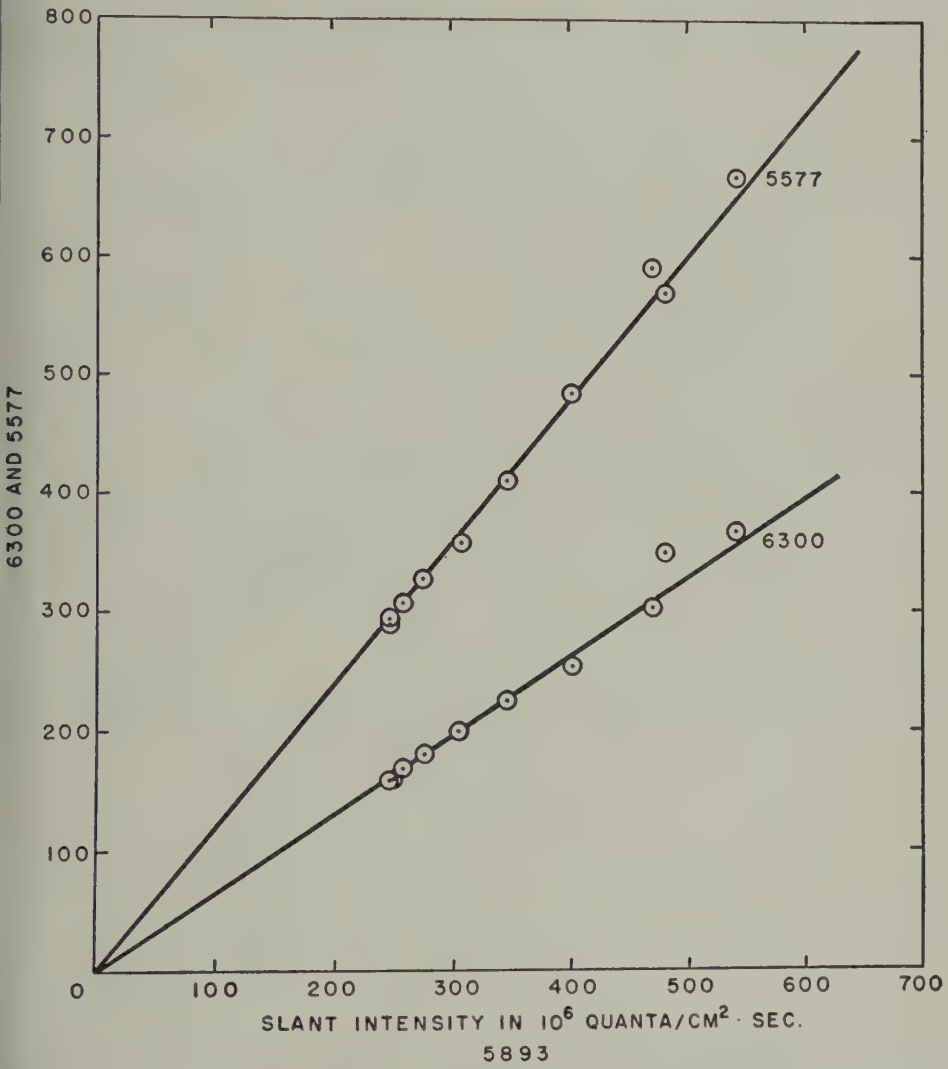

FIG. 11—CORRELATION OF SLANT INTENSITIES OF 5577, 5893, AND 6300 FOR JANUARY 6/7, 1951; THE POINTS INCLUDE AVERAGES OF 20, 18, AND 14 SURVEYS, RESPECTIVELY

nosphere radiations 5893 (sodium D) and 6300 forbidden oxygen ($^1D_2 - {}^3P_2$).
e same method of analysis and the same assumption as to the background
diation were made in all three cases. A plot of the slant intensities (that is,
ectly observed intensities at various zenith distances) of one color against

another will show up any gross error in the basic assumptions. If one of the col includes a substantial amount of extraneous radiation relative to the other, correlation curve does not in general extrapolate to the origin. In Figure 11

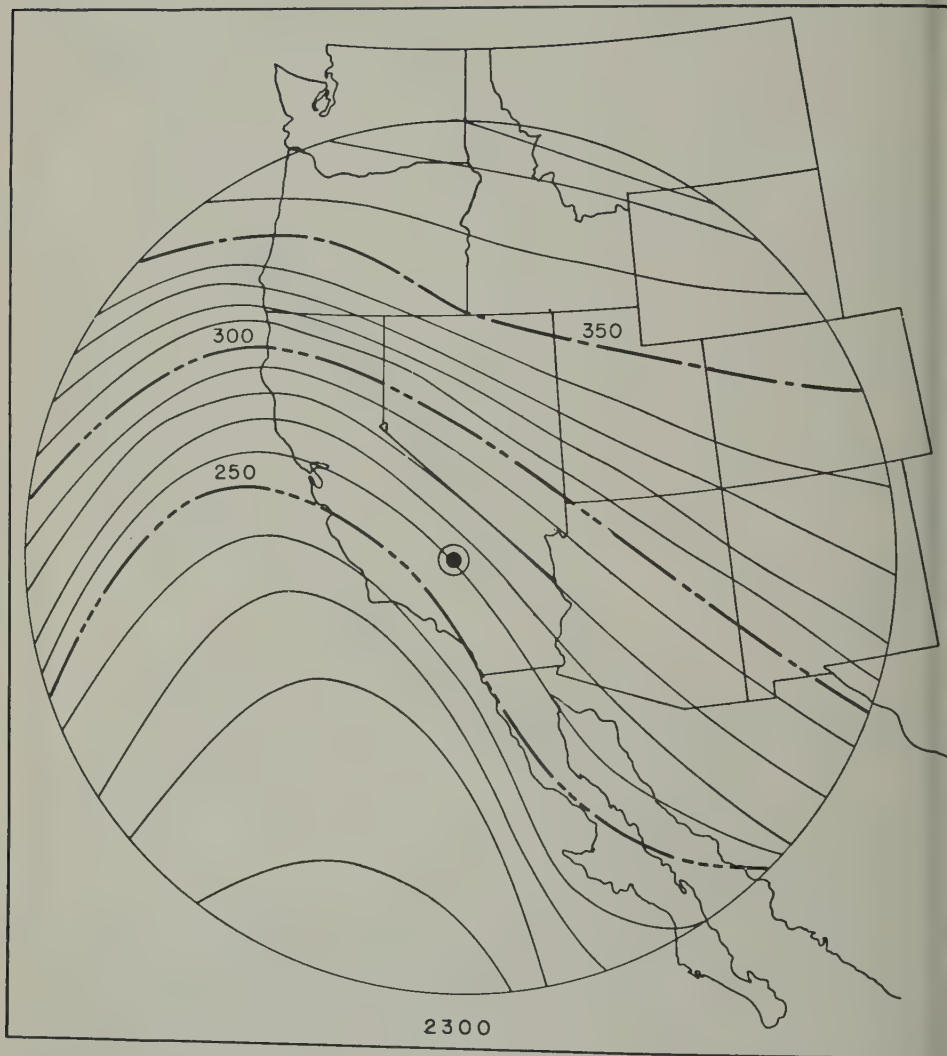

FIG. 12—ISOPHOTE PATTERN FOR $23^h 00^m$ PST ASSUMING TH HEIGHT TO BE 250 KM, SUPERIMPOSED ON A GEOGRAPHICAL MAP WITH THE OBSERVING STATION, CACTUS PEAK, IN THE CENTER

show plots of slant intensities of 5577 and 6300 against 5893, based on a lar amount of observational material (Assumption III in all cases). It is noted th a straight-line extrapolation of the curves comes very close to the origin. Ev this is not positive proof that Assumption III is correct, since there might

ıal or compensating systematic errors in all three cases, but we feel justified in ɔceeding with the general analysis with reasonable confidence that no serious or is likely. It is perhaps worth noting that the fact that there is no curvature the plots of Figure 11 is evidence that all three radiations occur at *approximately* same height. If one radiation were at, say, 50 km and another at 300 km, the iation of slant intensity with zenith distance of the two would follow different ɣs which would introduce curvature into the correlations.

In Figure 12 we show an isophotal map based on a height of emission of 250 ı. The circle represents observations at a zenith distance of 85°, which corre-ɔnds to a distance of 1,291 km (see Table 4) from Cactus Peak. It is noted that e western part of the United States plus part of northern Mexico and the adjacent cific Ocean are included.

In Figure 13 we show isophotal maps for each hour of the night. A number of ıeral features are noted, as follows:

(1) From astronomical twilight to $20^h\ 00^m$ PST there is a well-developed ximum in the west which moves westward with time. The balance of the sky ɔws no well-defined structure.

(2) From $20^h\ 00^m$ to $21^h\ 00^m$ PST the westward effect appears as a distortion the isophotes but the general picture suggests a transition between two phases.

(3) From $22^h\ 00^m$ to $03^h\ 00^m$ a distinct pattern is obvious. The isophotes run general in a WNW-ESE direction. A maximum to the north develops for the dnight, $01^h\ 00^m$, and $02^h\ 00^m$ maps. During this interval the isophotes are much ɔre crowded than during the early or late parts of the night.

(4) From $04^h\ 00^m$ to $05^h\ 00^m$ the intensity level of the entire sky decreases ɔidly. The general orientation of the isophotes changes to northwest-southeast $04^h\ 00^m$ and northeast-southwest at $05^h\ 00^m$. There is no apparent dawn bright-ing in the east corresponding to the twilight brightening in the evening in the st.

VI—DISCUSSION OF OBSERVATIONS

The series of isophote maps of Figure 13 constitutes a step-wise panorama in th space and time. It is of interest to inquire whether there is any general ttern which will describe the entire diurnal phenomenon in the form of a con-ıuous panorama. It may be assumed that the diurnal variation of intensity is a re time variation with no special motions of the excitation patterns. In this se, the changes of intensity are of a local nature. The maximum of intensity served at any particular geographical location will be due to a change in the ɔitation conditions in the local portion of the upper atmosphere. To explain the servations on such a basis, a mechanism must be found which undergoes diurnal anges so as to produce a distribution of intensity varying in time as indicated the successive maps of Figure 13 but also in space as shown by each individual ıp, but there would not necessarily be any continuity in the sequence of isophote tterns from hour to hour throughout the night.

Figure 13 strongly suggests, however, that there is some significance in both ace and time in the sequence of isophote patterns. This indicates the desirability exploring the possibility of a dynamic picture in which space motions of the

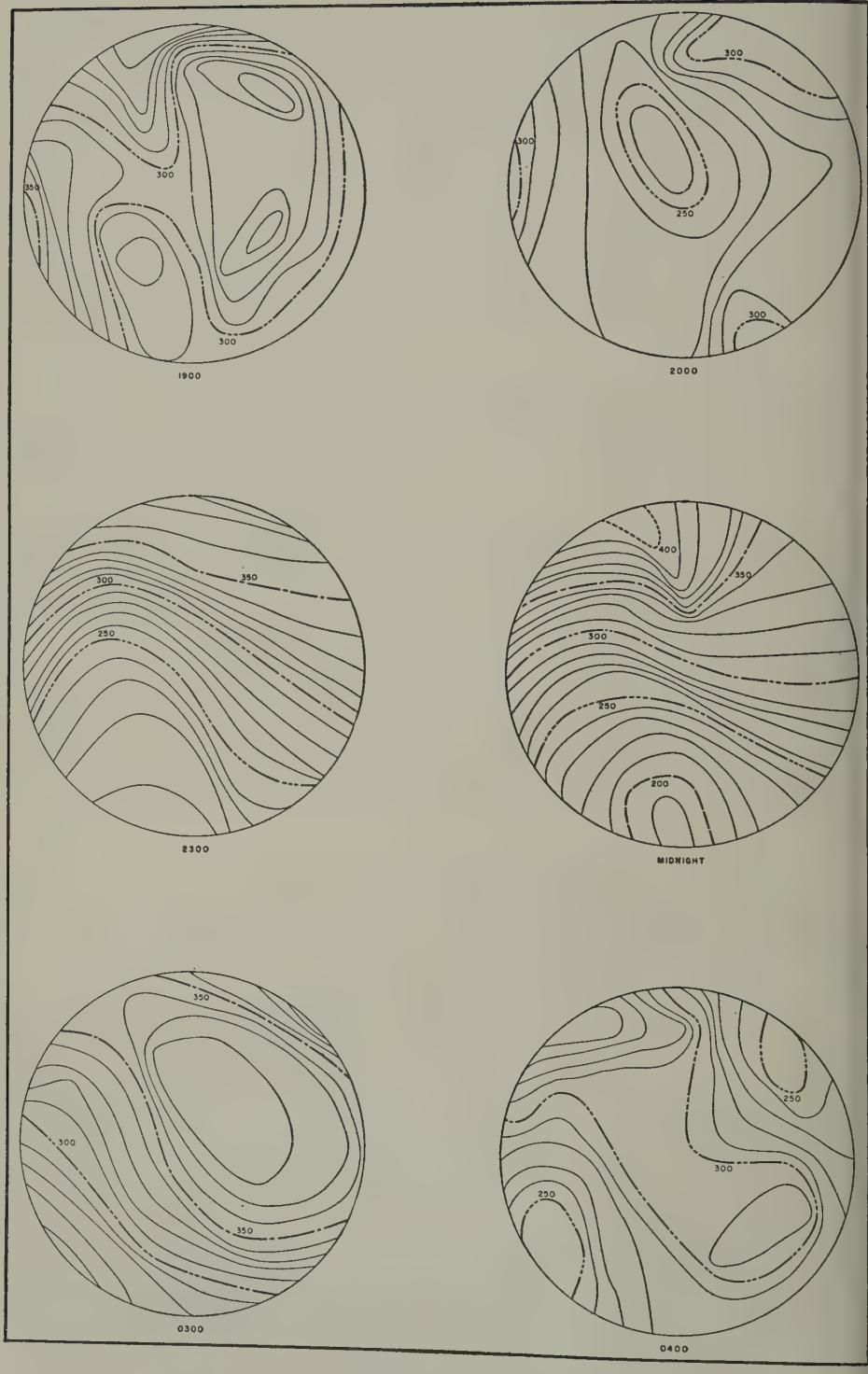
300
350
300
1900
300
300
250
300
2000
300
350
250
2300
400
350
300
250
200
MIDNIGHT
350
300
350
0300
250
300
250
0400

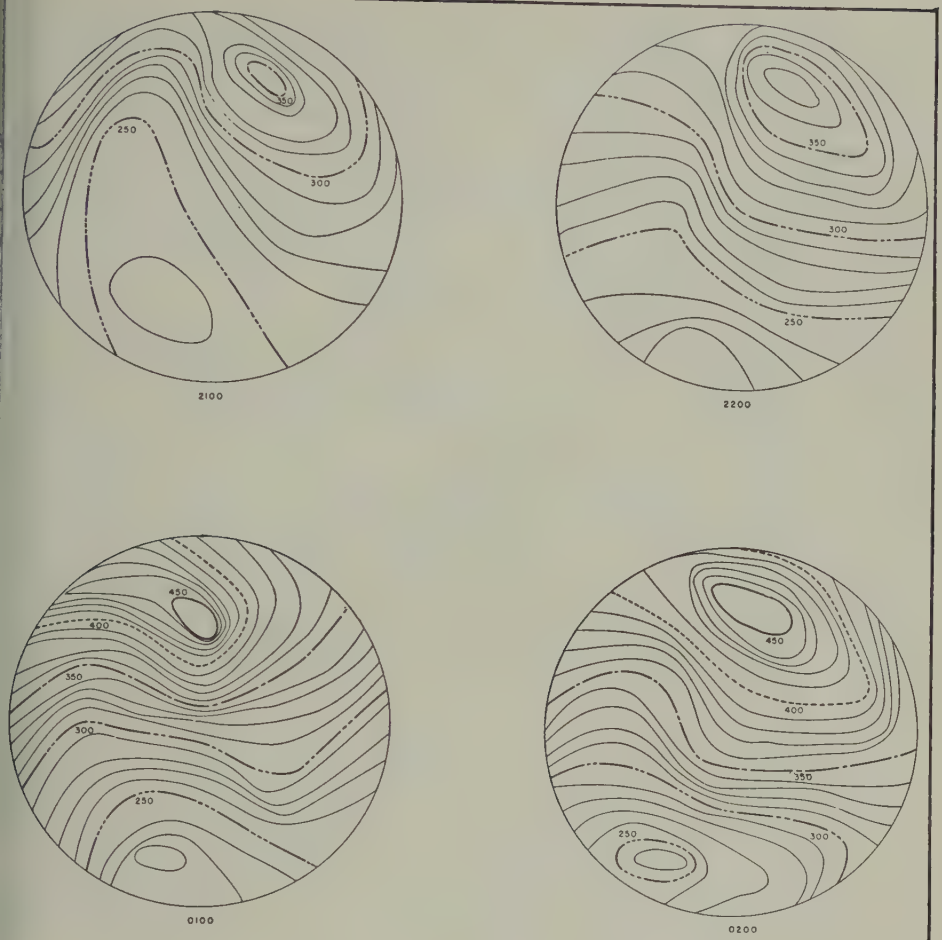

FIG. 13—ISOPHOTE MAPS OF THE INTENSITY OF 5577 ON JANUARY 6/7, 1951; UNIT IS 10^6 QUANTA/CM^2·SEC; NORTH IS UP, SOUTH DOWN, WEST TO THE LEFT, AND EAST TO THE RIGHT

excitation pattern are taking place during a night, not necessarily implying t motion of physical particles. In general, successive isophote maps must show so degree of overlapping of the patterns if space motion is a reality. This overl may be partially obscured if there is a pure time variation superimposed upon t space motion.

An apparent motion of the 300×10^6 isophote from north to south is obvio upon inspection of Figure 13. Between $21^h\ 00^m$ and $03^h\ 00^m$ the velocity of t motion is about 250 km per hour if the height to the emitting layer is 250 k However, we have not been able to rationalize the entire series of maps by general north-south motion of all the isophotes.

If we now look into the possibility of a strong west to east or east to we component of motion, we must take into account the possible effect of the earth rotation. Let the west to east component of linear velocity of the upper atmosph excitation as seen from the center of the earth be V_P and the linear velocity of t observer by virtue of the earth's rotation be V_E . Then the *apparent* velocity seen by an observer on the earth's surface from west to east of the excitation, V_A will be $V_A = V_P - V_E$. If the excitation patterns apparently move from we to east, as is the case of the prevailing winds in the troposphere of the northe temperate zone, then V_A is positive and $V_P > V_E$. If, on the other hand, t apparent velocity is from east to west, then V_A is negative and $V_P < V_E$. attempts to match the successive isophote maps of Figure 13, we have investigat the possibilities shown in Table 5.

TABLE 5—*Analysis of the 300 × 10⁶ diurnal isophote pattern*

V_A (1)	V_P (2)	Mean of maximum deviation (3)	Column (3) minus 20 × 10 (4)
$2\ V_E$	$3\ V_E$	37×10^6	17×10^6
V_E	$2\ V_E$	52	32
$1/2\ V_E$	$3/2\ V_E$	58	38
$-1/2\ V_E$	$1/2\ V_E$	41	21
$-\ V_E$	0	26	6
$-2\ V_E$	$-\ V_E$	37×10^6	17×10^6

The method employed is illustrated in Figure 14. In the event that there is apparent motion of the excitation pattern from east to west, then it follows th the portion of the pattern included in a sweep from the northern to the southe horizon (that is, the observer's meridian) at any given time is that portion whi will later appear to the west of the meridian and which has previously appear in the eastern part of the sky. The converse is true if the apparent motion is fr west to east. Thus it is possible to test east-west or west-east motions by compari time variations of the meridian observations with time-space variations of isophote maps.

In Figure 14*A* we show a time plot of the meridian observations throughc the night of January 6/7, 1951. Only the 200, 300, and 400×10^6 isophotes

nown. The ordinate scale has been fixed by assuming a height of emission of 250 m. The abscissa scale is basically a time scale, but in order to illustrate the effect f a superposition of successive complete isophote maps we made one hour on ne abscissa correspond to V_E . In other working plots, not shown here, we em-loyed abscissa scales of one hour equal to $\frac{1}{2}V_E$ and $2V_E$. The successive hourly sophote maps of Figure 13 were superimposed on meridian-time plots such as

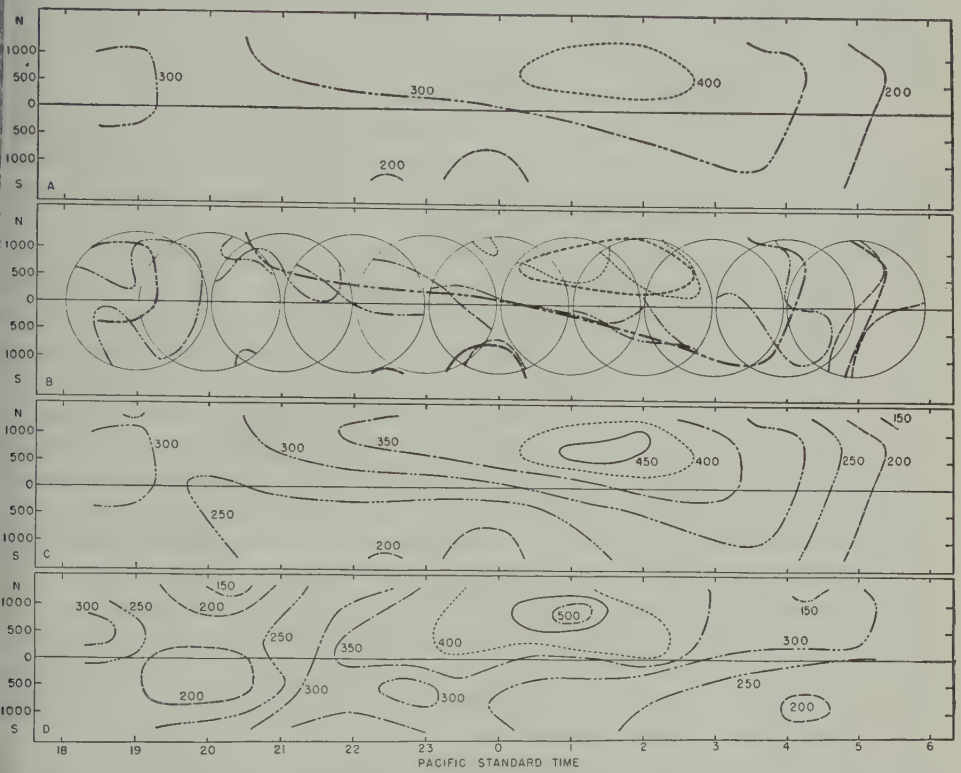

FIG. 14A—TIME PLOT OF THE ISOPHOTES OBTAINED FROM ONLY THE NORTH-SOUTH OBSERVATIONS ON JANUARY 6/7, 1951

FIG. 14B—SUPERPOSITION OF ISOPHOTE MAPS OF FIGURE 13 ON FIGURE 14A (SEE TEXT)

FIG. 14C—SAME AS FIGURE 14A BUT WITH SMALLER INCREMENTS BETWEEN ISOPHOTE LINES

FIG. 14D—COMPOSITE ISOPHOTE MAP FOR THE PREVIOUS NIGHT, JANUARY 5/6, 1951

igure 14*A* to estimate the quality of the fit between the diurnal pattern built p from the two approaches. An example of such a matching attempt is shown Figure 14*B*, in which it has been assumed that $V_A = -V_E$. Each of the hourly aps of Figure 13 has been superimposed on Figure 14*A*, including only the 200, 00, and 400 $\times$ 10^6 isophotes in order to avoid the confusion of too much detail.

Since the 300×10^6 isophote persists throughout most of the night, it is instructiv to follow the match of its segments from individual maps and the composite curv from Figure 14*A*. It is noted that usually a fairly satisfactory general match occurs Attention is called to the fact, however, that a part of this match is forced by th method of analysis, since the composite curve must intersect the segments on th meridian of each map except for the fact that the smoothing of each is done inde pendently. A significant criterion of the match is therefore the extreme departure of the segments from the composite curve, which may be due to errors of observa tion, to time variations superimposed on the space variations, or to an erroneou assumption as to the apparent velocity of the excitation pattern.

In column 3 of Table 5 we show the mean of the extreme departures of th segments from the composite curve for isophote 300×10^6 throughout the nigh for six different assumed east-west excitation velocities. It is not possible to mak a strictly objective evaluation of the significance of column 3 of Table 5, sinc we do not know the random errors inherent in the drawing of the isophotes. W estimate, however, that all the observational and analytical uncertainties are o the order of 20×10^6.* In the fourth column of Table 5 we show the residual afte subtracting 20×10^6 from the entries of column 3. This residual represents devia tions due to (1) true time variations plus (2) the effect of an erroneous assumptio as to the east-west component of motion. It is noted that the best case is that o $V_A = -V_E$ or $V_P = 0$. Thus, within the precision of the present analysis, w find that the best description of the observations is obtained if the general excita tion pattern apparently moves from east to west so as to just counteract the wes to east rotational velocity of the earth. In other words, the excitation pattern ma be considered to maintain its essential identity on the night side of the earth an the observer appears to move through the pattern as the earth rotates.

The entire case does not rest upon the data presented in Table 5. During th last two hours of the night, it is impossible to reconcile the motions correspondin to $V_A = 2V_E$ and $V_A = V_E$ when the 200 and 250×10^6 isophotes are matched so that these velocities must be ruled out.

We should like at this point to return to the matter of possible systemati errors in the present analysis. The principal potential source of error was brough out under section V above in the discussion of Assumptions I, II, and III. It i of interest to follow the implications of the two Assumptions I and II which w did not use.

Assumption I would have allowed for no background light through the 557 filter excepting that due to integrated star light and zodiacal light and is, therefor a limiting case. If we had used this assumption in our analysis, the amount background to be subtracted from the observations would have been less and th absolute intensities higher by about 21 per cent. The variation of the deduce

*This estimate of the uncertainty represents the unanimous opinion of ourselves and two our colleagues, all of whom have had extensive experience in making isophote maps. The estimat were made independently and prior to the calculations resulting in the entries of column 3 Table 5. In column 4 of Table 5 we have taken the arithmetic difference of the errors to indica the order of magnitude of the residual error, since we do not consider the data sufficiently accura to justify a refined treatment according to the theory of least squares.

pper atmosphere residual with increasing zenith distance would have been slower han that shown in Table 3 based upon Assumption III. The height deduced om the observations would have been 300 km instead of 250 km. In constructing he isophote maps of Figure 13, the general shapes of the patterns would have een the same but the over-all absolute intensity level would be raised by 21 er cent. The geographical coverage corresponding to the height of 300 km is bout 12 per cent greater than that for 250 km (see Table 4). The building up of composite contour map for the entire night from the separate hourly maps as e did in Figure 14*B* could be accomplished in a similar manner, but the hourly isplacement of each successive map would correspond to 1,510 km rather than ,350 km, as deduced in the use of Assumption III.

A similar set of consequences in the opposite sense would result from the use f Assumption II, which assigns a greater background intensity of an upper tmosphere component by a factor of two to the 5577 filter than to the 5303 ontrol filter. In Table 6 we show a summary of the consequences of the use of he three assumptions. It is our judgment that we have bracketed between As-umptions I and II the extreme possibilities as far as systematic errors are con-erned.

TABLE 6—*Results based on respective assumptions*

Assumption	Relative intensity level	Deduced height of emission	Apparent east–west velocity of pattern	Ratio of pattern velocity to earth's rotational velocity at latitude 36° north
		(*km*)	(*km/hour*)	
I	1.21	300	1,510	1.1
II	0.79	150	940	0.7
III	1.00	250	1,350	1.0

From the last column of Table 6 it is noted that if the apparent east-west notion of the excitation pattern of 5577 in the nightglow for January 6/7, 1951, s made approximately equal to the linear velocity of rotation of the earth at atitude 36° for Assumption III, deviations from this are +10 per cent in the ase of Assumption I and −30 per cent in the case of Assumption II. These devia-ions cannot be considered as significant in connection with the deduced rate of pparent motion of the excitation pattern in view of the approximate nature of he supporting evidence for such a motion (Table 5).

Quite independent of the question of the objective reality of a semi-fixed xcitation pattern on the night side of the earth such as we have suggested, we hould like to call attention to the value of plotting observational data for an ntire night as in Figures 14 and 15. As graphical representation of empirical data, uch plots permit a visualization of the diurnal changes of intensity of a nightglow mission, not only for an observer's zenith, but also for geographical locations ithin a circle of approximately 1,000 kilometers.

In Figure 14*C* is shown the isophote pattern for the night of January 6/ 1951, in which a smaller increment is used for successive isophote lines than f Figures 14*A* and 14*B*. For comparison, Figure 14*D** shows a similar pattern o tained for the previous night. It is seen that both nights have a well-develope maximum to the north of Cactus Peak of approximately the same intensity leve On January 5/6 the maximum occurred earlier than on January 6/7. A differen is also noted in that the later night shows a definite slope to the pattern as thoug

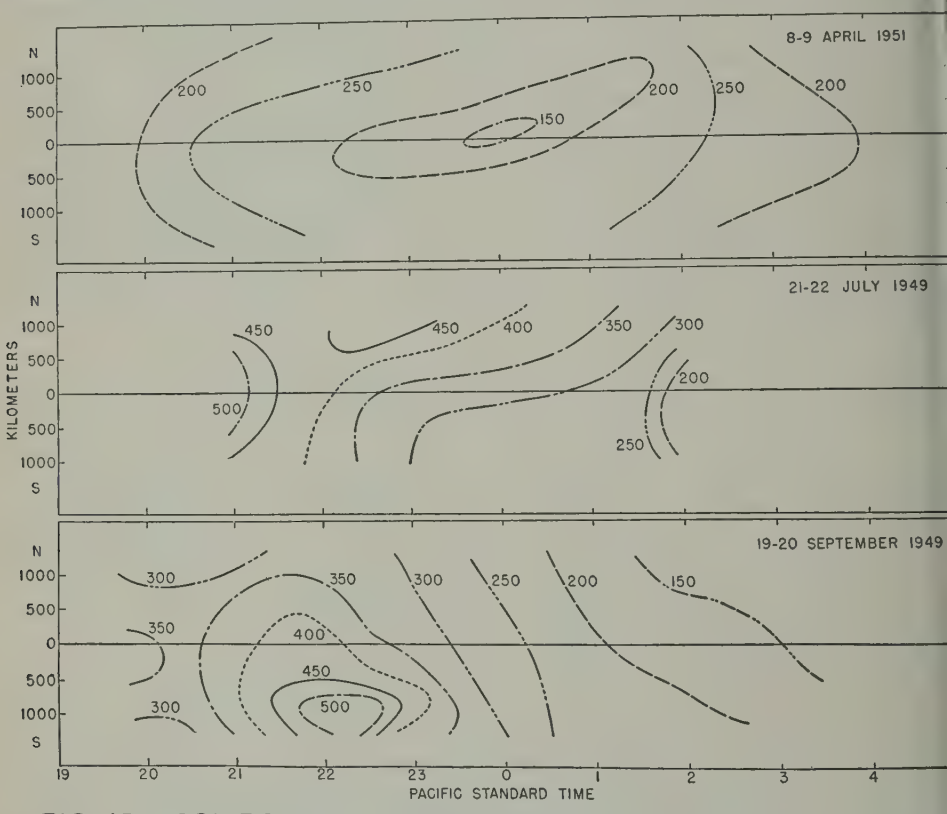

FIG. 15—COMPOSITE ISOPHOTE MAPS FOR THE NIGHTS OF APRIL 8/9, 1951, JULY 21/22, 1949, AND SEPTEMBER 19/20, 1949

there were a north-south motion of the excitation pattern superimposed upon t general east-west rotational effect. However, the general similarity of the two nigh supports our proposal that the earth's rotation through an excitation pattern responsible for a large amount of the diurnal variation, since it is reasonable expect that successive nights will show similar configurations if, during a sin night, we are dealing with a relatively fixed pattern.

*A critical study of the night of January 5/6, 1951, is in progress by our colleagues, E. Ashburn and Dorothy Davis Locanthi. We are indebted to them for permission to include Fig 14*D* in the present discussion.

It is planned to make a systematic study of all of our observational material d to accumulate further observations over another year in order to investigate e matter of seasonal variations in the excitation patterns of 5577. We have amined our data for the nights of April 8/9, 1951, July 21/22, 1949, and Sep- mber 19/20, 1949, and show in Figure 15 the results of an analysis of the north- uth sweeps similar to that resulting in the plots of Figure 14. For the April servations, we find that there is a suggestion of a minimum near midnight, eceded and followed by slight maxima. The entire intensity level of the night low. The July observations suggest the existence of a maximum off-scale to the rth. The September night shows a well-developed maximum to the *south* of actus Peak, occurring well before midnight.

Referring back to Figures 1 and 2, it is seen that the variation with time of the nith intensity at Cactus Peak for the night of January 6/7, 1951, is typical of ariations occurring on other nights. The maximum of intensity is a little above the verage of all the nights plotted, but higher values are observed, notably on Sep- mber 19/20, 1949, and July 21/22, 1949. The time of maximum occurs at about $2^h\ 30^m$ PST, which is the latest of any of the ten nights recorded. From a com- arison of Figures 14 and 15, it is obvious that there is a wide variation in the geo- raphical pattern of the isophotos and that the night of January 6/7 does not present, in detail, the pattern to be expected every night. Independent checks of ne apparent east-west motion of the excitation pattern, such as deduced for anuary 6/7, are being made for other nights and will be reported in later com- unications. An objective test will best be accomplished by a comparison of simul- neous observations at two stations separated in longitude but having the same titude. It is of interest that on the night of September 19/20, 1949, we observed multaneously from Cactus Peak and from a station in the White Mountains (100 iles to the north). A plot of the diurnal variation from the White Mountain bservations shows a pattern similar to that in Figure 15 for Cactus Peak. A maxi- um of the same order of intensity occurs to the south at the same time at both ations. The absolute calibration of the two photometers was not sufficiently curate for a good estimate of the height of the emission by "triangulation" ethods, but the apparent displacement of the patterns as seen from the two ations confirms that the strong increase of intensity to the southward was actually change in local zenith intensity in the geographical sense, such as we have assumed the detailed analysis given in this paper.

VII—CONCLUSIONS

The picture of the diurnal variations of the 5577 emission in the nightglow veloped in this study is as follows. The emission takes place in the general cinity of the *F*-layer of the ionosphere. It is characterized by a semi-fixed in- nsity pattern during a given night which maintains its orientation on the dark de of the earth, thus giving time variations when viewed by an observer at a ven geographical location as the earth rotates. For observers at the same latitude t different longitudes, the present picture predicts that during a given night ere will be similar diurnal patterns when referred to local civil time. The in- nsity pattern has major changes between nights widely separated in time through-

out the year. The maximum intensity may be to the north of latitude +36°, to t south, or in an indeterminate location. Because of the approximate nature of t evidence supporting the present picture, we prefer to consider it as a worki hypothesis rather than an established fact.

If the excitation pattern is fixed in its general features on the night side the earth, it follows that the entire phenomenon must be associated in some in mate way with the sun. Two possible mechanisms suggest themselves to us where the sun can affect the excitation of oxygen atoms directly in the night sky.

It is recalled that Maris and Hulburt [25, 26, 27] have developed a theory the polar aurora in which the ultraviolet light of the sun on the daylight side the earth is responsible for the appearance of ionized particles on the night si which excite the auroral spectrum. The ions are directed toward the earth's surfa by the earth's magnetic lines of force. One of the principal difficulties of the theo has been the necessity of postulating that the particles originating in the earth exosphere must go to extreme heights (30,000 to 50,000 km) before being ioniz in order to account for the observed auroral zone of maximum intensity. Becau of this and other difficulties [28], the theory that the sun is the direct source the particles causing the polar aurora finds wider acceptance. We should like suggest consideration of the possibility that the Maris-Hulburt theory might applied to the case of the nightglow. If the zone of maximum intensity for t nightglow is at lower latitudes than the polar aurora and if the height of the emitti layer is as great as 250 km, the difficulties associated with the Maris-Hulbu theory in connection with its application to the polar aurora may not be so seve for the nightglow.

Another possibility is that the nightglow radiation may be evidence of ion spheric winds such as have been deduced for the 100-km region in the dayti from systematic studies of variations of intensity of the earth's magnetic field [2 Such winds on the day side of the earth might set up counterparts on the nig side which would be expected to have significant seasonal variations as the su declination changes. If the excitation mechanism is associated with charg particles in such an ionospheric wind, a correlation is anticipated between t direction of motion of the particles and the local direction of the earth's magne field. The maximum energy will occur when the particles move at right angles the magnetic lines of force. No definite wind pattern is obvious from our compos isophote maps, but it is interesting that the intensity always falls toward sunri suggesting that in this region the motion is parallel to the magnetic lines of for as would be expected if the nocturnal wind motion is set up by contact with t daytime wind centered near the subsolar point.

ACKNOWLEDGMENTS

We are indebted to a number of our colleagues for assistance in the preparati of this report—Mr. Pierre St. Amand for help with the observing at Cactus Pe Dr. R. F. Sanford and Dr. Dorothy Davis Locanthi for help with the computi Mr. E. V. Ashburn and Mr. D. R. Williams for a critical reading of the ma script; Dr. F. T. Rogers, Jr., for administrative aid and encouragement. We h also profited by stimulating conversations with Dr. O. R. Wulf.

The project was supported by a research grant from the Office of Naval search, Project NR-082-045.

References

[1] Lord Rayleigh, Proc. R. Soc., A, **106**, 117 (1924).
[2] J. C. McLennan, J. H. McLeod, and H. J. C. Ireton, Trans. R. Soc. Can., **22**, 397 (1928).
[3] Lord Rayleigh, Proc. R. Soc., A, **124**, 395 (1929).
[4] J. V. Karandikar, Indian J. Phys., **8**, 547 (1934).
[5] Lord Rayleigh, and Spencer Jones, Proc. R. Soc., London, A, **151**, 22 (1935).
[6] R. Grandmontagne, Paris, C.-R. Acad. sci., **200**, 878 (1935).
[7] N. M. Dobrotin, I. M. Frank, and P. A. Cherenk, DAN (Doklady Academy of Nauk), No. 1, 110 (1935).
[8] A. A. Levedev and I. A. Khvostikov, DAN, No. 1, 118 (1935).
[9] V. I. Cerniajev, I. A. Khvostikov, and K. B. Paschin, J. Physique, **7**, 149 (1936).
[10] H. Garrigue, Paris, C.-R. Acad. sci., **202**, 1807 (1936).
[11] H. Garrigue, Paris, C.-R. Acad. sci., **205**, 491 (1937).
[12] A. A. Vasmut, V. N. Verstmer, C. U. Tibilod, and C. I. Freidert, DAN No. 19, 4 or 5 (1938).
[13] D. R. Barber, Lick Obs. Bull., **19**, 105 (1941).
[14] J. Dufay, and Tcheng Mao-Lin, Ann. Géophys., **2**, Fasc. 3, 189 (1946).
[15] C. F. Rodionov, E. H. Pavlova, and E. V. Rdultovskaiy, Reports of the Academy of Science, U.S.S.R., **66**, No. 1, 55-57 (1949).
[16] For a description of the instrument, see D. G. Marlow and J. C. Pemberton, Rev. Sci. Instr., **20**, 724 (1949).
[17] For a detailed discussion of the method of analysis with our two-color photometer, see F. E. Roach and D. Barbier, Trans. Amer. Geophys. Union, **31**, 7 (1950).
[18] Astroph. J., **85**, 213 (1937).
[19] See F. E. Roach, H. B. Pettit, and D. R. Williams, J. Geophys. Res., **55**, 183 (1950) for an estimate of the height of the OH bands; also A. B. Meinel, Astroph. J., **112**, 120 (1950) for a discussion of intensities.
[20] Zs. Astroph., **16**, 201 (1938).
[21] Bull. Astron. Inst. Netherlands, **2**, 75 (1924).
[22] Trans. Amer. Geophys. Union, **31**, 7 (1950).
[23] See, for example, C. T. Elvey, Gassiott Committee Report published by The Physical Society of London, pp. 16-21 (1948).
[24] Paris, C.-R. Acad. sci., **226**, 1208 (1948).
[25] Phys. Rev., **33**, 412 (1929).
[26] Phys. Rev., **33**, 1046 (1929); Trans. Amer. Geophys. Union, p. 131 (1931).
[27] Phys. Rev., **34**, 344 (1929); **34**, 1167 (1929).
[28] A critical discussion of the Maris-Hulburt theory is found in Chapter 25 of Geomagnetism, by S. Chapman and J. Bartels, Oxford, Clarendon Press (1940).
[29] Mass motions of charged particles in the ionosphere have been suggested by O. R. Wulf as a possible contributor to auroral excitation; see Terr. Mag., **50**, 185 (1945).

A METHOD FOR OBTAINING THE WAVE SOLUTIONS OF IONOSPHERICALLY REFLECTED LONG WAVES, INCLUDING ALL VARIABLES AND THEIR HEIGHT VARIATION*

BY J. J. GIBBONS AND R. J. NERTNEY

Ionosphere Research Laboratory, The Pennsylvania State College, State College, Pa.

(Received April 16, 1951)

ABSTRACT

A method is presented for obtaining solutions to the one-dimensional wave equation $\pi''/\pi = -K_0^2\epsilon^2(x)$ which arises in the course of the application of the wave theory to the study of the ionosphere. The π's represent characteristic wave functions of the ionosphere, K_0 the propagation constant of free space, $\epsilon(x)$ the complex index of refraction of the ionosphere, and the primes denote differentiations with respect to the space coordinate x. The method has been applied to the following "E-layer" problem with good results.

Operating frequency	—150 kc/sec
Angle of incidence	—Normal
N (electron density)	—Chapman spatial distribution with various values of maximum electron density
ν (collisional frequency)	—Exponentially decreasing with height
H (scale height)	—10 km (constant)
Earth's magnetic field	—Evaluated at 100 km over State College, Pennsylvania
Dispersion theory	—Appleton-Hartree (Sellmeyer)

An example of the method for obtaining the wave functions and reflection coefficients is carried out in detail, and reflection coefficients are presented for five different values of maximum electron density. This method is compared with the ray optics and the W.K.B. method. The results are compared very briefly with experiment.

Introduction—In the course of the application of the wave theory to the problem wave propagation in the ionosphere it becomes necessary to obtain solutions a pair of coupled wave equations [see 1 of "References" at end of paper]. The

*This work has been sponsored in part by the Geophysical Research Directorate of the Air rce Cambridge Research Laboratories.

usual method of attack on the problem consists of neglecting the coupling term and obtaining solutions to the so-called uncoupled equations. These solutions ar then modified by variational methods to yield the solutions to the coupled pa of equations. We shall concern ourselves here with the first phase of the problem namely, the solution of the uncoupled equations.

The differential equation which we desire to solve is of the form

$$\frac{\pi''}{\pi} = -K_0^2\epsilon^2(x) \equiv -K_0^2[\mu(x) - j\chi(x)]^2 \quad \ldots\ldots\ldots\ldots\ldots\ldots(1$$

where ϵ is a complex function of x and the primes denote differentiation wit respect to x. In the case of the ionospheric problem, x will denote height in one-dimensional wave equation, K_0 the propagation factor of free space, and the complex refractive index. The π's are wave functions associated with th electric vector of the field. The exact nature of this relationship will be discusse later.

Consider a function pair of exponential form

$$\pi_{1,2} = \frac{1}{\sqrt{p}} \exp\left\{\pm j \int p \, dx\right\} \quad \ldots\ldots\ldots\ldots\ldots\ldots(2$$

We now have, writing our equation in terms of the parameter p, a pair exact solutions to the differential equation:

$$\frac{\pi''_{1,2}}{\pi_{1,2}} = -p^2 + \frac{3}{4}\left(\frac{p'}{p}\right)^2 - \frac{1}{2}\frac{p''}{p} \quad \ldots\ldots\ldots\ldots\ldots\ldots(3$$

Next consider the wave equation which we desire to solve

$$\frac{\pi''}{\pi} = -K_0^2\epsilon^2 \quad \ldots\ldots\ldots\ldots\ldots\ldots\ldots\ldots(4$$

Now, ϵ is a relatively well-behaved function; it has no singular points in th region of interest. There is, however, one difficulty; $3/4 \mid \epsilon'/\epsilon \mid^2$ and $1/2 \mid \epsilon''/\epsilon \mid$ a not much less than $\mid K_0^2\epsilon^2 \mid$ everywhere. This means that the W.K.B. solutio ($p = K_0\epsilon$) are not good approximations everywhere. Further, of course, $K_0^2\epsilon^2$ complex and, therefore, p necessarily must be complex. Let us now modify equatio (3). Let $p = kf^{1/2}e^{iv}$. In terms of f and v, we then obtain

$$Re\frac{\pi''_{1,2}}{\pi_{1,2}} = -k^2 f\cos 2v - \frac{1}{4}\frac{f''}{f} + \frac{5}{16}\left(\frac{f'}{f}\right)^2 - \frac{1}{4}v'^2 = G(f, v) \quad \ldots\ldots($$

$$Im\frac{\pi''_{1,2}}{\pi_{1,2}} = -k^2 f\sin 2v - \frac{1}{2}v'' + \frac{1}{4}\frac{f'}{f}v' = H(f, v) \quad \ldots\ldots\ldots\ldots($$

Now we have exact solutions to an equation:

$$\frac{\pi''_{1,2}}{\pi_{1,2}} = Re\frac{\pi''_{1,2}}{\pi_{1,2}} + i\,Im\frac{\pi''_{1,2}}{\pi_{1,2}} = G(f, v) + i\,H(f, v) \quad \ldots\ldots\ldots\ldots($$

We desire solutions to the equation

$$\frac{\pi''}{\pi} = K_0^2\epsilon^2 = R(x) + i\,I(x) \quad \ldots\ldots(8)$$

Now, if it were possible, we would determine f and v such that

$$R(x) = G(f, v) \quad \ldots\ldots(9)$$

$$I(x) = H(f, v) \quad \ldots\ldots(10)$$

nd we would then have exact solutions to the original wave equation. The de-ermination of f and v to satisfy equations (9) and (10) is, of course in general, ust as impossible in terms of the elementary functions and operations as was the olution of the original equation. In fact, all that our new solutions have added to he original equation is the elementary operations of integration and exponentia-ion, and the problem appears nearly as hopeless as before. This is not true, how-ver, since what we have done is to separate in the $G(f, v)$ equation the "reflection" erms $(f'/f)^2$ and (f''/f) from the linear term in f; that is, we find that in a region f small partial reflections, the term in f predominates. On the other hand, in a egion of considerable reflection, the terms in $(f'/f)^2$ and (f''/f) are the domi-ating terms. A similar situation exists in the $H(f, v)$ equation. Further, in practice 've find for the type of region $(K_0^2\epsilon^2)$ in which we shall be interested that v is such hat $\cos 2v \simeq 1$, $\sin 2v \simeq 2v$, and $(1/4)v^{12} \ll \mid G(f, v) \mid$ (except in the neighbor-ood of $G(f, v) = 0$). The condition $\cos 2v \simeq 1$ and $\sin 2v \simeq 2v$ becomes a poorer pproximation when we go deep into a reflection region, but in this case $k^2 f \cos v$ and $k^2 f \sin 2v$ have become negligible by virtue of f becoming very small, as 've shall see later; in fact, it is immediately obvious from the terms in f'', f', v'', v' nd correction terms in the W.K.B. solutions.

The problem—Let us consider now the ionospheric problem which we desire o solve. This ionospheric configuration consists of an exponential ν (collision requency) varying with a scale height of 10 km. This exponential ν is fixed in pace by assigning a value of $\nu = 0.8 \times 10^5$ sec^{-1} at 115 km. This absolute value f ν is determined at a lower height from wave interaction data. Superimposed n this ν is a Chapman N (electron density) distribution. This Chapman N is xed in space by locating the N_{max} at 115 km. The value of N_{max} is specified by ssigning a value of f_c, where f_c is the critical frequency of the equivalent collision-ree layer. Note that this is not a true Chapman N, since the diurnal and seasonal eight variation of N_{max} has been removed. The value of f_c is related to N_{max} hrough

$$\omega_c = \left(\frac{4\pi e^2 N_{max}}{m}\right)^{1/2} \quad \ldots\ldots(11)$$

hese N, ν distributions are plotted in Figure 1. The value of H_m (earth's magnetic eld) is that for State College, Pennsylvania, evaluated at 100 km. This value is .535 oersted at an angle of 70° 52′ with the horizontal. The value of operating requency is 150 kc/sec and the incidence is normal. The values of f_c which we hall consider are 0.55, 1.1, 2.2, 3.0, and 4.4 Mc.

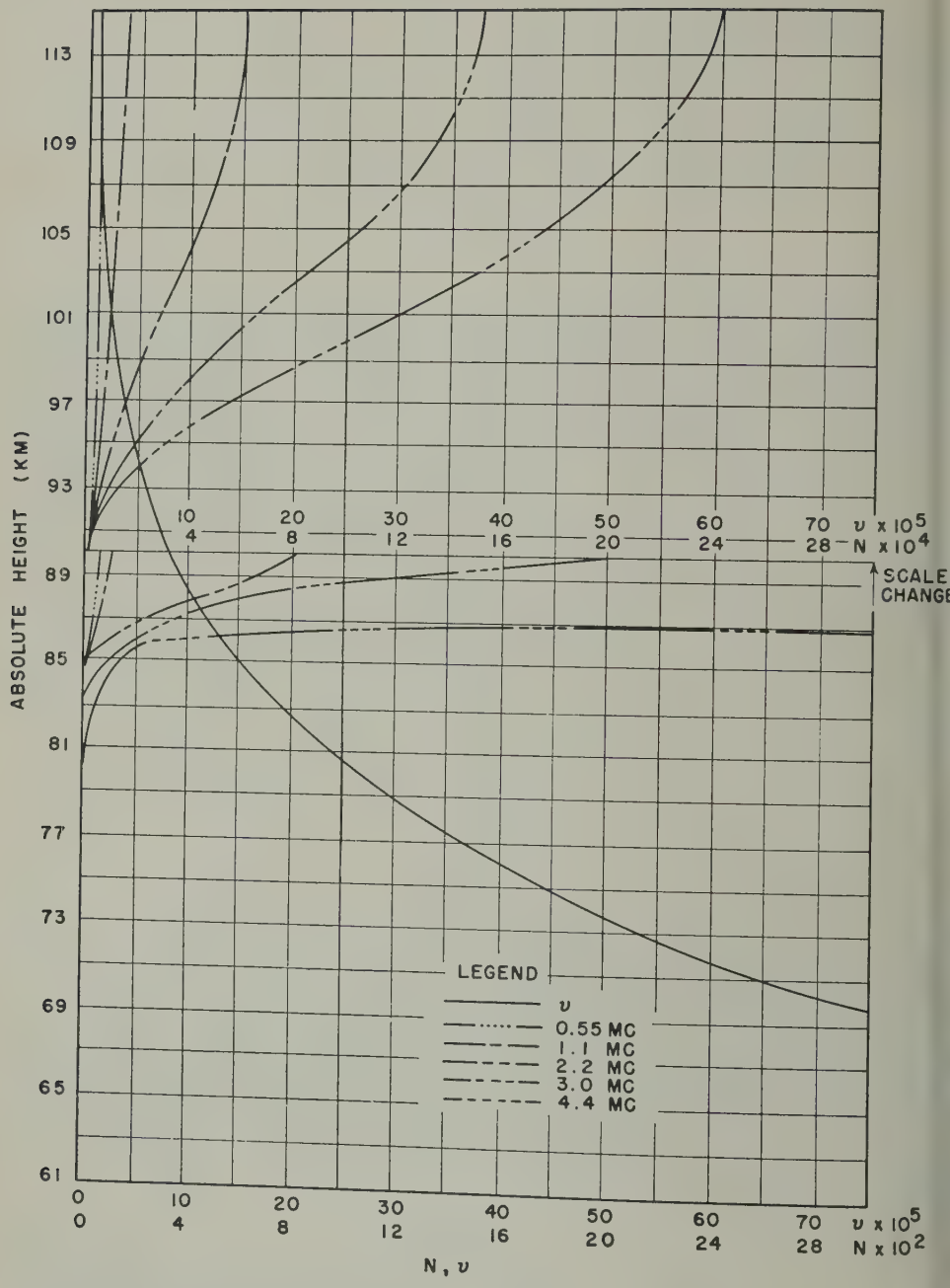

FIG. 1—Electron density (N) and electron collisional frequency (ν) as a function of height (The N distribution consists of a Chapman spatial distribution with N_{max} fixed at 115 km for all values of f_c . These N, ν distributions should represent rather typical E-layer configurations.)

As was mentioned earlier, the application of Appleton-Hartree (Sellmeyer) heory leads to a pair of "coupled" wave equations. If we neglect coupling effects, e obtain two wave equations corresponding to the so-called "ordinary" and extraordinary" components. We shall adopt the convention that a magneto-ionic component" is defined in such a manner that its polarization and index of refraction are continuous as the wave traverses the ionized medium; that downgoing omponent having left-handed polarization as it leaves the influence of the ionized nedium will be referred to as the "ordinary" component. This is possibly in conict with certain "sign conventions" for designating ordinary and extraordinary components," but seems to us a more logical method of handling the problem han allowing discontinuous behavior of a "component."

Let us now proceed to the solution of the two "uncoupled" differential equations vhich give rise to the "ordinary" and "extraordinary" waves.

The extraordinary wave—If we examine the indices of the extraordinary component, we see that $| K_0^2\epsilon^2 | \gg | \epsilon''/\epsilon |$ and $| \epsilon'/\epsilon |^2$ everywhere. This means that partial eflections are always very small and the W.K.B. approximation ($p = K_0\epsilon$) is a ood approximation everywhere.

The ordinary wave—If we examine the indices for the ordinary component, ve find that the condition $| K_0^2\epsilon^2 | \gg | \epsilon''/\epsilon |$ and $| \epsilon'/\epsilon |^2$ no longer holds everywhere nd we must have recourse to our method of solution in terms of the "p" functions.

Application—The method of application of this method shall be graphical curve tting. Our solutions, however, will be exact solutions expressed in the analytical orm of their own differential equation. That is, we shall select analytic functions and v such that $G(f, v) \simeq R(x)$ and $H(f, v) \simeq I(x)$ when $R(x)$ and $I(x)$ are lotted as functions of the variable x alone. We then obtain exact solutions of a ifferential equation, which is nearly the equation we desire to solve. This method f curve fitting is, it seems, the logical way to attack the problem because of the esponse of the magneto-ionic medium "im grosse" to the "wave theory" treatnent. That is, we shall produce exact wave solutions for a medium whose plotted ndex values are very similar to the plotted values of the medium for which we esire solutions. We are not seeking to match the medium at specific points such s "reflection points" but rather to obtain similar gross characteristics. This nethod has the obvious limitation of destroying the explicit functional relationship etween the solutions and the various parameters other than x. This, however, s made necessary by the extremely complicated nature of the complete Appleton-Iartree dispersion equation. It is difficult to imagine the existence of any approximate solution which does not require differentiation and/or integration on ϵ vhich would require numerical processes for obtaining ϵ' and $\int \epsilon \, dx$. These numerical processes would, of course, destroy the functional relationship as effectively s our method.

An example—The method is best illustrated by an example. If we consider a ypical E-layer index, as obtained from the Appleton-Hartree equation with xponential ν and Chapman N, we find that these curves have the same general iape for all the f_c's considered. Now, the order of procedure in applying our nethod is important, but the order and the general form of the f, v functions emain the same for all problems of this general type. For convenience we shall

measure the space coordinate x in kilometers with respect to 85-km absolut height.

First, we shall consider matching $G(f, v)$ to R. Let us anticipate two facts which will later be established, namely, that $\cos 2v \simeq 1$ in the region where th term in $(f \cos 2v)$ is of appreciable magnitude, and secondly that $1/4(v'^2)$ is every where small compared with $R(x)$ [except in the neighborhood of $G(f, v) = 0$ of course, and the only effect there will be a slight shift of the zero]. Then th equation to be satisfied by $f(x)$ is

$$R(x) = -K_0^2 f - \frac{1}{4}\frac{f''}{f} + \frac{5}{16}\left(\frac{f'}{f}\right)^2 \quad \ldots\ldots\ldots\ldots\ldots\ldots (12)$$

Now, let us first select an f_1 , $f_1 = k(a - x)^l$; now, if we refer to Figure 2 for $f_c = 3.0$ Mc, we see that this approximation is a good one to the left of $x = b$ if $k = 2.57, l = 1/4$ and $a = 5.9$. In general, we may adjust the curvature of $G(f)$ with the parameter l and the position of the steep trailing edge with a. Now that k and f have been selected, let us proceed to select an f_2 which will join "smoothly" on f_1 at $x = d$ and provide a $G(f, v)$ which will match R in the region to the right of $x = g$. We shall use the function $f_2 = Ae^{mz^2}$ where $z = (x - c)$. Now, by properly choosing A, m, and c, it is possible to match f_1 and f_2 at $x = d$, $g < d < b$, such that, $f_1(d) = f_2(d)$, $f_1'(d) = f_2'(d)$, and $G(f, v)$ clings to $R(x)$ in the region $x > g$. These values are $A = 0.9$, $m = -2$, $c = 5.30$. Immediately the objection may be raised that a match of f and f' is not sufficient since we have a second-order differential equation. It is true that a slight discontinuity in the "index" arises by virtue of the terms in f'', but this is very small since (1) we are coupling the solutions in a regon where $f_{1,2}''$ is quite small and (2) f_1'' and f_2'' are nearly equa because of the coincidence of the knees of the f_1 and f_2 curves in the neighborhood of d. In effect, we have worked a boundary value problem across a small discontinuity in the index. The effect of this may be shown to be small.

Now proceed to the imaginary match in Figure 3. Three "v" functions are necessary; v_1 , v_2 , and v_3 . The first, v_1 , is very simple to evaluate. This is the which is valid in the region where the W.K.B. solution is a good approximation and is equal to

$$v_2 = \frac{I}{-2k^2 f} \quad \ldots\ldots\ldots\ldots\ldots\ldots\ldots\ldots (13)$$

The v_3 function is valid in the region where the f_2 appearing in the first term of $H(f, v)$ has caused this term to become very small compared to the terms in v' and v''. The form of this function is

$$v_3 = -py + e \quad \ldots\ldots\ldots\ldots\ldots\ldots\ldots\ldots (14)$$

where $e = 3.185$, $p = 0.539$, and $y = x$ for this example.

This function will cause $H(f, v_3)$ to cling to I in the region to the right of some point i. These two v functions are then joined by some bridging function v_3 . The function matches v_3 such that $v_3(j) = v_2(j)$ and $v_3'(j) = v_2'(j)$, where $j > i$. The match on v_1 is such that $v_1(k) = v_2(k)$, where k is a point in the region for which

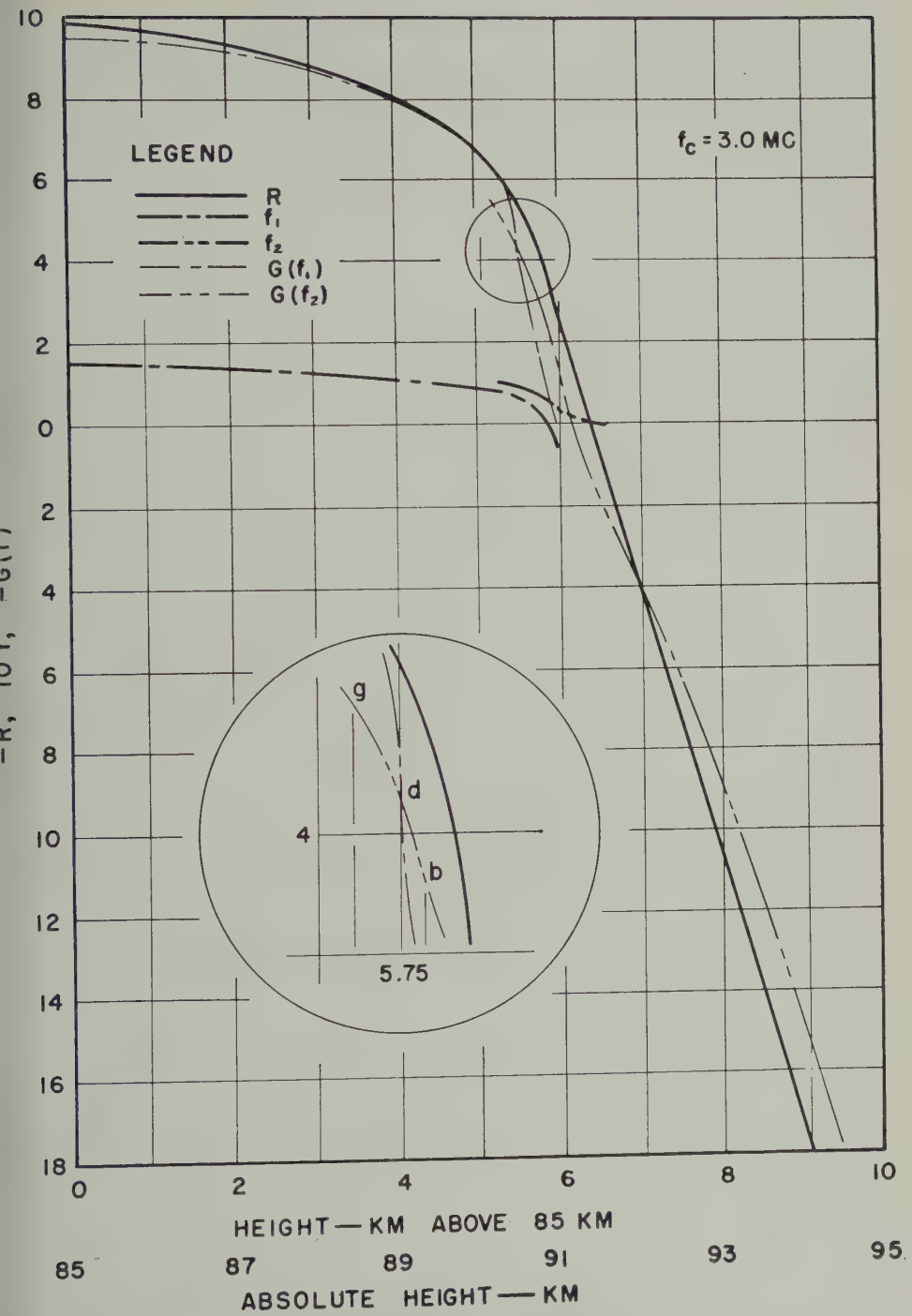

FIG. 2—The matching problem for $Re\,[-K_0^2\epsilon^2]$

(The quantities $-R = Re\,[-K_0^2\epsilon^2]$, $-G(f)$, and f are given as functions of height. The coordinate "x" is measured with respect to 85 km.)

v_1 is a good approximation. The only requirement on the derivatives at k is that $v_2'(k)$ and $v_2''(k)$ be small.

A hyperbola asymptotic to v_3 and the tangent to $v_1(k)$ is usually a good bridging function. Once this hyperbola has been determined we may discard v_2 , since it served only as a construction line for the hyperbola v_3 .

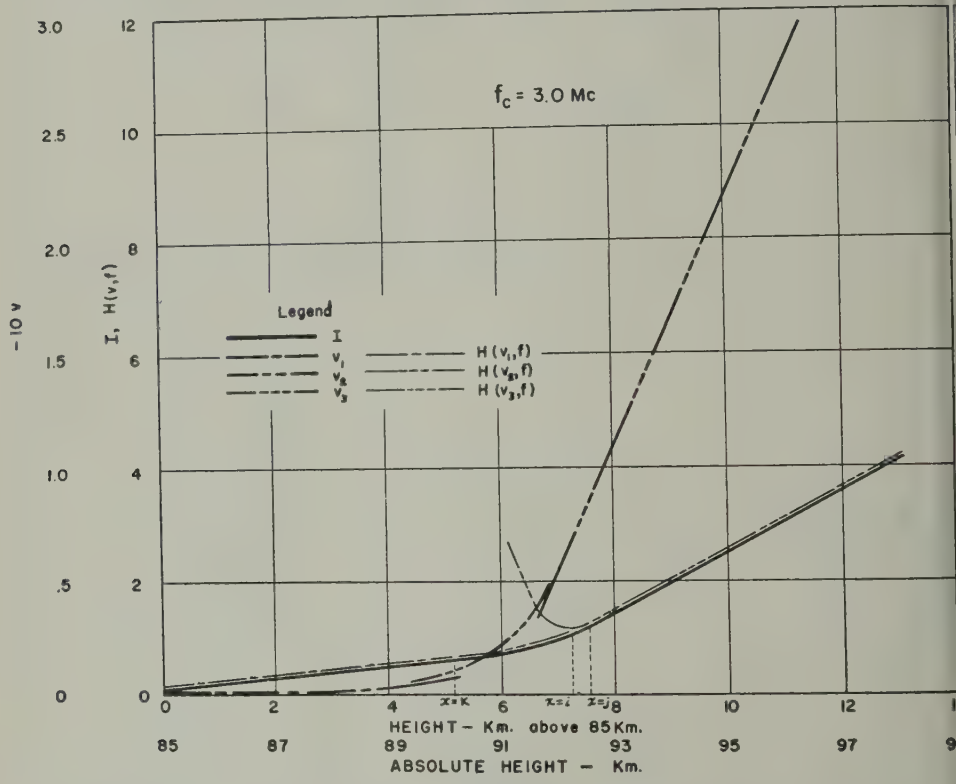

FIG. 3—The matching problem for $Im\,[-K_0^2\epsilon^2]$
(The quantities $I = Im\,[-K_0^2\epsilon^2]$, $-H(v, f)$, and v are given as functions of height. The coordinate "x" is measured with respect to 85 km.)

The same arguments concerning the small discontinuities introduced by f' and f'' in $G(f, v)$ hold also for $H(f, v)$, since $v_2''(j)$ and $v_3''(j)$ are very nearly equal to zero.

We now have determined f_1 , f_2 , v_1 , v_2 , v_3 such that $G(f, v) \simeq R$ and $H(f, v) \simeq I$ in a region extending several kilometers to the right of the point where $(K_0^2\epsilon^2) = 0$.

Now, let us consider the solutions π_1 and π_2 written in terms of f and v.

$$\pi_{1,2} = \frac{1}{kf^{1/2}(1 + iv)^{1/2}} \exp\left\{\pm j \int kf^{1/2}(1 + iv)\, dx\right\} \quad \ldots\ldots\ldots (1$$

(since $\sin v \simeq v$ and $\cos v \simeq 1$)

We may now examine the solutions to determine the effect of the approximations on the validity of our solutions. Consider the function p. This function appears in two roles in our solution, namely, (1) as the phase and damping integral in the exponential, and (2) as a complex multiplier on the exponential. Now the phase and damping integral constitutes the "memory" of the solution and the complex multiplier is a "memoryless" function which depends explicitly only on the value of f and v at the point in the medium. Therefore, for purposes of obtaining reflection coefficients, it is important to know f and v and their two derivatives accurately at any matching points; other than this, the important thing is that the integral of $kf^{1/2}$ and $kf^{1/2}v$ through the region of interest be known quite accurately. The magnitude of the error in determining the reflection coefficient may be estimated roughly by distorting the f and v curves and noting the effect on the $G(f, v)$ and $H(f, v)$ curves. This has been done for the examples given here, and indications are that the absorptions are in error at most by ± 0.1 neper and the phases are at most ± 0.1 radian in error. The effect of the mismatch

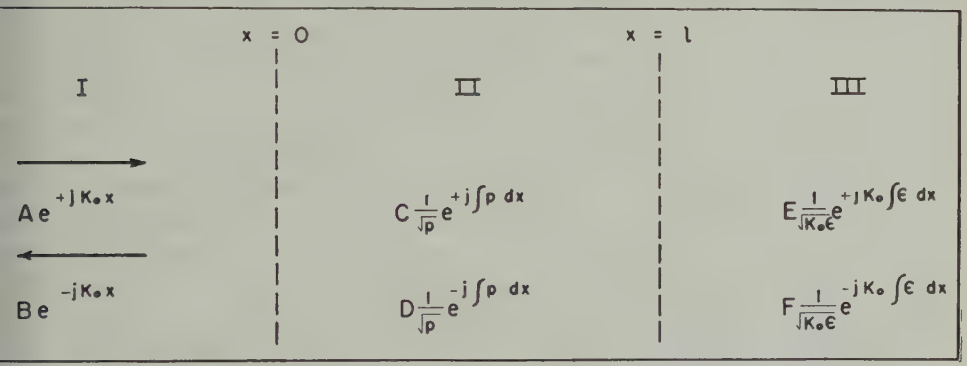

FIG. 4—The boundary value problem for the determination of the reflection coefficient (The form of the solution to be used in each of the regions is indicated.)

on f'' and v'' has also been examined. The effect of this mismatch is to cause the index to change discontinuously as we shift from, say, the f_1 function to the f_2 function. It was pointed out earlier that this effect is small. For example, the magnitude of this effect in the f_1 , f_2 match is to cause the real part of the index to change discontinuously on the order of hundredths of units in a region where it should be varying continuously with a derivative of about 1 unit—km^{-1}. The magnitude of the real part of the index at this point is around 0.4, so that the *relative* discontinuity is small. A qualitative test which may be performed to determine the effect of this mismatch is to change the match point on the f_1-f_2 functions so as to change the magnitude of the mismatch. The mismatch may be increased by a factor of two or greater from that which was obtained in the example without changing the reflection coefficient a measurable amount. In view of the present knowledge of the ionosphere and existing experimental techniques, the procedure should be sufficiently accurate to compare postulated N, ν distributions with experimental results. These tolerances can be reduced in the future by more careful curve fitting if this becomes necessary.

Reflection coefficient—We now desire to determine the reflection coefficient o the layer from these solutions. We shall obtain the reflection coefficients by workin an appropriate boundary value problem on the π functions. This boundary valu problem is represented schematically in Figure 4.

These π functions in regions II and III are not the ordinary electromagnetic field components. Since we are interested in obtaining answers in terms of, say the electric vector **E** which we may measure with our receiving equipment, a word is in order regarding the connection between the π functions and the electric vector of the electromagnetic field.

Let us use the notation of Rydbeck [1] with the exception that now the x axis denotes the direction of propagation, the y axis is transverse to the earth's magnetic field, and the z axis is longitudinal to the earth's field.

It may be shown for our "ordinary" wave that $E_y = (1 - u^2)^{-1/2}\pi$, where $u = E_z/E_y$ is the characteristic polarization of the "ordinary" magneto-ionic component; and we may obtain the electric vector at any point from these two relations. As we approach the lower surface of the layer, it becomes necessary to introduce the concept of "limiting polarization." This "limiting polarization" attains at some point in the layer where the perturbing effect of the electrons becomes so small as to produce no further measurable effect on the wave's polarization as the wave travels down through space to the receiver. Booker [3] has indicated theoretically the existence of such a phenomenon, and we have further experimental and theoretical evidence of this. In this case, let us place a further restriction on the origin of x, $x = 0$ in Figure 4. Let this restriction be that the origin is sufficiently far to the left that u is essentially constant. Finally, we assume that u and u' are everywhere continuous in x. We now see that our condition of maintaining continuity on π and π' (through the continuity on p and p') is sufficient, along with the continuity of u and u', to insure proper behavior of the **E** and **H** field vectors, and the reflection coefficient deduced for the π functions is exactly that which will be experienced by an electromagnetic wave incident from below the layer polarized with the "ordinary" polarization.

Since the special type of boundary value problem is determined by the particular ionospheric configuration, we shall make certain simplifying assumptions peculiar to all the problems for which we present results here. The extension to more general cases is obvious. In order to do this, let us divide the ionosphere into three regions: I, II, III. Region I is a region near the bottom of the layer where the ionization has become so small that we may use the free space solutions $e^{\mp jK_0 z}$. Region II is included in the region for which we have constructed "p" solutions. It will be specifically defined later; the only requirement at present is that the "p" solutions are defined everywhere in II. Region III is a region in which the W.K.B. solutions are valid. Again, this region will be defined specifically later. At present, the regions I, II, and III may overlap, so we let the coordinate system be defined such that $x = 0$ is the boundary between regions I and II and $x =$ between regions II and III. Next, consider the boundary value problem as indicated in Figure 4. Note again that the lower limit on the integral for each wave solution is arbitrary because of the arbitrary coefficients on the solutions. Let us match on π and π'. At $x = 0$

$$\pi : A + B = C + D \quad \ldots\ldots(16)$$

$$\pi' : jK_0A - jK_0B = j\sqrt{p}\,C - j\sqrt{p}\,D + S(p') \quad \ldots\ldots(17)$$

here $S(p')$ includes the terms in p' arising from the differentiation.

At $x = l$

$$: C\frac{1}{\sqrt{p}}\exp\left\{+j\int_0^l p\,dx\right\} + D\frac{1}{\sqrt{p}}\exp\left\{-j\int_0^l p\,dx\right\}$$

$$= E\frac{1}{\sqrt{K_0\epsilon}} + F\frac{1}{\sqrt{K_0\epsilon}} \quad \ldots\ldots(18)$$

$$' : jC\sqrt{p}\exp\left\{+j\int_0^l p\,dx\right\} - jD\sqrt{p}\exp\left\{-j\int_0^l p\,dx\right\}$$

$$-\frac{C}{2}p^{-3/2}p'\exp\left\{+j\int_0^l p\,dx\right\} - \frac{D}{2}p^{-3/2}p'\exp\left\{-j\int_0^l p\,dx\right\}$$

$$= jE\sqrt{K_0\epsilon} - jF\sqrt{K_0\epsilon} - \frac{E}{2}\frac{\epsilon'}{K_0^{1/2}\epsilon^{3/2}} - \frac{F}{2}\frac{\epsilon'}{K_0^{1/2}\epsilon^{3/2}} \quad \ldots\ldots(19)$$

Now consider E and F. For all the examples presented here we find that for l ufficiently large $\epsilon \simeq 0 - j\chi(x)$. Let us assume that there are no other "close" eflection regions. "Close" will be defined in terms of $\chi(x)$, that is, a "distant" eflection region will be one so distant that $\int \chi(x)\,dx$ is large enough so that the ave transmitted through the plane at l will be negligible upon its return from ny reflection region to the right. We shall also assume that there are no "close" egions of classical transmission. These assumptions are made because they are ufficient for our immediate problems. The effect of such "close" regions is to omplicate the boundary value problem. These conditions will hold for the cases f interest. This being true, we set the coefficient of the positive exponential $=0$, hat is, $E = 0$ (in this region $u \simeq$ constant; $\pi \simeq$ constant $\times E_z$).

Further, by proper selection of the origin, $S(p')$ may be made as small as we ke. As this is done, $\sqrt{p}$ approaches K_0 and equations (16) and (17) fall out as n independent set

$$A + B = C + D$$

$$A - B = C - D$$

$$A = C$$

$$B = D$$

Now, nothing has been said about the validity of the W.K.B. solutions in gion III. At present III is defined such that $\epsilon \simeq 0 - j\chi(x)$. Let us further ecify that $|(\chi'/\chi)^2|$ and $|\chi''/\chi|$ must be $\ll |K_0^2\chi^2|$. Again, in all of our E-layer roblems, there exist such regions for sufficiently large l.

Now consider the equations (18) and (19). For all our examples the behavior of p and ϵ are such that in equation (19) the terms containing p' dominate on the left side of the equation and the terms *not* containing ϵ' dominate on the right at $x = l$. Then equations (18) and (19) reduce to

$$C \frac{1}{\sqrt{p}} \exp\left\{+j \int_0^l p \, dx\right\} + D \frac{1}{\sqrt{p}} \exp\left\{-j \int_0^l p \, dx\right\} = F \frac{1}{[-jK_0\chi(x)]^{1/2}} \quad \ldots (20)$$

$$-\frac{C}{2} \frac{p'}{p^{3/2}} \exp\left\{+j \int_0^l p \, dx\right\} - \frac{D}{2} \frac{p'}{p^{3/2}} \exp\left\{-j \int_0^l p \, dx\right\} = -jF\sqrt{-jK_0\chi(x)} \quad \ldots (21)$$

Eliminating F, we see that

$$-\frac{C}{D} = \exp\left\{-2j \int_0^l p \, dx\right\} \quad \ldots (22)$$

From (21), $F = 0$. Now F is not truly zero. This result comes about in going from equation (19) to equation (21). Inclusion of the terms not containing p' will give a small F but will not effect the reflection coefficient appreciably. The reason for coupling the "p" solutions to W.K.B. solutions is as follows: If we examine the behavior of the "p" solutions, we see that, as we go deeply into the region III, the p becomes very small and we have (examining the Wronskian) a degeneracy on the linear independence condition. As a result it becomes difficult to work with these solutions in region III, since the total wave function is acquired by obtaining the difference between the two linearly independent wave functions whose numerical values are very large and whose variations are very nearly equal. Now we may use *any* pair of linearly independent solutions and it is convenient to use the W.K.B. solutions. The linear combination of the W.K.B. solutions is, of course, identical with the linear combinations of the "p" solutions (to the degree of approximation involved).

Now, we have already determined that $A = C$ and $B = D$. The reflection coefficient of the layer then is

$$R = \frac{A}{B} = \frac{C}{D} = -\exp\left\{-2j \int_0^l p \, dx\right\} \quad \ldots (23)$$

or in terms of f and v

$$R = -\exp\left\{-2j \int_0^l kf^{1/2}(\cos v + i \sin v) \, dx\right\} \quad \ldots (24)$$

Results—The quantities $kf^{1/2}$ $(\cos v) \simeq kf^{1/2}$ and $kf^{1/2} \sin v \simeq kf^{1/2}v$ are shown in Figures 5 and 6, respectively. The results of planimetric integrations on these quantities are indicated in Table 1. The values of absorption are tabulated in the form log ρ, since this is the usual method of presenting E-layer absorptions. The phase change on reflection is tabulated including the "$(-)$" sign in equation (23), but this is removed when the phase heights are calculated. This is done since the behavior of our reflection seems to be more similar to metallic reflection with phase reversal than to the "high pass filter" type phase change on reflection of $\pi/2$. This may be seen by examining the behavior of the boundary value problem

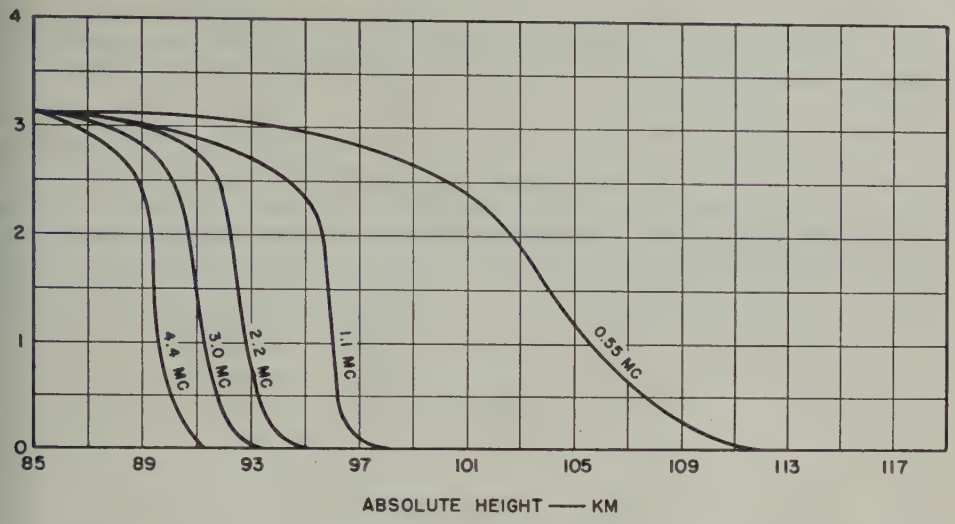

FIG. 5—The phase integrands
(The quantity $2\int_0^l kf^{1/2}\,dx + \pi$ yields the phase angle φ of the reflection coefficient $R = \rho e^{i\varphi}$. This quantity is shown as a function of height for the various N distributions of Fig. 1.)

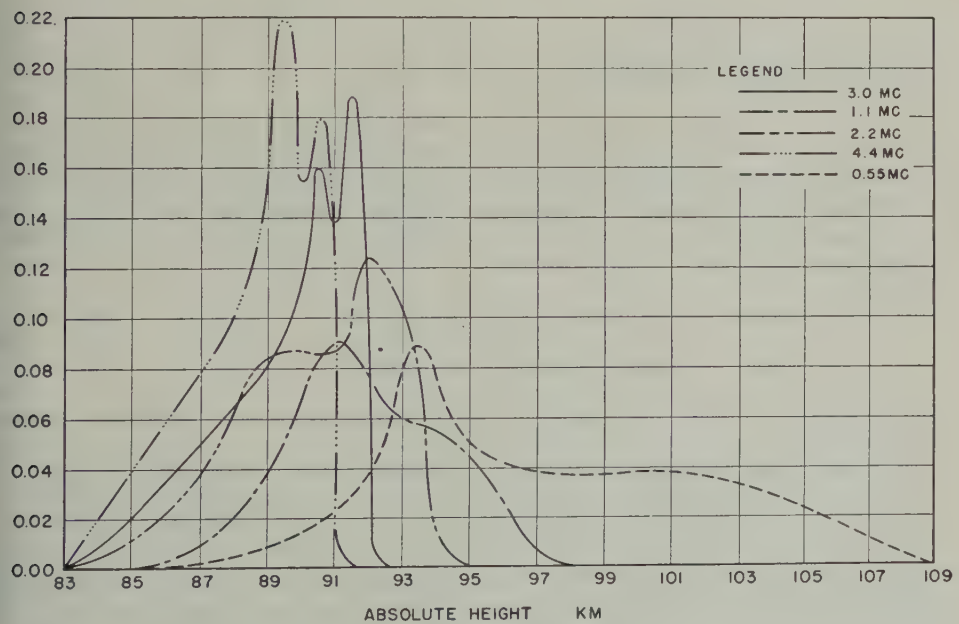

FIG. 6—The absorption integrands
(The quantity $2\int_0^l kf^{1/2}\,v\,dx$ yields the absorption log ρ of the reflection coefficient $R = \rho e^{i\varphi}$. This quantity is shown as a function of height for the various N distributions of Fig. 1.)

as we introduce a metallic reflector at the lower surface of the ionosphere and allow it to move upward through the reflection region. This technique also shows us that there is no ambiguity regarding the number of "full wave-lengths" of phase path in the medium.

TABLE 1—*Tabulated results (E-layer characteristics)*

(The quantities log ρ and φ of the reflection coefficient $R = \rho e^{i\varphi}$ are tabulated for the five ionospheric configurations considered. The phase heights are also indicated. The "phase height" is the height at which a metallic reflector would have to be placed in free space to result in a similar phase change.)

f_c	Ordinary component		Phase height†
	Reflection coefficient		
	log ρ	Phase shifts* (from 85 km)	
Mc/sec	*nepers*	*radians*	*km*
0.55	1.50	$57.5 + \pi$	103
1.1	1.0	$31.2 + \pi$	95
2.2	1.25	$22.5 + \pi$	92
3.0	1.25	$17.8 + \pi$	91
4.4	1.50	$13.0 + \pi$	89

*Including a reversal of sense on the electric vector $\Delta\varphi = \pi$.
†Not including the above phase reversal.

Comparison with other methods—The question immediately arises as to how this scheme compares with other common methods of solution. With this in mind, let us digress for a moment to discuss the W.K.B. method. The "W.K.B. method of solution" has several connotations, but we shall refer first to solutions of the W.K.B. *form*

$$\frac{1}{\sqrt{\epsilon}} \exp\left\{\pm j \int \epsilon \, dx\right\} \quad \ldots\ldots\ldots\ldots\ldots\ldots\ldots\ldots (25)$$

used as a pair of solutions to our wave equation without recourse to bridging functions.

Let us consider two regions, I and II of constant $\epsilon = \epsilon_0$, extending to $x = \mp\infty$ respectively, which are connected by a region III of variable $\epsilon(x)$ joining smoothly on the two regions of constant ϵ_0. Now, if we consider a wave traveling to the right in semi-infinite region I and perform a boundary value problem to determine the reflection coefficient (remembering that there is no downgoing wave in the region III and that $\epsilon(x) \to \epsilon_0$ and $\epsilon'(x) \to 0$ as we go from region III to regions I and II), we find that there is no downgoing wave in region I and the reflection coefficient is always zero. Further, the wave experiences in traversing the layer phase and amplitude changes given by exp $\{\pm jK_0 \int \epsilon(x) \, dx\}$, exactly the ray optical result. This result is obviously incorrect. Since $\epsilon(x)$ is perfectly arbitrary

t is well known that reflections may occur from minima in the indices of refraction, and in fact it is this type of reflection with which we are usually concerned in our onospheric studies. The reason for this incorrect value of the reflection coefficient ies in the fact that, as soon as the *relative* changes in the index $| \epsilon'/\epsilon |^2$ and $| \epsilon''/\epsilon |$ become large compared to $| K_0^2 \epsilon^2 |$, the W.K.B. solutions became solutions to another lifferential equation quite different from our wave equation. This may be seen by substituting the solutions directly into the wave equation. In other words, the so-called "impedance matching" factor $1/\sqrt{\epsilon}$ introduces no improvement over the ray optical treatment in a problem of this kind. We may, of course, in many cases determine the dissipative portion of the reflection coefficient by locating the zeros of the index ϵ in the complex distance plane and using the methods of contour

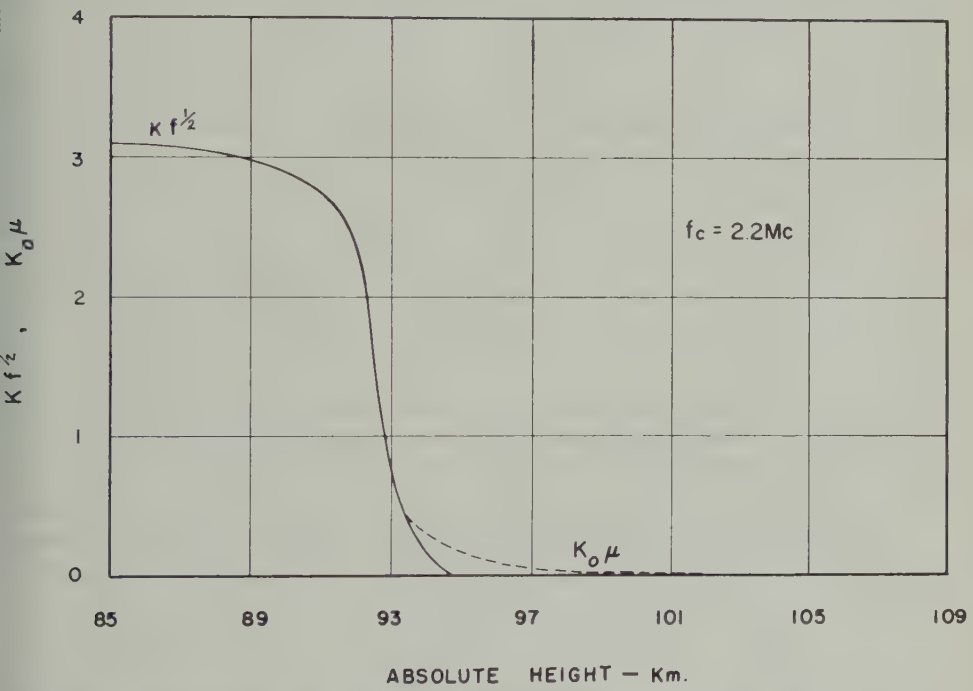

FIG. 7—The comparison of the "p-solution" phase integrand $kf^{1/2}$ with the quantity $K_0\mu$ for a typical ionospheric configuration

(It may be noted that the ray optical result for phase change on a wave $\Delta\varphi = \int_a^b K_0\mu \, dx$ is very nearly equal to the p-solution result $\Delta\varphi = \int_a^b kf^{1/2} \, dx$. There is no "reflection point" defined for the ray optical case with collisions, however.)

ntegration, but this is fraught with computational difficulties both in obtaining he values of the indices as functions of the complex variable z and in the applica- ion of the method in a practical case. Further, if we wish to obtain the phase of he reflected wave, it becomes necessary to bridge the region in which $| \epsilon'/\epsilon |^2$ nd $| \epsilon''/\epsilon |$ become large with wave functions which do not depend for their validity on the condition $| K_0^2 \epsilon^2 | \gg | \epsilon'/\epsilon |^2$ and $| \epsilon''/\epsilon |$, which is similar in principal to our method of solution.

The phase and absorption integrals obtained from the ray optical treatment (or an attempt to use solutions of the W.K.B. form which give the same result) are compared with the results of using our "p" solutions in Figures 7 and 8.

Let us examine the form of $kf^{1/2}$. This is the quantity which must be integrated to yield the phase path. This is not too different from the ray optical result (see Figure 7). The absorption integrals are quite different, however, as is seen in Figure 8. If we examine the quantity $kf^{1/2}v$, we find good agreement between $kf^{1/2}v$ and $K_0\chi$ till we approach the reflection point. In fact, the first maximum

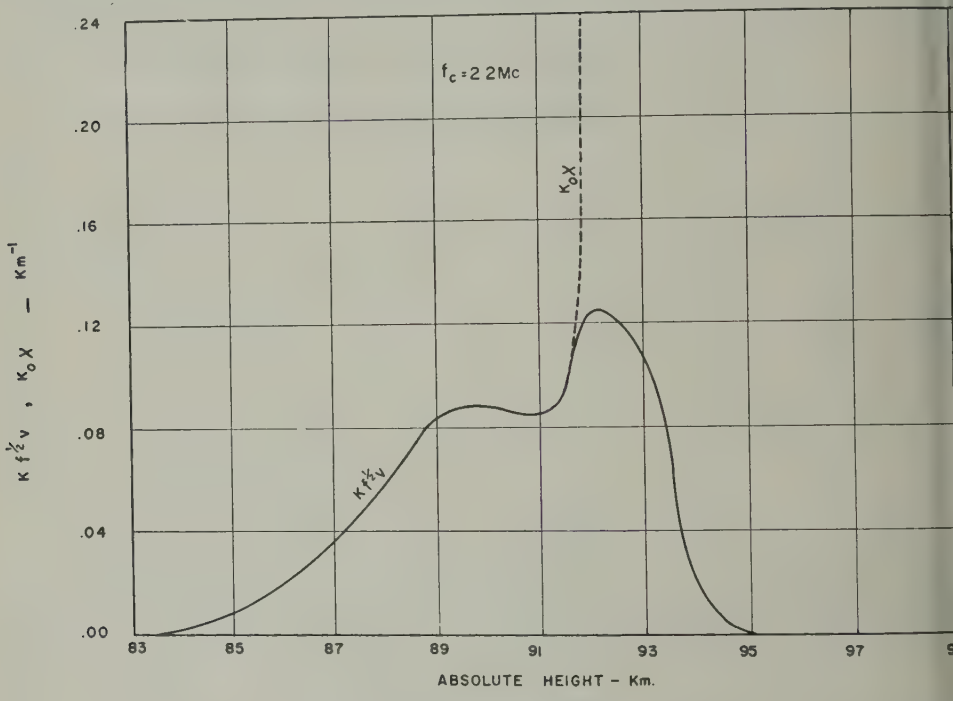

FIG. 8—The comparison of the "p-solution" absorption integrand with the quantity $K_0\chi$ for typical ionospheric configuration

(It may be noted that the ray optical result for absorption $\log \rho = \int_0^l K_0\chi \, dx$ is very nearly equal to the "p-solution" result $\log \rho = \int_0^l kf^{1/2} v \, dx$ until we enter a region of considerable reflection. The effect of the "p-solutions" is to terminate this integral as the wave diminishes due to partial reflections.)

in $kf^{1/2}v$ arises directly from a corresponding maximum in χ itself. We see now however, that the effect of the "p" functions is to terminate the absorption integral by causing the integrand to go to zero. The second maximum in the integrand arises for the following reason. Remember that these integrals represent an effect coupled to the lower face of the layer, that is, they represent the impedance of the entire layer as seen by a wave incident on the lower face. Now the absorption represents the ability of the medium to extract energy from a wave incident on the lower face. We have two effects as we enter a region of reflection; (1) due to the increase in N, with ν remaining relatively large, the medium has a great

ility to extract energy from a wave of given amplitude, an (2) due to partial flections, less of the wave is present as we go deeper into the reflection region. his means that the energy extracted from the incident wave by a given path ngth Δh becomes small, that is, the energy density deep in the reflection region ecomes so small as to become incapable of effecting the wave pattern below the yer. The reflections then result in a decoupling effect.

Since the first of these effects tends to increase the absorption and the second decrease it, the net result is the second maximum observed in the absorption tegrands.

Comparison with experiment—The comparison of our results with experiment ill be reported in detail in a following paper, but it seems that a few words re-arding this point would be in order.

In the first place, it is immediately obvious to anyone familiar with *E*-layer bsorptions that these values are far too low. The phase heights seem to be fairly nsistent with the experimental data, but exact comparison is impossible at the resent time because of the difficulty in comparing these results with the experi-ental group (or better "signal") heights. The theoretical phase heights are in eneral slightly less than the mean experimental signal heights, which is con-stent with ionospheric dispersion theory in sense.

The discrepancy in the absorption results, along with certain other experi-ental evidence which includes 150-kc/sec vertical incidence polarization results, 50-kc/sec short-range oblique incidence results, 16-kc/sec absorption results, and 6-kc/sec height results, has led us to postulate an electron "*D*-layer" lying below he *E*-layer. This study is being conducted presently and work on two preliminary -layer configurations makes it seem likely that a *D*-layer model may be con-ructed which will be consistent with the experimental evidence indicated above.

Acknowledgments—The authors wish to express their appreciation to Dr. A. H. Vaynick for his advice and assistance in this work, and also to Mrs. Pearl Laird or assistance in programing and carrying out the numerical calculations.

Portions of this work are to be submitted by R. J. Nertney in partial fulfillment f the requirements for the Ph.D. degree in the Department of Physics, the ennsylvania State College.

References

[1] O. E. H. Rydbeck, On the propagation of radio waves, Trans. Chalmers Univ., No. 34 (1944).

[2] G. N. Watson, Bessel functions, 2nd ed., Macmillan Co., New York (1944).

[3] H. G. Booker, Oblique propagation of electromagnetic waves in a slowly-varying non-isotropic medium, Proc. R. Soc., A, **155**, 235-257 (1936).

THE *D*-LAYER OF THE IONOSPHERE

BY A. P. MITRA

Institute of Radiophysics and Electronics,
University of Calcutta, India

(Received May 9, 1951)

ABSTRACT

This paper discusses in two parts the lowermost region of the ionosphere, namely, the *D*-layer. In Part I, a résumé of the present state of our knowledge is given. In Part II, new theoretical studies are made on the formation and structure of the layer, based on contemporary knowledge. It is assumed that the *D*-layer is produced by ionization of O_2 at the first ionization potential, as first suggested by S. K. Mitra, *et al.* The number densities of electrons and ions are calculated for various heights, taking due account of the variations of atmospheric temperature and effective recombination coefficient with height. The number density distribution of electrons does not show any maximum; that of ions, however, gives a maximum at nearly the same height as that of the rate of ion production. The distributions obtained have been used to give (*i*) the variation of reflection height with solar zenith angle (for long and very long waves), and (*ii*) values of the coefficient of reflection for various frequencies at the low frequency range.

INTRODUCTION

The idea that there might exist a layer of ionization below the *E*-layer is as l as our knowledge of the several ionospheric layers. Experimental investigations the ionosphere, such as propagation of long and very long waves, absorption of ves reflected from the *E*-layer, multiple reflection of atmospherics received in ytime at great distances from the source, all indicate the existence of such a er. But, compared to the other layers, *E*, *F*1, and *F*2, our knowledge about e *D*-layer is very vague and insufficient. This is because direct experimental nding of this layer is seldom possible. As a matter of fact, the little knowledge at we possess comes mainly from indirect experimental sources. How scanty our owledge is will be evident from the fact that we do not even know if the ionization tribution in the *D*-layer has a definite maximum or not. This insufficiency of owledge is particularly deplorable, as the layer is believed to exercise immediate ntrol on the propagation of radio waves, especially the long and very long waves,

and is the only available reflecting layer during a fade-out. A fuller study of the *D*-region is thus very necessary for both theoretical and practical reasons.

In view of the above, a detailed study of the region is proposed to be made in this paper. This will be in two parts. In the first part, a résumé of the present state of our knowledge of this layer will be given, for the reason that the little information we possess of the *D*-layer is still mostly scattered. In the second part, an attempt will be made to develop a theory of the formation of the *D*-layer based on contemporary knowledge.

PART I

PRESENT STATE OF KNOWLEDGE OF THE *D*-LAYER

1—*Two types of D-layer*

The recorded observations of the *D*-layer show as though there are two types of *D*-layer, one normal or regular and the other sporadic.

(*i*) *The normal type*—The normal type is an ionospheric layer below the *E*-layer. It is effective in daytime for the propagation of very long waves* and is evidently the more important type. Pfister [see 1 of "References" at end of paper] places the maximum of negative ion concentration of the layer at a height of about 60 km. According to Bates and Seaton [2], the electron concentration has a base at about 75 km and a maximum at about 90 km.

(*ii*) *The sporadic type*—This type is observed mainly in the tropics at about the 60-km level in the frequency range of 1.0 to 3.5 Mc/sec. This type was first observed by the Indian workers [3], and has, since then, been reported by many other observers. These observations have been summarised by Ellyett [4]. The behavior of the sporadic *D*-echoes are yet ill-understood, and, in many cases, there is considerable divergence of evidence. From extensive experiments at Picrain Islands, Ellyett concludes that the sporadic *D*-layers show both a summer and a winter minimum of activity. It has also been reported that this type of the *D*-layer is appreciably absorbing (*E*-echo strength was observed to weaken with increase in *D*-echo strength). Night-time sporadic *D*-echoes have also been reported [4]. It is clear that the sporadic *D*-layer cannot be considered as homogeneous in character.

2—*Experimental investigations regarding the D-layer*

(*a*) *Long and very long wave propagation data*—One of the most fruitful methods of studying the lowermost regions of the ionosphere—the region of the *D*-layer—is to study the propagation characteristics of long and very long waves incident obliquely or normally. Such studies were started in England before the last Great War. An extensive discussion is given by Bracewell and others (Cambridge) in reference [8]. They are now being made also in the U.S.A. and in Germany. Unfortunately, much of the data collected have not yet been properly interpreted

*Waves of length between 1 and 10 km (frequencies between 300 and 30 kc/sec) are called "long" and those of length greater than 10 km (frequencies less than 30 kc/sec) are called "very long."

This is because, due to the great length of the waves, the comparatively simple ray treatment of the wave propagation phenomena is not applicable.

A summary of the main results obtained, as have bearing on the *D*-layer, is given below.

(*i*) *Ionization density*—From the propagation data of waves of frequency 16 kc/sec, Budden, Ratcliffe, and Wilkes [6] estimated that the number density of electrons at the reflection level was about $2 \times 10^2/cm^3$. Weekes, in a private communication to Bates and Seaton [2] reports that the most recent work gives a slightly different value of $2.5 \times 10^2/cm^3$. Bremmer's calculations [7], however, give a much larger value ($2.5 \times 10^3/cm^3$; see Table 1).

(*ii*) *Reflection height*—The very long waves are found to be reflected from the range of heights 70–80 km during the day (Table 1) and 90–95 km during the night. The daytime reflection is assumed to occur at the tail of a Chapman region. The reflecting height varies with the solar zenith angle. At vertical incidence, the law of variation is similar to that for regions *E* and *F*1 (Table 1), namely

$$h(\chi) = h_0 + H(t) \log f(\chi)$$

where $h(\chi)$ and h_0 are the apparent heights of reflection for $\chi = \chi$ and $\chi = 0^0$, and $f(\chi)$ is the Chapman function of χ, being approximately equal to sec χ for $\chi < 85°$. A closer inspection, however, showed that the height variations are not quite symmetrical about midday and the straight lines obtained for afternoon readings do not correspond exactly to those obtained with morning readings. On higher frequencies, the variations were much more irregular. On 70 and 130 kc/sec, plots of h against log $f(\chi)$ do not give straight lines at all. [8].

For oblique incidence, diurnal changes of apparent reflection height on a frequency of 16 kc/sec, received at a distance of 220 km, are approximately the same as for vertical incidence. At a distance of 540 km, however, there are differences. The height starts to decrease suddenly at about one hour before ground sunrise, remains almost constant throughout the day, and increases rapidly near sunset. For a frequency of 127.5 kc/sec, the variations are identical with those at vertical incidence for a distance of 300 km, but change considerably when the distance is increased to 900 km.

The values of the scale height $H(t)$ have also been studied for the above cases. For 16 kc/sec, the over-all mean value of $H(t)$ is 5.5 ± 0.1 km; for 43 kc/sec, 4.8 ± 0.1 km; and for 70 and 113 kc/sec, somewhere about 2.8 km. $H(t)$ is also found to have a seasonal variation with a semi-annual period.

(*iii*) *Reflection coefficients*—The variations of the reflection coefficient with frequency and with the time of the day are also significant. Anderson [5] in 1931 plotted the attenuation coefficient against the frequency computed from long-distance propagation data and compared it with the Austin-Cohen formula. Good agreement was observed with the formula except in the neighbourhood of 45 kc/sec. Here the attenuation is much greater.

At noon on a summer day, when the downcoming waves are at their weakest, the reflection coefficient for 16 kc/sec is about 0.1, whereas it is less than 0.001 for 100 kc/sec, and only about 0.005 for 2 Mc/sec. The difference between long and

very long waves is not so marked in winter, and is hardly noticeable at night at any time of the year.

The diurnal variations of reflection coefficient in summer for a frequency of 16 kc/sec measured at almost vertical incidence are as follows: Sudden decrease of amplitude before ground sunrise, constancy of the coefficient throughout all the daytime, sudden increase in amplitude near sunrise, and symmetry of the curve about midday. In winter, the decrease before sunrise and increase near sunset are not so marked, and the variation of the reflection coefficient during the day has a gradual, though small, change. At higher frequencies (70 kc/sec) in summer a second sudden decrease in the coefficient occurs at about one and one-half hours after sunrise, reducing the amplitude to a very small daytime value.

The variation of reflection coefficient with frequency is also very significant. In Figure 1 are plotted, after Bracewell and others [8], the measured magnitudes of the "conversion coefficient" against radio wave frequency, for different times of day and season. (By the "conversion coefficient" $_{\parallel}R_{\perp}$ is meant that complex coefficient which relates the phase and amplitude of the vertically polarised radio wave component before reflection at the ionosphere to the phase and amplitude of the horizontally polarised wave component after reflection.) The "conversion coefficient" (and also the reflection coefficient at vertical incidence) is very small, particularly at summer noon, for waves between 30 and 100 kc/sec. This implies a very considerable absorption of these waves in the lower ionosphere.

Mention may also be made of the recent observations by Benner [9] on the diurnal variation of the vertical incidence ionospheric absorption at 150 kc/sec. He observed that a plot of $\log \mid \log \rho \mid$ *versus* $\log \cos \chi$ gives a morning slope of 0.675 and an afternoon slope of 0.76.

Measurements at oblique incidence give certain curious results. On a summer day, the reflection coefficient on a frequency of 16 kc/sec is about 0.15, when measured at a distance less than 300 km, but becomes as high as 0.32 when measured at a distance of between 500 to 800 km. There appears to be a rather sudden change in both reflection coefficient and reflection height near 400 km [see also Section 2*a*(*ii*)].

(*b*) *Short wave propagation data*—Short waves reflected from the upper layers suffer absorption twice during their up and down passage through the *D*-layer. Study of the variation of the signal strength of such waves with time (diurnal, seasonal, and solar cycle), on the assumption that there has been no loss at reflection, gives important information regarding the *D*-layer characteristics. Thus, if the layer is assumed to have a Chapman distribution of ionization, then the absorption suffered by a wave reflected (from the *E*-layer) in the double passage can be easily calculated from the relation

$$\log_e \rho = \frac{R}{(f \pm f_L)^2} \cos^n \chi$$

where R is a constant, f the wave frequency employed, f_L the gyro-frequency corresponding to the component of the earth's magnetic field along the ray path, and n a constant indicating the power of $\cos \chi$. Appleton has compared the reflection coefficient (that is, the *D*-layer absorption) thus calculated with observed results.

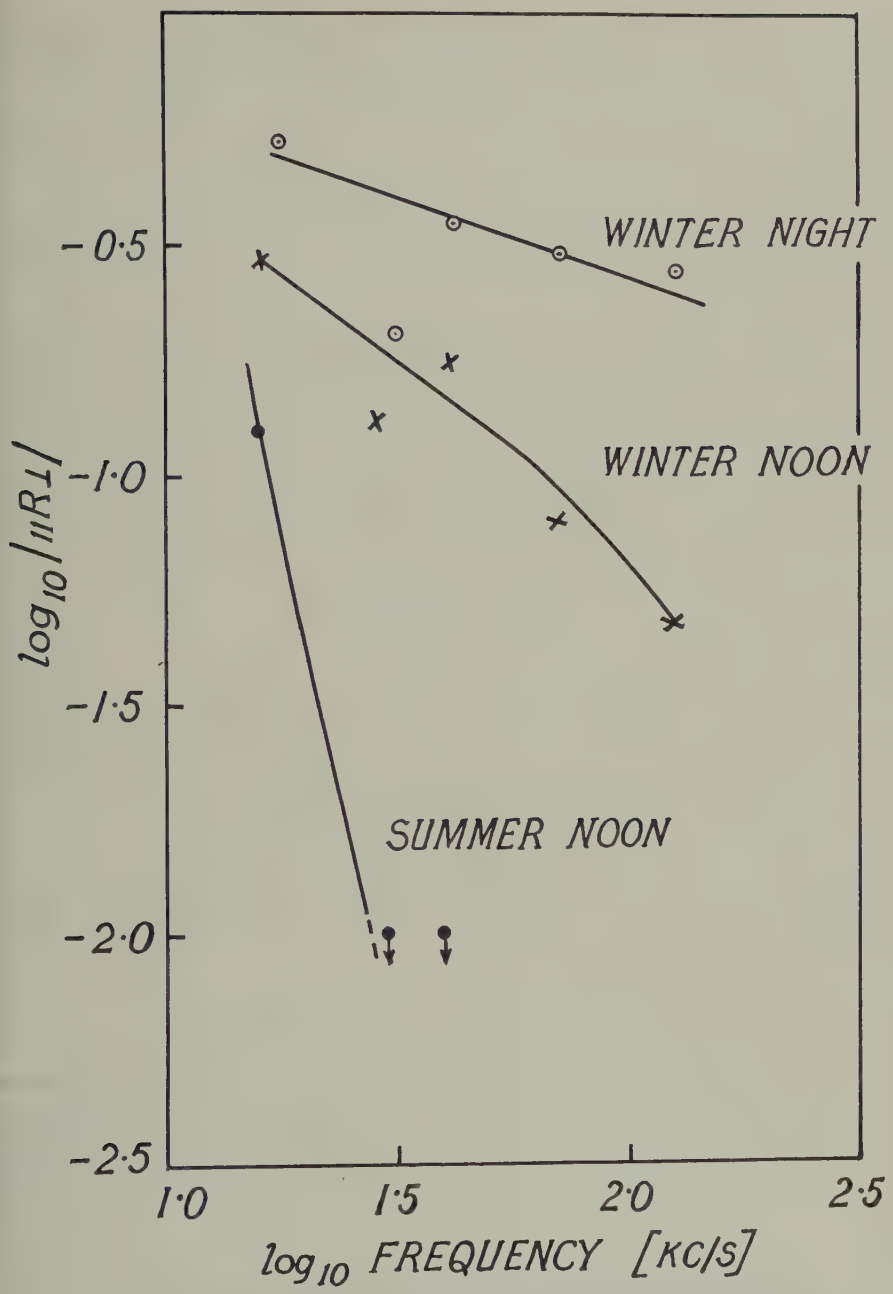

FIG. 1—Experimental curves giving variation of conversion coefficient $|{}_{\parallel}R_{\perp}|$ with frequency for different times of the day and season. Arrows indicate upper limits to measured values at the times when the signal was less than the noise (after Bracewell and others, Reference 8.)

There seems to be general agreement between the two. Appleton's [10] observations further show that the *D*-layer is markedly solar controlled, with a seasonal change of 2 or 3 to 1 from summer to winter. There is also a solar cycle variation of the *D*-region ionization density. This appears to be about 2.7 : 1 in summer and 1.4 : 1 in winter.

According to Bates and Seaton's calculations, based on short wave absorption data collected by Piggot, the electron concentration at the maximum of the layer (90 km) is about $1.5 \times 10^4/cm^3$ at midday (Table 1), with a recombination coefficient of about $3 \times 10^{-8}/cm^3$.

(*c*) *Results from fade-out phenomenon*—There are strong reasons to believe that the radio fade-out (also known as the Mögel-Dellinger effect) which causes dislocation of short and medium wave radio traffic in the sunlit hemisphere is produced by sudden increase of ionization in the lowermost absorbing region of the ionosphere. As such, detailed study of the wave propagation phenomena during radio fade-outs throws important light on the ionization characteristics of the *D*-region.

It has been observed that during radio fade-outs there is a sudden change of phase of the sky wave. This phase change (called sudden phase anomaly—S.P.A.) is due to a sudden lowering of the reflection height and has been studied in great detail for very long waves (16 kc/sec) in England.

The average lowering of the virtual height of reflection is found to be 4 km, but may even be as much as 15 km.

The intensity of the reflected wave is not affected in the same manner for all frequencies during a fade-out. As already noted, the short and medium waves are highly absorbed. For very long waves (16 kc/sec), however, at moderately steep incidence, the intensity is hardly, if at all, affected. [8]. There is even an increase in the field strength for oblique incidence [11]. It has also been reported that atmospherics (which are known to possess a quasi-periodicity of the order of a thousand cycles per second) of distant origin increase greatly in number. For frequencies higher than 30 kc/sec at vertical incidence, the amount of enhancement falls off progressively up to a limit which is variable, but which lies between 43 and 150 kc/sec. Beyond this limit, strong attenuation is found.

During a radio fade-out, the strength of the upper atmospheric current system (in the illuminated half of the atmosphere) which produces the so-called quiet-day variations of the terrestrial magnetic elements appears to undergo a marked increase in intensity. There is little doubt that this increase is due to increased conductivity produced by extra-ionization in the region near the *D*-layer. But whether this region is identical with the region in which the quiet-day current system is ordinarily produced by the tidal oscillations, or whether it is at a different level, is not yet known with certainty. If it is the former, then this simply means that during a solar flare the solar ultraviolet radiation which produces the *D*-region ionization is greatly intensified. If it is the latter, then this means that during a flare some new ionizing radiation is emitted from the bright spots on the sun. Unfortunately, in the absence of reliable information, no decision in this respect can be made yet. Nicolet's [13] attractive suggestion that the fade-out ionization is due to ionization of NO by $\lambda 1300$ appears to favour the latter case. But, it must be noted that the ionization rate for this process is as large as $10/cm^3/sec$ at 75 km and $40/cm^3/sec$ at 90 km

for normal conditions [2], and may quite possibly contribute to the over-all ionization of the normal D-region.

(*d*) *Lunar and solar magnetic variations and tidal oscillations in the D-region*—Appleton and Beynon's measurements [14] of absorption by the D-region reveal a lunar variation, with maximum occurring at 10.9 lunar hour. This result has been used by the authors to confirm the view (originally advanced by Martyn [15]) that the current systems for lunar magnetic variation are produced mainly in the D-region, where it has the correct phase for producing such variations.

The solar magnetic variations are also produced mainly in the D-region, as the solar flare evidence by McNish [16] has conclusively shown, but there are contributions also from regions E and $F1$, the latter, for this case, being in phase with the former. Cowling [17], however, has pointed out that on current ionospheric theory, as developed by Massey and his associates, it is not likely that the D-region has adequate conductivity to be mainly responsible for any of the magnetic variations. It may be remarked, however, that the conductivity of the regions must be due to ions, not to electrons, and that it can be adequate for producing the magnetic variations if there are nearly 10^4 ions per electron at heights of about 80 to 90 km.

TABLE 1—*D-layer experimental data*

Height of reflection of very long waves	Number density of electrons at about 70 km	Max. number density of electrons at about 90 km	Variation in reflecting height	Decrease in absorption during eclipse
km	cm^{-3}	cm^{-3}		
70 to 80	2×10^2 (Budden, *et al.*) 2.5×10^2 (Wilkes) 2.5×10^3 (Bremmer)	1.5×10^4 (Calculated by Bates and Seaton from the absorption data collected by Piggot)	Log sec χ law for very long waves	(*i*) 1 neper for 61 per cent solar disk in shadow; (*ii*) 1.3 nepers for 76 per cent in shadow

3—*Theoretical studies on the D-layer*

(*a*) *Origin of the D-layer*—The main source of ionization for the D-layer is the ultraviolet light from the sun. This is evident from measurements of reduction in the absorption during an eclipse. It has been found (Table 1) that, when 61 per cent of the solar disk is in shadow, the absorption is decreased by 1 neper from the control day value, and, when 76 per cent is in shadow, the absorption is decreased by 1.3 nepers [18].

The various theories suggested to explain the origin of the layer are discussed below.

(1) The most widely accepted theory is that the D-layer is produced by the ionization of O_2 at its first ionization potential (12.2 eV) as first suggested by Mitra, Bhar, and Ghosh [19]. This view is also accepted by Nicolet but with certain qualifications [see Section 2(*c*)].

(2) Jouast and Vassey [20] and later Vassey and Vassey [21] claim that labora-

tory experiments indicate that radiation of photon energy down to about 7 eV is so strongly absorbed by air that it is impossible for it to penetrate to the required levels. To avoid this apparent difficulty, they suggested that the operative mechanism might be photo-ionization of atomic sodium, the threshold energy of which is only 5.1 eV. The ionization rate for this process, however, is low [2]. Further, since the active radiation responsible for sodium ionization is not appreciably reduced during its passage through the atmosphere above the *D*-layer, the rate will not vary with the solar zenith angle. This is in direct conflict with observational data [see Section 2(*a*)]. It is, therefore, difficult to see how ionization of sodium can contribute to the *D*-layer ionization. At the same time, it is to be remembered that the experimental results of Schneider [22] (on which Jouast, Vassey, and Vassey's conclusions are based) have been confirmed by Hopfield [23]. Hopfield's work is particularly valuable, as he used a *continuous* light source. Experimental results of these two workers certainly indicate that photons of energy greater than 12 eV cannot reach the relevant atmosphere with sufficient intensity.

(3) According to Nicolet [13], there are three elements operative in the formation of the *D*-region. These are the following:

(*i*) A normal layer by ionization of O_2 at its first ionization potential (12.2 eV).
(*ii*) A layer more or less sporadic by ionization of sodium.
(*iii*) A layer of extra ionization of NO by radiation at λ1300 (during fade-out).

It is probable that both (*i*) and (*ii*) are ordinarily operative, the sporadic layer being embedded inside the normal *D*. The occasional prominence of the sporadic layer (in reflecting short waves) may be attributed to localised concentration of ionization inside the normal *D*. The possibilities of fade-out enhancement by NO have already been referred to in Section 2(*c*).

(*b*) *Structure of the D-layer*—Besides the nature of the ionizing radiation and the constituent ionized, one must also enquire into the structure of the layer, because a definite knowledge about the structure is essential for estimating the absorption suffered by short waves and understanding the propagation characteristics of long and very long waves. Unfortunately, our knowledge regarding the structure of the *D*-layer is yet very meagre.

The only source from which one can derive some information regarding the profile of the *D*-region ionization is from the interpretation, on theoretical grounds, of the propagation characteristics of long and very long waves.

The simplest assumption to explain the propagation characteristics of long and very long waves is to assume that the waves are being propagated in the spherical shell bounded by the surface of the earth and the lower boundary of the *D*-layer. The propagation is then of the type met in wave guides. It is found that for such type of propagation the number of lightly attenuated modes is small for very long waves. The mode picture for these waves is thus particularly convenient. The attenuation coefficients for the various modes depend upon the constants assumed for the *D*-layer, which may be partly or perfectly conducting. In particular, for a homogeneous, sharply-bounded region, the attenuation coefficient can be calculated

if the electrical conductivity of the region and its height above ground are known. Conversely, from the observed attenuation of very long waves, it is possible to estimate the conductivity of the reflecting layer. Bremmer [7] has calculated the reflection coefficient for a reflecting level at 70 km height, having a collisional frequency of about 10^6/sec. He found that for such a layer the number density of electrons is 2.5×10^3/cc, the electrical conductivity is 7×10^{-15} emu, and waves polarised with the electric vector in the plane of incidence have a minimum reflection coefficient for an angle of incidence of about 10° [7]. It will be noted that this density is much higher than that obtained experimentally by Budden, *et al.*

The mode picture has been further developed by Rydbeck [24]. Rydbeck has discussed the cases where the *D*-layer is (*i*) a homogeneous, sharply-bounded medium, (*ii*) a region of finite width in which ionization density varies parabolically with height, and (*iii*) a region in which ionization density varies as the square of the height above the level $N_e = 0$. For long waves, the behaviour was found to be similar for all the three cases. Hence no useful conclusion about the structure of the layer could be made from these works.

Booker [25], who was the first to take into consideration the effect of the earth's magnetic field, emphasised the fact that reflection for very long waves probably occurs where the complex refractive index changes by a large amount within a wave-length. The reflection level might be determined by the ionization gradient, but is more probably determined by gradient of collision frequency. This again brings home the fact that in interpreting the observed results of long and very long wave propagation, one must have recourse to the wave treatment rather than to the simpler ray treatment.

The differential equations for propagation in a stratified non-isotropic medium in the presence of a magnetic field were first given by Hartree [26]. Wilkes [27,28] has given solutions for frequency near 16 kc/sec for vertical incidence and later for oblique incidence. Wilkes showed that the diurnal changes of reflection height observed by Budden, *et al.*, could be explained with an ionospheric model in which N_e is proportional to the square of the height above the level where $N_e = 0$, the collisional frequency is constant, and the magnetic field vertical. Wilkes' model, however, could not account for all the changes of amplitude of the reflected wave. Stanley [29] considered a model in which the ionization varies exponentially with height. He showed that this particular model can account for most of the observed phenomena. He also showed that there is a region below the level of reflection (*cf.* Wilkes), the "tail" of the exponential, which plays a vital rôle in determining the variation of the reflected amplitude with frequency and with the time of the day.

Pfister [1] assumed two different models—one an effective ion layer and the other an effective electron layer. The ion layer was assumed to have a Chapman distribution of ionization. The profile of the electron layer was calculated, taking account of the variation of the recombination coefficient with height. It was found that the distribution could be represented by $N_e = (N_e)_0 \exp(1 + z - e^{-z} \sec \chi)$. This gives a distribution quite different from those in regions *E* and *F*. The electron density increases monotonically with height and trails off into the *E*-region without showing any well-defined maximum. With these models, Pfister calculated the reflection coefficient on the basis of the wave equation given by Wilkes for vertical

incidence, and the transmission values on the basis of the ray theory. The results obtained by him differed for the two models. The calculations showed that for the effective ion layer, the ion concentration had little influence on the amount of reflection, but much larger influence on transmissivity. A larger ion density extends the range of absorption to higher frequencies. For an effective electron layer, the reflection characteristic remains practically the same as for the ion layer, while transmission characteristics alter radically. Ordinary and extraordinary waves are separated and show large absorption, especially near gyro-frequency. Evidently it is important to decide between the two models. One way of doing this will be to study experimentally the behaviour of transmission near gyro-frequency. Unfortunately, as Pfister has pointed out, the reflection characteristics of the *D*-layer can hardly be separated from the transmission characteristics of the layer, and the desired analysis of the measurements is difficult to make.

It will be noticed from the above discussion (and also from Table 2) that different workers have used different structures of the *D*-layer in carrying out their calculations. It is difficult at this stage to decide which of these various structures is to be favoured.

Table 2—*Structure of the D-layer as assumed in theoretical studies of long and very long wave propagation characteristics*

Author	Assumed structure of the *D*-layer	Remarks
1. Bremmer	Homogeneous, sharply-bounded region	Number density of electrons at 70 km level is $2.5 \times 10^3/\text{cm}^3$
2. Rydbeck	(*i*) Homogeneous, sharply-bounded region	.....
	(*ii*) Region of finite width with parabolic distribution of ionization	.....
	(*iii*) Region in which the ionization density varies as the square of the height above the level $N_e = 0$	For long waves the behavior is similar for all the cases. No conclusion possible.
3. Booker	Region behaves as a metallic reflector	.....
4. Wilkes	(*i*) Same as in 2(*ii*)	Good agreement with observations on 16 kc/sec for case (*ii*)
	(*ii*) Same as in 2(*iii*)	
5. Stanley	Ionization varies exponentially with height	Method of calculation as in Wilkes. Better agreement with observations claimed.
6. Pfister	(*i*) Effective ion layer having a Chapman distribution	The two models give different results. No choice between these two has been made by Pfister.
	(*ii*) Effective electron layer expressed as $N_e = (N_e)_0 \exp(1 + z - e^{-z} \sec \chi)$	

PART II

STUDIES ON THE ORIGIN AND STRUCTURE OF THE *D*-LAYER

1—*Introduction*

It is clear from the works summarised in Part I that our knowledge concerning the origin and structure of the *D*-layer is far from satisfactory. This is particularly distressing, as a knowledge of the structure of the layer is essential for calculations of propagation parameters for all radio waves [see Section 3(*b*)].

In Part II of the paper, we will make an attempt to determine the structure of the *D*-layer, that is, determine the distribution with height of the number density of electrons and ions which go to form the *D*-layer. For this purpose we will start with the following plausible assumptions.

1. The whole of the *D*-layer is comprised in the region 30 km to 100 km.
2. The active atmospheric constituent is O_2 , which is ionized at its first ionization potential by $\lambda\lambda 1012 - 910$.
3. The temperature distribution in the regions will be assumed to be that as adopted by NACA (Fig. 2; also Table 3). (The atmospheric temperature distribution up to 100 km is known with much less uncertainty than in the region above. The distribution, of course, may be expected to vary with the hour of the day, the season of the year, and perhaps also with solar cycle. Nevertheless, the general shape of NACA standard variation is not deviated from.)
4. The atmospheric constituents are thoroughly mixed in this region. (This is corroborated by rocket data, at least up to 70 km [30].) The mean molecular mass is, therefore, constant and $H = kT/mg$ depends only on temperature.

TABLE 3

Region	Range	Temp. (T_0) at reference level	Temperature gradient (γ)	N_0
	km	°*K*	°*K*/*km*	cm^{-3}
I	32–50	220	9.2	5×10^{16}
II	50–63	350	0.0	4×10^{15}
III	63–76	350	−10.4	1.5×10^{15}
IV	76–83	240	0.0	3.5×10^{14}
V	83–100	240	4.5	1.4×10^{14}

2—*Rate of ion production*

To calculate the rate of ion production, we require a knowledge of the corresponding absorption coefficient. Unfortunately, this is not known with certainty. We know, however, that it is extremely small. Bates and Massey [31] place it at about

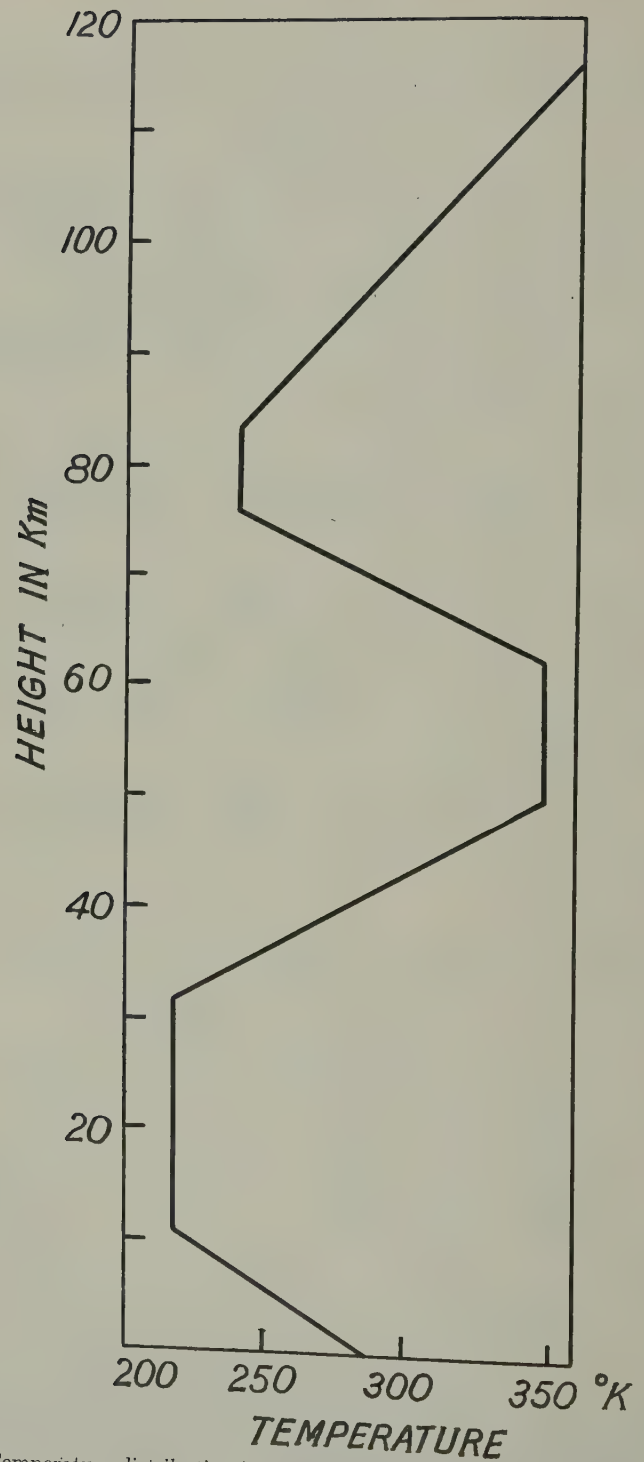

Fig. 2—Temperature distribution in the standard atmosphere as adopted by NACA

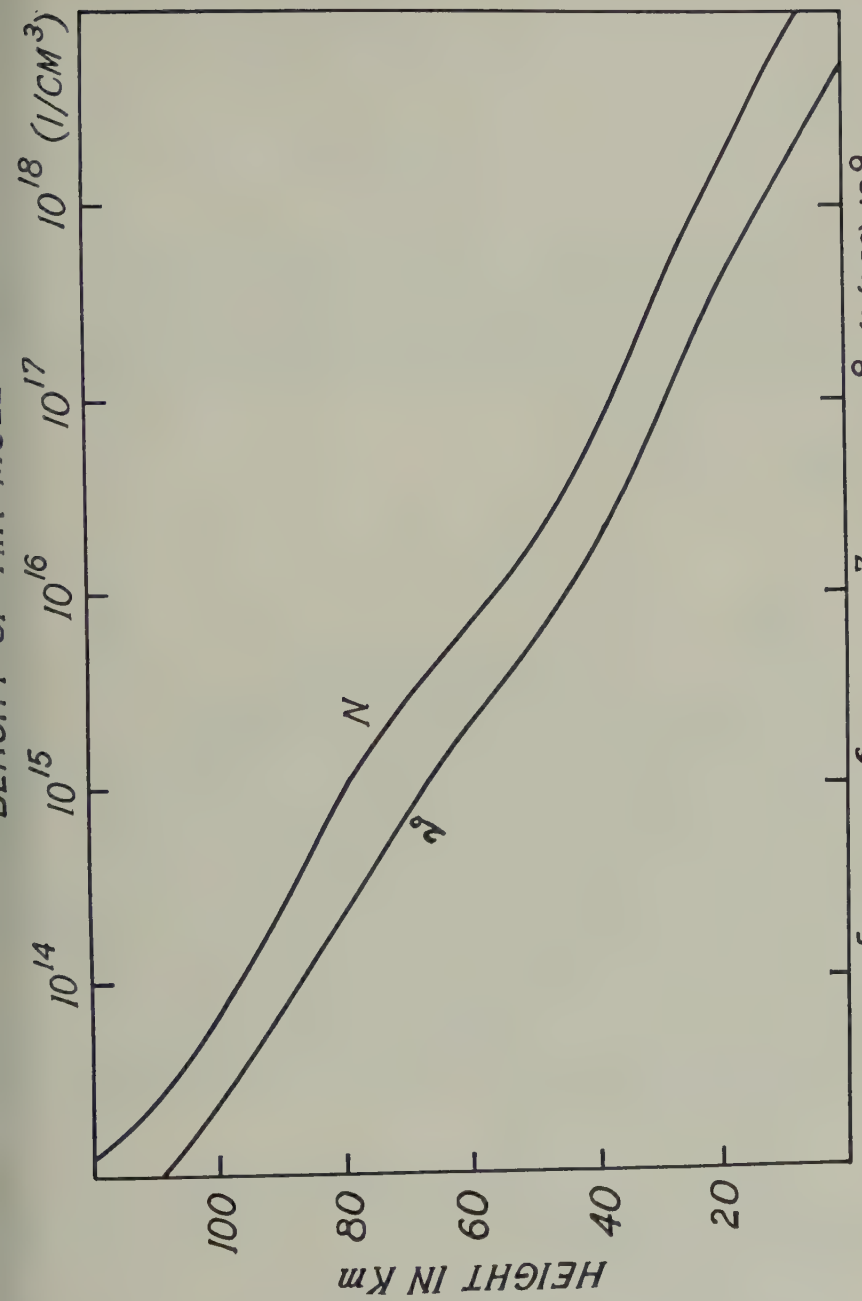

FIG. 3—Distribution of density and collisional frequency of air molecules in the standard atmosphere adopted by NACA

10^{-20}cm^2. But, values less than this are not at all improbable. We have, therefore, considered three different absorption cross-sections, namely, $A = 10^{-20}$cm^2, 10^{-21}cm^2, and 5×10^{-22}cm^2.

The number of available quanta at the first ionization potential is taken to be 2.5×10^9 [32].

Now, the rate of ion production for an *isothermal atmosphere* is given by the Chapman relation

$$q = AN_0Q \exp [-z - N_0AH \sec \chi \exp (-z)] \quad \ldots\ldots\ldots\ldots (1)$$

where A = atomic absorption coefficient, N_0 = density of neutral particles at the bottom of the region concerned, Q = available flux of solar quanta at the wavelengths concerned, z = reduced height equal to h/H where h is the height measured from the bottom of the layer concerned, H is scale height, and χ = solar zenith angle. For a *non-isothermal atmosphere*, equation (1) does not hold. If the temperature is assumed to vary linearly with height (as in the present case), then [33]

$$q = AN_0Q\left(1 + \gamma \frac{h - h_0}{T_0}\right)^{-(1 + T_0/H_0\gamma)} \cdot \exp\left[-AN_0H_0 \sec \chi\left(1 + \gamma \frac{h - h_0}{T_0}\right)^{-T_0/H_0\gamma}\right] \quad \ldots\ldots (2)$$

where γ = gradient of temperature, h_0 , T_0 = height of and temperature at the reference level, and H_0 = scale height at the reference level.

In calculating the rate of ion production at various heights, we shall use equation (1) for regions II and IV, and equation (2) for regions I, III, and V.

On the basis of the above formulae, the values of the rate of ion production for different heights for the three absorption cross-sections have been calculated for $\chi = 0°$, 45°, 60°, 80°, and 84°. Curves for $\chi = 0°$ are depicted in Figure 4.

It will be seen that the shapes of the curves are different from those given by the Chapman laws. This point will again be taken up in Section 4. It may be remarked here that, whenever we pass into regions of constant temperature, the height gradient of q suddenly increases. Further, maximum numbers of ions are produced in the region of low temperature for all the three absorption cross-sections chosen.

The effect of the absorption cross-section on the shape of the curve is quite large (Fig. 4). The curves move up with higher values of A and become sharper at the base. For $A = 10^{-20}\text{cm}^2$, the base is almost flat, and q increases from 400 to 1,000 within a distance of about 3 km.

3—*Determination of the effective recombination coefficient*

It has been shown by Bates and Massey [31] that the value of effective recombination coefficient may be expressed as

$$\alpha = \alpha_e + \lambda\alpha_i + \frac{1}{N_eT}\frac{dT}{dt} + \frac{1}{N_e(1 + \lambda)}\frac{d\lambda}{dt} \quad \ldots\ldots\ldots\ldots (3)$$

with

$$\lambda = \frac{\beta N_eN}{KN_eN + \rho N_e + \alpha_iN_e^2 + q - \alpha_eN_e^2} \quad \ldots\ldots\ldots\ldots (4)$$

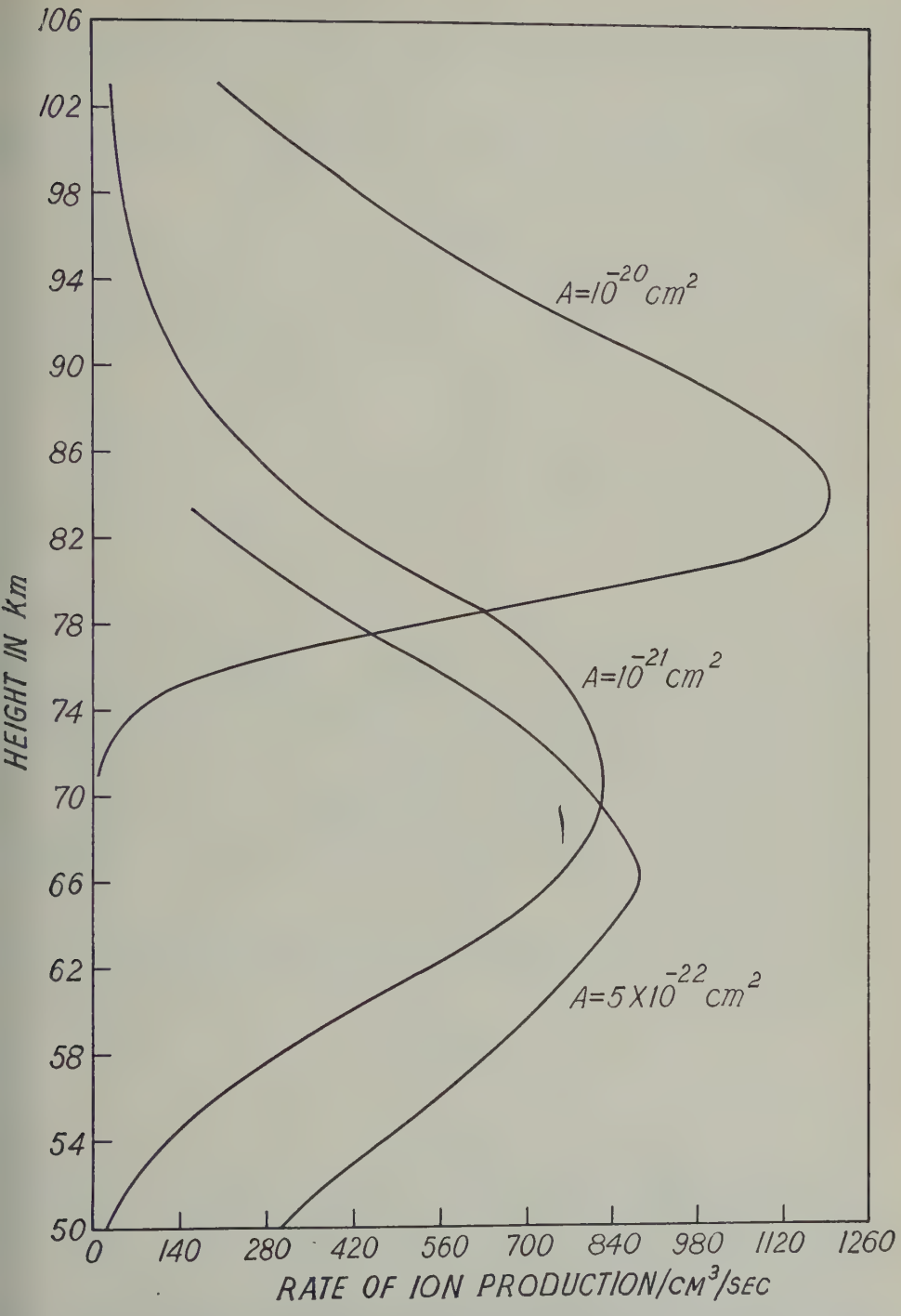

FIG. 4—Height distribution of the rate of ion production for three values of the absorption coefficient at the first ionization potential of O_2 : $A = 10^{-20}$ cm², 10^{-21} cm², and 5×10^{-22} cm²

where N_e = electron density, α_e = electronic recombination coefficient, λ = ratio of negative ions to electrons, β = coefficient of attachment, K = coefficient of collisional detachment, ρ = coefficient of photo-detachment, and α_i = coefficient of mutual neutralisation.

The values of the different coefficients likely to be important and their relation to pressure (that is, to height), if any, are given in Table 4.

Table 4

Type of reaction	Coefficient of reaction	Remarks
1. Attachment	$\beta = 10^{-14} + 1.5 \times 10^{-12}\, p$ cm³/sec (p in mm)	Bradbury [34]; pressure dependent
2. Photo-detachment	0.35/neg. ion/sec	Bates and Massey [31]
3. Mutual neutralisation	10^{-7} to 10^{-8} cm³/sec	Bates and Massey [31]
4. Collisional detachment	10^{-16} to 10^{-17} cm³/sec	Value uncertain; 5×10^{-16} adopted

It will be noted from Table 4 that the important operative processes are only attachment, photo-detachment, mutual neutralisation, and collisional detachment. On account of the relatively high gas densities involved, it is probable that electrons become attached to oxygen molecules mainly through the Block-Bradbury process. The coefficient β associated with this is given by $\beta = 10^{-14} + 1.5 \times 10^{-12} p$ (p in mm). The mutual neutralisation coefficient is usually assumed to lie between 10^{-7} to 10^{-8}cm³/sec. We adopt here the value 10^{-8}, agreeing with Bates and Massey [31] that the lower value is more probable. For the coefficient of collisional detachment, we accept a value of 5×10^{-16}cm³/sec. The photo-detachment rate is assumed to be 0.35/neg.ion/sec [31].

We see now that equations (3) and (4) can be further simplified. Assuming for N_e a value of 10^4/cm³, it is seen at once that $\alpha_i N_e^2$ and q are negligible in comparison to KN_eN and ρN_e. Further, both dT/dt and $d\lambda/dt$ are small terms. Hence

$$\lambda = \frac{\beta N}{(KN + \rho)} \qquad (5)$$

$$\alpha = \frac{\beta N \alpha_i}{(KN + \rho)} \qquad (6)$$

Now the Block-Bradbury detachment process is pressure dependent. Its value will then vary with height. Assuming the pressure-height distribution as given by NACA (Fig. 3), the variation of β with height has been calculated. In Figure 5, the variations with height of βN, KN, and ρ are depicted. In the same Figure is also drawn the variation of λ with height as calculated from equation (5).

Several interesting points may be noted here. Firstly, the variation of λ with height is determined largely by that of KN in the height range of 55 to 70 km. But

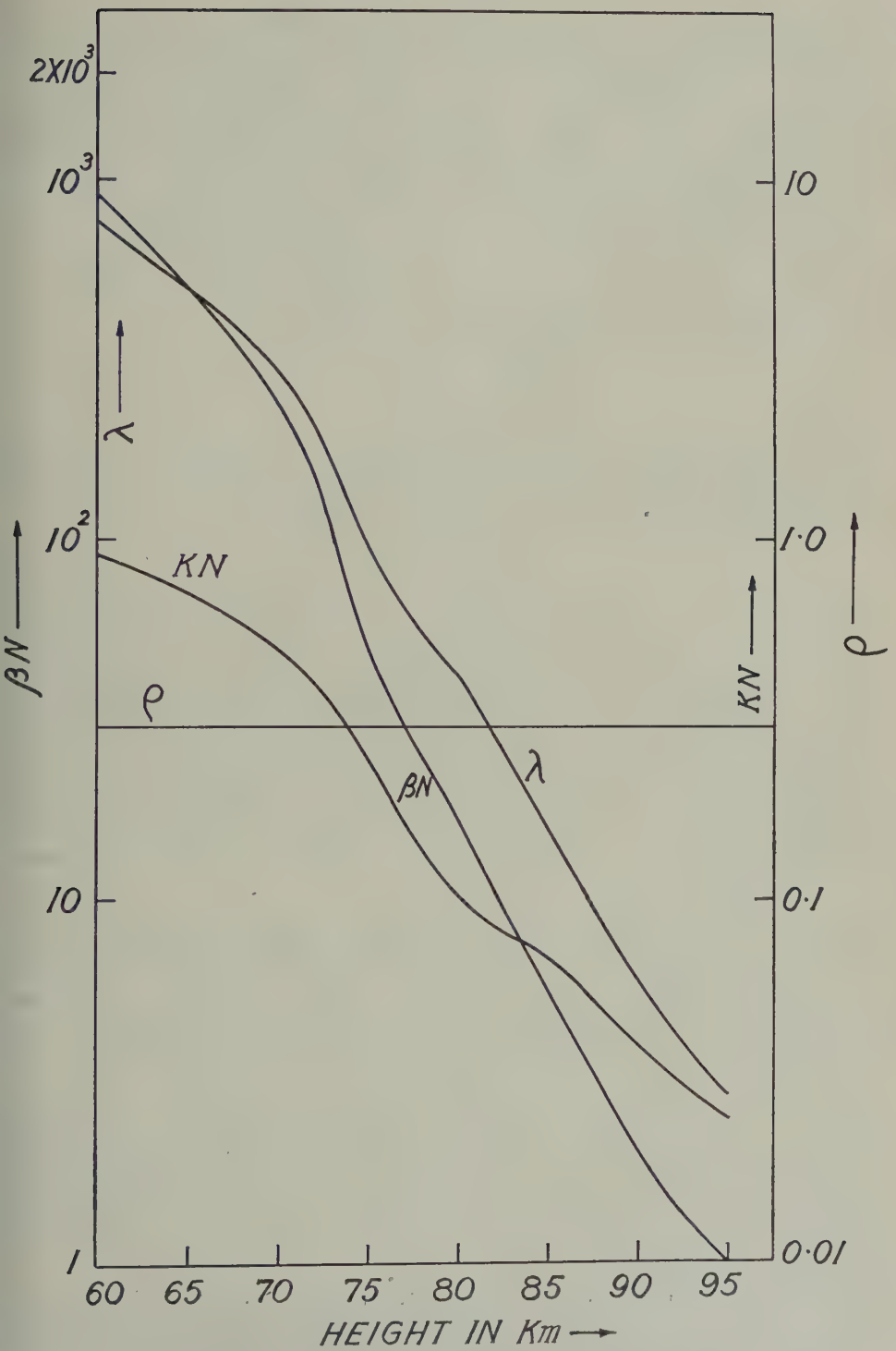

FIG. 5—Variation of the parameters βN, KN, ρ, and λ with height, used in calculating the recombination coefficient; β = coefficient of attachment, K = coefficient of collisional detachment, ρ = coefficient of photo-detachment, and λ = ratio of negative ions to electrons

at greater heights, the effect of ρ preponderates. Evidently, at very low heights, the coefficient of recombination varies little with height, the only variation being that due to β. Thus for the "tail" of the ionization region, where very long waves are assumed to undergo reflection, the variation of α with height is small, as was concluded by Budden, Ratcliffe, and Wilkes from independent reasonings [6]. At greater heights, the variation of α with height is rapid because of the variations of both β and N. Secondly, the value of λ is very great in the D-region. This, to us, seems to be the main difference between region D and the upper regions.

4—Variations of the number densities of electrons and ions with height

It may be shown after Bates and Massey [31] that

$$\frac{dN_e}{dt} = \frac{q}{1+\lambda} - \alpha N_e^2 \quad \ldots\ldots\ldots\ldots\ldots\ldots\ldots\ldots (7)$$

where λ and α are given by equations (5) and (6).

Now, we may expect a quasi-equilibrium condition to exist because of the large recombination rate. This is corroborated by the observed symmetrical variation of reflection height about noon [6]. We, therefore, put $dN_e/dt = 0$, so that

$$N_e = \sqrt{q/\alpha(1+\lambda)} \quad \ldots\ldots\ldots\ldots\ldots\ldots\ldots\ldots (8)$$

The distribution of N_e with height may be calculated with the help of this equation and of the curves giving variation of q and α with height. The calculated results are plotted in Figures 6*A*, 6*B*, and 6*C* for different value of the absorption cross-section A. It will be observed that the distribution curve has no well-defined maximum. It rises gradually to a value of about $10^4/cm^3$ and merges with the tail of region E. A slight dip in the value of the density distribution may, however, occur just below region E for lower values of A. It may also be noted that for a given value of N_e the corresponding height increases with decrease of A for heights below 78 km, but decreases above this height. The height gradient of ionization is steepest for lower absorption rates.

A striking feature of the results is the close agreement of the calculated number densities with the observed values. The maximum density (calculated from the absorption data) is about $2 \times 10^4/cm^3$ at about 90 km and about $10^2/cm^3$ at about 75 km (calculated from long wave propagation data). Both these values agree satisfactorily with our values. This supports the original assumption that the normal D-layer is produced by ionization of O_2 at its first ionization potential.

The variation with χ is also significant. With the decrease of χ, the height-density curves move up and also undergo significant changes in their shape. This result has important bearing on the reflection conditions of long and very long waves. A peculiar feature of the curves is the sudden increase of height gradient of ionization from 73 km to 76 km, noticeable only for lower values of A. This occurs for all values of χ. The gradient, however, is sharpest for $\chi = 0°$, and decreases as the value of χ increases.

It is also interesting to calculate the distribution of negative ions with height. The results are depicted in Figure 7. The negative ion concentration is found to have well-defined maxima. These are situated at about the same height where the rate

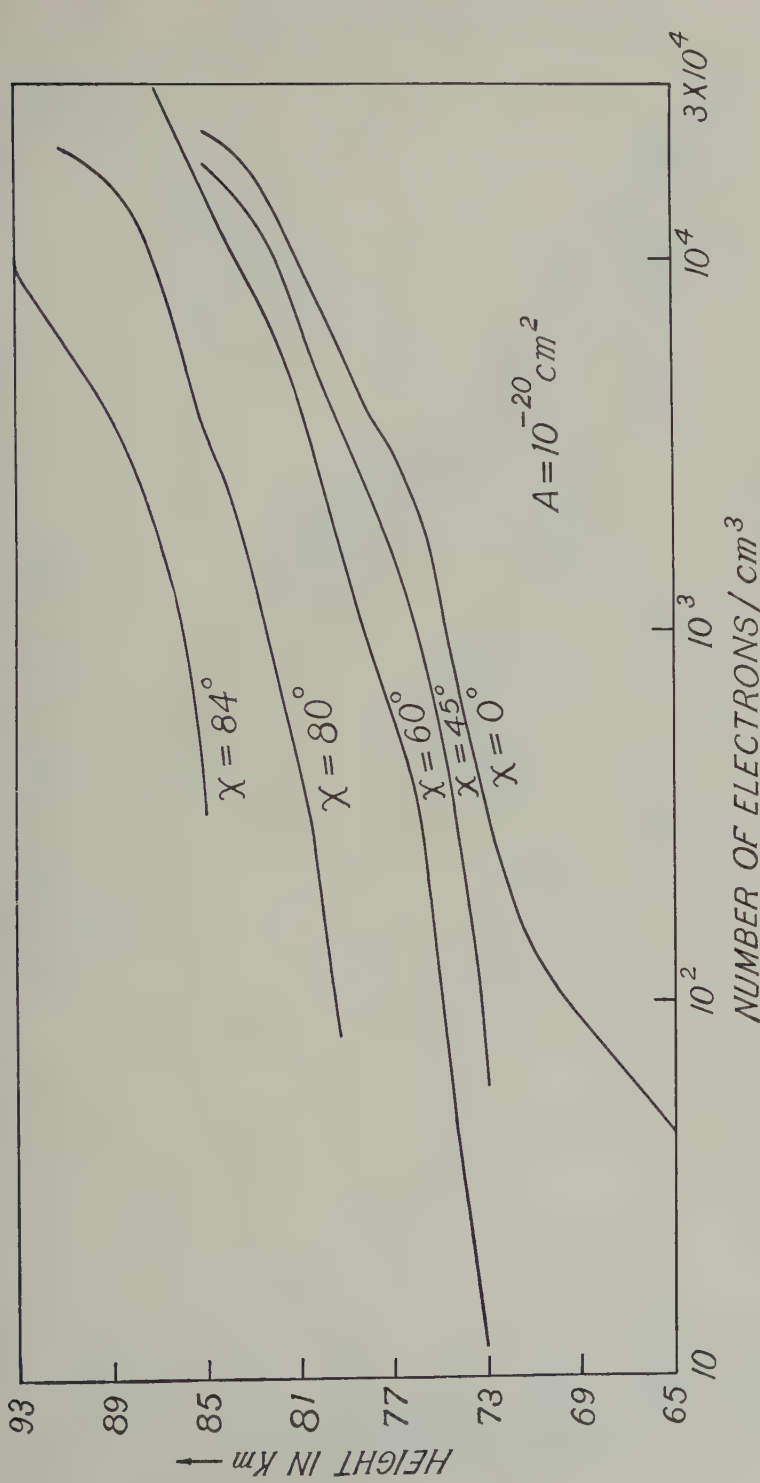

FIG. 64.—Theoretical curves showing the height distribution of number density of electrons for the case $A = 10^{-20}$ cm^3 for five different values of χ, namely, $\chi = 0°$, 45°, 60°, 80°, and 84°

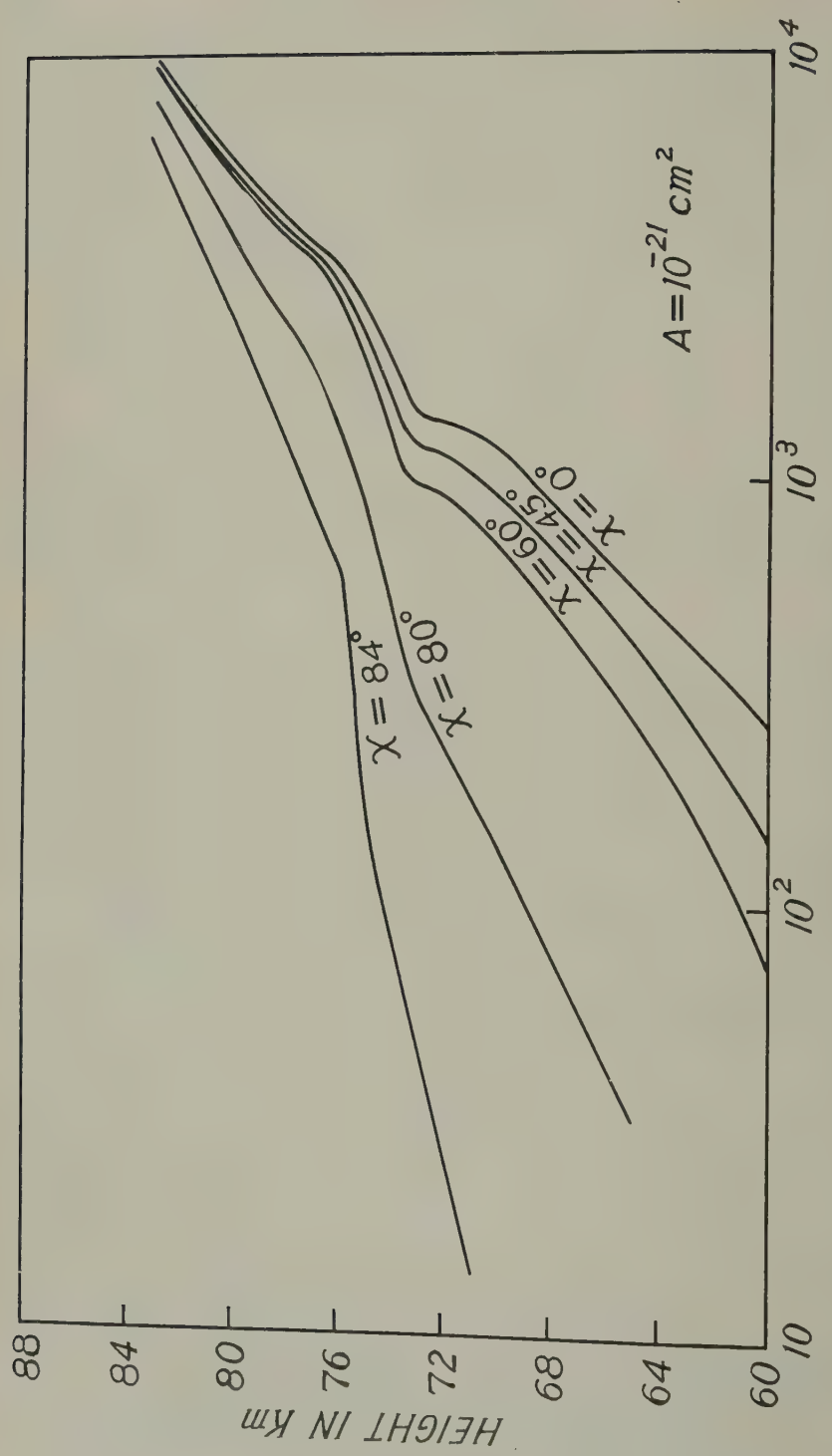

FIG. 6B—Theoretical curves showing the height distribution of number density of electrons for the case $A = 10^{-21}$ cm² for five different values of χ, namely, $\chi = 0°$, 45°, 60°, 80°, and 84°

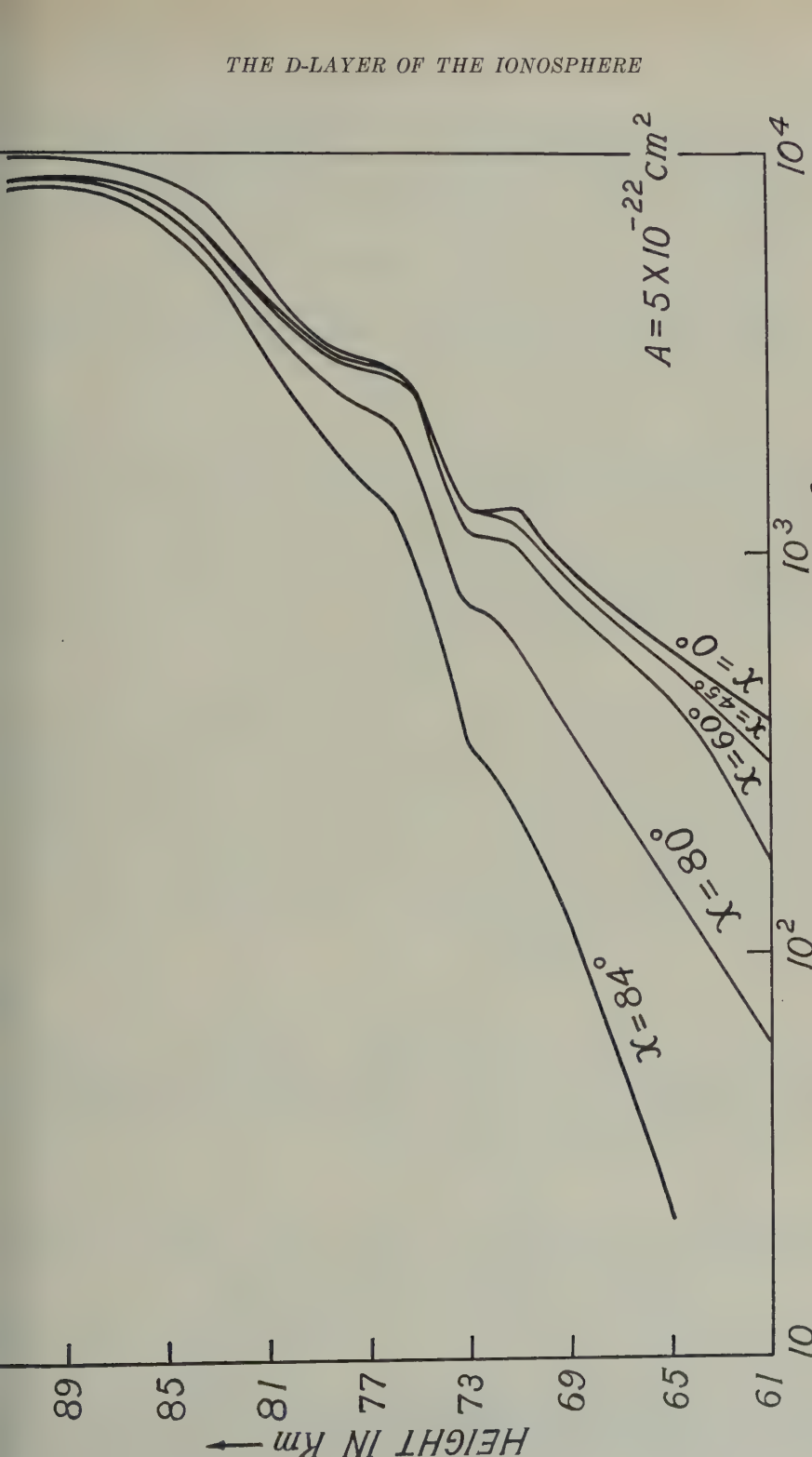

FIG. 6C—Theoretical curves showing the height distribution of number density of electrons for the case $A = 5 \times 10^{-22}$ cm^2 for five different values of χ, namely, $\chi = 0°$, 45°, 60°, 80°, and 84°

of ion production is also a maximum. The level of the maximum rises with increasing value of A, while the thickness of the negative ion layer decreases simultaneously. With increase in the value of χ, the negative ion layer moves up again with important changes in shape.

5—Variation of the effective height of reflection with solar zenith angle

It is usually believed that the long and very long waves are reflected from the tail of a Chapman region. On this assumption Budden, *et al.* [6] and later Wilkes [27,28] showed that the ionization density variation with χ is given by

$$N_e = P \exp \{-\sec \chi \, e^{-z}\} \quad \ldots\ldots\ldots\ldots\ldots\ldots (9)$$

for values of $\chi < 85°$, even when the effective recombination coefficient is assumed to vary exponentially with height. Equation (9) implies that the height variation of collisional frequency has no perceptible effect on the ionization at these levels and that with increase in the value of χ the layer as a whole moves up without any change of shape, so that to the upgoing long wave the same aspect is always presented, whatever the value of χ. The variation of the reflecting height with χ will, then, be given by the constancy of N_e, namely

$$h(\chi) = h_0 + H(t) \log \sec \chi$$

We now come to our ionization curves. Neither for electrons nor for ions the shape of the curves remains invariant with changes in χ. This invalidates the reasonings of Budden, *et al.* [6] and of Wilkes [27,28].

It is interesting to consider how, with the ionization curves we have obtained, the reflection height for any fixed value of N_e will vary with χ. In the discussion, we will not neglect the variation of collisional frequency with height.

We recall that at the low frequency range we deal practically with quasi-longitudinal propagation [25]. We have for this case

$$\mu^2 = 1 - \frac{\omega_N^2}{\omega^2 \pm \omega\omega_L - j\omega\nu} \quad \ldots\ldots\ldots\ldots\ldots\ldots (10)$$

where $\omega_N^2 = (4\pi/m)N_i e^2$, $\omega_L = (eH_L)/mc$, 2π times frequency, and $\omega = |H_L| =$ longitudinal component of earth's magnetic field. In the special case of long wave propagation and in the range of reflection where $\omega \ll \nu$, we may simplify this equation. Since $\omega_L \ll \nu$ (even for electrons), then

$$\mu^2 = 1 - \frac{j\omega_N^2}{\omega\nu}$$

We determine a level of the actual reflection height which is given by

$$|\mu^2 - 1| = \sin^2 \xi \qquad \text{or} \qquad \left(\frac{\omega_N^2}{\nu}\right) = \omega \sin^2 \xi \quad \ldots\ldots\ldots\ldots (11)$$

It is evident that for satisfactory evaluation of reflecting height, N_e and ν are to be known with sufficient degree of precision. The values of N_e at different heights for both ions and electrons have already been determined. The values of collisional frequency are, however, less certain. The collision frequency for air molecules up

about 100 km are known (Fig. 3). For ions, the collisional frequency will be proximately the same.

The collisional frequency for electrons will change because of the following two

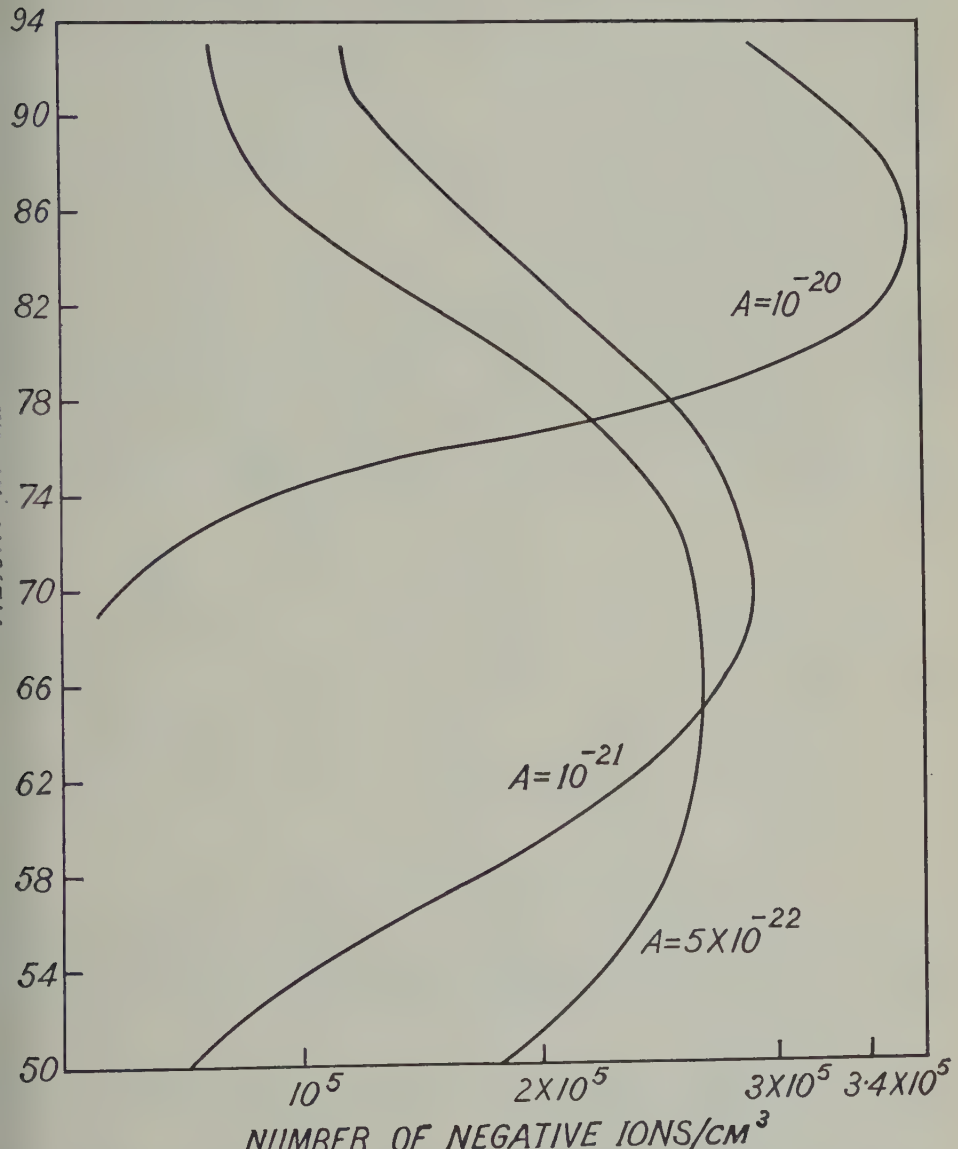

IG. 7—Theoretical curves showing the height distribution of number density of ions for $\chi = 0°$ for three values of absorption coefficients ($A = 10^{-20}$ cm^2, 10^{-21} cm^2, and 5×10^{-22} cm^2)

ctors: (*i*) In accordance with mobility relations, collisions are increased by the quare root of the mass ratio $\sqrt{m_i/m_e}$, that is, as $\sqrt{59 \times 10^3} : 1$; (*ii*) because f the geometry involved, collisions are reduced by a factor of $4\sqrt{2}$. This gives a

value of about 10^8/sec at a height of 60 km. It may be remarked, however, that the values of electronic collisional frequency at this height, as indirectly deduced from experimental investigations, are by no means consistent. Thus, according to Wilkes [27], the electronic collisional frequency at this height is not larger than 10^6/sec. In contrast to these observations, however, Stanley [29] has produced evidence that the collisional frequency may be much higher, of the order of 10^7/sec. Huxley's [35] observations on cross-modulation also indicate a larger value. We, therefore, make a compromise between these conflicting evidences by assuming that (ν electron/ν ion) is not 50 (which is the theoretical value), but only 5. The electronic collisional frequency at any height is then obtained by multiplying the ionic collisional frequency at that height by 5.

We now choose three values of ω, namely $\omega = 10^5$, $\omega = 2.7 \times 10^5$, and $\omega = 10^6$, corresponding to frequencies of about 16 kc/sec, 43 kc/sec, and 160 kc/sec, respectively. The variation of effective height of reflection with log sec χ for both these cases ($\sin \xi = 1$) are plotted in Figure 8. For each of the lower frequencies (16 kc/sec and 43 kc/sec), the mean curve is still a straight line, that for 43 kc/sec being a better fit. For 160 kc/sec, however, the law $h \propto \log \sec \chi$ no longer holds.

It is also interesting to note the effective values of $H(t)$ obtained with the help of these curves (Table 5). These values agree satisfactorily with those obtained experimentally.

Table 5

Exploring frequency	$H(t)$ calculated	$H(t)$ experimentally determined
kc/sec	*km*	*km*
16	5.5	5.5 ± 0.1
43	4.6	4.8 ± 0.1
113	2.6	2.8 ± 0.1

6—*Coefficient of reflection of long and very long waves*

The structure of the *D*-layer as we have obtained has been shown to explain satisfactorily the variation of reflecting height with solar zenith angle. We have yet to show that for low frequencies the reflection coefficients for this structure are of the right order.

It is not intended to make any elaborate study of the problem here. But a preliminary discussion of the same may be made on the basis of the electron and ion distributions we have obtained.

The reflection does not occur within an infinitely small altitude range. It is a continuous effect with a centre at the level given by equation (11). In the neighborhood of this point, the height variation of $(\mu^2 - 1)$ is approximated by a parabola [1], as

$$(\mu^2 - 1) = j\left(\frac{\omega}{c}\right)^2 K' s^2 \quad \ldots\ldots\ldots\ldots\ldots\ldots\ldots\ldots (12)$$

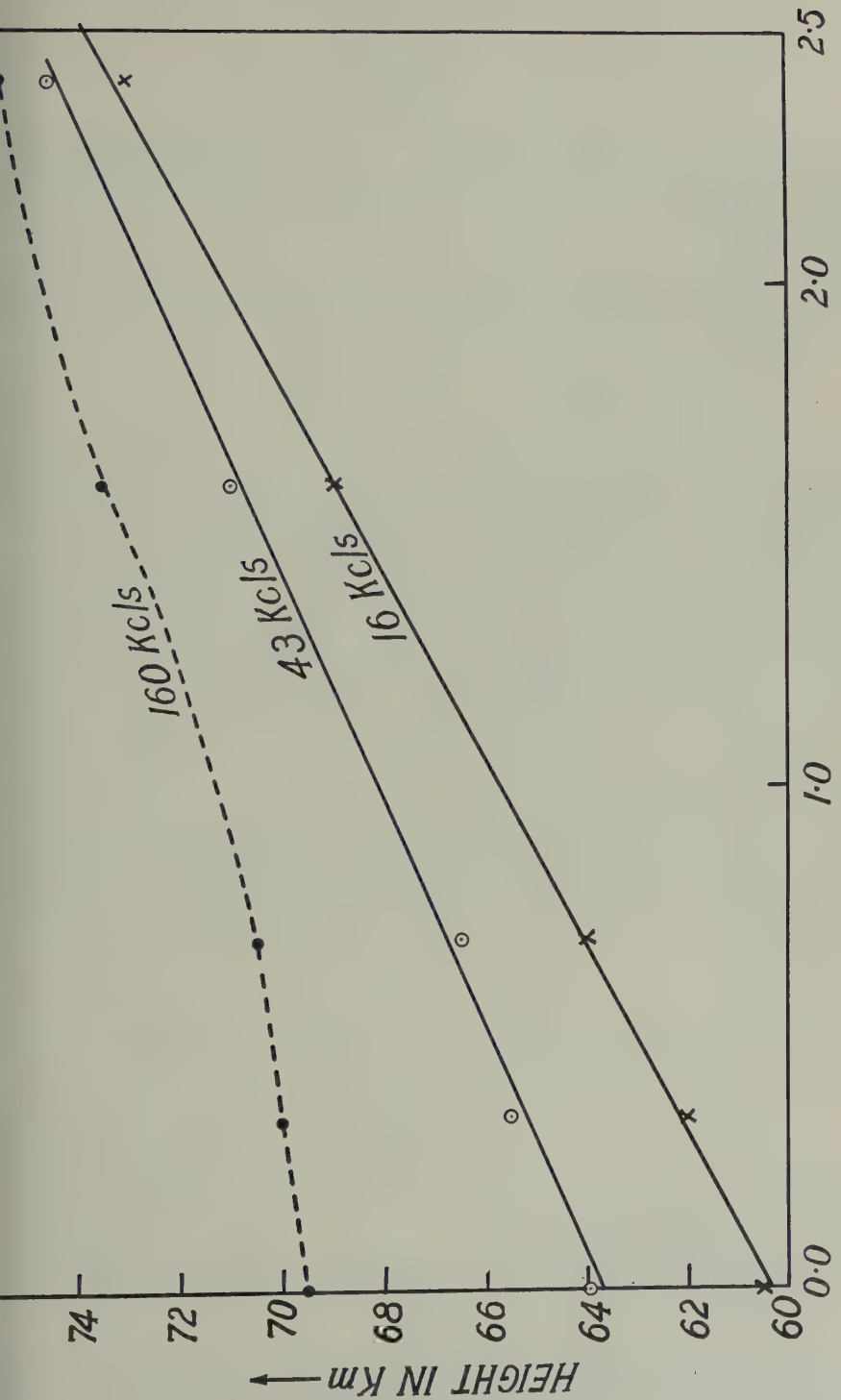

Fig. 8—Theoretical curves giving reflection height as function of solar zenith angle for the three frequencies 16 kc/sec, 43 kc/sec, and 160 kc/sec

where s is the coordinate of height, and K' is given by

$$\frac{1}{\sqrt{K'}} = \frac{2(\omega/c)\omega \sin \xi}{\mathrm{d}/\mathrm{d}h(\omega_N^2/\nu)} \quad \ldots\ldots\ldots\ldots\ldots\ldots\ldots\ldots (13)$$

where ξ is the angle of incidence of the incident wave, ν the collisional frequency of electrons or ions, and N_i the total number of electrons or total number of ions.

For the denominator in equation (13), we will have to take the value at the reflection point.

The function K' is related in a complicated way with the reflection coefficient. By means of the wave equation given by Wilkes [27] for a plane wave incident at an angle against the ground, it can be shown [1] that

$$\frac{\sin^2 \xi}{2} \sqrt{\frac{1}{jK'}} = \left(n + \frac{1}{2}\right) = \left| n + \frac{1}{2} \right| e^{-i\psi} \quad \ldots\ldots\ldots\ldots\ldots\ldots (14)$$

where $(n + \frac{1}{2})$ is a complicated function related with the reflection coefficient. The exact nature of the relation between $| n + \frac{1}{2} |$ and reflection coefficient has been calculated by Pfister [1] for various arguments (Fig. 9).

Evidently the value of the reflection coefficient depends on $\mathrm{d}/\mathrm{d}h(\omega_N^2/\nu)$, which will be different for electrons and ions. It is not known which of these determine the characteristics of the wave propagation at the low frequency range. Because of the very small mass of electrons, these may be the most effective even at these low heights. On the other hand, ions are so numerous at these heights that an effective ion layer may not be an impossibility. We shall, however, discuss here only the electron layer. Such a discussion, though incomplete, will be sufficient for our present purpose.

The electron density distributions we have obtained have several inflexions. As such, (ω_N^2/ν) *versus* height curve cannot be made to fit a single curve accurately. In fact, it is found to consist of four different exponential curves, one between 55–64 km, another between 64–73 km, a third between 73–75 km, and a fourth above 75 km. For an approximation, however, a single exponential curve may be assumed. Thus

$$(\omega_N^2/\nu) = e^{b(h-h_0)} \quad \ldots\ldots\ldots\ldots\ldots\ldots\ldots\ldots (15)$$

where $b \simeq 0.60/\mathrm{km}, 0.28/\mathrm{km}, 0.24/\mathrm{km}$ for $A = 10^{-20}\mathrm{cm}^2$, $A = 10^{-21}\mathrm{cm}^2$, and $A = 5 \times 10^{-22}\mathrm{cm}^2$, respectively. $| n + \frac{1}{2} |$ is then given by

$$\left| n + \frac{1}{2} \right| = \frac{\omega \sin \xi}{bc} \quad \ldots\ldots\ldots\ldots\ldots\ldots\ldots\ldots (16)$$

The reflection coefficients calculated with the help of this equation for $\chi = 0$ and $\sin \xi = 1$ are plotted in Figure 10.

It will be noted that the reflection coefficients fall off very rapidly with increasing frequency. This is in agreement with experimental observations.

7—*Conclusion*

In the preceding sections, we have considered the formation and structure of the normal D-region, starting with the assumption that the D-region ionization i

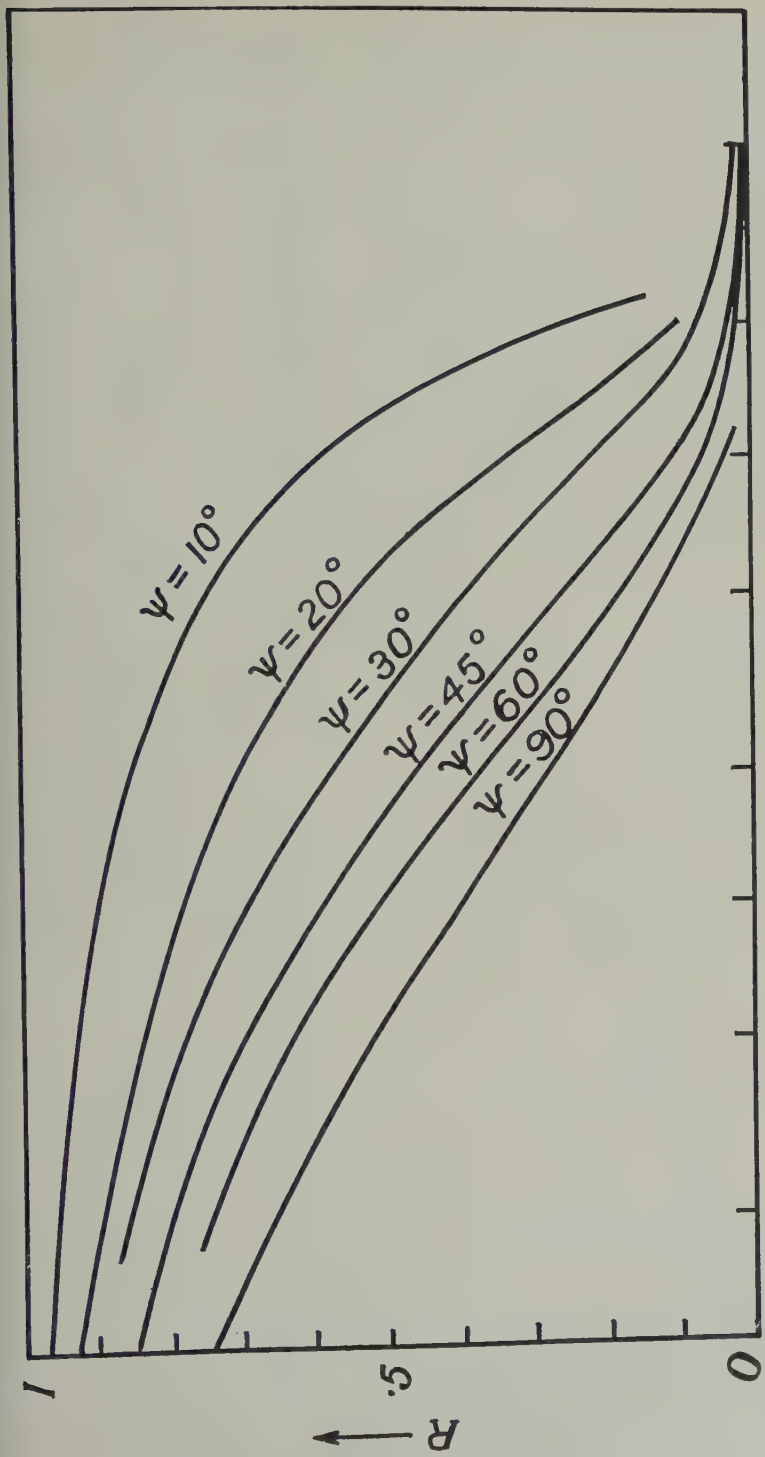

FIG. 9—Variation of reflection coefficient with $|n + 1/2|$ for different values of the argument ψ (after Pfister)

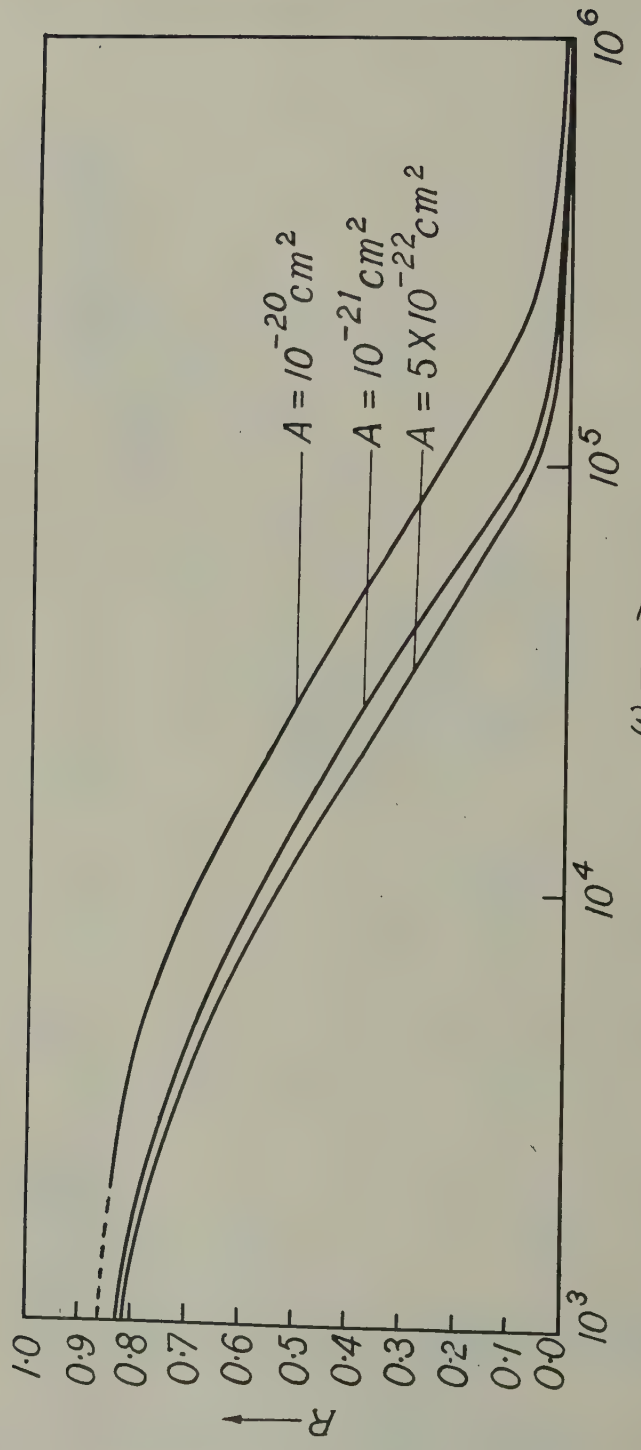

FIG. 10—Theoretical curves giving reflection coefficient as a function of frequency for the absorption coefficients $A = 10^{-20}$ cm², 10^{-21} cm², and 5×10^{-22} cm² ($\chi = 0°$ and $\xi = 1$)

caused by ionization of O_2 at its first ionization potential, as first suggested by S. K. Mitra, *et al.* It is satisfactory to note that the results obtained with this assumption conform to observed facts. The ionization rate is found to be sufficiently large and gives values of electron densities which are in very good accord with the observed values. Considerations of the height variations of atmospheric temperature and recombination coefficient have brought out the following significant facts.

Firstly, the distribution does in no way follow the Chapman law. The electron distribution, in particular, is quite different from that of the *E*- or the *F*-layer. It increases continuously with height, making it difficult to separate the *D*-layer from the *E*-layer. This wide divergence from the Chapman shape explains why it has not been possible to explain the propagation phenomena of long and very long waves (on the assumption of a Chapman distribution). The ion distribution, however, shows a maximum at nearly the same height where the rate of ion production is maximum, that is, it shows some similarity with the Chapman distribution.

Secondly, the variation of "reflecting" height with zenith angle as measured for long and very long waves receives ready explanations with the ionization distributions as obtained in this paper.

Thirdly, the reflection coefficients for various frequencies at the low frequency range as obtained by calculation show satisfactory agreement with experimental results.

The quantitative results as listed above are certainly encouraging, and show the assumption that the *D*-region is produced by the ionization of O_2 at the first ionization potential is justified.

ACKNOWLEDGMENT

The investigations described in the paper were carried out with the help of grants received from the Council of Scientific and Industrial Research, Government of India, and form part of the programme of the Radio Research Committee.

The author is indebted to Prof. S. K. Mitra for the suggestion of the problem and for constant guidance during the progress of the work.

References

[1] W. Pfister, Proceedings of the Conference on Ionospheric Research, State College, Pennsylvania (1949); J. Geophys. Res., **54**, 315 (1949).
[2] D. R. Bates and M. J. Seaton, Proc. Phys. Soc., B, **63**, 129 (1950).
[3] S. K. Mitra and P. Syam, Nature, **135**, 953 (1935).
[4] C. D. Ellyett, Terr. Mag., **52**, 1 (1947).
[5] N. Anderson, Proc. Inst. Radio Eng., **19**, 1150 (1931).
[6] K. G. Budden, J. A. Ratcliffe, and M. V. Wilkes, Proc. R. Soc., A, **171**, 188 (1939).
[7] H. Bremmer, Terrestrial Radio Waves, Elsevier Publishing Co., Inc., New York (1949).
[8] R. N. Bracewell, K. G. Budden, J. A. Ratcliffe, T. W. Straker, and K. Weekes, Proc. Inst. Elec. Eng., **98**, pt. 3, 221 (1951).
[9] A. H. Benner, Proc. Inst. Radio Eng., **38**, 685 (1950).
[10] E. V. Appleton, Mixed Commission on Ionosphere, U.R.S.I., Bruxelles, p. 14 (1948).
[11] R. Bureau, Transactions of the Edinburgh meeting, 1936, Internat. Union Geod. Geophys., Assoc. Terr. Mag. Electr., Bull. 10, 429 (1937); Nature, **139**, 110 (1937).
[12] Schonland, Elder, Hodges, Phillips, and Van Wyk, Proc. R. Soc., A, **176**, 180 (1940).
[13] M. Nicolet, Mixed Commission on Ionosphere, U.R.S.I., Bruxelles, p. 50 (1948).
[14] E. V. Appleton and W. J. G. Beynon, Nature, **164**, 308 (1949).

[15] D. F. Martyn, Proc. R. Soc., A, **194**, 445 (1949).
[16] A. G. McNish, Terr. Mag., **42**, 109 (1937).
[17] T. G. Cowling and R. Borger, Nature, **161**, 515 (1948).
[18] British National Committee for Scientific Radio, U.R.S.I., proceedings, p. 128 (1947).
[19] S. K. Mitra, J. N. Bhar, and S. P. Ghosh, Indian J. Phys., **12**, 455 (1938).
[20] R. Jouast and E. Vassey, Paris,C.-R. Acad. sci., **213**, 139 (1941).
[21] A. Vassey and E. Vassey, Cahiers de Physique, **9**, 28 (1941).
[22] E. G. Schneider, J. Optical Soc. Amer., **30**, 128 (1940).
[23] J. J. Hopfield, Astroph. J., **104**, 208 (1946).
[24] O. E. H. Rydbeck, Trans. Chalmers Univ., No. 34 (1944).
[25] H. G. Booker, Proc. R. Soc., A, **150**, 267 (1935).
[26] D. R. Hartree, Proc. R. Soc., A, **131**, 428 (1931).
[27] M. V. Wilkes, Proc. R. Soc., A, **175**, 143 (1940).
[28] M. V. Wilkes, Proc. R. Soc., A, **189**, 130 (1947).
[29] J. P. Stanley, J. Atmos. Terr. Phys., **1**, 65 (1950).
[30] K. F. Chackett, F. A. Paneth, and E. J. Wilson, Nature, **164**, 128 (1949).
[31] D. R. Bates and H. S. W. Massey, Proc. R. Soc., A, **187**, 261 (1946).
[32] M. Nicolet, Inst. R. Met. Belgique, Mém. 19, 1–162 (1945).
[33] J. A. Gledhill and M. E. Szendrei, Proc. Phys. Soc., B, **63**, 427 (1950).
[34] M. E. Bradbury, Terr. Mag., **43**, 55 (1938).
[35] L. G. H. Huxley, Proc. R. Soc., A, **200**, 486 (1950).

EFFECTS OF IONOSPHERE DISTURBANCES ON LOW FREQUENCY PROPAGATION

By J. M. Watts and J. N. Brown

Central Radio Propagation Laboratory, National Bureau of Standards, Washington 25, D. C.

(Received May 10, 1951)

ABSTRACT

Results of vertical-incidence pulse observations at the Central Radio Propagation Laboratory, National Bureau of Standards, show that ionospheric storms have appreciable effects on the reflective properties of the *E*-region at night. Daytime effects of storms are limited primarily to periods of high absorption, coinciding with similar effects at higher frequencies. Data obtained at 160 kc indicate that the character of low frequency reflections at night may be a sensitive indication of storminess. Correlation is shown between magnetic *K*-indices and low frequency data. During storms, effects have been of such magnitude that they cannot be ignored in design of low-frequency navigational or high-speed communications systems.

Reflections from the ionosphere at vertical incidence have been observed at frequencies of 50, 100, and 160 kc at the Central Radio Propagation Laboratory, of the National Bureau of Standards, since January 1950. Most of the data obtained have consisted of virtual height *versus* time recorded on 35-mm film. A vacuum-tube pulse transmitter, delivering about 900-kw peak pulse power to a loop antenna, and a double conversion receiver connected to a dipole antenna have proved satisfactory for recording virtual height at 50 kc in the winter and at 100 and 160 kc during the summer high absorption period.

The film records have been studied with the purpose of determining the normal character of reflections and their abnormal variations. A summary of this material follows.

During the day, vertical-incidence reflections from the ionosphere at frequencies between 50 and 160 kc exhibit uniform virtual heights of about 90 km. This occurs with great regularity, and a single mode is nearly always received with little evidence of turbulence. Figure 1 is a section of height-*versus*-time record, illustrating the transition from night to day during a quiet period. In all illustrations, three-hour *K*-indices are given as a gauge of geomagnetic activity.

The night-time trace may be slightly spread even though conditions are quiet. The change in height from 100 to 90 km begins at about $05^h\ 25^m$, which agrees

closely with the local sunrise time of $05^h\ 26^m$ for August 18, 1950. The increasing absorption with sunrise is evidenced by the disappearance or weakening of the multiple traces.

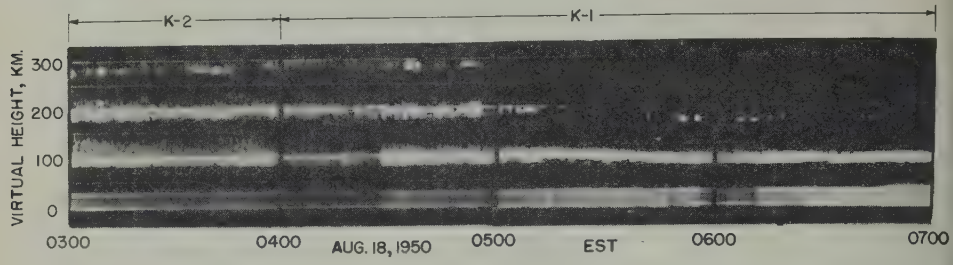

FIG. 1

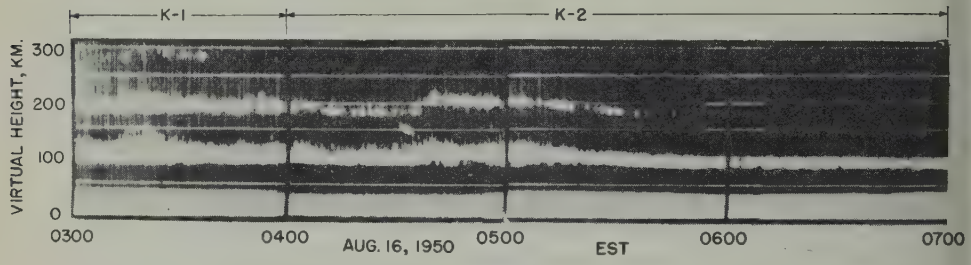

FIG. 2

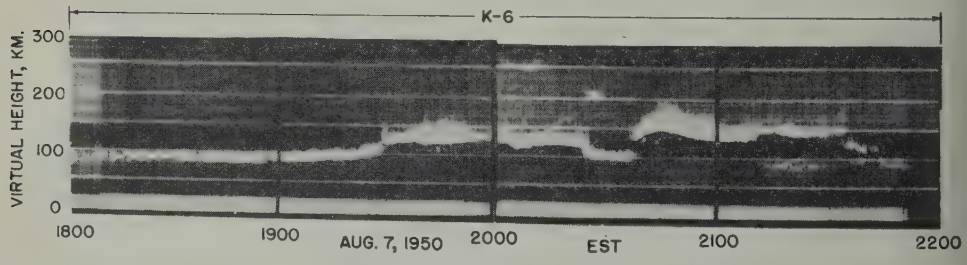

FIG. 3

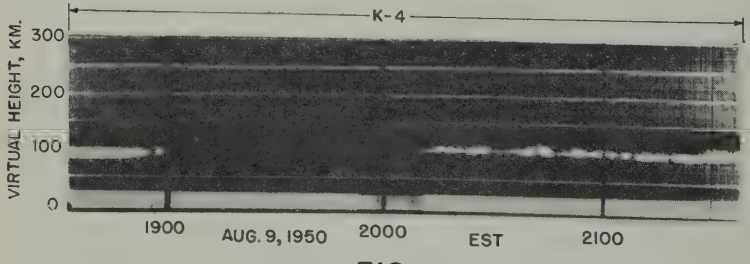

NOTE: MULTIPLY SCALED HEIGHTS IN ALL FIGS. BY 1.12 FOR CORRECTED VIRTUAL HEIGHTS.

FIG. 4

Figure 2 illustrates a phenomenon which is not unusual, although it occurs more often at night. At $04^h\ 40^m$, the lower level of reflection disappeared and a higher level appeared. The change is more easily seen in the multiple trace. The virtual

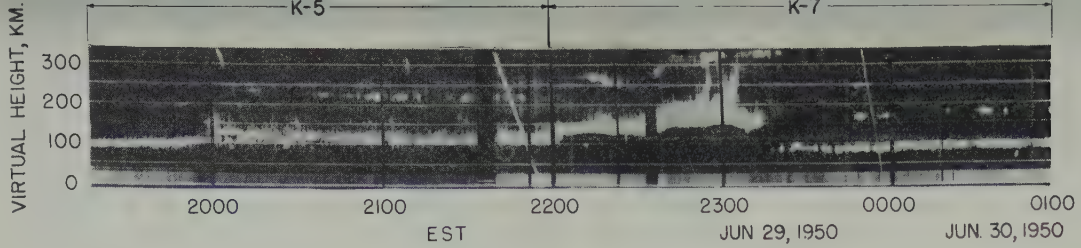

NOTE:
MULTIPLY SCALED HEIGHTS IN ALL FIGS. BY 1.12 FOR CORRECTED VIRTUAL HEIGHTS.

FIG. 5

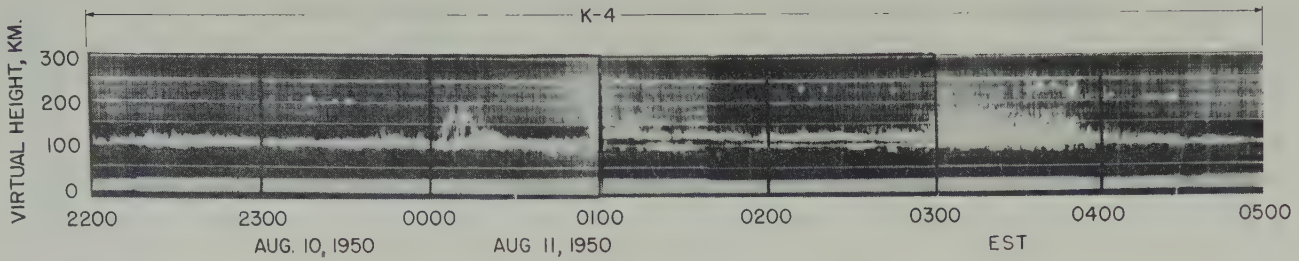

FIG. 6

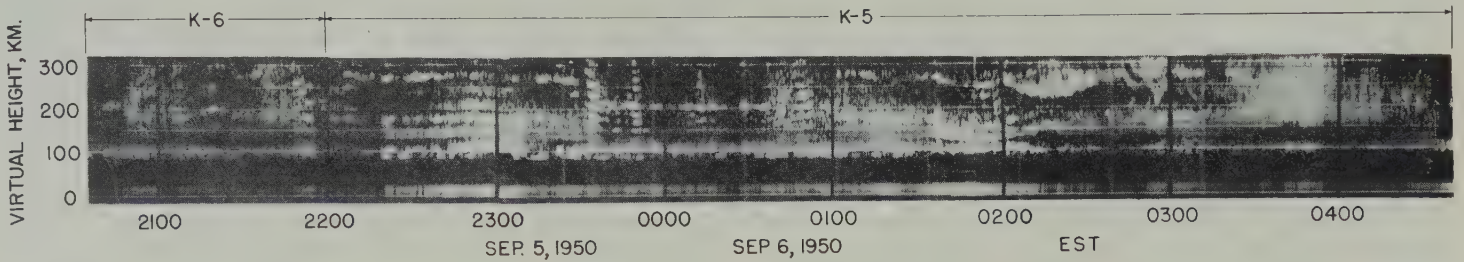

FIG. 7

height of the new reflection proceeded to decrease, and then the usual sunrise effect caused a further lowering.

The increase in layer height at sunset is usually not as abrupt as the decrease at sunrise. For this reason, the record in Figure 3 is especially interesting. Figure 3 shows a sunset period on a day which was definitely disturbed according to both high-frequency transmission standards and geomagnetic standards. At $19^h\ 30^m$, the trace showed a cusp strongly suggestive of group retardation, which is often observed at higher frequencies near critical frequencies of layers. This, indeed, may have been produced by the real *E*-layer critical frequency as it decreased to, and then went below, the observing frequency (160 kc). After $19^h\ 30^m$, all semblance of a regular, stable, reflecting region ceased. The abrupt changes in height centered about $20^h\ 30^m$ should be noted, and also the weakening of all reflections after $21^h\ 10^m$. The record of Figure 4 was made on a moderately disturbed day, and no abrupt changes of height were noted. However, the fade-out of $19^h\ 00^m$ to $20^h\ 10^m$ occurred at the same time as a fade-out at higher frequencies, and also a fade-out on a 100-kc, 1500-km oblique incidence path.

Figure 5 illustrates another possible *E*-layer critical frequency observed at $20^h\ 00^m$, similar to that in Figure 3. The fact that this record was made near midsummer could account for the later time for the *E*-layer critical to drop to 160 kc. From $20^h\ 00^m$ to $22^h\ 00^m$, a slightly spread echo was returned. At $22^h\ 05^m$, that echo was supplanted by a diffuse reflection of changing virtual height, which lasted until $23^h\ 15^m$, when the original low-level trace reappeared.

Another type of trace which may be recorded during a disturbance is shown in Figure 6. The geomagnetic index observed at that time represents a moderately disturbed condition, yet the low-level reflection was absent all night and irregular layers at heights of 100 and 130 km were recorded. Just before $01^h\ 00^m$, both of these layers were recorded simultaneously, and several interlayer reflections resulted. At $03^h\ 00^m$ to $04^h\ 00^m$, extensive scattering was evident.

Figure 7 is more complicated than many high-frequency ionospheric records. Low absorption and the presence of several reflecting boundaries have resulted in many traces due to direct reflections, indirect reflections from interlayer reflections, scattered reflections, and combinations of multiple reflections of all of those types. The lower level was apparently a partial, but unstable, reflector most of the night. Enough energy was propagated through it to reveal the structure above.

As a further check of the correlation between ionospheric disturbances and the geomagnetic *K*-index numbers, the records between sunset and sunrise for the months of May to November, 1950, were scaled to determine what percentage of the operating time appeared to be disturbed. The following conditions were chosen as criteria in deciding whether or not an echo pattern was disturbed: Absence of the normal 80 to 100-km level return, presence of extra layers at abnormally high virtual heights, spread echo patterns when associated with some other indication of disturbed conditions, weakened or absent echo patterns when coincident with high-frequency sudden ionosphere disturbances. The three-hour magnetic *K*-index numbers for the night-time operating period of each day were added and normalized by dividing by the number of operating hours. Figure 8 shows the comparison of these two quantities for a typical month, October 1950.

The conclusions to be drawn from these low frequency records must necessarily e tentative. The observing period has been short, May 1950 to November 1950. peration at fixed frequency yields data having the same limitations suffered by ne pioneer high-frequency observations performed many years ago at a few fixed requencies. A comparison of the 50-kc and 160-kc data indicates that the type of isturbance characterized by the night-time absence of the low-level reflection ccurs less often at the lower frequencies. Also, the duration of disturbance and its everity are less at 50 kc than at 100 and 160 kc. Conclusions derived from vertical-ncidence data may not be valid at oblique incidence, but it seems evident that the

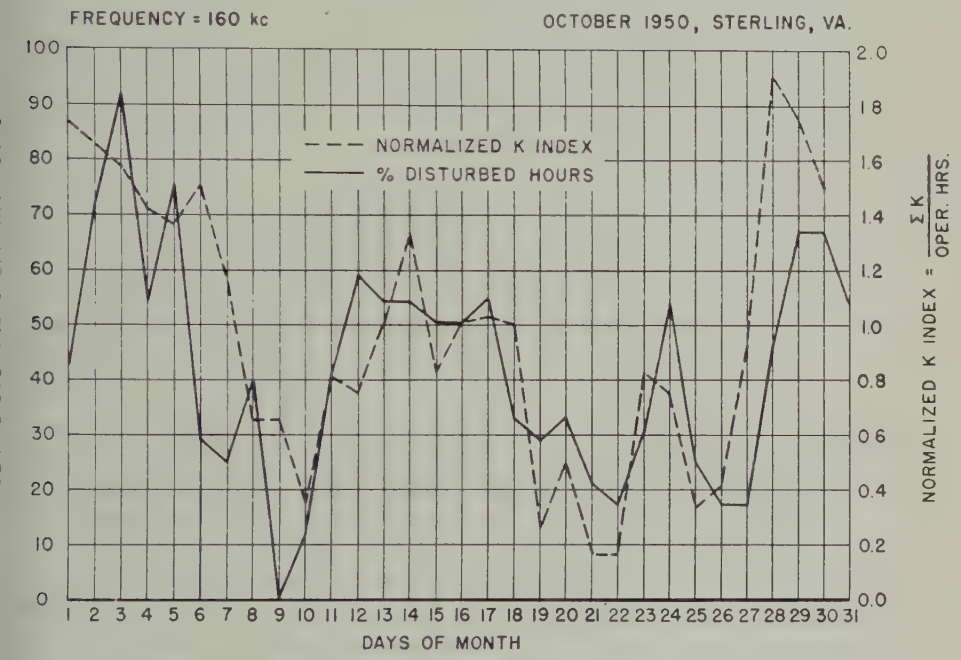

FIG. 8—CORRELATION OF PERCENT DISTURBED OPERATING TIME AND NORMALIZED MAGNETIC K INDICES (CHELTENHAM) (RESTRICTED TO HOURS BETWEEN SUNSET AND SUNRISE)

nformation cannot be ignored in the design of certain low-frequency navigational ystems or high-speed communication systems.

A more satisfactory understanding of ionospheric layer-structure in the *E*-egion will require the use of sweep-frequency equipment, similar to the automatic quipment now in use at the higher frequencies and covering the frequency range f 50 kc to 1 Mc. It is intended, when such apparatus is available, to pursue in-estigations using these techniques. Thus, the transition from *E*-region to *F*-region eflection at vertical incidence would be recorded during each frequency sweep hroughout the night, adding more information concerning the probable sources f ionization in the night-time *E*-region.

References

J. N. Brown and J. M. Watts, Ionosphere observations at 50 kc, J. Geophys. Res., **55**, 179-181 (1950).

R. A. Helliwell, Ionospheric virtual height measurements at 100 kilocycles, Proc. Inst. Radio Eng., **37**, 887-894 (1949).

C. Williams, Low-frequency radio-wave propagation by the ionosphere, with particular reference to long-distance navigation, Proc. Inst. Elec. Eng., **98**, Pt. 3, 81-103 (1951).

THE MODES OF FORMATION OF THE IONOSPHERIC LAYERS

By J. H. Piddington

Division of Radiophysics, Commonwealth Scientific and Industrial Research Organization, Sydney, Australia

(Received May 21, 1951)

ABSTRACT

Ionospheric measurements made during eclipses are analyzed and, together with recently acquired solar data, are used in a reexamination of the theories of the ionosphere. It is shown that:

(*i*) The rates of disappearance of electrons in all the principal layers may be much higher than hitherto believed. If so, then the number of ionizing quanta needed is also greatly increased.

(*ii*) There is probably a non-solar source of electron production in region *E* (and perhaps region *D*). It may be the electric currents flowing in the upper atmosphere which are also manifested by fluctuations in the earth's magnetic field.

(*iii*) Solar ionizing radiation does not appear to originate (principally) either throughout the corona or near the photosphere, but in regions of rapid temperature transition in the chromosphere and lower corona. Excess emission occurs, as has been shown previously, from regions of disturbance, often near sunspots.

(*iv*) The emission spectrum of these regions may be strong in the quasi-Lyman spectrum of HeII and in X-rays of wave-length ranging down to about 3 Å. During flares, X-rays of wave-length less than 1 Å may be emitted.

(*v*) The *F*1 and *F*2 ionospheric layers may be accounted for if minor modifications of existing theories are made. The *E* and *D* layers may be formed by quanta of a few hundred and a few thousand electron volts, respectively, originating in the chromospheric transition region.

I—INTRODUCTION

Bates and Massey (1946) have discussed the various theories of formation of the ionospheric layers. They found that the *F*1 and *F*2 layers might reasonably be accounted for in terms of photo-ionization of O and N_2 by quanta in the range

13.5 eV to above 18.7 eV. No satisfactory theories of formation of the D* or *E* layers were available, however. Subsequently, Nicolet (1947) suggested that the *E* layers might be formed by a process of pre-ionization of O_2 and Hoyle and Bates (1948) examined an alternative theory involving ionization by quanta of energy about 325 eV (or perhaps 1,300 eV) originating in the solar corona. Finally, Bates and Seaton (1950) quantitatively tested various theories of formation of *D* region ionization and concluded that one, the ionization of NO by certain quanta in the range 10 eV to 11 eV, might be tenable.

The apparently satisfactory position outlined above has, unfortunately, deteriorated in the face of a number of criticisms of the various theories. Bates and Seaton (1950) found that a new determination of the absorption cross-section of O was rather low to account for the level of the *F*1 layer. Penndorf (1949) concluded that all molecular oxygen lay below the *E* region, thus raising a difficulty for the preionization theory. Bates (1949) found that observations during the twilight flash showed a very small number of N_2^+ ions. If ionization were due to 325 eV quanta as suggested by Hoyle and Bates, these ions should be plentiful. Objections to the NO theory of the *D* layer may be found in a very high value of apparent recombination coefficient and other factors discussed below.

In the present communication, further data concerning the ionosphere are sought among the results of radio observations made during a number of eclipses. Although most of the results have been published for some years, no systematic investigation has, apparently, been made. The following conclusions are reached:

(*i*) Values of effective recombination coefficients in regions *E*, *F*1, and *F*2 are much higher (perhaps by a factor of 10) than the usually accepted values. This implies, of course, a corresponding increase in the numbers of ionizing quanta.

(*ii*) There may be two and perhaps three sources of electron production in region *E*.

(*iii*) The ionizing radiation responsible for regions *D*, *E*, and *F*1 does not originate throughout the corona.

(*iv*) The radiation is emitted more strongly from certain regions of disturbance associated with sunspots. Evidence of this has already been given by Higgs (1942), Rydbeck (1946) and Waldmeier (1947). It appears likely that the radiation is emitted mainly from chromospheric levels, the photosphere playing a minor, perhaps negligible, role.

In the second part of this paper, the formation of the ionospheric layers is discussed in the light of the above new evidence and of other solar and terrestrial data obtained in the past few years. It is concluded that existing theories may, with modification, satisfactorily explain the formation of regions *E*, *F*1, and *F*2. It is suggested, however, that quanta from the quasi-Lyman spectrum of HeII may play

*The limited experimental evidence available is insufficient to prove the existence of a discrete *D* layer. In the present communication, all ionization lying below the *E* region is referred to as "*D* region ionization." The level of transition from the *D* to the *E* region cannot, at present, be defined, but it is taken that the *E* layer does not depart greatly from a simple Chapman layer. The lower boundary of *D* region is probably at a level of about 50 km.

n important, even a major, part. A theory of the origin of part at least of D region onization in terms of X-rays of wave-length about 1Å to 3Å is presented.

II—EFFECTIVE RECOMBINATION COEFFICIENTS

The effective recombination coefficient α of a region may be found by using he formula

$$\frac{dN}{dt} = Q - \alpha N^2 \quad \ldots\ldots\ldots\ldots\ldots\ldots\ldots\ldots (1)$$

vhere N is the electron density and Q the rate of electron production. As Q varies liurnally or during an eclipse, N will vary in a manner depending on α.

(*a*) *The E and F1 regions*—Determination of α_E from observations of diurnal ariations of critical frequency have been made by Best, Farmer, and Ratcliffe 1938) and others, a value of about 1×10^{-8} cm^3 sec^{-1} being indicated. However, he results seem far from conclusive; for example, their winter observations give a est fit for an infinite value of α. Also, in interpreting the observations, the following ossibilities have been overlooked. The distribution of ionization in region E may liffer considerably from a simple Chapman region, contributions being made by uanta with a wide range of energies; it is shown below that even the radiation esponsible for the D region may cause an appreciable effect in E region. It is also hown that a non-solar source of ionization may be present. These effects would ender the determinations of α from observations of diurnal variations open to onsiderable doubt.

Since changes in Q are much more rapid during eclipses, the results provide a nore reliable method of finding α. Values of α_E and α_{F1} are listed in Table 1. Results for the 1935 eclipse—referred to in subsection IV(*a*)—are omitted because he percentage of totality was too small, as also some of those for the 1945 eclipse ecause they are not as conclusive as those of McLeish, who observed a total clipse.

Table 1

Eclipse	Observer	α_E cm^3 sec^{-1}	α_{F1} cm^3 sec^{-1}	Time lag φ
1932	Kirby, *et al.* (1934)	....	....	Zero
1940	Gilliland (1942)	2×10^{-8} to 1×10^{-7}	$10^{-8} - 10^{-7}$	Zero
1940	Higgs (1942)	1.7×10^{-8}	....	Zero
1944	Ledig, *et al.* (1946)	....	....	Negative
1944	Baral and Mitra (1944)	....	....	Positive
1945	McLeish (1948)	1.6×10^{-8}	1.4×10^{-8}	Positive
1947	Bosson, *et al.* (1947)	0.2×10^{-8} to 0.7×10^{-8}	1×10^{-9} to 3×10^{-9}	Positive

In determining α from eclipse data, it has been assumed that Q is proportional o the unobscured area of the solar disk. Equation (1) then allows theoretical clipse curves to be drawn for different values of α. These curves have a time lag φ ehind the optical eclipse curve, and a minimum value of electron density N_m. Experimental and theoretical eclipse curves are illustrated in Figure 1, which is re-

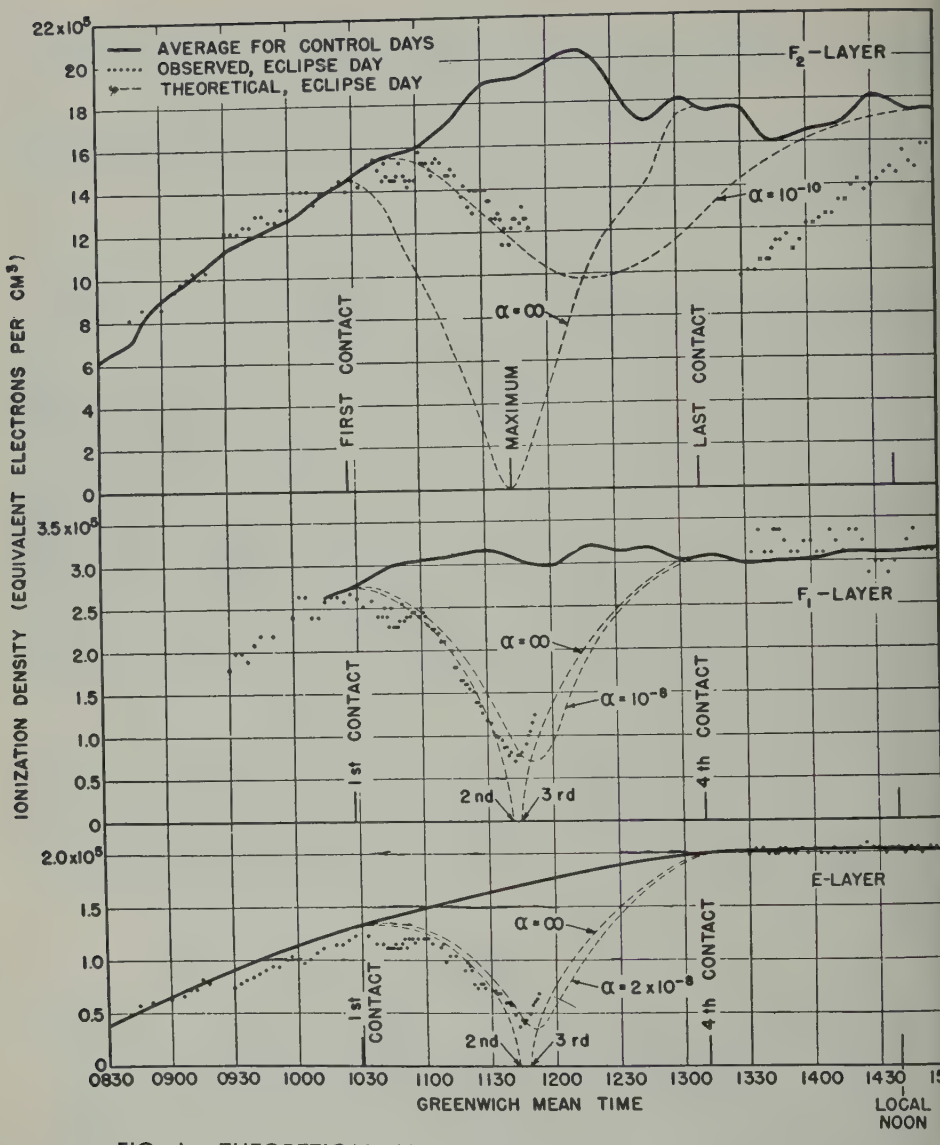

FIG. 1—THEORETICAL AND EXPERIMENTAL VALUES OF ELECTRON DENSITY IN THE IONOSPHERIC LAYERS DURING AN ECLIPSE (REPRODUCED FROM A PAPER BY T. R. GILLILAND IN THE NATIONAL GEOGRAPHIC SOCIETY (U.S.), SOLAR ECLIPSE SERIES NO. 2)

produced from Gilliland's (1942) paper. It will be seen (for the E and $F1$ regions that, although the theoretical and experimental curves give the same value of N_m they have quite different values of φ. Gilliland remarked on this and suggested a lower and an upper limit of α_E of 2×10^{-8} cm^3 sec^{-1} and 1×10^{-7} cm^3 sec^{-1} to match the observed values of N_m and φ, respectively. Higgs (1942) found

milar discrepancy, and suggested that it was due to an irregular distribution of the ources of ionizing radiation over the solar disk. However, Gilliland's results show ot only a very sharp and definite minimum during totality but even a small increase ı ionization during the same period.

The anomaly may be explained either by the presence of some ionizing agency uring totality, or by the continued existence of a small proportion of ions which isappear very slowly. A combination of the two effects is also, of course, a possiility. In Table 2 of subsection IV(*a*), it is shown that the proportion of residual onization varies considerably from one (total) eclipse to another. This would seem o favour the first possibility, since the proportions of different ions (say O^+ and N_2^+) ight be expected to remain reasonably constant. Furthermore, evidence of the xistence of a solar ionizing agency during totality is given in subsection IV(*b*), here it is shown that some ionizing radiation originates in regions situated well bove the photosphere and which may not be eclipsed at totality. The contribution o N_m by residual ionization is discussed in the following section. It should be emembered that, if some ions disappear much more slowly than others, then there re actually two effective recombination coefficients. The one discussed here applies o the larger proportion of ions.

It remains to explain the fact that on three occasions positive values of φ *were* btained as shown in Table 1. The results of Bosson, *et al.*, are most interesting, as ney show a considerable lag, indicating very small values of α_E and α_{F1}. However, lthough there is a marked asymmetry in the general shape of both eclipse curves, evertheless the minimum values of electron density were, in each case, recorded uring totality. Furthermore, the eclipse curves show a general similarity to a plot f the unobscured active areas of the sun for the period of the eclipse (Haikin and hikhachev, 1948). Similarly, during the eclipse observed by McLeish, there was a arked concentration of sunspots near the eastern limb. There was no marked oncentration of spots on the solar limb during the eclipse observed by Baral and Iitra. However, the observations of E region critical frequencies were so widely paced (about 25 minutes) that it could not be stated definitely that the minimum id not occur at eclipse maximum (of 87 per cent). The eclipse curves of Ledig, *et al.*, owed a small negative value of φ. It is tentatively concluded that asymmetry bserved has been caused by irregular distributions of the sources of ionizing adiation. The evidence for such irregularity is discussed in detail in section IV.

The best estimates of α_E and α_{F1} can be made from Gilliland's curves. Considera-on of the rates of change of slope of the eclipse curves during totality suggests alues of 2×10^{-7} cm^3 sec^{-1} and 1×10^{-7} cm^3 sec^{-1} for E and $F1$ regions, respecvely. However, the determination is very uncertain and perhaps the safest course to take 1×10^{-7} cm^3 sec^{-1} and 5×10^{-8} cm^3 sec^{-1} as the best estimates (rather han the upper limits) of α_E and α_{F1}, respectively. These are much higher than the sually accepted values of 1×10^{-8} cm^3 sec^{-1} and 4×10^{-9} cm^3 sec^{-1} (Bates and Massey 1946).

It is possible that the large values of α deduced from eclipse observations may e peculiar to eclipse conditions. For example, if the value of λ (ratio of negative ns to electrons) were controlled mainly by a process of photodissociation, it ight increase during the eclipse as the photons causing dissociation were cut off.

This would result in an increase in the proportion of negative ions and a more rapid decrease in the value of N. However it seems more probable that λ is limited by collision detachment (Bates and Massey, 1946), in which case λ could increase only if that process were slowed. Such an effect might be possible if detachment by collision with excited particles was important; such particles might be expected to disappear in the absence of solar radiation. In that case, a high value of α during the night would also be expected. A decision between the importance of various factors involved must await more detailed knowledge of the processes of attachment and detachment.

The extremely large values of α_E and α_{F1} determined above, increase the already considerable difficulties of explanation which have been discussed by Bates and Massey (1947). They do seem, however, to accord with more recent experimentally determined values mentioned by Bates (1950) and may, as he points out, be due to a process of dissociative recombination.

If such a process does determine α_E , then the value of α in D region would be greater by a factor at least as great as the ratio of molecular densities. At 90 km, the lower limit of α would be about 1×10^{-5} cm^3 sec^{-1}.

(*b*) *The F2 region*—Determination of α for the $F2$ region is more difficult than for lower regions. Appleton (1937), using observations of the diurnal variation of critical frequency, found a value of 8×10^{-11} cm^3 sec^{-1}; Martyn (1947), however, suggested that tidal motions would be so large as to invalidate the method. Woolley (1946) and Allen (1946) favour a value of about 1×10^{-11} cm^3 sec^{-1}. However, Woolley's value is chosen to conform with a black-body sun at 6000°K., which may be far from representing the actual conditions. Allen's result is based on a statistical analysis of sunspot numbers and ionospheric characteristics. He finds maximum correlations corresponding to delays up to several weeks of the ionospheric data behind the spot numbers. The delay for the $F2$ region is more than one day behind the average for the lower regions, and Allen concludes that this indicates slow recombination in the $F2$ region. However, as D and E regions probably have different origins,* the delay might be caused by other factors. It is only permissible therefore, to compare delays for regions $F1$ and $F2$, which is done in a later paper (Allen, 1948), the difference being only 0.6 of a day. If $F1$ and $F2$ regions have an identical origin, this might indicate a value of α of a few times 10^{-11} cm^3 sec^{-1}. If however, the origins are not identical, as is possible, then α cannot be found from the data. The value of α found from night-time decay of ionization density is about 3×10^{-11} cm^3 sec^{-1} (see Bates, 1949).

Unfortunately, eclipse observations of $F2$ ionization do not provide a simple method of finding α. Estimates ranging from 4×10^{-11} cm^3 sec^{-1} (Higgs, 1942) to 1×10^{-9} cm^3 sec^{-1} (Wells and Shapley 1946, McLeish 1948) have been made. It would seem that tidal or random effects invalidate the method.

One other method remains, based on the fact that $F1$ and $F2$ regions probably have a common origin (or very nearly so). Bates (1949) has shown that knowing α_{F1} and the relative gas and electron densities, α_{F2} may be determined. He found a value of 1.1×10^{-10} cm^3 sec^{-1}, but if the above estimate of α_{F1} is used, this leads to the extremely large value of about 1×10^{-9} cm^3 sec^{-1}. It is unlikely that th

*That is, are not formed by ionization of the same gas by the same radiation.

elative gas densities used are much in error and, although Bates considered that nly O was ionized, the result is unchanged if other gases are also affected. One ossibility is that the proportion of N_2 decreases with height. If this were the case nd if the absorption cross-section of N_2 were greater than that for N (in a part of he spectrum where quanta were plentiful), then our estimate of α_{F2} might be too arge. However, the value found is not inconsistent with a recent determination by Becker and Dieminger (1950), who decided that α_{F2} was not less than 2×10^{-10} m^3 sec^{-1}.

Summing up, it would seem that values of α_{F2} obtained from a simple interpretation of observational data may not give even an approximation to the true rate f electron disappearance. For example, the thickness of $F2$ region may be so large hat as electrons disappear at the level of maximum density the value of this maximum may remain nearly unchanged, while the level where it is found rises. The osition is then further complicated by tidal effects which, as Martyn (1947) has hown, may cause large vertical movements of the ions. The best estimate of α_{F2} nay lie between 1×10^{-9} cm^3 sec^{-1} and 1×10^{-10} cm^3 sec^{-1}.

III—A NON-SOLAR SOURCE OF ELECTRON PRODUCTION

Nocturnal values of α_E have been determined by Appleton (1937) and others, s about 2×10^{-9} cm^3 sec^{-1}. However, as Bates and Massey (1946) have pointed ut, these are probably too low because of the neglect of sources of ionization. They ssume a value of 1×10^{-8} cm^3 sec^{-1}, equal to the daytime value.

If the much larger value of α found above obtains during the night, then there nust be a considerable source of electron production. Observed rates of decay of onization are so small (leading, as seen above, to values of α_E of about 2×10^{-9} m^3 sec^{-1}) that we have, approximately

$$Q = \alpha N^2$$

Putting $N = 10^4$ cm^{-3} and $\alpha \geq 10^{-7}$, $Q \geq 10$ cm^{-3} sec^{-1}, about one per cent of the nidday rate of electron production.

A similar calculation suggests that there is also a night-time source of electron roduction in the upper D region.

An alternative to the presence of a nocturnal ionizing agency is that a proportion f daytime ions disappears very slowly. For example, in the E region, the ions conerned may be O^+ and N_2^+, the former disappearing much more slowly than the atter. Let A, n, n^+, and α be the absorption cross-section number of neutral and onized particles and effective recombination coefficient, and let subscripts 1 and indicate reference to O^+ and N_2^+, respectively. It may easily be shown that $n_1^+/n_2^+ = A_1 n_1 \alpha_2 / A_2 n_2 \alpha_1$. If nocturnal ionization is due to the persistence of O^+, nen we have for E layer: $n_1^+/n_2^+ \sim 0.1$, $n_1/n_2 \sim 0.5$, and $\alpha_2/\alpha_1 = 50$ (taking $\alpha_1 = \times 10^{-9}$ cm^3 sec^{-1} and $\alpha_2 = 1 \times 10^{-7}$ cm^3 sec^{-1}). Thus, $A_1/A_2 = 1/250$, which is onsiderably smaller than the likely ratio according to Bates and Massey (1946). Even if this mechanism played an important part in E region, it seems unlikely hat it could be important in D region as well, where a corresponding balance etween the various parameters would have to exist under very different conditions.

It is concluded that most of the ions concerned are probably formed by a nocturna ionizing agency.

Dufay and Dufay (1947) have measured the intensity of the negative banc system of N_2 in the twilight flash. The emission was mainly from a region at a leve of 100 km $\pm$ 25 km, and was observed some time after sunset (on the ground) when radiation reaching the layer concerned must traverse lower layers. They found that the intensity varied with magnetic and auroral activity, and was not visibl during very quiet periods. Bates (1949) analyzed these results, and showed that th proportion of N_2^+ ions was a minute fraction of the total ions present. He pointe out that the simplest explanation of this conclusion was that N_2 was not appreciably ionized by solar radiation. An alternative explanation was also given in terms of the relatively rapid disappearance of N_2^+ ions in the manner discussed above. The ob servations of Dufay and Dufay and the analysis of Bates may also be explained in terms of the rapid recombination of all the ionization in the region concerned, and the presence of a nocturnal ionizing agency. This agency would appear to be connected in some way with magnetic disturbances.

In speculating on the possible sources of night-time electron production, ioniza tion by solar ions is ruled out on several counts; for example, several investigations have shown that improbably high kinetic energies are needed to penetrate to the low levels concerned. Ionization by meteors has been discussed by Lovell (1950) who found the effect too small to be appreciable.

The most likely source of electron production appears to be electric currents flowing in the regions concerned. The existence of such currents is indicated by fluctuations of the magnetic elements. A low proportion of N_2^+ ions, as found by Bates, would be anticipated because of the higher ionization potential of N_2 . In addition to ionization by collision, excitation and subsequent emission of radiation would occur and might explain the results of Dufay and Dufay, particularly the correlation of intensity with magnetic and auroral activity. Such emission might also be the explanation of the light of the night sky (non-polar aurora), many properties of which are explicable in terms of excitation by electric currents (Rayleigh and Jones, 1935).

IV—THE REGIONS OF ORIGIN OF THE SOLAR IONIZING RADIATION

In considering the formation of the ionospheric layers, it has been customary to consider the radiation as originating on the solar disk and having intensity corresponding to a black body at about 6000°K. Such a simplification was justified, in view of our limited knowledge of the solar atmosphere. The simplification was not without its dangers, however, and may, as shown above, have led to misinterpretation of eclipse results. A totally different source of some ionizing radiation has been suggested by Hoyle and Bates (1948), who suggest a coronal origin. It is proposed to examine eclipse and other data to find, if possible, just where the regions are from which the radiation is emitted.

(*a*) *Observations of the ionosphere during eclipses*—It has been shown above that in E and $F1$ regions (and, presumably, D region) the apparent recombination coefficient is so large that equation (1), even during an eclipse, reduces to

$$Q = \alpha N^2 \quad \ldots\ldots\ldots\ldots\ldots\ldots\ldots\ldots\ldots\ldots (2$$

Again, since the critical frequency f of a region is related to the maximum electron density,

$$N \propto f^2 \quad \ldots\ldots\ldots\ldots\ldots\ldots\ldots\ldots\ldots\ldots (3)$$

Therefore

$$Q \propto f^4 \quad \ldots\ldots\ldots\ldots\ldots\ldots\ldots\ldots\ldots\ldots (4)$$

This fourth-power law has been verified by Allen (1948). He found values of 3.72 and 4.90 for E and $F1$ regions, respectively, but concluded that the theoretical value of 4 is probably the best estimate.

It is now evident from proportionality (4) that values of critical frequency measured during an eclipse allow relative values of Q to be determined. Knowing the parts of the solar atmosphere and disk which are obscured at each instant, it is possible to make some deductions as to the regions of origin of the ionizing radiation. In particular, the theory of origin throughout the corona may easily be tested.

If N and N' are the values of maximum electron density in a layer before, and at, eclipse maximum, and Q and Q' the corresponding rates of electron production, then $(N/N')^2 = Q/Q'$. Values of N/N' and of Q/Q' for a number of eclipses and for regions E and $F1$ are listed in Table 2. Where critical frequency data are quoted in the reference, the proportionality (3) is used. Blank spaces indicate that suitable data were not available. Data obtained by Henderson (1933) at the 1933 total eclipse are omitted because a satisfactory method of determining critical frequencies had not been developed.

TABLE 2

Eclipse	Reference	Percent totality	N/N'		Q/Q'		N'	N'
			E region	F_1 region	E region	F_1 region	E region	F_1 region
Aug. 31, 1932	Kirby, *et al.* (1934)	90	3.3	2.5	10	6.2	....	....
Feb. 3, 1935	Kirby, *et al.* (1936)	35	1.2	1.1	1.4	1.3	....	....
Oct. 1, 1940	Gilliland (1942)	100	4.3	4.1	19	17	4×10^4	7×10^4
Oct. 1, 1940	Higgs (1942)	100	2.9	....	8.4	....	3×10^4	6×10^4
Jan. 25, 1944	Ledig, *et al.* (1946)	88	2.4	2.5	5.9	6.3	....	....
Jul. 20, 1944	Baral and Mitra (1944)	87	1.8	....	3.1	....	....	....
Jul. 9, 1945	Gejer and Akerlind (1947) at Sörmjöle	99	2.4	2.4	5.7	6.0	4×10^4	7×10^4
Jul. 9, 1945	Gejer and Akerlind (1947) at Hörnsjö	99	1.6	3.1	2.4	9.8		
Jul. 9, 1945	Gejer and Akerlind (1947) at Östersund	95	2.3	2.7	5.4	7.3	....	....
Jul. 9, 1945	Gejer and Akerlind (1947) at Tromsö	93	2.0	2.3	3.8	5.4	....	....
Jul. 9, 1945	McLeish (1948)	100	2.3	3.2	5.3	10	3×10^4	6×10^4
May 20, 1947	Bosson, *et al.* (1947)	100	2.8	4.0	7.8	16	6×10^4	11×10^4

(*b*) *Coronal emission*—Let us assume that the corona has uniform temperature and composition. The number of any particular type of quanta emitted from a small volume is proportional to the number of collisions between the types of ion involved, which, in turn, is proportional to N_e^2 , where N_e is the electron density in the region concerned. Since appreciable reabsorption of high energy quanta is not likely (Woolley and Allen, 1948), the rate of electron production in the ionospheric layers is given by

$$Q \propto \int N_e^2 \, dv \qquad (5)$$

The integration is throughout the unobscured volume of the corona. Reasonable values of N_e are given by Allen's (1947) distribution, so that relative values of Q under different conditions may be calculated. This is done in Appendix I for non-eclipse and total eclipse conditions, and it is found that the ratio of the values of Q is 2.03. Thus, if all the radiation responsible for, say, the E layer, originated in the corona, the decrease in flux density at eclipse totality would only be in the ratio of about 2/1. This ratio may be compared with the values of Q/Q', listed in Table 2. The averages for the total or near total eclipses are 7.6 and 11.6 for regions E and $F1$, respectively. It would seem that, even if there is a considerable departure from the conditions of uniformity assumed above, it is most unlikely that a large proportion of the E or $F1$ region ionizing agency originates throughout the corona (according to Allen's coronal electron density distribution).

It may be noted that, if there were any appreciable lag in ionization equilibrium during the course of the eclipse (as there is for region $F2$), then the observed value of Q/Q' would be smaller than the ratio of flux densities of ionization; the discrepancy between the experimental results and a theory of coronal origin would be greater.

One determination of N/N' for D region was made by Ledig, *et al.* (1946) for the 1944 eclipse, using as a measure of electron density the minimum frequency observable after reflection from a higher region. The minimum frequencies before the eclipse and at totality, f_m and f_m' , depend on the total absorption in the D region. The absorption at any given level, and hence the total absorption, varies as N and inversely as the square of the frequency, so that $(f_m/f_m')^2 \propto N/N'$ as in (3). The value of $(N/N')^2$ or Q/Q' for region D was 11, so that the ionizing agency was reduced to 9 per cent of its pre-eclipse strength, while the proportion of visible solar disk was reduced to 12 per cent of the full disk. Evidently the agency responsible for region D does not have its origin throughout the corona.

The existence of evidence of a coronal origin of ionizing radiation has been claimed by Waldmeier (1947) and Wells and Shapley (1946). Waldmeier discusses eclipse results, comparing variations in E region ionizing agency with the eclipsing of regions known for high coronal-line (λ5303) intensity or for concentration of faculae. He shows that the ionizing radiation may originate largely in regions of disturbance in the solar atmosphere; the actual sources need not, however, be in the corona but might be much lower, the connection with coronal emission being explained in terms of a common agency causing both phenomena. Waldmeier's conclusions are not, however, invalidated by the eclipse results analyzed above

It has been shown that the radiation does not originate *throughout* the corona, but it may, as seen below, originate near the base of the corona.

Shapley and Wells have suggested that a drop in $F2$ critical frequency some time before first contact of the 1944 eclipse was due to the obscuration of a source of ionizing radiation far out in the corona. In view of the low rate of disappearance of electrons in the $F2$ region, the inference is not likely to be correct. Furthermore, their records show other, unexplained, irregularities in $F2$ eclipse curves occurring at other times.

(*c*) *The emitting regions*—Beyond showing that most of the E and $F1$ ionizing agency does not originate throughout the corona, the eclipse results do not provide a very definite indication of the vertical extent of the emitting regions. The residual value of Q at totality for the total eclipses varies from about 5 per cent to 20 per cent for E region and from about 5 per cent to 10 per cent for $F1$ region. The residual ionizing agency may originate in emitting regions projecting beyond the moon's limb or from the corona generally or from the terrestrial agency discussed above. Until more data are available, a decision cannot be made. However, as the value for both E and $F1$ regions is of the same order (which would not be expected for coronal radiation) and is much greater than the night-time agency (10 per cent instead of 1 per cent), the first-mentioned possibility is favoured.

Gilliland (1942) pointed out that an increase in electron density occurred in both regions during totality (just after second contact). The limb of the moon at mid-eclipse covered the solar atmosphere to a level of about 33,000 km, so that if the effect were real it would indicate radiation from a considerable height. McLeish's (1948) results indicate a decrease in radiation after totality, which also suggests a fairly concentrated source of radiation at a considerable height. It would seem that, although the evidence is far from conclusive, radiation may be emitted from regions as high as some tens of thousands of kilometres above the photosphere.

An estimate of the lower level of the radiation regions may be obtained from observations of thermal radio-frequency radiation from the sun. These have been discussed by Piddington (1950), who derived a relationship between electron temperature T_e and optical depth τ, at frequency f, as follows:

$$T_e \simeq 4800 + 9{\cdot}1 \times 10^{13}(\pi f^2 \tau)^{-1/2}$$

The observational results include frequencies up to 24,000 Mc/sec, and more recent results of Hagen (1949) extend the range up to 35,000 Mc/sec. At that frequency, values of T_e for optical depths of 1 and 2 are 6300°K. and 5800°K. The smoothness and continuity of the data suggest that the electron (and, presumably, gas) temperature continues to fall as the photosphere is approached. The regions from which most of the radio-frequency emission emerges are generally optically very thin for visible and ultra-violet frequencies, so that the (visible) black-body sun lies at a much lower and cooler level, perhaps about 5000°K. Even a 6000°K. black-body sun does not satisfactorily account for the ionized layers (Bates and Massey, 1946) and the discrepancy is greater for larger values of α. It is concluded that the general black-body radiation, emerging from below levels of a few thousand kilometres, may play an insignificant part in the formation of the ionosphere.

The work of Higgs (1942), Allen (1946, 1948), Rydbeck (1946), and Waldmeier (1947) shows that the ionizing agency originates largely in "active" areas which may be associated with sunspots, faculae, flocculi, and excessive emission of coronal lines. The eclipse results of Bosson, *et al.* (1947) and Gilliland (1942) provide further evidence; obscuration of large spot groups coincides with apparent decreases in the ionizing agency of 50 per cent and 20 per cent, respectively, for both E and $F1$ regions.

It would seem, therefore, that the solar ionizing radiation originates mainly in the upper chromosphere and lower corona, between a few thousands and some tens of thousands of kilometres; the distribution over the disk is irregular, a large proportion of the radiation emerging from "hot regions" associated with sunspots and other regions of disturbance.

Observations of solar radio-frequency radiation have recently led to the discovery of strongly emitting or "bright" patches on the solar disk, responsible for a slowly varying component of radiation. These patches are usually associated with sunspot groups or other regions of disturbance and, as Piddington and Minnett (1951), have shown, they probably emit thermal radio radiation corresponding to temperatures up to about 1×10^7°K and consist of large volumes of gas at unusually high temperatures and pressures. Waldmeier and Müller (1950) have discussed the same component of solar radiation and suggested an origin in regions of "coronal condensation," also at high temperatures and pressures.

As far as the limited data show, the "hot regions" emitting radio waves and those emitting ionizing radiation are roughly coincident and have periods of existence considerably greater than sunspots. Evidence for the long life of regions emitting ionizing radiation has been given by Allen (1948), while Christiansen, Yabsley, and Mills (1950) have found regions of intense radio emission coinciding with those occupied by extinct sunspots. It is likely that these regions were formed during the lives of the spots. It is possible, therefore, that the regions emitting ionizing radiation and those emitting radio noise may be identical, and if so some of them (away from sunspots) may also be identical with regions emitting particles which travel to the earth in a few days and cause mild magnetic activity (Piddington and Minnett). Others (permeated by spot magnetic fields) may be the source of more violent magnetic storms. Some evidence in this direction is offered by Allen (1946), who observed a large decrease in ionospheric electron density during a period when the sunspot number did not decrease. This unexpected phenomenon was accompanied by considerable magnetic activity and could have been due to the gases of hot regions "blowing out" and thereby causing magnetic activity and decreasing the ionizing radiation.

Ionizing radiation from the undisturbed sun does not originate (substantially) either throughout the corona or in the relatively cool gases in the lower chromosphere. It is presumably emitted, therefore, from the transition region and Woolley and Allen (in press) have shown that this region is capable of emitting a considerable amount of Lyman radiation. Additional radiation from the "hot regions" is also likely to be emitted, largely from the transition regions between the extremely hot (1×10^7°K or more) gases and the cool chromospheric or prominence material. These transition regions may exist at considerable heights, at levels which would

normally lie within the corona. It would be of considerable interest to make exact measurements of the location of strong sources of ionizing radiation and simultaneous measurements of sources of radio-frequency emissions. Such measurements would be possible during an eclipse if a number of electron-density measuring sets and radio noise sets were suitably distributed in the manner of Christiansen, *et al.*

In the following section the emission spectra of transition regions are considered.

V—THE SPECTRUM OF IONIZING RADIATION

Woolley and Allen (in press) have advanced reasons why the transition regions should have very large temperature gradients, most of the temperature change occurring within a range of a few thousands of kilometres. The chief reason against a smaller gradient is that an embarrassingly large quantity of Lyman radiation would be emitted. Such a steep gradient is not at variance with a model proposed by Piddington (1950), whose results apply to the average conditions over the solar disk. A series of steep temperature gradients over limited areas, between which the pressures differed, would result in a lower average gradient as determined.

Let us consider the changing composition of the gas in moving from a region at a temperature a few times 10^3°K to one of 1×10^6°K $- 1 \times 10^7$°K. The cold, dense gas consists mainly of H and He, with a small proportion of protons and electrons and atoms or singly charged ions of O, N, Ne, C, Mg, Si, Fe, and other metals, perhaps in that order of abundance (Woolley and Allen, 1948). As the temperature rises, the proportion of H atoms decreases to a very small value at 2×10^4°K. At 3×10^4°K most of the He is singly ionized, and at 5×10^4°K there is very little He at all. At higher temperatures only electrons, protons, He nuclei, and highly stripped atoms of O, N, etc., are found in appreciable proportions. Thus each region of cold dense gas is surrounded by successive sheaths of HeI and HeII, with smaller proportions of heavier atoms.

Now consider an electron moving in the very hot gas beyond these sheaths. The collision frequency with protons is given approximately (for example, Piddington, 1950) by

$$\nu = 50\, N_e T_e^{-\frac{3}{2}}$$

where N_e and T_e are the electron density and temperature, a Maxwellian velocity distribution being assumed. The average electron velocity is

$$V = \left(\frac{8kT_e}{\pi m}\right)^{1/2}$$

where k is Boltzmann's constant and m the electronic mass. The collision cross-section of protons is therefore given by

$$\sigma = \frac{\nu}{N_e V} = 50\, V^{-4}\left(\frac{8k}{\pi m}\right)^{3/2}$$

$$= 1{\cdot}2 \times 10^{19} V^{-4}$$

In the low temperature regions where $T_e \sim 10^4$°K., σ is large (about 10^{-12} cm^2), so that collisions with protons are by far the most frequent. At temperatures of

1×10^{6}°K and 1×10^{7}°K, the values of σ are about 8×10^{-17} cm^2 and 8×10^{-1} cm^2, respectively. It is evident that the fastest electrons will have the longest fre paths and will penetrate furthest through the transition region, thus causing marked departure from conditions of even local thermodynamic equilibrium.

Consider an electron with energy a few times the average for a gas temperatur of 1×10^{7}°K. There will be a few of these in regions where the gas temperature i 1×10^{6}°K and a considerable proportion when the temperature is 1×10^{7}°K When $N_e = 10^{10}$ cm^{-3}, the mean free path of the electron (for collision with proton only) is about 1,000 km, so that the electron might penetrate well into the coole gas without colliding with a proton. The collision cross-sections for ions other tha protons do not fall off rapidly and may be taken roughly as 10^{-16} cm^2. The mea free path for collision with these ions (assumed to be present in a proportion of 10 with hydrogen) is about 1,000 km, so that even though they are present in a smal proportion there is a roughly equal chance of a collision. The mean free path fo helium (one part in six with hydrogen, cross-section about 2×10^{-17} cm^2) is 300 km so that a collision is even more likely.

As a fast electron penetrates into a cooler region it may collide with a heavie atom (O, N, metals, etc.) at any level. It passes through successive "sheaths" o HeII and HeI and may collide with those particles. Finally it may reach the H level and collide with a hydrogen atom. Any of the ions or atoms involved may loos one or more electrons. Because of the relatively high electron density, recombinatio will be rapid and high-energy quanta may be emitted. Such a mechanism migh explain the mysterious phenomenon of the appearance of strong HeII lines low i the chromosphere and at the edges of prominences (Cillié and Menzel, 1935) These lines indicate the emission of quanta of energy about 50 eV from region where singly ionized metal atoms are also found. Under conditions of local thermo dynamic equilibrium at 6000°K, and a pressure corresponding to the middle of th chromosphere, the ratio of ionized to neutral helium is about 10^{-11}. At much highe temperatures, singly ionized metal atoms do not exist in appreciable numbers.

The fast electron (say about 4,000 eV) discussed above may doubly ionize H or may remove a K-level electron from atoms with atomic numbers up to abou 20 (Ca). Faster electrons, normally occurring in much smaller proportions, woul be capable of removing K-level electrons from the heavier elements.

The resulting emission spectrum might be expected to show the followin features:

The H Lyman spectrum with head at 13.5 eV.
The HeI spectrum with head at 24.6 eV.
The HeII quasi-Lyman spectrum with head at 54 eV.
Line and continuous emission from atoms of O, N, Ne, C, etc., ranging u to some hundreds of electron-volts (as discussed by Woolley and Alle 1948).
K-series X-ray emission lines from elements with atomic numbers up t about 20 (giving quanta with $\lambda \sim 3$ Å).
L-series X-rays from heavier atoms, also in the same wave-length range.
A smaller proportion of K-series lines for the heavier atoms, wave-lengt ranging perhaps to less than 1 Å. The proportion of these very hig

energy quanta might be expected to increase during periods of unusual disturbance. According to Giovanelli's (1948) theory of flares, it would seem that high energy electrons might be provided in large quantities, resulting in turn in a large increase of hard X-radiation. The emission, during flares, of particles which travel to the earth with speeds of 1,500 km sec^{-1} provides some evidence of the existence of very high energy particles. If the emitted gas is a mixture of electrons and protons, the average energy per particle is about 5700 eV, corresponding to radiation of wave-length about 2 Å.

It is not proposed to speculate on the emission of even more energetic quanta or particles. However, observations of increases of cosmic radiation during flares (for example, Forbush, Gill, and Vallarta, 1949) suggest that such radiation (and, presumably, some gamma-radiation) may result from extreme cases of solar disturbances.

VI—FORMATION OF THE IONOSPHERIC LAYERS

The discussions by Bates and Massey (1946), Bates and Seaton (1950), and others indicate that the formation of the ionospheric layers is far from being fully understood. As fresh evidence is provided by the eclipse and radio noise observations, it may be permissible to indulge in further speculation on the processes involved.

The level of the maximum ionization density of a layer is found by using the well-known formula, due to Chapman (1931)

$$n = \frac{\cos \chi}{AH} \qquad \ldots\ldots\ldots\ldots\ldots\ldots\ldots\ldots\ldots\ldots (6)$$

where n is the density of the particles causing absorption and A their absorption cross-section. H is the scale height of the atmosphere and χ the zenith angle of incident radiation. This formula is used below in calculating the values of n for the various layers. A value of 0.8 for $\cos \chi$ is used.

(*a*) *The F2 layer*—Bates (1949) has examined an earlier hypothesis of Bradbury that the $F1$ and $F2$ layers have a common origin (the ionization of atomic oxygen) and that separate layers result from different values of α. He concluded that radiation capable of accounting for the observed rate of ion production in the $F1$ layer would provide adequate $F2$ ionization. The analyses of Allen (1946, 1948) described in section III seem to support this conclusion and, further, to indicate different origins of the D, E, and F region ionization.

The absorption cross-section of N_2 at its second ionization potential may be as large as 1×10^{-16} cm^2 (Bates and Massey, 1946). Ionization would tend to form a layer where the density of N_2 is about 1×10^9 cm^{-3} (for a scale height of, say, 50 km). It might account for a G layer if such exists (Menzel and Bailey, 1947).

(*b*) *The F1 layer*—Bates and Massey (1946) consider that the ionization of atomic oxygen (and, perhaps, N_2 or N) at its first ionization potential may account for the $F1$ layer. Bates and Seaton (1950) refer to new calculations of A for atomic oxygen and conclude that the layer might be formed below the $F1$ layer. However, as they point out, other processes may play a part. The values of A for N at its

first ionization potential or for O at its second ionization potential are large enoug to provide a layer at about the correct level. If, as suggested in section V, the numb of ionizing quanta does not fall off rapidly above 13.5 eV (as it would for a 6000° black-body sun), these processes would be more important and the level of the F layer could be accounted for satisfactorily.

An interesting alternative, or additional, agency is the quasi-Lyman spectru of HeII. The values of A for O, N, and N_2 are of the order 1×10^{-16} cm^2 and 4×10^{-19} cm^2 for quanta of 20 eV and 180 eV, respectively. A value of about $1 \times 10^{-}$ cm^2 is not unlikely for quanta of about 50 eV; the resulting layer would then be about the $F1$ level.

(*c*) *The E layer*—The difficulties of accounting for the E layer by the theori of Nicolet (1945) or Hoyle and Bates (1948) have been discussed by Bates an Seaton (1950) and briefly mentioned in section I. A further objection to the secon theory is posed in section IV, where it is shown that the ionizing radiation do not originate throughout the corona.

It would seem that the possibilities of quanta up to at least 30 eV have bee explored and found wanting. Fortunately, considerations in section V suggest tha quanta may be plentiful with energies much above 20 eV. There appears to b insufficient evidence to decide on the important region of the solar spectrum Quanta in HeII spectrum (about 50 eV) are probably absorbed too quickly to b effective at E-region levels but they may be important. Another possibility a quanta of energy above about 300 eV which, as Hoyle and Bates have shown, migh be expected to form a layer at the correct height. Higher energy quanta, als from transition regions in the solar atmosphere, might also be effective.

An objection to any theory of ionization by high energy quanta has been ind cated by Bates (1949), who found a very small proportion of N_2^+ ions in the twilig flash, whereas high energy quanta would ionize N_2 as easily as the other component However, as indicated in section III, this phenomenon is easily explicable in term of rapid disappearance of daytime ions and replacement by others, formed b electric currents or some other agency.

It is possible that the agency responsible for D region is partially absorb in E region and plays an appreciable part in its formation. Such could be the case as suggested below, the agency in question were X-rays. If α increases in the sam ratio as n (the density of absorbing atoms or molecules), then the proportion p of region ionization due to the D region agency is (Bates, 1949) approximate $(N_D/N_E)^2 \exp(1)$, N_D and N_E being the maximum electron densities in the tw layers. Reasonable values of N_D and N_E at midday (Bates and Seaton, 1950) a 1.5×10^4 cm^{-3} and 1.5×10^5 cm^{-3}, giving a value of p of about three per cen It is possible, however, that the D layer is much more spread than a Chapman lay due to a frequency spread of the ionizing quanta. Also α may increase more rapid than n. In either case, p is increased, as it also is for larger values of χ. It wou seem that the effect may be important, particularly in determining α_E by observi diurnal changes of electron density. It has often been stated that E region is n affected by a solar flare and its attendant increase in D-region ionization. This wou seem to be an argument against the above conclusion. However, ionization duri a flare seems to be formed predominantly at a lower level than the normal D lay

that the above computations would have to be revised for this radiation. Also iggs (1942) has reported that an increase in *E*-region electron density of as much 30 per cent *has* been observed at Mount Stromlo after an eruption and, more cently, Dieminger and Geisweid (1950) have measured increases of about 70 r cent during a major disturbance.

(*d*) *The D region*—In view of the apparent complexity of ion distribution tween about 50 and 100 km, it is probably desirable to discuss a *D* "region" ther than "layer." A number of theories have been suggested to account for is ionization by quanta in the range below 13.5 eV, above which level (to at ast 30 eV) absorption by O is too strong to permit penetration. These theories ve been discussed quantitatively, as far as data permit, by Bates and Seaton 950), who conclude that only one, the ionization of NO by quanta in the range eV to 11 eV, may be tenable. The quanta concerned enter the atmosphere through o groups of windows of widths about 5*A* and 20*A*, for which the values of *A* r NO) are 2×10^{-21} cm^2 and 5×10^{-21} cm^2, respectively.

A serious objection to the NO theory seems to be posed by the results of very ng wave observations of Bracewell, Budden, Ratcliffe, Straker, and Weekes 951), who find daytime levels of reflection of 16 Mc/sec waves as low as 70 n. They have also observed decreases in heights of reflection during a solar flare as much as 15 km, bringing the level down as low as 55 km. According to estimates Piggott, quoted by Bates and Seaton (1950), the daytime level of the electron nsity maximum in *D* region is at about 90 km. There is, evidently, a very large read of ionization.

The NO theory of *D* region, as outlined by Bates and Seaton, should result proximately in the formation of two overlapping Chapman layers with maxima ss than one scale height apart. If the maximum of the upper (and normally more nse) layer is at 90 km, then the lower will be at about 84 km, and the electron nsity at 64 km (about 3 scale heights lower) will have fallen by a factor of about $\times 10^8$ to a value of virtually zero. Such a distribution is not consistent with the sults of Bracewell, *et al.*

Bates and Seaton have pointed out that the NO theory may explain a decrease the level of reflection of very long waves during a flare. While this is true quali- tively, it does not appear capable of explaining the long-wave results. The separa- on of the two overlapping layers is too small to account for more than a fraction of e maximum observed drop in level of 15 km. The remainder would have to be counted for by a strengthening of the lower layer by a very large factor. The diffi- lty is accentuated by a probable increase in α with decreasing level. It is con- uded, therefore, that while ionization of NO may play some part in the formation ionization below 100 km, it probably does not account for the whole of it and ay play an insignificant part.

In view of the apparent complexity of the *D* region, as indicated by the long- ve results at Cambridge mentioned above, it would seem likely that two or more n producing agencies are operative. There appears to be four main possibilities follows:

(*i*) *X-rays*—In view of the considerations of Bates and Massey (1946) and Bates d Seaton (1950), it would seem that, in addition to quanta capable of ionizing

NO, the only others which might be sufficiently penetrating lie in the range abov 30 eV. There seems little likelihood of finding a sufficiently penetrating radiatio in the range 30 to 180 eV, and beyond this range absorption coefficients are reason ably well known, so that we may calculate the X-ray wave-length appropriate t the formation of a given layer.

Consider a layer having a maximum at 90 km, where the molecular density i about 3×10^{14} cm^{-3} and the scale height about 8 km. From equation (6), the ap propriate value of A is about 3×10^{-21} cm^2, corresponding to a mass absorptio coefficient of 60 gm^{-1}. Such an absorption coefficient is experienced by X-ray of wave-length about 3 Å, energy about 4,000 eV (Compton and Allison, 193 p. 522). Ionization at much lower levels would probably require more energeti quanta, although there might be some spreading of ionization by secondary particle released by the original quanta. During unusually large flares, Bracewell, *et a* (1951), have observed the level of reflection of very long waves to fall as low a 55 km. This might be considered a lower limit of ionization and, according t equation (6), indicates an absorption cross-section of about 4×10^{-23} cm^2, whic obtains for X-rays of wave-length about 0.7 Å.

(*ii*) *Quanta capable of ionizing NO*—Part of *D*-region ionization, as Bates an Seaton have shown, may be caused by this agency.

(*iii*) *A downward extension of the E layer*—Some of the theories of formation o the *E* layer lead to the prediction of a "tail" at the base of the layer in which ioniza tion extends down considerably below a simple Chapman region. This is particularl so if the ionizing agency consists of quanta of a few hundred electron-volts, a suggested by Hoyle and Bates. Apart from secondary ionization effects, the antici pated spread of energies in the incident quanta would cause a spread in the laye formed. Such a distribution is consistent with the results of an analysis by Stanle (1950) of some long-wave reflection coefficients.

(*iv*) *Electric currents*—It was shown in section III that some *E*- and *D*-regio ionization may be caused by electric currents. The effect was small in *E* region an is probably also small in *D* region. Thus in sub-section IV(*b*), it was shown tha *D*-region ionization during an eclipse, as indicated by short-wave absorption, closel followed the optical eclipse, suggesting that ionization was mainly due to a direc solar agency. However, that electric currents may play a part is suggested by long wave results of Bracewell (1949), who found that during periods of considerab magnetic activity the apparent height of reflection remained for some days at abou 75 km instead of rising to about 90 km at sunset as it usually did.

Although each of the above sources of ionization in the *D* region may play som part, it appears unlikely that sources (*iii*) or (*iv*) could account for the sudde increase in ionization which may accompany a flare and which causes long wav to be reflected from levels below 60 km. The most likely agency would seem to b X-rays.

VII—ACKNOWLEDGMENTS

The author wishes to thank Prof. H. S. W. Massey, Dr. D. F. Martyn, an Dr. R. N. Bracewell for helpful suggestions, and Dr. T. R. Gilliland and th National Geographic Society (U.S.) for permission to reproduce Figure 1.

References

Allen, C. W. (1946), Terr. Mag , **51**, 1.
Allen, C. W. (1947), Mon. Not. R. Astr. Soc., **107**, 426.
Allen, C. W. (1948), Terr. Mag., **53**, 433.
Appleton, E. V. (1937), Proc. R. Soc., A, **162**, 451.
Appleton, E. V., and R. Naismith (1940), Proc. Phys. Soc., **52**, 402.

Baral, S. S., and S. K. Mitra (1944), Science and Culture, **10**, 175.
Bates, D. R. (1949), Proc. R. Soc., A, **196**, 562.
Bates, D. R. (1950), Phys. Rev., **78**, 492.
Bates, D. R., and H. S. W. Massey (1946), Proc. R. Soc., A, **187**, 261.
Bates, D. R., and H. S. W. Massey (1947), Proc. R. Soc., A, **192**, 1.
Bates, D. R., and M. J. Seaton (1950), Proc. Phys. Soc., **63**, 129.
Becker, W., and W. Dieminger (1950), Zs. Naturf., *5a*, 308.
Best, J. E., F. T. Farmer, and J. A. Ratcliffe (1938), Proc. R. Soc., **164**, 96.
Bosson, F., J. F. Denisse, R. Gallet, and P. Seligmann (1947), Relations entre les phénomènes solaires et géophysiques, Colloque International, Lyon.
Bracewell, R. N. (1949), Ph.D. Thesis, Cambridge.
Bracewell, R. N., K. G. Budden, J. A. Ratcliffe, T. W. Straker, and K. Weekes (1951), Proc. Inst. Elec. Eng., **98**, Pt. 3, 221.

Chapman, S. (1931), Proc. R. Soc., A, **132**, 353.
Christiansen, W. N., D. E. Yabsley, and B. F. Mills (1950), Aust. J. Sci. Res., **2**, 506.
Cillié, G. G., and D. H. Menzel (1935), Harvard College Observatory, Circular No. 410.
Compton, A. H., and S. K. Allison (1935), X-rays in theory and experiment, Macmillan, London.

Dieminger, W., and K. H. Geisweid (1950), J. Atmos. and Terr. Phys., **1**, 42.
Dufay, M., and J. Dufay (1947), Paris, C.-R. Acad. sci., **224**, 1834.

Forbush, S. E., P. S. Gill, and M. S. Vallarta (1949), Rev. Mod. Phys., **21**, 44.

Gejer, S., and P. Akerlind (1947), Terr. Mag., **52**, 479.
Gilliland, T. R. (1942), Nation. Geog. Soc., Solar Eclipse Ser., No. 2, 88.
Giovanelli, R. G. (1948), Mon. Not. R. Astr. Soc., **108**, 163.

Hagen, J. P. (1949), A study of radio-frequency radiation from the sun, U. S. Naval Research Lab., Report 3504.
Hagen, J. P., R. B. Jackson, and C. B. Strang (1947), Observations on May 20, 1947 total eclipse of the Sun, U. S. Naval Report.
Haikin, S. E., and B. M. Chikhachev (1948), Bull. (Izvest.) Acad. Sci. Phys. Ser., **12**, 38.
Henderson, J. T. (1933), Can. J. Res., **8**, 1.
Higgs, A. J. (1942), Mon. Not. R. Astr. Soc., **102**, 24.
Hoyle, F., and D. R. Bates (1948), Terr. Mag., **53**, 51.

Kirby, S. S., L. V. Berkner, T. R. Gilliland, and K. A. Norton (1934), Proc. Inst. Radio Eng., **22**, 247.
Kirby, S. S., T. R. Gilliland, and E. B. Judson (1936), Proc. Inst. Radio Eng., **24**, 1027.

Ledig, P. G., M. W. Jones, A. A. Giesecke, and E. J. Chernosky (1946), Terr. Mag., **51**, 411.
Lovell, A. C. B. (1950), Science Progress, **38**, 22.

Martyn, D. F. (1947), Proc. R. Soc., A, **189**, 241.
McLeish, C. W. (1948), Can. J. Res., A, **26**, 137.

Menzel, D. H., and D. K. Bailey (1947), Relations entre les phénomènes solaires et géo physiques, Colloque International Lyon, p. 163.

Nicolet, M. (1945), Mem. R. Met. Inst. Belgium, **19**, 1.

Penndorf, R. (1949), J. Geophys. Res., **54**, 7.
Petrie, W. (1950), J. Geophys. Res., **55**, 143.
Piddington, J. H. (1950), Proc. R. Soc., A, **203**, 417.
Piddington, J. H., and H. C. Minnett (1951), Aust. J. Sci. Res., A, **4**, 131.

Rayleigh, Lord, and H. S. Jones (1935), Proc. R. Soc., A, **151**, 22.
Rydbeck, O. E. H. (1946), Göteborg, Chalmers Tekn. Högsk. Handl., No. 53.

Waldmeier, M. (1947), Terr. Mag., **52**, 333.
Waldmeier, M., and H. Müller (1950), Zs. Astroph., **27**, 58.
Wells, W. H., and A. H. Shapley (1946), Terr. Mag., **51**, 401.
Woolley, R. v. d. R. (1946), Proc. R. Soc., A, **187**, 102.
Woolley, R. v. d. R., and C. W. Allen (1948), Mon. Not. R. Astr. Soc., **108**, 292.
Woolley, R. v. d. R., and C. W. Allen, Ultra-violet emission from the chromosphere, Mon Not. R. Astr. Soc. (in press).

APPENDIX I

In Figure 2 are shown three portions of the corona marked I_1 and (two annula rings) I_2 . If Q_1 and Q_2 are also the rates of electron production in the ionospheric

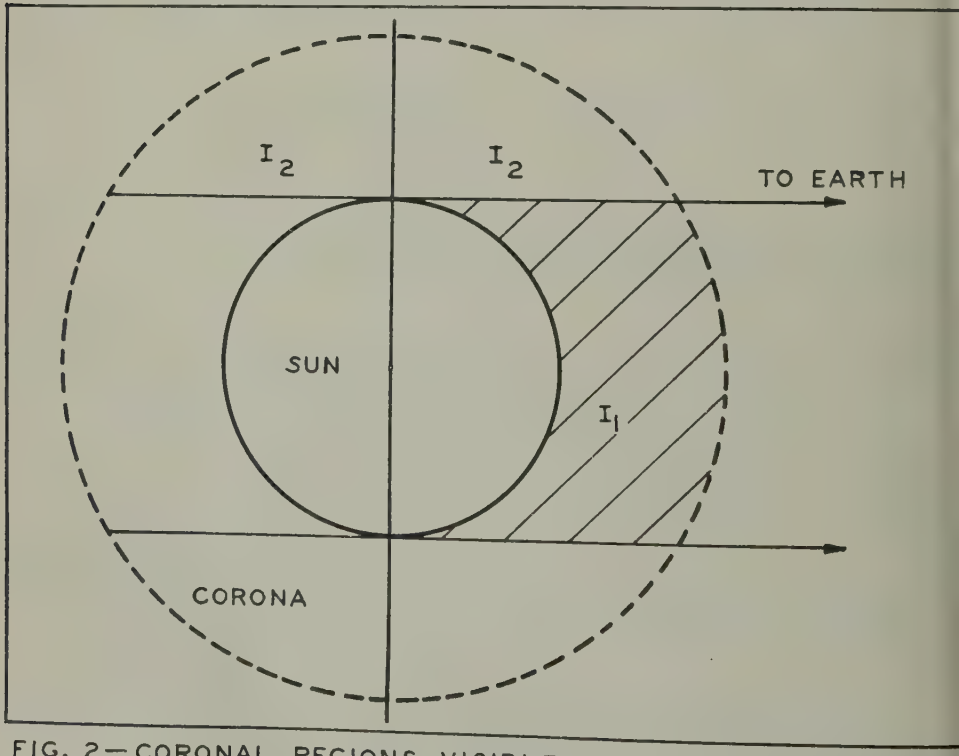

FIG. 2—CORONAL REGIONS VISIBLE AND NOT VISIBLE DURIN A TOTAL ECLIPSE

yers due to radiation from these regions, and if the moon is assumed to subtend ıe same angle as the sun at eclipse, then the ratio of flux density of quanta before ıd at totality of the eclipse is $Q_1 + 2Q_2/2Q_2$. The values of Q_1 and Q_2 may be etermined by using proportionality (5) and Allen's (1947) values of coronal ectron densities, given by

$$N_e = 10^8(1{\cdot}55\eta^{-6} + 2{\cdot}99\eta^{-16})$$

here $\eta = R/R_0$, R_0 = radius of the solar disk, and R = radius to the point oncerned.

It may be shown that

$$Q_1 + Q_2 = K\int_1^\infty (1{\cdot}55\eta^{-5} + 2{\cdot}99\eta^{-15})^2\,\mathrm{d}\eta \quad \ldots\ldots\ldots\ldots\ldots\ldots(7)$$

$$Q_2 = K\int_1^\infty (1 - \eta^{-2})^{1/2}(1{\cdot}55\eta^{-5} + 2{\cdot}99\eta^{-15})^2\,\mathrm{d}\eta \quad \ldots\ldots\ldots(8)$$

here $\mathrm{d}\eta$ is an elementary shell. The integral in equation (7) may be found readily, nd that in (8) by putting

$$(1 - \eta^{-2})^{1/2} = \cos\theta$$

hen it reduces to

$$\sum \int_0^{\pi/2} l \sin^{2m}\theta \cos^2\theta\,\mathrm{d}\theta,$$

$$(l = 2{\cdot}40K,\ 9{\cdot}27K,\ 8{\cdot}95K$$

$$m = 4,\ 9,\ 14)$$

hich may be determined.

We find $Q_1 = 0.64K$ and $2Q_2 = 0.62K$.

Thus at a full eclipse, the rate of electron production, if it originated in an Allen ype corona, should be reduced in the ratio $(Q_1 + 2Q_2)/2Q_2 = 2.03$. This result, hich applies equally well for ultra-violet and radio-frequency radiation (provided ıe optical depth of the corona is everywhere small), may be tested at radio fre-uencies.

Hagen, Jackson, and Strang (1947), observing at 9350 Mc/sec, found that flux ensity of observed radiation at totality was 4 per cent of maximum. Piddington 1950) has shown that at (approximately) the same frequency $Q_1 + Q_2 = 6.8$ er cent of the full flux density; therefore, $2Q_2 = 4.4$ per cent, in close agreement ith the 4 per cent found by Hagen, *et al.* Again at 200 Mc/sec, Haikin and hikhachev (1948) found 40 per cent residual radiation at totality. This is less ıan the 50 per cent expected from an optically thin corona, because at that fre-uency the degree of reabsorption is appreciable.

LIST OF GEOMAGNETIC OBSERVATORIES AND THESAURUS OF VALUES*

BY H. FREEBORN JOHNSTON

Central Radio Propagation Laboratory, National Bureau of Standards, Washington 25, D. C.

(Received June 25, 1951)

ABSTRACT

The list of magnetic observatories gives for the 72 stations in operation the geographic position and the abbreviation for each one. Among the newer observatories, either in operation or under construction, are Nurmijärvi in Finland, Průhonice in Czechoslovakia, Memanbetsu in Japan, El Abiod, Beni-Abbès and M'Bour in French Colonial Africa, and Muntinlupa in the Philippine Islands. Speaking in general terms, the annual values are for recent years and follow after those published in the September 1948 issue of the Journal of Terrestrial Magnetism and Atmospheric Electricity. Values for the year 1950 have been supplied by several observatories; in fact, many more than expected, a pleasant augury of recrudescent interest in geomagnetism. Values over comparatively extended periods are tabulated for La Quiaca, Pilar, and Laurie Island (Orcadas), all in Argentina.

The observers-in-charge of world-wide geomagnetic observatories have been ssiduous in supplying indices of magnetic activity to the Committee on Charac-erization of Magnetic Activity within a few days after the end of each month. As they were derived, they have also taken the opportunity to kindly include nonthly and annual mean values of the magnetic elements for all days. In addition, ome of the values supplied have been for earlier years and are corrections of or dditive to those which have been published in the excellent Thesaurus by John . Fleming and W. E. Scott, which have appeared in many issues of the Journal f Terrestrial Magnetism and Atmospheric Electricity. Table 1 gives a list of the bservatories, their abbreviations, and geographic positions. The annual values re given in Table 2, the successive columns indicating the observatory by abbrevi-tion, the year, the declination (D) with E for East and W for West, the horizontal ntensity (H), the vertical intensity (Z) with + for the north end of the dip-eedle below the horizontal and − when above, and a final one for descriptive emarks. When there is no suffix to the annual value, it has been derived from all ays. The suffix "a" indicates absolute observations, "p" preliminary values for l days, "x" less reliable values, and "i" incomplete values.

*Presented at the Ninth General Assembly, International Union of Geodesy and Geophysics, fore the Association of Terrestrial Magnetism and Electricity, August 21 to September 1, 1951, Brussels, Belgium.

Table 1--List of magnetic observatories
(with abbreviations and geographic position)

Observatory	Ab.	Lat.	Long.	Observatory	Ab.	Lat.	Long.
		° ′	° ′			° ′	° ′
Thule	Th	76 32N	68 54W	San Miguel	SM	37 46N	25 39W
Tromsø	Tr	69 40N	18 57E	Zinsen	Zi	37 30N	126 38E
Godhavn	Go	69 14N	53 31W	San Fernando	SF	36 28N	6 12W
Abisko	Ai	68 21N	18 49E	Kakioka	Ka	36 14N	140 11E
Kiruna	Ki	67 50N	20 14E	Tokio	Tk	35 41N	139 45E
Sodankylä	So	67 22N	26 39E	Ksara	Ks	33 49N	35 53E
College 3rd site	Co	64 52N	147 50W	El Abiod	EA	32 54N	0 33E
Dombås	Do	62 05N	9 06E	Tucson	Tu	32 15N	110 50W
Nurmijärvi	Nu	60 30N	24 42E	Zô-Sè	ZS	31 06N	121 11E
Lerwick	Le	60 08N	1 11W	Beni-Abbès	Be	30 07N	2 10W
Lövo	Lo	59 21N	17 50E	Helwan	He	29 52N	31 20E
Sitka	Si	57 03N	135 20W	Tamanrasset	Ta	22 48N	5 32E
Rude Skov	RS	55 51N	12 27E	Honolulu 1st site	Ho	21 19N	158 04W
Eskdalemuir	Es	55 19N	3 12W	Honolulu 2nd site	Ho	21 18N	158 06W
Meanook	Me	54 37N	113 20W	Teoloyucan	Te	19 45N	90 11W
Wingst	Wn	53 45N	9 04E	Alibag	Al	18 38N	72 52E
Witteveen	Wi	52 49N	6 40E	San Juan	SJ	18 23N	66 07W
Swider	Sw	52 07N	21 15E	Muntinlupa	Mn	14 22N	121 01E
Niemegk	Ni	52 04N	12 40E	M'Bour	MB	14 22N	16 57W
Abinger	Ab	51 11N	0 23W	Kodaikanal	Kd	10 14N	77 28E
Manhay	Ma	50 18N	5 41E	Jaluit	Jl	5 55N	169 39E
Průhonice	Pr	49 59N	14 33E	Tatuoca	Tt	1 12S	48 31W
Fürstenfeldbruck	Fu	48 10N	11 17E	Elisabethville	El	11 40S	27 28E
Chambon-la-Forêt	CF	48 01N	2 16E	Huancayo	Hu	12 03S	75 20W
O'Gyalla	OG	47 52N	18 11E	Apia	Ap	13 48S	171 46W
Nantes	Na	47 15N	1 34W	Tananarive	Tn	18 55S	47 32E
Toyohara 1st site	Ty	46 58N	142 45E	Mauritius	Mu	20 06S	57 33E
Surlari	Su	44 41N	26 15E	La Quiaca	LQ	22 06S	65 36W
Castellaccio	Ca	44 26N	8 56E	Vassouras	Va	22 24S	43 39W
Memanbetsu	Mm	43 54N	144 12E	Watheroo	Wa	30 19S	115 52E
Agincourt	Ag	43 47N	79 16W	Pilar	Pi	31 40S	63 53W
Istanbul-Kandilli	IK	41 04N	29 04E	Hermanus	Hr	34 25S	19 14E
Ebro	Eb	40 49N	0 31E	Toolangi	To	37 32S	145 28E
Coimbra	Ci	40 12N	8 25W	Amberley	Am	43 10S	172 44E
Toledo	Tl	39 53N	4 03W	Magallanes	Mg	53 09S	70 54W
Cheltenham	Ch	38 44N	76 50W	Macquarie Island	MI	54 30S	158 57E
				Laurie Island	LI	60 44S	44 47W

Table 2--Annual values of geomagnetic elements at observatories

Ob.	Year	D	H	Z	Remarks
		° ′	γ	γ	
Th	IPY2	81 21.2W	4570	+55757	August 1932 to July 1933
Tr	1945	1 45.7W	11199	+50503	
	1946	1 34.6W	11179	+50554	
	1947	1 26.5W	11174	+50585	
	1948	1 18.4W	11156	+50594	
	1949	1 10.5W	11153	+50620	
Go	1931	57 23.9W	8228	+55484	
	1939	55 13.8W	8171	+55171	
	1940	55 02.4W	8163	+55162	
	1941	54 52.3W	8162	+55158	
Ai	1945	0 16.1E		+47020	
	1946	0 25.6E		+47043	
	1947	0 34.1E	11680x	+47068	x, these values are less reliable
	1948	0 41.7Ex	11685x	+47068x	

Table 2--Annual values of geomagnetic elements at observatories (continued)

Ob.	Year	D	H	Z	Remarks
		° ′	γ	γ	
Al	1949	0 50.0Ex	11686x		Continued
	1950	1 00.6Ex	11672x	+47138x	x, these values are less reliable
Co	1940	4 09.2E	11916	+49552	
	1941	4 18.4E	11890	+49583	
	1942	4 25.2E	11882	+49617	
	1948	5 04.0E	11772	+49676	
	1949	5 12.6E	11765	+49687	
Co	1945	29 41.8Ep	12597p	+55360p	2nd site. p, preliminary value
	1948	29 21.2Ep	12589p	+55370p	3rd site. Preliminary station differences,-
	1949	29 19.6Ep	12599p	+55406p	2nd site minus 3rd site in D +14.6E,
	1950				in H + 5γ, and in Z -100γ.
Do	1946	6 16.0W	13837	+47509	
	1947	6 08.5W	13815	+47549	
	1948	6 01.0W	13790	+47569	
Le	1947	11 12.9W	14358	+47002	
	1948	11 05.1W	14366	+47009	
	1949	10 52.9W	14373	+47037	
	1950	10 45.3W	14383	+47039	
Lo	1947	0 35.4W	15218	+47055	
	1948	0 28.1W	15213	+47072	
	1949	0 20.7W	15208	+47101	
	1950	0 12.2Wp	15220p	+47131p	p, preliminary value
Li	1948	29 21.1E	15503	+55011	
	1949	29 18.8Ep	15507p	+55005p	p, preliminary value
	1950	29 16.4Ep	15512p	+54986p	
LS	1947	3 27.1W	16677	+45419	
	1948	3 19.7W	16676	+45435	
	1949	3 12.2W	16675	+45465	
Ls	1947	11 57.1W	16525	+45154	
	1948	11 48.9W	16537	+45158	
	1949	11 40.9W	16549	+45172	
	1950	11 33.2W	16569	+45194	
Me	1943	25 28.8E	12732	+59200	
	1944	25 22.3E	12752	+59167	
	1945	25 16.1E	12753	+59124	
	1946	25 10.4E	12792	+59339	
	1947	25 02.2E	12790	+59204	
	1948	24 57.7E	12811	+59258	
	1949	24 52.2E	12813	+59220	
	1950	24 45.8E			
Mn	1944	5 16.4W	17622	+44286	
	1947	4 52.1W	17597	+44373	
	1948	4 44.5W	17608	+44426	
	1949	4 36.4W	17613	+44442	
	1950	4 29.3W	17622	+44461	
Mi	1947	6 07.1W	17940	+43891	
W	1939	0 44.1W	18319a	+44106a	a, absolute observations
	1940	0 36.8W	18313a	+44193a	
	1941	0 29.3W	18303a	+44242a	
	1942	0 23.1W	18296a	+44283a	

Table 2--Annual values of geomagnetic elements at observatories (continued)

Ob.	Year	D	H	Z	Remarks
		° ′	γ	γ	
Sw	1943	0 16.7W	18284a	+44371a	Continued
	1944	0 10.6W	18267a	+44385a	a, absolute observations
	1945	0 03.7W	18263a	+44456a	
	1946	0 03.6E	18234a	+44514a	
	1947	0 10.0E	18225a	+44544a	
	1948	0 16.8E	18217a	+44566a	
	1949	0 23.1E	18210a	+44619a	
	1950	0 30.3E	18220a	+44650a	
Ni	1943	3 46.0W	18421	+43558	
	1944	3 38.4W	18422	+43601	
	1945	3 30.8W	18418	+43640	
	1946	3 22.1W	18400	+43688	
	1947	3 14.4W	18399	+43731	
	1948	3 06.5W	18404	+43761	
	1949	3 00.4W	18404	+43788	
Ab	1947	9 43.1W	18577	+43246	
	1948	9 35.4W	18593	+43255	
	1949	9 27.5W	18607	+43273	
	1950	9 19.7W	18628	+43288	
Ma	1946	6 38.2W	19101	+42855	
	1947	6 27.7W	19103	+42895	
	1948	6 17.4W	19105	+42912	
	1949	6 10.5W	19115	+42945	
	1950	6 04.6W	19149	+42963	
Pr	1946				Continuous registration began 1946
Fu	1945	4 06.1W	20316	+41621	
	1946	3 57.4W	20299	+41666	
	1947	3 49.8W	20299	+41690	
	1948	3 42.2W	20308	+41715	
	1949	3 35.4W	20313	+41753	
	1950	3 27.7W	20330	+41789	
CF	1947	7 52.4W	20095	+41682	
	1948	7 44.7W	20109	+41695	
	1949	7 36.8W	20121	+41715	
	1950	7 29.1W	20138	+41714p	p, preliminary value
OG	1943	1 33.3W	20669	+41650	
Na	1948	9 17.2W	20410	+41306	
	1949	9 09.6W	20432	+41370	
	1950	9 02.7W	20457	+41428	
Ty	1934	8 59.9W	20535	+44604	1st site
Ca	1943	5 43.6W	22194	+38937a	a, absolute observations of inclination
	1944	5 35.1W	22189	+38954a	
	1945	5 27.8W			The registrations in H and the observed I
	1946	5 19.7W			for July 1, 1945 to February 1, 1946 we
	1947	5 11.0W	22116	+39123a	burned.
	1948	5 02.5W	22222	+39155a	
	1949	4 55.0W	22225	+39147a	
	1950	4 47.7W	22240	+39195a	
Mm	1950	8 06.5Ei	26457i	+41834i	i, incomplete, November only, all days

Table 2--Annual values of geomagnetic elements at observatories (continued)

b.	Year	D	H	Z	Remarks
		° ′	γ	γ	
g	1943	7 30.8W	15309	+56459	
	1944	7 30.1W	15314	+56406	
	1945	7 27.7W	15322	+56392	
	1946	7 25.8W	15311	+56361	
	1947	7 22.3W	15338	+56370	
	1948	7 22.8W	15355	+56300	
	1949	7 21.1W	15362	+56244	
	1950	7 22.0W	15430	+56344	
ĸ	1947	1 59.9E	24846i	+38439i	i, incomplete, October to December only
b	1943	8 27.7W	23634	+36760p	p, preliminary value
	1944	8 19.3W	23665	+36794p	
	1945	8 11.5W	23679	+36787p	
	1946	8 03.4W	23690	+36817p	
	1947	7 54.9W	23724	+36879p	
	1948	7 47.0W	23734		
	1949	7 38.7W	23765		
	1950	7 31.4Wp	23803p		
i	1951	11 11.8Wa	23797a	+36478a	a, absolute observations January to March
l	1947	9 42.7W	23961	+36296	
	1948	9 35.4W	23983	+36291	
	1949	9 27.3W			
	1950	9 19.2W	24048	+36285	
h	1948	7 04.0W	18248	+53839	
	1949	7 04.4Wp	18281p	+53838p	p, preliminary value
	1950	7 04.2Wp	18320p	+53829p	
M	1948	16 52.3W	23899a	+39222a	a, absolute observations
	1949	16 45.7W	23951a	+39169a	
	1950	16 40.1W	24015a	+39142a	
i	1938	6 11.6Wa	30130a	+40383a	a, absolute observations
F	1947	10 21.9W	25554	+33656a	a, absolute observations of inclination
	1948	10 15.0W	25595	+33608a	
	1949	10 07.7W	25622	+33591a	
	1950	10 01.4W	25678	+33614a	
a	1948	6 15.2W	29934	+35016	
	1949	6 17.4W	29961	+35036	
	1950	6 19.7W	29998	+35041	
k	1899	4 33.7Wi	29856i	+34400i	i, incomplete, November excepted
	1911	5 00.6Wi	30025i	+34640i	i, incomplete, August excepted
s	1946	2 11.8E	28774	+32747	
	1947	2 13.9E	28790	+32833	
	1948	2 15.8E	28812	+32901	
	1949	2 17.9E	28824	+32971	
	1950	2 20.5E			
u	1948	13 32.1E	26027	+44323	
	1949	13 29.2Ep	26015p	+44285p	p, preliminary value
S	1943	3 25.9W	33469	+33997	
	1944	3 26.2W	33504	+34012	

Table 2--Annual values of geomagnetic elements at observatories (continued)

Ob.	Year	D	H	Z	Remarks
		° ′	γ	γ	
Ta	1941	7 13.0W	32035	+17999	
	1942	7 06.5W	32035	+17958	
	1943	6 59.9Wi	32049i		i, incomplete, March excepted
	1944	6 53.7W	32091		
	1945	6 46.2W	32122		
Ho	1946	10 28.1E	28350	+23145	1st site
	1947	10 28.6Ei	28349i	+23150i	i, incomplete, January and February
	1947	11 35.4Ei	28669i	+22933i	2nd site. i, incomplete, April to December
	1948	11 36.3E	28638	+22953	Station differences,- 1st site minus 2nd
	1949	11 37.4E	28600	+22979	site in D -1°06.0E, in H -335γ and in Z
	1950	11 37.9Ep	28566p	+23003p	+237γ -- p, preliminary value
Te	1947	9 37.2Ei	....	+32823i	i, incomplete, Jan. 1 to Apr. 24. H inoperativ
	1948	9 28.4E	....	+32929i	i, incomplete, Apr. to Dec. H inoperative
	1949	9 25.0E	30566	+32878	
	1950	9 21.6E	30506	+32794	
Al	1946	0 41.2W	38152	+17770	
SJ	1948	6 22.0W	27460	+35612	
	1949	6 26.1Wp	27483p	+35522p	p, preliminary value
	1950	6 30.3Wp	27509p	+35438p	
Mn	1951	0 33.0Ei	38850i	+10010i	i, incomplete, January only, all days
Kd	1950	1 55.0Wa	39480a	+2457a	a, preliminary absolute value
Jl	1938	7 51.5Eai	34170ai	+2779ai	a, absolute obsn's. i, incomplete, Sep. to De
	1939	7 49.9Ea	33880a	+2726a	
	1940	7 51.9Ea	33980ai	+2704ai	i, incomplete, January to October
Tt	IPY2	12 34.6W	29025	+11745	September 1933 to January 1934
El	1932	9 33.0W	23784	-24628	
	1933	9 31.1W	23789	-24687	
	1934	9 27.7Wi	23749i	-24755i	i, incomplete, January to May
	1938	9 14.1W	23566	-24809	
	1939	9 11.4W	23509	-24815	
	1940	9 08.8W	23457	-24831	
	1941	9 05.8W	23408	-24837	
	1942	9 02.8W	23382	-24831	
	1943	8 59.5W	23340	-24853	
	1944	8 57.0W	23312	-24867	
	1945	8 55.0W	23280	-24879	
	1948	8 51.2W	23202	-24884	
	1949	8 49.3W	23172	-24890	
	1950	8 47.2W	23142	-24877	
Hu	1947	6 22.0E	29195	+1061	
	1948	6 17.1E	29149	+1046	
	1949	6 12.2E	29102	+1028	
Ap	1947	11 16.9E	34841	-20613	
	1948	11 20.1E	34857	-20578	
	1949	11 25.1E	34873	-20547	
	1950	11 30.4Ep	34862p	-20506p	p, preliminary value
Tn	1939	9 16.6Wi	21142i	-28895i	i, incomplete, March excepted
	1940	9 25.3W	21068	-28783	On Jan. 1, H decreased by 77γ to IMS
	1941	9 39.1Wi	21081i	-28836i	i, incomplete, May and June excepted

Table 2--Annual values of geomagnetic elements at observatories (continued)

o.	Year	D	H	Z	Remarks
		° ′	γ	γ	
n	1942	9 51.2Wa	21064a	-28803a	Continued
	1943	9 58.6Wa	21020a	-28787a	a, absolute observations
	1944	10 07.4Wa	21012a	-28799a	
	1945	10 12.1Wa	20981a	-28802a	
	1946	10 25.8Wa	20940a	-28783a	
	1947	10 34.5Wa	20890a	-28753a	
	1948	10 35.8W	20867	-28770	
	1949	10 45.1W	20817	-28710	
	1950	10 51.2W	20795	-28695	
u	1946	15 00.5W	22358	-30182	
	1947	15 10.5W	22355	-30237	
	1948	15 22.1W	22339	-30290	
	1949	15 30.1W	22326	-30337	
	1950	15 39.6W	22321	-30395	
Q	1926	5 14.9E	26397i	-5828	1926-31, scalings exactly on the hour by
	1927	5 05.5E	26353	-5801	L.M.T. which is 65°36′ west of Greenwich.
	1928	4 57.3E	26324	-5801	a, absolute observations
	1929	4 48.3Ei	26291i	-5779i	i, incomplete, Jan. and Feb. excepted
	1942	3 20.9E	25898	-5927	1942-48, scalings exactly on the hour 60° W.
	1943	3 15.3Ei	25852i	-5964i	Gr. i, incomplete, October excepted
	1944	3 07.9Ei	25799i	-5972i	i, incomplete, January excepted
	1945	3 01.3E	25748	-5997	
	1946	2 55.2E	25680	-6046	
	1947	2 50.0E	25618	-6065	
	1948	2 44.9E	25556	-6083	
i	1945	14 19.4W	23508	-8330	
	1946	14 26.0Wa	23449a	-8408a	a, absolute observations
	1947	14 33.4Wa	23310a	-8437a	
	1948	14 39.9Wa	23228a	-8530a	
	1949	14 47.6Wa	23173a	-8590a	
	1950	14 55.4Wa	23096a	-8692a	
a	1948	2 51.2W	24816p	-51913p	p, preliminary value
	1949	2 49.9Wp	24825p	-51966p	
	1950	2 48.6Wp	24838p	-52029p	
i	1905	9 51.4E	25892	-12655	1905-1931, scalings exactly on the hour by
	1915	8 31.9E	25550	-12302	L.M.T. which is 63°53′ west of Greenwich
	1916	8 22.9E	25506	-12265	
	1932	6 11.4E	24607	-11945	1932-1948, scalings exactly on the hour by
	1936	5 47.6E	24396	-11969	60° west of Greenwich. N.B. Final con-
	1937	5 41.7E	24333	-11979	stants have now been adopted for the per-
	1938	5 35.9E	24264	-11996	iod 1936.0 to date
	1939	5 30.4E	24200	-12015	
	1940	5 24.9E	24132	-12032	
	1941	5 18.5E	24062	-12049	
	1942	5 12.0E	24012	-12054	
	1943	5 05.8E	23938	-12059	
	1944	4 59.3E	23874	-12061	
	1945	4 53.7E	23802	-12059	
	1946	4 48.8E	23718	-12067	
	1947	4 43.5E	23644	-12063	
	1948	4 37.3E	23572	-12065	
	1949	4 31.0E	23493	-12067	1949.0, hourly mean scalings by 60° WGMT,
	1950	4 24.6E	23417	-12065	i.e. 00 to 01, 01 to 02, etc.

Table 2--Annual values of geomagnetic elements at observatories (concluded)

Ob.	Year	D	H	Z	Remarks
		° ′	γ	γ	
Hr	1947	23 46.6W	13809	-28734	
	1948	23 47.6W	13739	-28642	
	1949	23 48.8W	13664	-28557	
	1950	23 48.8Wp	13592p	-28464p	p, preliminary value
To	1948	9 23.9Ep	22894p	-56419p	p, preliminary value
	1949	9 29.2Ep	22872p	-56430p	
	1950	9 34.1Ep			
Am	1946	19 07.7E	22192	-55219	
	1947	19 14.5E	22189	-55213	
	1948	19 22.3E	22188	-55201	
	1949	19 30.9E	22181	-55200	
	1950	19 39.2E	22177	-55186	
Mg	IPY2	17 46.4E	26001	-29981	January to August 1933
MI	1950	23 58.0Eai	13434ai	-51250ai	a, absolute observations. i, incomplete, A
LI	1906	5 11.7Ei	25655i		1906-31, scalings exactly on the hour by L.M.T. which is 44°47′ west of Greenwi i, incomplete. For D, - March, April, N vember and December excepted. For H
	1908	5 01.7Ei	25433i		January only. i, incomplete, Jan., Feb., Mar., Oct. excepted
	1909	4 57.0Ei	25436i	-35603ia	i, incomplete. Last 17 days of Jan., last 1 of Feb., and last 10 of Sep. excepted. a,
	1913	4 42.3E			absolute observations of inclination, Jan
	1914	4 39.8E			and Sep. excepted
	1915	4 36.1Ei			i, incomplete, January to April only
	1917	4 27.9E			
	1918	4 19.2E			
	1919	4 14.3E			
	1920	4 10.8E			
	1921	4 05.9E			
	1922	4 00.1E			
	1923	3 54.7E			
	1924	3 50.6E			
	1925	3 44.7E			
	1926	3 39.9E			
	1927	3 34.7E	24300		
	1928	3 31.3E			
	1929	3 23.3Ei	24157		i, incomplete. For D, - Jan. to Mar. exce For H, - Jan. to May excepted
	1930	3 19.4E	24097		
	1931	3 14.8E	24049	-33174a	a, absolute observations of inclination
	1932	3 10.3E	23975	-32970a	1932-47, scalings exactly on the hour 45° Gr.
	1933	3 06.2E	23900	-32735a	
	1934	3 02.6E	23827	-32971a	
	1935	2 59.4E	23753	-32877a	
	1936	2 55.7E	23678	-32796a	
	1937	2 51.4E	23597	-32687a	
	1938	2 48.3E	23519	-32584a	
	1940	2 40.5E	23360	-32430a	
	1941	2 38.4E	23285	-32264a	
	1942	2 34.7E	23208	-32133a	
	1943	2 32.2E	23142	-31996a	
	1944	2 29.2E	23074	-31909a	
	1945	2 26.9E	23011	-31849a	
	1946	2 25.4E	22917	-31707a	
	1947	2 23.7E	22845		

GEOMAGNETIC AND SOLAR DATA

FINAL RELATIVE SUNSPOT-NUMBERS FOR 1950

Table 1 contains the final sunspot-numbers for 1950 for the whole disk of the ı, based on observations made at the Zurich Observatory, supplemented by ies furnished by other cooperating observatories. Table 2 gives the number of

TABLE 1—*Final relative sunspot-numbers for the whole disk of the sun for 1950*

ay	Jan.	Feb.	Mar.	Apr.	May	June	July	Aug.	Sep.	Oct.	Nov.	Dec.
1	101	60	95	72	144	88	70	94	49	41	78	82
2	100	38	75	80	146	84	58	110	59	41	62	80
3	92	33	90	122	132	84	58	106	49	41	57	82
4	84	36	128	133	130	66	66	84	51	50	67	75
5	76	53	134	136	129	58	75	90	31	50	79	61
6	85	43	148	139	139	54	88	83	27	45	94	46
7	84	32	184	151	130	50	98	76	23	54	80	85
8	86	20	187	114	121	70	77	72	24	78	55	108
9	64	29	163	120	108	65	67	70	38	84	61	94
0	83	43	150	109	105	108	68	75	31	79	60	94
1	75	66	156	88	101	102	78	70	28	68	46	96
2	85	72	128	91	71	72	68	74	37	88	48	115
3	83	85	124	95	69	95	67	84	65	75	42	94
4	80	125	133	97	60	101	98	68	85	72	61	79
5	75	144	130	103	47	94	75	80	80	106	81	59
6	70	156	110	120	57	84	89	93	83	103	62	42
7	82	154	100	120	61	83	96	106	85	99	66	26
8	91	166	108	85	79	78	83	93	87	74	58	19
9	110	197	101	90	86	78	102	114	80	50	50	7
0	130	190	90	93	89	66	130	113	65	48	36	0
1	155	170	80	85	92	55	108	103	58	27	22	7
2	163	162	70	70	112	86	125	95	51	20	18	0
3	150	137	76	96	128	107	115	115	44	22	16	0
4	157	113	72	128	162	108	108	103	56	32	13	31
5	140	96	73	138	142	128	96	92	41	30	20	39
6	130	80	80	142	134	113	118	77	45	37	32	56
7	110	73	73	119	131	97	112	76	49	51	64	58
8	111	82	69	160	121	74	110	55	38	55	74	35
9	98		97	153	109	82	112	58	49	95	69	41
0	118		100	154	86	78	106	58	32	107	73	23
1	82		78		72		100	54		80		43
an	101.6	94.8	109.7	113.4	106.2	83.6	91.0	85.2	51.3	61.4	54.8	54.1

TABLE 2—*Daily numbers of sunspot-groups for 1950.*

Day	Jan.	Feb.	Mar.	Apr.	May	June	July	Aug.	Sep.	Oct.	Nov.	Dec.
1	6	8	11	8	11	8	7	6	4	5	5	1
2	8	6	9	8	12	7	5	7	6	4	4	7
3	5	5	9	11	10	6	6	8	6	3	4	6
4	6	5	12	11	10	7	6	6	5	4	6	7
5	8	8	12	10	10	4	8	5	4	4	7	6
6	8	6	14	10	12	5	7	7	3	4	6	6
7	7	4	16	12	12	5	6	6	3	5	5	6
8	8	3	14	10	11	7	7	6	2	6	4	6
9	6	3	13	12	10	6	6	6	4	7	4	6
10	7	5	10	10	11	9	5	7	3	7	4	6
11	6	7	13	6	9	9	6	5	2	6	4	6
12	7	7	9	6	8	7	5	6	3	8	4	7
13	6	8	9	5	7	7	6	7	4	9	3	6
14	7	9	13	6	6	7	8	5	8	6	5	6
15	7	9	12	6	5	6	6	6	8	7	6	5
16	7	9	10	6	6	5	6	8	7	7	4	3
17	8	9	10	6	6	4	8	9	7	6	4	2
18	8	10	10	5	8	4	7	7	6	4	3	3
19	8	14	9	5	8	6	9	9	6	4	4	1
20	10	11	9	5	8	6	11	10	5	5	3	0
21	11	11	7	6	8	7	8	10	5	3	2	1
22	11	11	7	5	10	8	8	9	5	1	3	0
23	13	11	8	6	9	9	7	11	5	2	2	0
24	13	9	8	8	11	11	8	9	6	2	1	3
25	14	9	7	9	9	10	8	8	3	2	1	3
26	12	8	8	10	10	7	9	8	3	4	3	3
27	12	9	8	8	8	7	10	9	4	5	5	3
28	9	9	8	10	8	7	10	7	3	6	5	1
29	10		10	9	10	8	11	6	5	9	5	2
30	12		8	10	7	8	9	6	4	9	5	2
31	7		8		8		7	4		6		3
Mean	8.6	8.0	10.0	8.0	9.0	6.9	7.4	7.2	4.6	5.2	4.0	3.

spot-groups on each day for the year 1950. The yearly mean of the group-numbe is 6.9, against 11.6 in 1949. The yearly mean of the relative numbers is 83 against 134.7 in 1949. After the very high and prolonged maximum of sunspo activity in 1947, solar activity at first diminished very slowly, and it was n until 1950 that there occurred a considerable decrease. Solar activity during 19 dropped to about 60 per cent of the activity in 1949. At the end of 1950, the fi three spotless days occurred. Figure 1 gives a graphical representation of the da relative sunspot-numbers for 1950, the times being plotted as abscissas and t

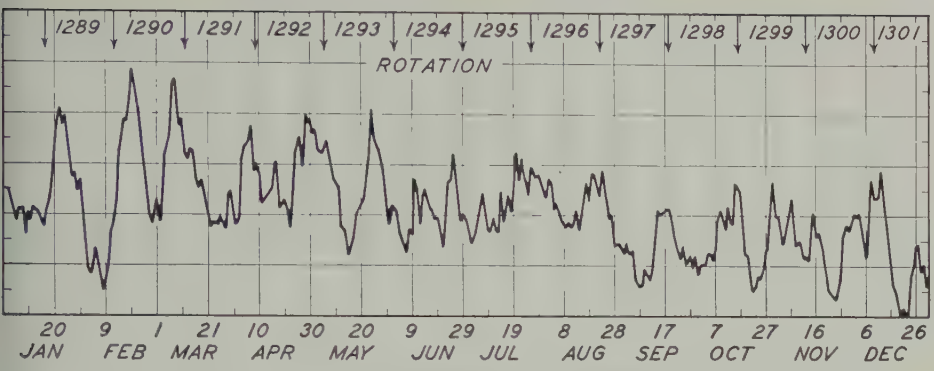

FIG. 1—DAILY RELATIVE SUNSPOT-NUMBERS FOR 1950

ıtive numbers as ordinates. The limits of successive solar rotations are indicated vertical arrows in the upper edge of the diagram.

M. Waldmeier

ss Federal Observatory
urich, Switzerland, April 18, 1951

INTERNATIONAL DATA ON MAGNETIC DISTURBANCES, FIRST QUARTER, 1951

Sudden commencements followed by a magnetic storm or a period of storminess (s.s.c.)

S.C.'s given by five or more stations are in italics. Times given are mean valu with special weight on data from quick-run records.

1951 January 16d 09h30: Wi Tl.—*21d 10h57:* nine.—21d 11h10: El.—2 08h15: Es.—26d 15h22: Wn.—30d 05h50: Wi.—30d 06h56: Ka Pi El Ap.

1951 February 04d 11h09: Sw.—*05d 04h24:* six.—05d 05h19: El.—07d 17h Do.—21d 17h38: Sw.—*22d 06h11:* five.—*27d 00h28:* twenty-four.—28d 04h Ab.—*28d 14h17:* fourteen.

1951 March *06d 07h50:* twenty-four.—07d 12h27: Do Wn Ab Va.—14d 12h Do.—*16d 10h04:* six.—17d 08h28: Do.—22d 09h50: Sw Tl El Hr.—22d 14h Wn.

Sudden commencements of polar or pulsational disturbances (p.s.c.)

1951 January 02d 19h30: El.—02d 23h25: El.—03d 22h00: Wn.—05d 14h So El.—05d 20h09: Wn Te.—05d 21h37: Te El.—06d 19h18: So Wn.—1 00h53: Wn.—11d 22h05: Wn.—16d 21h14: Wn.—18d 21h00: Wn.—20d 00h Tl.—23d 18h25: So.—24d 19h47: Tr Wn.—26d 18h21: El.

1951 February 01d 01h24: Tl El.—01d 20h20: Do Fu.—02d 20h39: Wn 03d 19h28: So Wn.—04d 10h53: To.—05d 23h53: CF.—06d 01h02: CF.— *18h24:* five.—08d 21h11: El.—10d 21h50: Fu.—10d 22h10: El.—11d 23h00: Wn 11d 23h59: Wn.—12d 02h57: Wn.—12d 17h30: Fu El.—12d 21h47: Fu.— 22h47: Do.—13d17h46: Fu Wn.—13d 19h13: Do So Wn Fu.—14d 18h06: El.—14d 20h43: Wn.—*15d 22h42:* five.—16d 19h43: So.—16d 20h28: Tr Wn 22d 23h24: Tl.—23d 02h10: CF Va.—25d 21h22: Wn Fu El.—26d 13h50: To 27d 02h37: Wn Tl.

1951 March 01d 03h27: Va El.—02d 23h10: Wn Fu.—04d 21h05: Fu 04d 22h13: Wn CF El.—06d 03h28: Wn.—06d 19h48: Do Wn Fu.—07d 00h Wn.—07d 20h40: El.—10d 18h08: Fu.—11d 16h10: Fu El.—11d 18h39: Fu E 12d 00h42: Ch.—*12d 19h30:* five.—13d 14h15: Tl Va.—14d 19h30: Fu El.— 01h00: El.—16d 19h54: Wn.—17d 16h52: Wn Fu.—19d22h30: Tr.—21d 21h Wn.—21d 22h04: Wn Fu.—22d 23h35: El.—24d 16h04: Wn.—24d 19h05: Tl El.—26d 22h08: Do Wn.—27d 21h30: Wn.—30d 01h11: Fu.

Other impulses found in the magnetograms

1951 January 02d 08h38: Va El.—02d 09h39: Do Tl Va El.—02d 16h Tl.—04d 22h00: Te.—05d 12h55: El.—08d 20h50: El.—09d 02h27: Te.— 12h40: Te.—10d 17h59: El.—10d 21h23: El.—11d 11h01: El.—11d 19h05: E 15d 02h26: Va.—15d 03h13: Va.—16d 15h39: Tl.—19d 00h15: Te.—20d 15 El.—26d 03h29: Ka El.—30d 00h39: El.—30d 13h20: Te.—31d 08h44: V 31d 09h55: Va.—31d 17h37: So.

magnetic planetary three-hour-range indices Kp, preliminary magnetic character-figures, C, and final selected days, January to March, 1951

January 1951

1	2	3	4	5	6	7	8	Sum
3o	3 −	2 +	2 −	3 −	3o	3 −	3 −	21 −
3o	4o	4 −	3 −	4 −	3o	4o	3 +	27 +
3 +	5o	2 +	2o	2 +	2o	3 −	3 +	23o
3 −	2 +	1 −	0 +	0 +	2o	2 −	3 −	13 −
2o	2o	1 +	2 −	2o	2o	4 −	4 −	18 +
2o	2o	1c	1o	1o	1 −	2 +	0 +	10 +
0 +	2 −	2 −	1 +	1o	1o	1o	1 +	9 +
2o	1 −	3o	3 −	3o	2 +	2 −	1 −	16o
1 +	2 +	2 +	2 +	2 −	1o	0 +	1 −	12o
1o	1o	1 +	0o	1o	4o	4 +	3 +	16o
5o	2o	4 −	2 +	2 −	2 +	4 −	4o	25 −
4 +	4 −	4 −	4 −	3o	3o	2 +	2o	26 −
3 +	4o	4o	2 +	2 −	1 +	4 −	3o	23 +
3 +	3o	3o	3o	3 +	3o	3 −	3 +	25 −
4 +	4 +	3o	2 +	3 +	3 −	3 +	4o	27 +
4 −	2 −	3 −	3 +	4o	4 −	3 +	5 −	27o
4o	4 −	3o	2o	1 −	1 +	1 +	1 +	17 +
1o	2 −	1o	1o	2 +	2 +	1o	3 −	13o
4 −	3 −	2 +	2o	3 +	2 +	3o	4 −	23o
4o	2o	1o	1 +	2 +	2 +	1 −	1 −	14 +
1o	0o	1 −	3o	4o	5 −	4 −	5o	22o
5 +	5o	6 −	4 +	5o	5o	5 +	6o	42 −
5 −	3 −	4 −	4o	3 +	4 −	4 −	3 +	29o
2 −	3o	3 −	3 −	3 +	2 −	2 +	2 +	20 −
2 −	2 +	2 +	2o	3 −	2 −	2 +	2 −	17 −
1 −	1 +	2 −	2 +	2 +	4 −	4 −	4 −	19 +
3 +	5 −	4o	3 −	2 +	3o	3o	3 +	26 +
4 −	4 −	3 −	3 +	3 +	3 +	4 +	4 −	28o
2o	3o	3o	4 −	2 +	3 −	3 −	4 −	23o
3o	2 +	3 +	3 −	2o	3 +	3o	4o	24 −
4 +	6 −	7 −	5 +	4o	4 +	4 +	4 +	39o

February 1951

1	2	3	4	5	6	7	8	Sum
5o	5 −	4o	3o	2 +	1 +	4 −	4o	28o
3 −	2 +	1o	0 +	1 −	1o	1o	2 +	11 +
2 −	1o	1 −	0 +	0 +	1 +	2 +	2 −	9 +
0 +	0o	2o	4o	3o	3o	3 −	2o	17o
1 −	3o	3o	3o	4o	3 +	4 +	4 −	25o
6o	6o	4 +	4o	2o	2 −	1 +	2 +	28 −
3 +	3 +	2 +	1 +	1 +	3 −	2 +	3 −	19 +
3 −	2o	2 +	3o	3 −	5 −	5 +	4o	27 −
3 +	4 −	4 −	3o	4 +	5 −	4o	5 −	31 +
4o	4o	4 +	3 −	3o	2 +	4 −	5o	29o
5 −	4 −	3o	3o	3 −	4o	4 −	5 −	29 +
5 +	5 +	4o	3 +	4 −	4o	5 +	4 +	35 +
4o	4 −	3 +	4o	4o	3o	3 +	4 −	29o
3o	3 −	2 +	2 +	2o	2o	4 −	3o	21o
2o	1o	1 +	1 +	2 −	1 −	1o	2 +	11 +
1 −	0 +	0 +	0 +	0 +	1o	1 +	1o	5 +
1 −	0o	0 +	0 +	1o	1o	3 −	2 +	8 +
3 +	2o	2o	3 +	3 −	3o	3 +	2o	22 −
1o	2 +	2 +	4o	3 −	2 +	2o	3o	20 −
2 +	2 +	1 +	2 +	1 +	1 −	1o	1 −	12o
2o	2 +	2 +	2o	3 −	3 −	3o	3o	20o
4 +	4 +	5o	5 −	5o	4 +	5 −	5 +	38 −
6 −	5 −	6 +	6 −	5 +	5 −	6 −	6o	44o
5o	5o	5o	4 +	4 +	5 +	4o	4 −	37 −
4o	3 +	2o	3o	3 −	3o	3 −	5 −	25 +
2 +	3 +	3o	3 −	4 −	4o	4 −	2 +	25o
7o	6 −	5 −	3 +	4o	4o	5 −	5 −	38o
5o	7 −	7c	5o	4 +	4 −	3 +	4o	39o

March 1951

1	2	3	4	5	6	7	8	Sum
4 +	4 +	3 −	3 +	3o	2 +	1 +	1 +	23 -
0o	0 +	1 +	2o	3 +	2 +	1 +	2 +	13o
2 −	3o	4o	3 −	2o	2 +	2 −	1 −	18o
0o	3o	3o	1 +	2o	1 +	1 +	3o	15o
0 +	2o	3 −	2 −	1o	2 −	1o	0 +	11 −
1 +	3 +	5o	3 +	3 +	3 −	3 −	3 −	24 +
4 −	3 +	2 +	4 +	6o	4 +	5o	5o	34o
4 −	3o	4 −	6 −	5 −	5 +	5o	5 −	36 −
4 +	4o	4o	4 −	3 +	4 −	4o	6o	33o
5o	6 −	5o	3 +	4 +	4 −	4o	4o	35o
4o	4 −	4 +	3 +	3o	5o	5 −	3 −	31 −
4 +	4 +	4o	5o	5 −	4 −	4o	2o	32o
3o	3 +	3 +	5 −	5o	6 −	7 −	6 +	38o
5o	5 −	5 −	3 +	5 −	5 −	6 +	4 −	37o
6o	4o	3o	2 +	2 +	2o	2 −	1 −	22o
1 −	3o	3o	4 +	3 +	3o	4 −	3o	24o
2o	2 −	5 +	5 +	3o	4 −	3 −	3 −	26 +
3o	3 +	3 +	5 +	3o	3o	3 −	4o	28 −
3 +	3o	4 −	2o	1 −	2 −	2 −	1 +	17 +
1 −	1o	1o	4o	4o	3 −	1o	1 −	15o
1 −	1o	2o	2 −	1 +	1o	2o	4 −	13 +
4o	4 −	3o	5 −	5 −	6 −	6o	6 −	37 +
4o	4o	3 +	4 −	4o	4o	5o	4 +	32 +
4 −	3o	3 −	3 +	4 −	3 +	4 +	4o	28o
4 −	5 −	2 −	4 +	3 +	3 −	1 +	3o	25 −
3 +	3 −	3 +	3 +	3o	2 +	4 −	4 −	25 +
3 +	5 −	3o	3 −	2 +	2 +	2 −	2o	22o
2 +	1 −	0 +	0o	1o	1 +	1o	1 +	8o
1 −	4 +	5 +	4o	5 −	4o	4o	4 +	31 +
4 −	3 −	2o	3 −	3 −	1 +	1o	2 −	18 −
1 +	2 −	3o	2 +	2 −	3 +	2 +	1 +	17o

Final *C*, 1951		
Jan.	Feb.	Mar.
0.6	1.2	0.8
1.1	0.1	0.5
0.7	0.0	0.4
0.2	0.8	0.4
0.7	1.2	0.1
0.2	1.3	0.9
0.0	0.5	1.5
0.5	1.1	1.4
0.2	1.1	1.1
1.0	1.2	1.3
1.1	1.2	1.2
0.9	1.3	1.2
0.8	0.9	1.6
0.8	0.7	1.4
1.0	0.2	1.0
1.0	0.0	1.0
0.5	0.3	0.9
0.3	0.6	0.9
1.1	0.6	0.5
0.6	0.2	0.7
1.2	0.7	0.4
1.6	1.5	1.5
1.2	1.7	1.1
0.5	1.4	1.0
0.3	1.0	0.9
1.2	0.9	0.9
0.8	1.6	0.6
1.0	1.6	0.1
0.6		1.2
0.9		0.7
1.6		0.6

Final selected days

Jan.	Feb.	Mar.
Five quiet		
4	2	2
6	3	4
7	15	5
9	16	21
18	20	28
Five disturbed		
2	22	7
21	23	10
22	24	13
23	27	14
31	28	22
Ten quiet		
4	2	2
6	3	3
7	4	4
8	7	5
9	15	19
17	16	20
18	17	21
20	18	28
24	20	30
25	21	31

1951 February 01d 14h54: Va.—02d 07h20: So.—04d 16h33: Do.—05d 10h3
Sw.—05d 14h25: Wn Ma Tl Va.—06d 08h13: Do Sw Va.—07d 00h35: Tl.-
08d 07h00: Te.—08d 11h11: Sw.—09d 21h05: El.—10d 06h58: Sw.—12d 07h5
Sw.—14d 12h12: Tl.—21d 06h11: Hu.—21d 14h37: Te.—22d 05h20: Tl El.-
22d 07h21: Va.—25d 02h02: Ap.—27d 16h21: Tl.—27d 20h24: Ab Tl.—27
23h22: Ab Tl.—27d 21h53: Ab.

1951 March 02d 20h54: Ap.—07d 07h15: El.—07d 10h15: Sw.—10d 04h5
Sw.—10d 14h38: Ma.—13d 00h14: Ch.—13d 08h39: Sw.—13d 17h40: Fu El.-
13d 19h30: Fu El.—15d 07h57: So.—16d 14h30: Va El.—16d 15h55: Va.—21
07h00: Pi.—21d 19h30: Te.—22d 15h41: Va.—27d 03h15: Ch.—28d 12h20: Es.-
29d 03h09: Te.

Preliminary report on solar-flare effects

Effects confirmed by ionospheric or solar observations are in italics.

1951 January 01d 16h27: Pi.—02d 09h40: Wi Ma.—08d 20h42: Pi.—14d 13h4
14h09: Va.—14d 17h17-27: Va.—16d 15h21: Pi.—20d 15h25: Pi.—20d 15h42-5
Va.—20d 15h37-20h18: Tu.—*22d 16h25-48:* Wi Va Pi.—31d 09h55: Va.—31
12h13-28: Va.

1951 February 05d 14h25?: Eb.—10d 11h11-30: Do.—12d 17h29: Pi.—14
11h21-45: Tl.—16d 16h16-17d 01h24: Tu.—*19d 14h00-30:* CF Hu Hr.—21d 17h2
Hu Pi.—22d 05h19?: Eb.—22d 06h11-20: Eb.—22d 20h50-59: Va.—*24d 14h30-4*
CF Hu.—24d 15h15-16h03: Va.—*25d 14h00-35:* CF.—*26d 01h55-02h30:* Ka Am.-
27d 16h31-37: Eb.—28d 14h16-15h27: Ch SJ.

1951 March *01d 11h10-21:* CF.—*01d 11h57:* CF.—*01d 15h18:* Hu.—02d 20h5
21h06: Ch Tu Ho Hu.—03d 11h36: CF magn−, sol +.—12d 13h06-15: Va.-
12d 13h49-58: Va.—16d 19h16-43: Tu.—17d 18h50-19h04: Ho Pi.—18d 11h2
CF magn−, sol +.—20d 10h41-50: Va.—20d 15h22-53: Tl Hu Pi.—22d 14h5
15h06: Va.—24d 11h28-34: CF magn−, sol+, ion+.—28d 12h20-30: Tl.—2
03h04?: Ap.—30d 14h03: Do.

Committee on Characterization of Magnetic Disturbances

J. Bartels, *Chairman*
University
Göttingen, Germany

J. Veldkamp
Kon. Nederlandsch Meteorologisch Institu
De Bilt, Holland

OVISIONAL SUNSPOT-NUMBERS FOR APRIL TO JUNE, 1951

ependent on observations at Zurich servatory and its stations at Locarno and Orosa)

Day	April	May	June
1	41	62	38
2	27	56	38
3	24	78	37
4	20	51	26
5	40	46	65
6	61	20	103
7	69	26	115
8	78	17	130
9	75	32	138
10	74	84	137
11	84	102	133
12	88	125	147
13	78	155	159
14	103	170	163
15	118	184	158
16	126	212	147
17	130	220	152
18	148	229	157
19	150	204	146
20	132	180	138
21	149	180	134
22	144	154	123
23	140	140	93
24	119	117	63
25	115	114	60
26	114	93	63
27	114	87	48
28	98	81	45
29	81	51	43
30	65	48	18
31		46	
ans.....	93.5	108.5	100.6
. days.....	30	31	30

Mean for quarter: 101.0 (91 days)

M. Waldmeier

iss Federal Observatory
Zurich, Switzerland

CHELTENHAM THREE-HOUR-RANGE INDICES *K* FOR APRIL TO JUNE, 1951

[*K*9 = 500 γ; scale-values of variometers in γ/mm: $D = 5.3$; $H = 2.6$; $Z = 4.1$]

Gr. day	April 1951		May 1951		June 1951	
	Values *K*	Sum	Values *K*	Sum	Values *K*	Sum
1	3113 0023	13	4565 2456	37	3442 3444	28
2	3332 3354	26	7244 4545	35	2443 3354	28
3	5344 3545	33	5343 3345	30	4222 2122	17
4	5543 4545	35	5334 3333	27	2332 2223	19
5	5643 5333	32	1323 1133	17	3332 2233	21
6	4553 4445	34	3341 2122	18	3353 3332	25
7	5633 3344	31	2322 1113	15	4432 2235	23
8	4443 2234	26	0101 2122	9	4442 3333	26
9	4443 2233	25	2333 2346	26	4313 2212	18
10	5344 3133	26	3545 5443	33	1113 2222	14
11	4443 2124	24	3234 3344	26	2312 2334	20
12	4322 1224	20	4433 2332	24	5233 2233	23
13	5534 5334	32	1122 0112	10	3233 3223	21
14	5343 2223	24	2432 0245	22	1200 1356	18
15	3212 2222	16	5333 3233	25	4443 3544	31
16	2110 1124	12	4433 2223	23	4243 3332	24
17	4233 2131	19	4444 3334	29	3111 2446	22
18	1146 6534	30	5523 1233	24	6754 2324	33
19	4233 2223	21	3221 1123	15	3655 2333	30
20	2533 3445	29	2221 2022	13	4101 2114	14
21	5544 3334	31	2100 0001	4	2341 2313	19
22	5543 4354	33	3101 2323	15	2213 2123	16
23	4522 2113	20	2224 2254	23	3221 1123	15
24	2444 5345	31	4323 3333	24	1212 2123	14
25	5643 3444	33	2232 2244	21	4454 5453	34
26	5222 1221	17	3222 3556	28	3342 2342	23
27	1332 2333	20	4533 1112	20	2241 2334	21
28	3122 1322	16	2321 2211	14	3333 2234	23
29	4423 2322	22	1152 2233	19	3211 2343	19
30	0110 1212	8	2135 3222	20	3421 2232	19
31			2323 1244	21		

Ralph R. Bodle
Observer-in-Charge

Cheltenham Magnetic Observatory
Cheltenham, Maryland, U.S.A.

PRINCIPAL MAGNETIC STORMS

(Advance knowledge of the character of the records at some observatories as regards disturbance

Observatory (Observer-in-Charge)	Greenwich date	Storm-time GMT of begin.	Storm-time GMT of ending[1]	Sudden commencement Type[2]	Amplitudes[3] D	H	Z	C-figure, degree of activity[4]	Maximal activity on K-scale 0 to 9 Gr. day	Gr. 3-hr. period	K-index	Ran D	H
(1)	(2)	(3)	(4)	(5)	(6)	(7)	(8)	(9)	(10)	(11)	(12)	(13)	(1
	1951	*h m*	*d h*		′	γ	γ					′	γ
College (M. L. Cleven)	Apr. 2	07 45	11 18	.....	....	....	....	ms	3	6	7	340	178
									4	5, 6	7		
									5	4	7		
									6	4, 5	7		
	Apr. 12	21 30	14 20	.....	....	....	....	ms	13	5	7	270	123
	Apr. 18	06 55	19 13	s.c.*	−10	+63	−39	ms	18	4, 5	7	230	136
	Apr. 19	23 30	23 07	.....	....	....	....	ms	21	4	7	150	141
	Apr. 24	07 30	26 13	.....	....	....	....	ms	25	3	7	260	152
	May 1	06 00	4 19	.....	....	....	....	ms	1	4, 7	6	250	131
									2	4, 5, 6	6		
									4	4	6		
	May 9	07 00	12 19	.....	....	....	....	ms	10	5	7	230	135
									11	4	7		
	June 2	03 10	3 14	.....	....	....	....	ms	2	5	6	70	93
	June 14	17 51	16 16	s.c.*	−17	−130	+18	ms	15	6	6	180	99
									16	4	6		
	June 17	17 06	20 03	s.c.*	−27	−84	+38	ms	18	2	6	170	144
									19	3, 4	6		
Sitka (J. H. Nelson)	Apr. 2	00 ..	10 15	.....	....	....	....	ms	5	2	7	84	83
	Apr. 12	22 ..	14 15	.....	....	....	....	ms	13	4, 5	7	88	6
	Apr. 18	06 53	19 03	s.c.	−5	42	+8	s	18	5	9	205	130
	Apr. 20	00 ..	23 07	.....	....	....	....	ms	21	4, 5	7	94	80
	Apr. 24	08 ..	26 10	.....	....	....	....	s	25	3	8	148	11
	May 1	05 ..	4 19	.....	....	....	....	ms	2	4, 5	7	108	83
									4	4	7		
	May 9	07 ..	12 19	.....	....	....	....	s	10	5	8	81	10
	May 16	00 ..	18 04	.....	....	....	....	ms	17	4	7	43	5
	May 23	09 ..	24 03	.....	....	....	....	ms	23	5	6	41	3
	May 26	10 40	27 06	.....	....	....	....	ms	27	2	7	63	7
	May 30	07 ..	30 14	.....	....	....	....	ms	30	4	7	34	5
	June 2	03 ..	3 15	.....	....	....	....	ms	2	3	6	39	3
	June 6	03 ..	6 18	.....	....	....	....	ms	6	3	6	33	3
	June 14	17 51	16 21	s.c.*	+2	64	−2	m	14	7, 8	5	47	2
									15	5	5		
									16	4	5		
	June 17	17 02	19 22	s.c.*	+3	35	−2	s	18	2	8	93	12
									19	3, 4	8		
	June 25	04 29	26 13	s.c.*	−4	50	−4	ms	25	4, 6	6	50	4
Cheltenham (R. R. Bodle)	Apr. 2	19 ..	11 08	.....	....	....	....	ms	5	2	6	35	
	Apr. 12	22 ..	14 12	.....	....	....	....	m	13	1, 2	5	19	
	Apr. 18	06 53	19 03	.....	....	....	....	ms	18	1, 2	6	38	1
	Apr. 20	14 ..	23 06	.....	....	....	....	m	20	8	5	15	1
									21	1	5		
	Apr. 24	05 ..	26 02	.....	....	....	....	ms	25	2	6	28	
	May 1	05 ..	5 00	.....	....	....	....	ms	2	1	7	46	
	May 9	17 ..	10 21	.....	....	....	....	ms	9	8	6	21	1
	May 17	02 ..	18 05	.....	....	....	....	m	18	1, 2	5	21	
	May 26	15 ..	27 05	.....	....	....	....	ms	26	8	6	13	
	May 29	06 21	29 08	.....	....	....	....	m	29	3	5	15	
	June 14	17 50	16 22	s.c.	6	17	2	ms	14	8	6	9	
	June 17	17 01	18 05	s.c.	3	33	4	ms	18	2	7	58	
	June 18	18 15	19 15	s.c.	3	59	4	ms	19	2	6	13	
	June 25	02 ..	26 09	.....	....	....	....	m	25	5	5	11	

[1]Approximate time of ending of storm construed as the time of cessation of reasonably marked disturbance moveme traces; more specifically, when the *K*-index measure diminished to 2 or less for a reasonable period.

[2]s.c. = sudden commencement; s.c.* = small initial impulse followed by main impulse (the amplitude in this case is t *main impulse only*, neglecting the initial brief pulse); . . . = gradual commencement.

[3]Signs of amplitudes of *D* and *Z* taken algebraically; *D* reckoned positive if towards the east and *Z* reckoned posit tically downwards.

[4]Storm described by three degrees of activity: *m* for moderate (when *K*-index as great as 5); *ms* for moderately sev *K* = 6 or 7); *s* for severe (when *K* = 8 or 9).

PRINCIPAL MAGNETIC STORMS—Continued

ory / er- / ge)	Green-wich date	Storm-time: GMT of begin.	Storm-time: GMT of ending[1]	Sudden commencement: Type[2]	Sudden commencement: Amplitudes[3] D	H	Z	C-figure, degree of activity[4]	Maximal activity on K-scale 0 to 9: Gr. day	Gr. 3-hr. period	K-index	Ranges: D	H	Z
	(2)	(3)	(4)	(5)	(6)	(7)	(8)	(9)	(10)	(11)	(12)	(13)	(14)	(15)
	1951	*h m*	*d h*		′	γ	γ					′	γ	γ
	Apr. 1	23 ..	14 15	.....	.....	.....	.....	ms	7	2	6	19	128	....
ap-	(*Note:* Apr. 8-12 only moderately disturbed; 13th badly disturbed)													
	Apr. 18	06 53	26 05	s.c.	−1	+51	+7	ms	18	4	6	18	181	65
	May 1	01 ..	4 15	.....	.....	.....	.....	ms	1	8	6	17	214	53
									2	1	6			
	May 9	18 ..	12 09	.....	.....	.....	.....	ms	9	8	6	25	126	....
	May 25	18 46	27 11	s.c.	0	+18	0	m	25	8	5	11	136	20
									26	6, 8	5			
									27	2	5			
	June 14	17 50	16 12	s.c.	+2	+14	+1	ms	14	8	6	12	115	18
	June 17	17 01	20 03	s.c.	+2	+15	0	ms	18	2	7	23	174	57
	(*Note:* Probably 60 per cent of range in *Z* is due to normal diurnal-variation)													
	Apr. 18	06 52	19 04	s.c.	+1	+24	−5	ms	18	4, 5	6	10	125	36
lig)	May 1	16 ..	2 02	(*Note:* Very rough period with one *K*-index of 6, but not considered a storm.)										
	May 25	18 48	27 05	s.c.	0	+13	−3	m	26	7, 8	5	13	145	42
									27	1, 2	5			
	June 17	17 01	19 12	s.c.	0	+10	−5	ms	17	8	6	13	150	40
	Apr. 18	06 54	19 12	s.c.	1	28	12	ms	18	4	7	14	141	59
ite)	May 9	17 50	11 18	.....	.....	.....	.....	m	9	8	5	13	124	70
	June 17	17 00	19 12	s.c.	1	22	12	ms	19	2	6	13	173	36
Geo-	Apr. 2	12 00	6 05	.....	.....	.....	.....	ms	2	6	7	9	249	41
uan-	Apr. 18	06 52	23 05	s.c.	+1	+38	+8	ms	18	5, 6	7	11	436	62
	May 1	04 56	4 03	.....	.....	.....	.....	ms	1	7	6	9	402	41
ecke)	May 9	02 27	12 21	.....	.....	.....	.....	ms	10	5	7	12	307	60
	May 25	18 47	27 04	s.c.	0	+42	+1	m	26	6, 8	5	4	375	42
	June 17	17 01	18 16	s.c.	+2	+101	+7	ms	17	8	6	7	393	29
	June 25	04 28	25 23	s.c.	0	+23	+3	ms	25	6	6	4	167	35
	Apr. 1	22 45	7 13	.....	.....	.....	.....	m	3	1, 2, 7	5	6	142	21
King)									6	3	5			
	Apr. 18	06 52	19 03	s.c.	.....	+21	−4	ms	18	4	6	5	137	33
	May 1	00 45	3 12	.....	.....	.....	.....	m	1	3, 4, 7, 8	5	4	163	32
									2	1, 4	5			
	May 9	06 30	12 07	.....	.....	.....	.....	m	9	8	5	4	142	33
									10	2, 4	5			
	May 16	22 45	18 07	.....	.....	.....	.....	m	18	2	5	5	76	25
	May 22	05 00	24 20	.....	.....	.....	.....	m	22	4	5	5	97	18
	May 25	18 45	27 11	.....	.....	.....	.....	m	26	7, 8	5	5	167	26
	May 31	20 00	3 14	.....	.....	.....	.....	m	27	2	5	4	90	12
									2	3	5			
	June 5	20 15	7 14	.....	.....	.....	.....	m	6	3	5	3	114	27
	June 17	17 00	18 16	s.c.	+1	+21	−8	ms	17	8	6	6	189	37
	Apr. 1	21 ..	10 07	.....	.....	.....	.....	m	2	5, 6, 8	5	22	112	120
									3	4, 5, 6, 7	5			
k)									4	6	5			
									5	2	5			
									6	8	5			
									7	1, 5, 7, 8	5			
									8	8	5			
	Apr. 12	21 ..	14 15	.....	.....	.....	.....	m	12	8	5	17	110	100
									13	1, 5	5			

(*Note:* Hermanus continued on next page.)

PRINCIPAL MAGNETIC STORMS—Concluded

Observatory (Observer-in-Charge)	Greenwich date	Storm-time GMT of begin.	Storm-time GMT of ending[1]	Sudden commencement Type[2]	Amplitudes[3] D	H	Z	C-figure, degree of activity[4]	Maximal activity on K-scale 0 to 9 Gr. day	Gr. 3-hr. period	K-index	Ran D	E
(1)	(2)	(3)	(4)	(5)	(6)	(7)	(8)	(9)	(10)	(11)	(12)	(13)	(1
	1951	*h m*	*d h*		′	γ	γ					′	γ
Hermanus— *Continued* (A. M. van Wijk)	Apr. 18	06 53	19 13	s.c.	+1	+30	+15	ms	18	4	7	21	19
	Apr. 19	21 ..	23 09	.....	....	....	....	m	20	7, 8	5	18	9
									21	1, 3, 4	5		
									22	7	5		
									23	2	5		
	Apr. 24	06 ..	26 06	.....	....	....	....	m	24	7, 8	5	17	10
									26	1	5		
	May 1	00 ..	5 00	.....	....	....	....	ms	1	8	7	37	17
	May 9	17 ..	12 21	.....	....	....	....	ms	9	8	6	25	14
	May 25	18 47	27 12	s.c.	+1	+10	+9	ms	26	8	6	17	14
	June 3	00 07	3 02	——Large bay——				m	3	1	5	.....	...
	June 6	04 ..	6 18	.....	....	....	....	m	6	4	5	12	6
	June 14	17 50	16 12	s.c.	+1	+10	+8	..	16	1, 2	4	12	6
	June 17	17 01	18 16	s.c.	+1	+7	+6	ms	17	8	6	20	10
									18	4	6		
	June 18	23 14	19 17	s.c.	+2	+12	+11	m	19	3, 4	5	12	8
	June 25	04 28	26 17	s.c.	+2	+9	+9	..	25	4, 5, 6, 7	4	11	10
									26	4	4		
Watheroo (L. S. Prior)	Apr. 2	12 00	7 21	.....	....	....	....	ms	3	4	6	22	14
	Apr. 12	23 00	13 17	.....	....	....	....	m	12	8	5	10	10
									13	1, 4, 5	5		
	Apr. 18	06 54	18 23	s.c.*	+3	+45	−23	ms	18	4	7	17	23
	Apr. 24	08 00	26 02	.....	....	....	....	m	24	5	5	15	12
									25	5	5		
	May 1	05 00	4 23	.....	....	....	....	ms	2	5	6	30	13
	May 9	20 00	10 22	.....	....	....	....	ms	9	8	6	24	9
	June 14	17 52	15 03	s.c.*	+2	+25	−19	m	14	8	5	11	6
	June 17	17 04	18 11	s.c.	+1	+28	−10	ms	18	1	6	21	14
	June 18	23 14	19 19	s.c.	+1	+10	−5	m	19	2, 6	5	12	10
	June 25	04 29	25 23	s.c.*	+2	+12	−15	m	25	5	5	12	10
Amberley (J. W. Beagley)	Apr. 2	12 44	8 14	s.c.?	0	+7	−2	m	3	2	5	19	13
									4	3, 5	5		
									5	4	5		
									6	3, 8	5		
	Apr. 12	21 57	14 13	.....	....	....	....	m	13	5	5	21	6
	Apr. 18	06 53	19 12	s.c.	−2	+38	+4	ms	18	4, 5	6	24	11
	Apr. 20	14 18	23 06	.....	....	....	....	m	21	1, 4	5	23	13
				(*Note:* Abrupt ending at $23^d\ 06^h\ 16^m$)									
	Apr. 24	04 42	26 12	.....	....	....	....	m	24	3	5	21	11
									25	3, 5, 6	5		
	Apr. 30	22 51	5 10	.....	....	....	....	ms	1	4	6	38	11
	May 5	23 30	6 09	.....	....	....	....	m	6	3	5	13	
	May 9	00 54	12 07	.....	....	....	....	m	10	3, 5	5	17	11
									11	4	5		
	May 25	18 46	27 12	s.c.*	....	−8	....	m	26	8	5	12	11
	May 30	05 52	30 16	.....	....	....	....	m	30	4	5	14	
	June 6	01 37	6 17	.....	....	....	....	m	6	3	5	16	11
	June 14	17 52	16 16	s.c.	+3	+18	−14	m	14	8	5	11	11
	June 17	17 02	18 16	s.c.	+2	+26	−9	ms	17	8	6	17	11
	June 18	23 15	20 05	s.c.*	−2	+17	+8	ms	19	4	6	16	11

LETTERS TO EDITOR

)MMENTS CONCERNING THE PAPER "FINE STRUCTURE OF THE LOWER IONOSPHERE" BY R. A. HELLIWELL, A. J. MALLINCKRODT, AND F. W. KRUSE, JR.

We read with great interest in the March, 1951, issue of this JOURNAL (**56**,). 1, pp. 53-62) the above paper concerning the characteristics of the lower ıosphere, as determined by long-wave pulse techniques. Our Laboratory has o been conducting long-wave, vertical-incidence pulse experiments for some time a frequency of 150 kc/sec. From an extensive series of group height, absorption, larization and, more recently, change of phase height measurements, we have en able to develop a model of the lower ionosphere which appears to satisfy the eoretical and experimental results on a diurnal and seasonal basis at this fre- ency.[1] The available experimental results on other long wave-lengths have also en considered, and we should like to take this opportunity to call attention to other interpretation as to the cause of two apparent "reflection" heights, pointed t by the above authors.

The model, as far as the E-region is concerned, for night-time May and June, ound $01^h\ 00^m$ to $03^h\ 00^m$, is essentially constant and may be described as follows:

$$N = 10^4 e^{1/2(1-x-e^{-x})} \text{ electrons/cm}^3$$

$$h_{max} = 115 \text{ km} = \text{height of maximum ionization}$$

$$x = \text{height measured in scale units with respect to } h_{max}$$

$$\nu = \text{exponentially decreasing with scale height of 10 km}$$

$$\nu_c = (5.348 \times 10^5) \text{ sec}^{-1} \text{ at 94 km}$$

Earth's magnetic field = constant = 0.535 oersted at an angle of 70° 52′ with the horizontal

We shall consider first the 150 kc/sec results, which we have studied in greatest ail. In the case of 150 kc/sec waves incident vertically on this model, we find t, neglecting the effects of coupling,[2] there will be a wave of "ordinary" polari- ion "reflected" from the level where $N \cong 3{,}000$. This corresponds to the well own $X = 1 + Y$ reflection level which occurs in the collision-free case and at eight of about 100 km in our model.

[1] "The lower E and D regions of the ionosphere as deduced from long-wave measurements," by . Gibbons, H. J. Nearhoof, and R. J. Nertney; submitted for presentation at the URSI-IRE ting, Cornell University, October 8-10, 1951.

[2] "A method for obtaining the wave solutions of ionospherically reflected long waves, including ariables and their height variation," by J. J. Gibbons and R. J. Nertney, J. Geophys. Res., **56**, 3, pp. 355-371 (1951).

If we consider the coupling[3] and modify our unperturbed wave solutions fo the "ordinary" and "extraordinary" waves, by use of variational methods, i becomes evident that there will be waves scattered in the forward (direction o propagation of the unperturbed wave) and in the backward (opposite to th direction of propagation of the unperturbed wave) directions by these "unper turbed" waves. The region of maximum coupling occurs in the neighborhood o the well-known $X = 1$ reflection level. For 150 kc/sec, this occurs at a value o $N \cong 300$ (which is at about 91 km in our model).

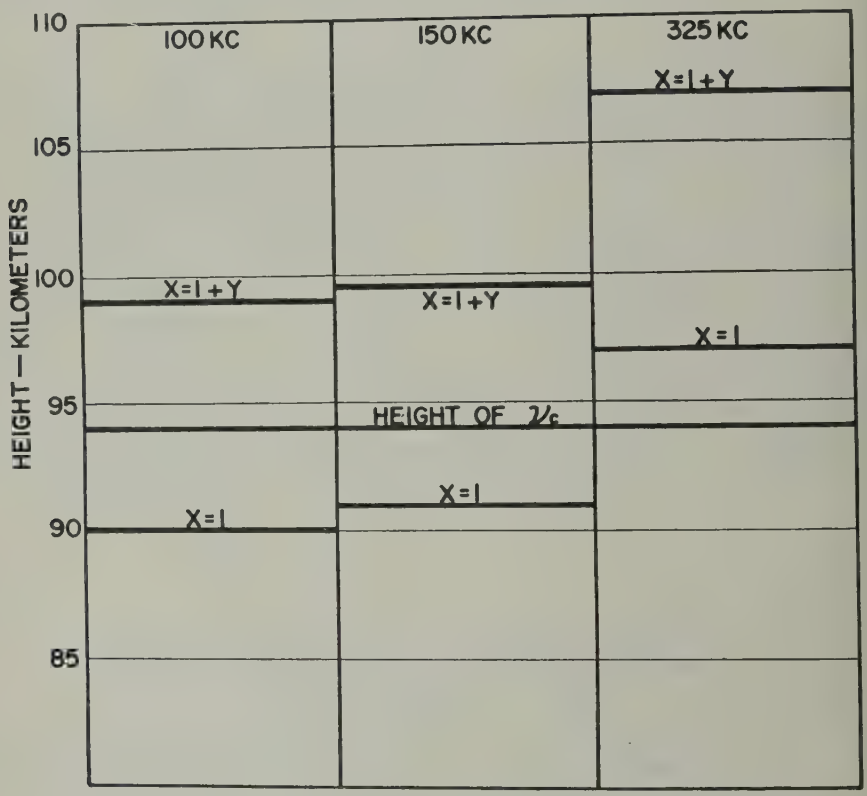

FIG. 1—HEIGHT OF THE CRITICAL POINTS IN THE E-LAYER MODEL FOR 01^h00^m TO 03^h00^m, MAY AND JUNE

It is beyond the scope of this Letter to discuss in detail the mechanics of su a complicated reflection mechanism, but the results to be expected are as follo

With a transmitted pulse of linear polarization, we might expect to see, first hop, an echo originating at about 91 km, having left-handed rotation and ve nearly linear polarization. This echo should have maximum strength someti

[3]Technical Report No. 25, "Wave solutions, including coupling, of ionospherically reflec long radio waves and the derived characteristics of the lower ionosphere," Ionosphere Resea Laboratory, The Pennsylvania State College, State College, Pa. (July 1951).

er midnight when the E-layer critical frequency reaches its minimum value, ce, at this time, the $N \cong 300$ ($X = 1$) point is in closest proximity to the $\nu = \nu_c$ nt in our model. This corresponds to strongest coupling in our series of diurnal dels. We would expect to see a second echo also of left-handed polarization, ginating from the $N \cong 3{,}000$ point ($X = 1 + Y$) at around 100 km. Neither these echoes will be a pure magneto-ionic component, since the lower "coupling" ıo was excited by a transmitted wave consisting of both ordinary and extraor- ıary polarizations and the upper echo, which was a pure component on re- ːtion from the upper "reflection" region, has excited the other component by versing the coupling region.

From these results it becomes evident that, while the effect of the high collision the lower E-region has been to "smooth" the indices of refraction and appar- ly remove the $1 - X = 0$ reflection point, this apparent removal of the reflection ıdition is true only in the sense that we no longer have a reflection condition a single magneto-ionic component. The true effect of the collisions has been to ıceal a "reflection" condition in the coupling terms.

Considering other frequencies, if we locate the critical points $1 - X = 0$ and $+ Y = X$ in our model for 325 kc/sec, we find that they occur at 97 km and 7 km, respectively. The points are located at 90 km and 99 km for 100 kc/sec. These results are plotted in Figure 1 and may be compared with Figures 4 and n the above-named paper. The similarity of these Figures leads us to believe at there is strong likelihood that the splitting may be due to the above effects her than a true stratification.

It must be pointed out that our results are based on the analysis of the effects our model on c.w. waves and that the heights quoted are the *true* heights of the ɔupling" and "reflection" regions. For this reason, it is not surprising that the ɔarent height of the upper 325 kc/sec trace is greater than the true height licated by our model. It may also be noted that it is not difficult, with this ɔlanation of the splitting, to obtain a 300 kc/sec split which has its lower echo ng below the 150 kc/sec echo upper echo—an experimental fact which has been served.

This work has been supported in part by Contract No. AF19(122)-44 with the ited States Air Force, through sponsorship of the Geophysical Research Di- torate, Air Materiel Command.

R. J. Nertney

iosphere Research Laboratory,
The Pennsylvania State College,
State College, Pennsylvania, June 27, 1951

A NOTE ON CERTAIN CHARACTERISTICS OF THE NORMAL *E*-LAYE

Experimental determinations of equivalent height, h', as a function of wav frequency, f, for the *E*-layer of the ionosphere have been obtained to an accurac of ± 1 km, using high-power ionosphere measuring equipment developed by th Ionosphere Research Laboratory of The Pennsylvania State College.

As is well known, the task of converting equivalent height *versus* frequenc

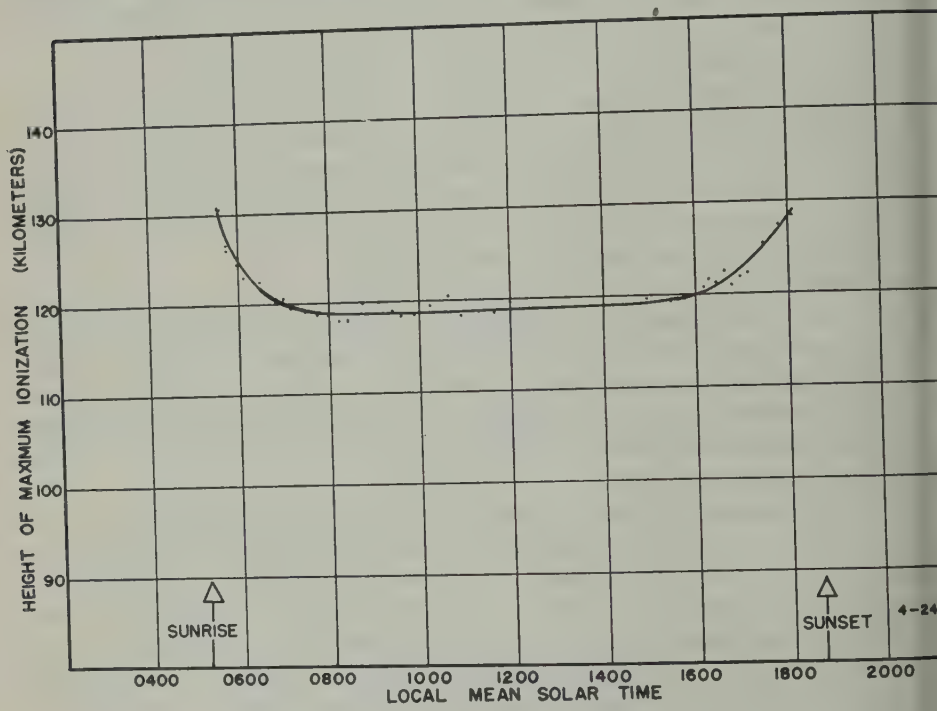

FIG. 1—DIURNAL VARIATION OF THE HEIGHT OF MAXIMU IONIZATION

data to true height *versus* frequency data in any quantity heretofore has b almost impractically time consuming. A method has been developed by Dr. J. Kelso,[1] however, which makes possible the conversion of $h' - f$ data to h_t data on a routine basis. The method is an extension of the work of Friedm and Krauss,[3] and a complete curve may be converted in approximately 15 min with the aid of computed tables.

Applying this method to our $h' - f$ data, procured during the last year have been able to obtain true height data for all our normal records. (It shoul

[1]J. M. Kelso, "A procedure for the determination of the electron density in the ionosph Technical Report No. 19, Ionosphere Research Laboratory, The Pennsylvania State Co State College, Pa. (Feb. 20, 1951).

[2]B. Friedman, Research Report EM-17, Washington Square College, Mathematics Res Group, New York University (1950).

[3]L. Krauss, Progress Report No. 6, Washington Square College, Mathematics Research G New York University (1950).

d that the method, at present, does not include the effects of collisions or the h's magnetic field.) From the true heights thus determined, it has been possible btain the diurnal variation of the height of maximum ionization, h_m , for the yer at State College. It has been noted that this variation does not follow pman theory, except possibly for about an hour after sunrise and an hour re sunset. Throughout most of the day, h_m remains at a relatively constant , which, for this latitude, was found to be between 115 and 120 km. In Figure 1

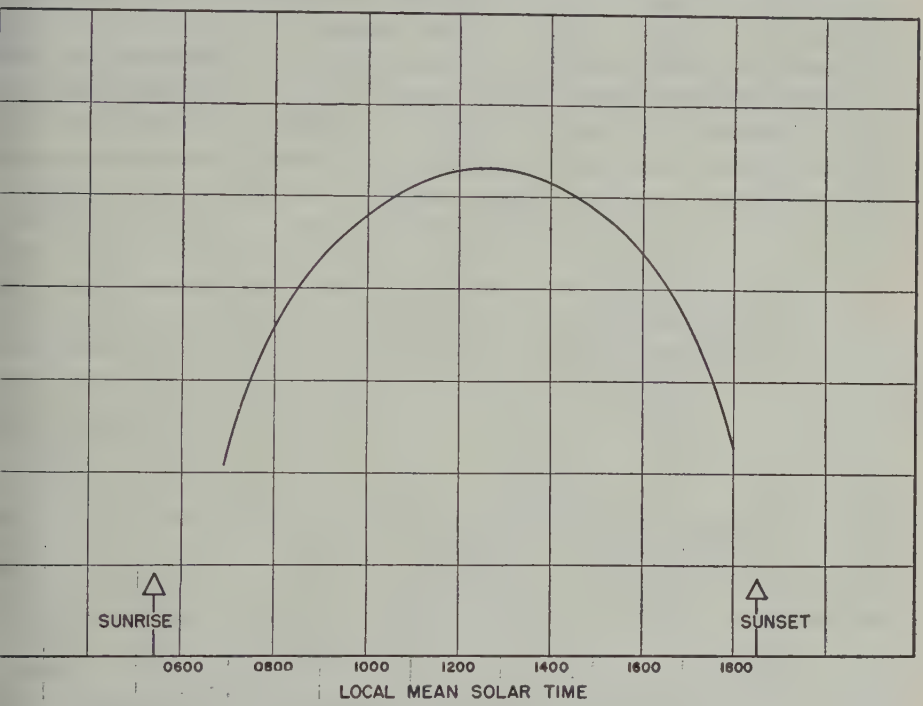

IG. 2—DIURNAL VARIATION OF ELECTRON DENSITY AT 115 KM ON APRIL 17, 1951

ıstrated a curve of the variation of h_m for 24 April 1951 in which the afore-ioned characteristics may be observed.

t should be noted that the use of the characteristic frequency method for rmining h_m ,[4], $f_{h_m} = 0.814\, f_{E_c}$, for these and other data yields similar $h_m - t$ es during most of the day, but does not do so for the hours between sunrise noon for the data examined to date. This is presumably due to the diurnal tion in the shape of the layer.

sing the above method, it is quite simple to obtain curves of the temporal tion of electron density at a constant height under simple theory conditions. xample of such a curve is shown for 17 April 1951 in Figure 2. Using a technique to Appleton,[5] in which times symmetrical about noon are chosen and for

. C. Jaeger, "Equivalent path and absorption in an ionospheric region," Proc. Phys. Soc., **59**, 47).

. V. Appleton, "Regularities and irregularities in the ionosphere," The Bakerian Lecture, R. Soc., A, **162**, 451-479 (1937).

which the rate of ion production, q, due to solar ultra-violet radiation is the sa one can determine an effective recombination coefficient, α', from the elect density - time curve using the equation

$$\frac{dN}{dt} = q - \alpha' N^2$$

From curves of the temporal variation of electron density in the region fr 108 to 120 km, we have found that, for any given height, α' is substantially c stant, but that there is a height variation suggestive of pressure dependence α' in the region under consideration. Values of α' were determined for times to five hours from solar noon and the average taken for each height. For the s day as in Figure 2, the average values of α' were determined and plotted in Figu

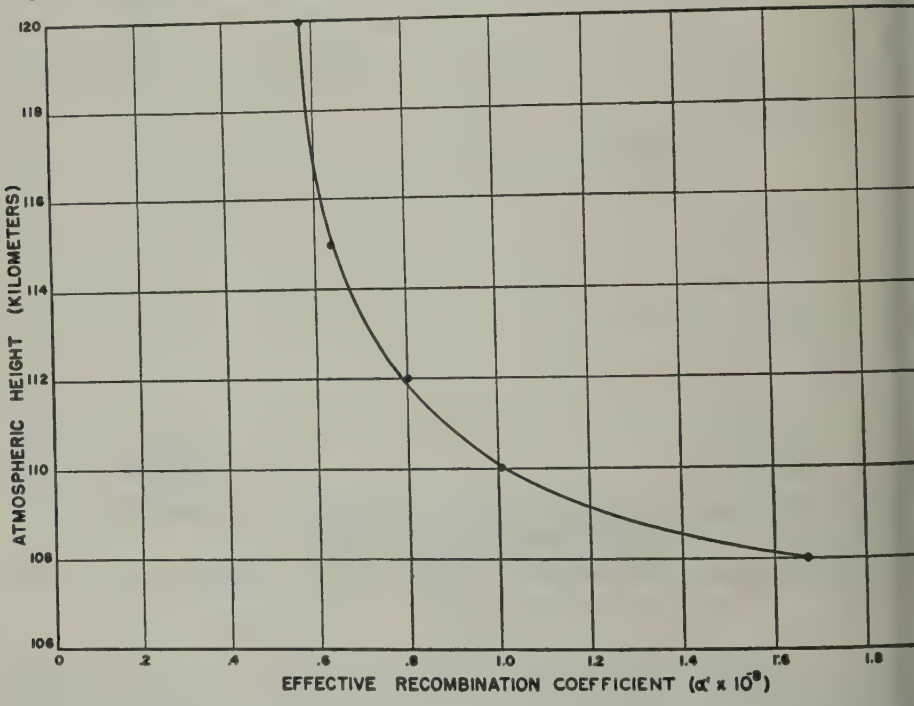

FIG. 3—VARIATION OF EFFECTIVE RECOMBINATION COEFFICI WITH HEIGHT, APRIL 17, 1951

The curve is seen to be exponential-like. If it were exactly exponenti pressure dependence of α' would be hard to deny. It is not exactly a true expon in this particular case, but the similarity is so striking that one might suspect further investigation might reveal some such correlation.

This work has been supported in part by contract No. AF(122)-44 wit United States Air Force, through sponsorship of the Geophysical Researc rectorate, Air Materiel Command.

C. H. Gra

Ionosphere Research Laboratory,
The Pennsylvania State College,
State College, Pennsylvania, June 27, 1951

NOTES

29) *Fall meeting of USA National Committee of URSI-IRE*—A meeting of the National Committee of the International Scientific Radio Union and the tute of Radio Engineers Professional Group on Antennas and Propagation be held on the campus of Cornell University, Ithaca, N. Y., on October 8, 9, 10, 1951. The School of Electrical Engineering will be the hosts. Sessions on ollowing topics will be held: Radio standards and methods of measurement, ospheric radio propagation, ionospheric radio propagation, extraterrestrial noise, circuit theory, and electronics.

30) *Geomagnetic surveys in Pakistan*—Dr. K. Wienert has been appointed by Technical Assistance Service of UNESCO to start observatories and a geo- netic field survey in Pakistan. The establishment of three observatories has proposed. If the regions prove satisfactory geomagnetically, one observatory oe located at Quella in Western Pakistan, and a second one at Dacca in Eastern stan.

31) *New edition of the Auroral Atlas*—A grant of 5,000 Norwegian crowns was e from the Temporary Commission for the Liquidation of the Polar Year -33 for reprinting the Auroral Atlas. The new edition will be ready soon.

32) *Solar eclipse*—The United States *Hydrographic Bulletin* (No. 16 of April 951) contained the following account of a solar eclipse observed in the Carib- Sea:

ourth Officer Daniel Karsh, of the American S.S. *Green Mountain State*, ain Ralph C. Spaulding, Master, reported that on March 7, 1951, from 25^m to 23^h 19^m GMT, in latitude 14° 05′ north, longitude 77° 21′ west, an se of the sun was observed. When the phenomenon was first seen the apparent of both sun and sky changed to a brilliant grayish-white which lasted until maximum eclipse occurred at 23^h 50^m GMT. As the eclipse decreased, the al sunset hues appeared, with the sun setting at 23^h 19^m GMT, while its r limb was still partially eclipsed. The sky was clear; wind northeast, force 2; t northeasterly sea; barometer 29.94 inches; air temperature 77° F.; sea erature 79°F.

33) *Aurora Borealis*—The United States *Hydrographic Bulletin* (No. 20 of 19, 1951) contained the following account of the Aurora Borealis in the h Atlantic:

hird Officer D. L. Higgins, of the American S.S. *American Manufacturer*, ain R. O. Patterson, Master, reported that on March 14, 1951, at 23^h 00^m , in latitude 52° 00′ north, longitude 24° 32′ west, an exceptionally brilliant ay of Aurora Borealis was observed. It appeared first as a bright fan-shaped esembling a large moonlit cloud in the northern sky. The arc of light spread it extended from a bearing of 280° to 030°, reaching to an altitude of 30° in enter and 20° on either end, the middle of the arc being 6° to 10° wide. Streaks ght resembling searchlight beams were interspersed along the entire arc, g and fading continually, and varying in brilliance from extremely bright es of silver-colored light to a dull glow. The phenomenon lasted for an hour, by 24^h 00^m GMT the bright fingers of light disappeared, the arc fading and

leaving a faint greenish glow on the northern horizon. By 03^h 00^m GMT, March the display was over completely. The sky was partly cloudy with occasion showers; wind WSW, force 6; sea rough; barometer 29.13 inches; air temperatu 43°F.

(34) *Geomagnetic activities of the United States Coast and Geodetic Survey*—T Inter-American Geodetic Survey observers continued on magnetic surveys in Sou America under the technical direction of the United States Coast and Geode Survey.

Reports containing reproductions of Cheltenham and Sitka magnetograms the first half of 1949 have been issued. "Magnetic hourly values, Cheltenha Maryland, 1948," the first publication in a new series giving hourly values p cessed by punched-card methods, was also issued.

"Instrucciónes para tomar mediciónes magnéticas," TC-297, has been pu lished by the United States State Department. This is a Spanish translation Captain Julio C. Roletti, of Uruguay, of "Directions for magnetic measurement by Daniel L. Hazard.

Dr. Clemente Garavito, of Colombia, is studying magnetic observatory ope tions at the United States Coast and Geodetic Survey under sponsorship of Inter-American Geodetic Survey.

The United States Coast and Geodetic Survey is cooperating with the Dep ment of Terrestrial Magnetism, Carnegie Institution of Washington, in the test of several special magnetic variometers.

(35) *Personalia*—Dr. *Otto Schneider*, who since 1948 has been Chief of Geophysical Division of the National Meteorological Service of Argentina, recei was appointed Technical Adviser to Director General of the Service, Carlos Nu Monasterio. His successor as Chief of the Geophysical Division is Dr. *Raimu Celeste*, a young Argentine scientist who has specialized in techtonophysics.

Dr. *J. A. Ratcliffe*, of the Physics Department, University of Cambridge, elected a Fellow of the Royal Society at a meeting held on March 15, 1951.

Our Associate Editor, Dr. *O. Lützow-Holm*, Director of the Geophysical servatory, at Pilar, Córdoba, Argentina, reports on the progress of a monume reduction of observatory records performed with the assistance of his staff du the past three years. The additional annual values of the magnetic elements rived for the three observatories operated by Argentina will be found elsewhe this issue of the JOURNAL. Values for Pilar are available from 1905 to 1950, re reduction being completed for 1905, 1915, 1916, 1932, and 1945-50. Annual va are now available for La Quiaca (operation under control of the Argentine N but reduction at Pilar) for 1920-33 and 1942-48, reduction being completed 1926-29 and 1942-48. Annual values are available for Laurie Island (Orcadas) 1905-47 with the exception of 1916 and 1939 (for the years 1913-26 only declina reductions are complete). It will be recalled that Dr. Lützow-Holm has al completed his ambitious program of 1,000 field stations in Argentina, thus ran his country with the best geomagnetically-mapped countries in the world.

Advice has been received that Father *Ch. Combier*, Director of the Observa de Ksara, in Lebanon, died on June 8, 1951. Rev. Dr. *J. Plassard* has been appo Director; his address is Observatoire de Ksara, par Zahle, Republic of Leban

LIST OF RECENT PUBLICATIONS

By W. E. Scott

Department of Terrestrial Magnetism,
Carnegie Institution of Washington,
Washington 15, D. C.

(Received July 23, 1951)

A—*Terrestrial Magnetism*

TELS, J., AND J. VELDKAMP. International data on magnetic disturbances, fourth quarter, 1950. J. Geophys. Res., **56**, No. 2, 283-287 (1951).

LE, R. R. Cheltenham three-hour-range indices *K* for January to March, 1951. J. Geophys. Res., **56**, No. 2, 288 (1951).

ARO, V. C. A., W. C. PARKINSON, AND H. W. UNTHANK. Sudden commencements and sudden impulses in geomagnetism: Their hourly frequency at Cheltenham (Md.), Tucson, San Juan, Honolulu, Huancayo, and Watheroo. J. Geophys. Res., **56**, No. 2, 177-195 (1951).

LAND, G. D. Combined analysis of gravity and magnetic anomalies. Geophysics, **16**, No. 1, 51-62 (1951).

GRAPHIC SURVEY INSTITUTE. Magnetic survey in Japan. Kyoto, J. Geomag. Geoelectr., **2**, No. 3, 89-94 (1950).

O, Y. On the magnetic moment of the residual magnetism of the rock. Kyoto, J. Geomag. Geoelectr., **2**, No. 3, 81-82 (1950).

O, Y., AND S. UTASHIRO. Investigation of the magnetic storm by the induction magnetograph. Kyoto, J. Geomag. Geoelectr., **2**, No. 3, 71-73 (1950).

NEVA, L. A. The anomalous geomagnetic field and its equivalent system of electric currents in the world's ocean. Doklady Akad. Nauk USSR, **71**, No. 1, 49-52 (1951). [In Russian.]

OKI, T. The KC type magnetometer for direct-vision. Kyoto, J. Geomag. Geoelectr., **2**, No. 3, 83-85 (1950).

AGAI, N., N. KAWAI, AND T. NAGATA. Recent progress in palaeomagnetism in Japan. Kyoto, J. Geomag. Geoelectr., **2**, No. 3, 61-65 (1950).

ATA, T. A reply to the comment by Prof. Ferraro on my article "Southward shifting of the auroral zone." J. Geophys. Res., **56**, No. 2, 292-294 (1951). [Letter to Editor.]

M. Geomagnetic activity characterized by the *K* indices. Kyoto, J. Geomag. Geoelectr., **2**, No. 3, 86-88 (1950).

S, INSTITUT DE PHYSIQUE DU GLOBE. Annales de l'Institut de Physique du Globe de l'Université de Paris et du Bureau Central de Magnétisme Terrestre. Publiées par les soins de J. Coulomb. Tome XXV. Paris, Imprimerie Nationale, 57 with 8 pages de graphiques (1950). 31 cm. [Contains values of the magnetic elements for Chambon-la Forêt in 1947-48, for Nantes in 1948, Tananarive in 1948-49, and Ksara in 1947-48.]

E, A. T., AND G. A. WILKINS. The daily magnetic variations in equatorial regions. J. Geophys. Res., **56**, No. 2, 259–263 (1951).

CIPAL MAGNETIC STORMS. Principal magnetic storms, January to March, 1951. J. Geophys. Res., **56**, No. 2, 289-291 (1951).

EIKIN, V. V. The magnetic field and the influence of the world's ocean on its pattern. Doklady Akad. Nauk USSR, **76**, No. 1, 57-60 (1951). [In Russian.]

ED STATES COAST AND GEODETIC SURVEY. Magnetograms, Cheltenham, Maryland, January-June 1949. Washington, D. C., U. S. Coast Geod. Surv., 61 pp. (1951). 25 cm.

United States Coast and Geodetic Survey. Magnetograms, Sitka, Alaska, January-June 19
Washington, D. C., U. S. Coast Geod. Surv., 65 pp. (1951). 25 cm.
Veldkamp, J. The geomagnetic field of the Netherlands reduced to 1945.0. K. Nederlands M
Inst., No. 134, 30 + 7 charts (1951). 34 cm.
Yoshimatsu, T. Diurnal and seasonal frequencies of occurrence of "sudden commencement
SC, in geomagnetism. Kyoto, J. Geomag. Geoelectr., 2, No. 2, 54-60 (1950).

B—*Terrestrial Electricity*

Akademische Verlagsgesellschaft. Das gewitter, ergebnisse und probleme der modern
gewitterforschung. Leipzig, Geest and Portig K.-G., 249 with figs. (1950). 23 cm. [Collect
and edited by H. Israël.]
Cardús, J. O. Sobre la rey de las fases en las corrientes telúricas. Rev. Geofísica, Madrid,
No. 35, 215-233 (1950).
Chalmers, J. A. The origin of the electric charge on rain. Q. J. R. Met. Soc., 77, No. 332, 249-2
(1951).
Maeda, K. On the electrical conductivity of the upper atmosphere. Kyoto, J. Geomag. Geoelec
2, No. 2, 45-53 (1950).
Malan, D. J., and B. J. F. Schonland. The electrical processes in the intervals between
strokes of a lightning discharge. Proc. R. Soc., 206, No. 1085, 145-163 (1951).
Yeh, T. C. Some measurements of the atmospheric electric potential over Mei-Tan. J. Chin
Geophys. Soc., 2, No. 2, 147-157 (1950).

C—*Cosmic Rays*

Biermann, L., and A. Schlüter. Cosmic radiation and cosmic magnetic fields. II. Origin
cosmic magnetic fields. Phys. Rev., 82, No. 6, 863-868 (1951).
Fan, C.-Y. On Fermi's theory of the origin of cosmic radiation. Phys. Rev., 82, No. 2, 211-
(1951).
Kato, Y., and T. Kanno. On the variations of the cosmic-ray intensity associated with the m
netic storm. Sci. Rep. Tôhoku Univ., Ser. 5, Geophysics, 2, No. 3, 153-157 (1950).
Sekido, Y., and T. Yagi. Deflection of cosmic rays in the solar magnetic field. Kyoto, J. Geom
Geoelectr., 2, No. 3, 77-80 (1950).
Sekido, Y., and S. Yoshida. On the diurnal variation of cosmic rays: Part II. Annual chang
the cosmic-ray diurnal variation. Kyoto, J. Geomag. Geoelectr., 2, No. 3, 66-70 (1950).
Unsöld, A. Cosmic radiation and cosmic magnetic fields. I. Origin and propagation of cosmic
in our galaxy. Phys. Rev., 82, No. 6, 857-863 (1951).

D—*Upper Air Research*

Adel, A. Atmospheric nitrous oxide and the nitrogen cycle. Science, 113, 624-625 (June 1, 19
Aspinall, A., J. A. Clegg, and G. S. Hawkins. A radio echo apparatus for the delineatio
meteor radiants. Phil. Mag., 42, No. 328, 504-514 (1951).
Berning, W. W. Charge densities in the ionosphere from radio doppler data. J. Met., 8, N
175-181 (1951).
Bracewell, R. N., K. G. Budden, J. A. Ratcliffe, T. W. Straker, and K. Weekes.
ionospheric propagation of low-and very-low-frequency radio waves over distances less
1000 km. Proc. Inst. Elec. Eng., 98, Pt. 3, No. 53, 221-236 (1951).
Central Laboratorium. A simple mechanism to obtain a logarithmic frequency scale us
capacity-linear condenser. 's-Gravenhage, Mededeling No. 32 R.L., 2 pp. with table and
(May 1951). [Prepared by Ir P.L.M. v. Berkel.]
Choudhury, D. C. Effect of vertical transport of ions caused by solar tides in F_2 region. I
J. Phys., 25, No. 1, and Proc. Indian Assoc. Cultivation Science, 34, No. 1, 1-7 (1951)
Christiansen, W. N., and J. V. Hindman. A long-period change in radio-frequency rad
from the "quiet" sun at decimetre wave-lengths. Nature, 167, 635-637 (April 21, 195

INGTON, A. E. Some characteristics of 10.7-centimetre solar noise, II. J. R. Astr. Soc. Can., **45**, No. 2, 49-61 (1951).

KSON, D. V. Nomogram and slide-rule for solution of spherical triangle problems found in radio communication. J. Geophys. Res., **56**, No. 2, 163-175 (1951).

RIG, R. Beiträge zur Höhenschwankung der *F*2-Schicht der Ionosphäre. Zs. angew. Phys., **3**, Heft 3/4, 96-103 (1951).

STERLING, K. Wellenausbreitung in der Ionosphäre bei Berücksichtigung des Erdmagnetfeldes bei schiefer Inzidenz II. Archiv Elektr. Uebertrag., **5**, Heft 5, 209-215 (1951).

SON, N. C. Radio observations of the aurora on November 19, 1949. Nature, **167**, 804-805 (May 19, 1951).

A, U. C. Reversal of polarization of microwaves from sunspots. Indian J. Phys., **25**, No. 1, and Proc. Indian Assoc. Cultivation Science, **34**, No. 1, 8-16 (1951).

ES, C. O. Wave packets, the Poynting vector, and energy flow: Part II—Group propagation through dissipative isotropic media; and Part III—Packet propagation through dissipative anisotropic media. J. Geophys. Res., **56**, No. 2, 197-206 and 207-220 (1951).

GRONE, A. H., W. H. Benson, Jr., and A. W. Stratton. Attenuation of radio signals caused by scattering. J. Applied Phys., **22**, No. 5, 672-674 (1951).

CHIN, K. E. Distribution of radiation across the solar disk at a frequency of 81.5 Mc/s. Nature, **167**, 889-891 (June 2, 1951).

KINLEY, D. W. R. Meteor velocities determined by radio observations. Astroph. J., **113**, No. 2, 225-267 (1951).

RA, S. N. Anomalous behavior of multiply reflected echoes from the ionosphere. Science and Culture, **16**, No. 9, 425-426 (1951).

RA, S. K. Atomic nitrogen in auroras. Nature, **167**, 897 (June 2, 1951).

ATA, T., N. Fukushima, and M. Sugiura. Electro-dynamical behaviour of the ionosphere region viewed from geomagnetic variations. Kyoto, J. Geomag. Geoelectr., **2**, No. 2, 35-44 (1950).

SON, J. H. Shortwave radio propagation correlation with planetary positions. RCA *Review*, **12**, No. 1, 26-34 (1951).

ERSON, A. M. The mechanism of *F*-layer propagated back-scatter echoes. J. Geophys. Res., **56**, No. 2, 221-237 (1951).

LIPS, G. J. A wide-band aerial system for circularly polarized waves, suitable for ionospheric research. Proc. Inst. Elec. Eng., **98**, Pt. 3, No. 53, 237-239 (1951).

ER, K. Ausbreitungsvorhersage für Kurzwellen mit Hilfe von Ionosphärenbeobachtungen. Archiv Elektr. Uebertrag., **5**, Heft 4, 154-167 (1951).

ER, G. Motion in the solar atmosphere as deduced from radio measurements. Nation. Bur. Stan., CRPL preprint No. 51-14, 3 pp. + table (Oct. 25, 1950).

BECK, O. E. H. Théorie de la triple décomposition magnéto-ionique. Onde Électrique, **31**, No. 288, 153-156 (1951).

TT, J. A note on the geomagnetic control of the F_2-layer critical frequency. Nation. Bur. Stan., CRPL preprint No. 51-13, 3 pp. + diagrs. (Oct. 24, 1950).

ER, C. L. Some observations of the variable 205 Mc/sec radiation of Cygnus A. J. Geophys. Res., **56**, No. 2, 239-258 (1951).

VICE DE PRÉVISION IONOSPHÉRIQUE MILITAIRE. Propositions et rapports de travaux en vue de l'Assemblée générale de l'URSI en Septembre 1950. S.P.I.M., No. R13, 26 pp. (Aug. 1950).

ER, S. F., E. Maple, and W. A. Bowen, Jr. Evidence for ionosphere currents from rocket experiments near the geomagnetic equator. J. Geophys. Res., **56**, No. 2, 265-281 (1951).

NCER, D. E. Separation of variables in electromagnetic theory. J. Applied Phys., **22**, No. 4, 386-389 (1951).

ATTON, A. W., D. F. Metcalf, and C. W. Tolbert. A study of tropospheric scattering of radio waves. Proc. Inst. Radio Eng., **39**, No. 6, 643-648 (1951).

'SON, F. G. Meteors. Sci. Amer., **184**, No. 6, 22-28 (1951). [Describes usefulness of radar and radio techniques in the detection and study of meteor showers and sporadic meteors.]

D, J. P. Observations of the spectrum of high-intensity solar radiation at metre wavelengths. III—Isolated bursts. Aust. J. Sci. Res., A, **3**, No. 4, 541-557 (1950).

Wilkins, A. F., and C. M. Minnis. Comparison of ionospheric radio transmission forecasts wit practical results. Proc. Inst. Elec. Eng., **98**, Pt. 3, No. 53, 209-220 (1951).
Williams, C. Low-frequency radio-wave propagation by the ionosphere, with particular referenc to long-distance navigation. Proc. Inst. Elec. Eng., **98**, Pt. 3, No. 52, 81-99 (1951). [Discussion of paper and author's reply are given, pp. 99-103.]

E—*Earth's Crust and Interior*

Baule, H. Seismische Geschwindigkeitsmessung im Karbongestein unter Tage. J. Geophys. Res **56**, No. 2, 157-161 (1951).
Benioff, H. Global strain accumulation and release as revealed by great earthquakes. Bull. Geo Soc. Amer., **62**, No. 4, 331-338 (1951).
Caloi, P., e F. Peronaci. Sulla superficie di discontinuita alla profondità di 950 km circa. An Geofis., Roma, **4**, No. 1, 107-110 (1951).
Gaskell, T. F., and J. C. Swallow. Seismic refraction experiments in the North Atlanti Nature, **167**, 723-724 (May 5, 1951).
Gutenberg, B. Revised travel times in southern California. Bull. Seis. Soc. Amer., **41**, No. 143-163 (1951).
Gutenberg, B. Crustal layers of the continents and oceans. Bull. Geol. Soc. Amer., **62**, No. 427-439 (1951).
Hafner, W. Stress distributions and faulting. Bull. Geol. Soc. Amer., **62**, No. 4, 373-398 (1951
Hubbert, M. K. Mechanical basis for certain familiar geologic structures. Bull. Geol. Soc. Ame **62**, No. 4, 355-372 (1951).
Hughes, D. S., and H. J. Jones. Elastic wave velocities in sedimentary rocks. Trans. Am Geophys. Union, **32**, No. 2, 173-178 (1951).
Jeffreys, H. Dynamic effects of a liquid core (II). Mon. Not. R. Astr. Soc., **110**, No. 5, 460-4 (1951).
Kerr, P. F. The earth's uranium. Sci. Amer., **184**, No. 5, 17-21 (1951).
Leet, L. D., D. Linehan, and P. R. Berger. Investigation of the T phase. Bull. Seis. Soc. Ame **41**, No. 2, 123-141 (1951).
Logie, H. J. The velocity of seismic waves on the Witwatersrand. Bull. Seis. Soc. Amer., **41**, No. 109-121 (1951).
Nakamura, S. T. On the seismic energy and the age of the earth. Sci. Rep. Tôhoku Univ., Ser. Geophysics, **2**, No. 3, 206-208 (1950).
Nettleton, L. L. On the use of geophysical tools. Mines Mag., **40**, No. 10, 49-52 (1950).
Pettersson, H. Die schwedische Tiefsee-Expedition 1947/48. Naturwiss., **38**, Heft 6, 125-1 (1951).
Poole, J. H. J., and C. F. G. Delaney. Origin of atmospheric argon and the radioactive dec constants of potassium-40. Nature, **167**, 680-681 (April 28, 1951).
Reich, H., O. Foertsch, and G. A. Schulze. Results of seismic observations in Germany on Heligoland explosion of April 18, 1947. J. Geophys. Res., **56**, No. 2, 147-156 (1951).
Rothé, J. P. La structure de l'Atlantique. Ann. Geofis., Roma, **4**, No. 1, 27-41 in French 117-125 translation in Italian (1951).
Schneider, O. La edad de la Tierra. An. Soc. Cient. Argentina, **151**, 57-70 (Febrero 1951).
Smart, W. M. The origin of the earth. Cambridge, University Press, 239 with 8 pls. and 42 f (1951).
Stoneley, R. Polarisation of the *S*-phase of seismograms. Ann. Geofis., Roma, **4**, No. 1, 3-8 English and 113-116 translation in Italian (1951).
Stose, A. J., and G. W. Structure of the Sugarloaf Mountain area, Maryland, as a key to Piedm stratigraphy. Bull. Geol. Soc. Amer., **62**, No. 6, 697-699 (1951).
Takeuchi, H. Diffraction of elastic waves by an elastic sphere. Geophys. Notes, **3**, No. 19, 28 (1950).
Tanni, L., and E. Niskanen. The geoidal undulations and disturbing masses. Helsinki, Ann. Fennicae, A. III, Geol.-Geog. 24, 20 pp. (1951).
Turner, F. J., and J. Verhoogen. Igneous and metamorphic petrology. New York, McGr

Hill Book Co., Inc., 490 pp. (1951). [Treatment of the origin and evolution of rocks that have crystallized or have been profoundly modified at high temperatures.]

TTON, J. T., AND J. O. MYERS. Geophysical surveying. Practical application to general problems. Mine and Quarry Eng., **16**, No. 10, 307-313, and No. 11, 341-346 (1950).

F—*Miscellaneous*

IA, M. Sur la densité, la température et la turbulence dans les couches inférieures de la chromosphere. Prague, Bull. Central Astron. Inst. Czechosl., **2**, No. 7, 97-100 (1951).

ŠKA, J. Sur l'effet terrestre apparent de l'activité solaire. Paris, C.-R. Acad. sci., **232**, No. 18, 1643-1645 (1951).

SSBERG, W. A forecast of solar activity. J. Geophys. Res., **56**, No. 2, 294-295 (1951). [Letter to Editor.]

KAWA, G. On the longitude effect of a corpuscular stream from the sun. Kyoto, J. Geomag. Geoelectr., **2**, No. 3, 74-76 (1950).

RNATIONAL COUNCIL OF SCIENTIFIC UNIONS. Report of the Executive Committee (edited by F. J. M. Stratton, General Secretary). Cambridge, University Press, 78 pp. (1951). 25 cm.

N, F. D. On the expulsion of corpuscular streams by solar flares. Mon. Not. R. Astr. Soc., **110**, No. 5, 477-482 (1951).

N, F. D. On investigation into the possibility of observing streams of corpuscles emitted by solar flares (II). Mon. Not. R. Astr. Soc., **110**, No. 5, 483-490 (1951).

, F. Discussion photométrique de récentes éclipses de Lune. Prague, Bull. Central Astron. Inst. Czechosl., **2**, No. 6, 86-88 (1951).

IONAL PHYSICAL LABORATORY. Report for the year 1950. Department of Scientific and Industrial Research, Wightman and Co., Ltd., London, 71 pp. (1951). 24 cm. [Issued under the authority of His Majesty's Stationery Office.]

IONAL RESEARCH COUNCIL. Proceedings of the Alaskan Science Conference of the National Academy of Sciences, National Research Council, Washington, November 9-11, 1950. Washington, D. C., National Research Council, Bull. No. 122, 216 pp. (April 1951). 25 cm. [Contains minutes and summaries of papers, Section of Geophysics.]

ERVATORIO ASTRONOMICO DE LA PLATA. Memoria anual, correspondiente al año 1948. Prepared by Captain G. O. Wallbrecher, Director. Buenos Aires, pub. Observatorio Astronomico de la Universidad Nacional de la Plata, Ser. Especial No. 9, 144 pp. with list of publications (1950). 27 cm. [Contains sections on terrestrial magnetism, seismology, and gravity.]

T, W. E. List of recent publications. J. Geophys. Res., **56**, No. 2, 299-306 (1951).

TKA, Z. The H_α-emission from chromospheric flares. I—Observations. Prague, Bull. Central Astron. Inst. Czechosl., **2**, No. 6, 81-86 (1951).

TKA, Z. The H_α-emission from chromospheric flares. II—General features of the asymmetry. Prague, Bull. Central Astron. Inst. Czechosl., **2**, No. 7, 100-103 (1951).

DMEIER, M. Provisional sunspot-numbers for January to March, 1951. J. Geophys. Res., **56**, No. 2, 288 (1951).

NOTICE

When available, single unbound volumes can be supplied at $3.50 each and single numbers 1 each, postpaid.

Charges for reprints and covers

Reprints can be supplied, but prices have increased considerably and costs depend on the ber of articles per issue for which reprints are requested. It is no longer possible to publish a dule of reprint charges, but if reprints are requested approximate estimates will be given when y proofs are sent to authors. Reprints without covers are least expensive; standard covers title and author) can be supplied at an additional charge. Special printing on covers can also pplied at further additional charge.

Fifty reprints, without covers, will be given to institutions paying the publication charge of per page.

Alterations

Major alterations made by authors in proof will be charged at cost. Authors are requested, fore, to make final revisions on their typewritten manuscripts.

lers for back issues and reprints should be sent to Editorial Office, 5241 Broad Branch Road, , Washington 15, D.C., U.S.A.

Subscriptions only are handled by The Johns Hopkins Press, Baltimore 18, Maryland, U.S.A.

CONTENTS—Concluded